

Proceedings of two courses on

## COMPUTATIONAL MECHANICS I (elastoplasticity)

May 10-14, 2010

and

## COMPUTATIONAL MECHANICS II

December 1 - 3, 2010

held under the project

**Educational and scientific collaboration CR-Iceland:  
computational mechanics, geothermal energy and further applications**

(supported by EEP/Norway funds).



at Institute of Geonics AS CR Ostrava

Project organizer: Prof. Dr. Radim Blaheta (Institute of Geonics AS CR Ostrava)

Assoc. Prof. Dr. Jan Valdman (University of Iceland)

## **Preface**

These proceedings resulted from two courses - Computational Mechanics I and II, which were held at the Institute of Geonics AS CR with many participants from VSB - Technical University of Ostrava in May and December 2010.

The first course was focused on computational plasticity and lectured by Jan Valdman from the University of Iceland. The second course covers broader scope of topics from computational mechanics – damage mechanics, fluid dynamics, acoustics, contact problems, homogenization, solving problems of identification of material parameters, preconditioning for saddle point systems and aspects of a posteriori error computation, FEM, BEM, adaptiveness and parallel computing. The presented topics have lot of applications, among other covering geothermal energy and other geo engineering fields.

The courses Computational Mechanics I and II were supported by EEP/Norway funds via the project BG FTA 4th call - EČ 049-4V- Collaboration of CR and Island on education and science: Computational mechanics, geothermal energy and other applications.

This support and the work of all lecturers from Iceland, Sweden and the Czech Republic is highly appreciated.

Prof. Radim Blaheta  
project coordinator

# COMPUTATIONAL MECHANICS I (elastoplasticity)

May 10-14, 2010

activity: 5 lectures and 3 computer exercises designed for students, PhD students and researchers given by Jan Valdman (University of Iceland) on Mathematical modelling of elastoplasticity.

topics:

- modelling of elastoplasticity using rheological models
- introduction to theory of variational inequalities and their discretization with Finite Element method
- implementation details of a time-dependent two-dimensional problem in Matlab

# COMPUTATIONAL MECHANICS II

December 1 - 3, 2010

activity: 13 lectures given by 11 speakers

participants and their talks (ordered according to schedule):

- D. Lukáš (VSB-TU) - Parallel BEM-based methods
- J. Valdman (U Iceland) - A posteriori error estimates (3 talks)
- H. Palsson (U Iceland) - Computational fluid dynamics with OpenFOAM (2 talks)
- O. Axelsson (I Geonics) - Preconditioning for saddle point problems
- M. Neytcheva et al. (U Uppsala) - On an augmented Lagrangian-based preconditioning of Oseen type problems
- J. Kruis (CTU Prague) - Damage mechanics analysis with arc-length solver
- Z. Dostal (VSB-TU) - T-FETI based scalable algorithms for contact problems
- O. Vlach (VSB-TU) - Quasistatic contact problems
- T. Kozubek (VSB-TU) - Scalable algorithms for dynamics contact problems
- V. Vondrak (VSB-TU) - Efficient parallel contact shape optimization
- A. Markopoulos (VSB-TU) - MATSOL - implementation methods
- R. Blaheta et al. (I Geonics) - Computational (geo) micromechanics, Identification of material parameters (2 talks)
- S. Sysala (I Geonics) - Elasto-plasticity: selected topics

Original posters to both conferences (in czech and english),  
slides to COMPUTATIONAL MECHANICS I (elastoplasticity)  
by Jan Valdman

and

some abstracts to COMPUTATIONAL MECHANICS II

follow.

Additional information can be found on web pages of Institute of Geonics AS CR Ostrava

<http://www.ugn.cas.cz/?l=en&a=&p=events/2010/kvp/index.php>

<http://www.ugn.cas.cz/?l=en&a=&p=events/2010/wcm/index.php>





Srdečně zveme všechny zájemce na týdenní kurz



## VÝPOČETNÍ PLASTICITA

**přednášející dr. JAN VALDMAN** z University of Iceland, Reykjavík  
Kurz je podporovaný fondy EHP/Norska a je určen  
pro studenty, doktorandy a další zájemce.

Účelem kurzu je popis základních mechanických modelů v elastoplasticitě a jejich matematického modelování. Speciální důraz bude věnován numerickým metodám a jejich realizaci v Matlabu.

Témata **přednášek** zahrnují:

- modelování elastoplasticity pomocí reologických modelů
- úvod do teorie variačních nerovnic a jejich diskretizace pomocí metody konečných prvků (FEM)
- implementace řešiče časově závislé 2D úlohy v Matlabu

Cílem navazujícího **počítačového praktika** je:

- implementovat jednoduché úlohy lineární elasticity pomocí metody konečných prvků
- rozšířit je pro případ elastoplastického modelu včetně časové závislosti

Pro práci v počítačovém praktiku se předpokládá vlastní počítač. Vlastní MATLAB (v. 7 a výše) je vítán. K dispozici bude WiFi přístup k omezenému počtu licencí.

### Program:

Zahájení **10. 5. 2010, 13:00**, J. Valdman, úvodní přednáška

Pokračování kurzu **11. - 14. 5. 2010** denně:

- |             |  |
|-------------|--|
| 9:00-10:30  | přednáška  |
| 10:30-11:00 | diskuze, občerstvení                               |
| 11:00-12:30 | počítačové praktikum: tvorba a využití SW (MATLAB) |

Přednášky i počítačové praktikum se budou konat v **konferenční místnosti Ústavu geoniky AV ČR**, Studentská 1768, areál VŠB TU Ostrava Poruba.

ÚGN AV ČR a KAM FEI VŠB TU

Odborný garant: Prof. Radim Blaheta



You are invited to participate at the course



## COMPUTATIONAL MECHANICS II

held under the project „Educational and scientific collaboration CR-Iceland: computational mechanics, geothermal energy and further applications“ (supported by EEP/Norway funds).

**The course is a free continuation of the course Computational Mechanics I (plasticity) and is designed for students, PhD students and researchers.**

### Program

#### 1.12. 2010 from 14.00

##### Opening

D. Lukáš (VŠB-TU) **Parallel BEM-based methods**

J. Valdman (U Iceland) **Aposteriori error estimates (1)**

H. Palsson (U Iceland) **Computational fluid dynamics with OpenFOAM(1)**

#### 2.12. 2010 from 9.00

J. Valdman (U Iceland) **Aposteriori error estimates (2)**

H. Palsson (U Iceland) **Computational fluid dynamics with OpenFOAM(2)**

O. Axelsson (I Geonics) **Preconditioning for saddle point problems**

M. Neytcheva (U Uppsala) **Augmented Lagrangian preconditioning**

##### from 13.00

J. Kruis (CTU Prague) **Damage mechanics analysis with arc-length solver**

Z. Dostál (VŠB-TU) **T-FETI based scalable algorithms for contact problems**

O. Vlach (VŠB-TU) **Quasistatic contact problems**

T. Kozubek (VŠB-TU) **Scalable algorithms for dynamics contact problems**

V. Vondrák (VŠB-TU) **Efficient parallel contact shape optimization**

A. Markopoulos (VŠB-TU) **MATSOL - implementation methods**

#### 3.12. 2010 from 9.00

J. Valdman (U Iceland) **Aposteriori error estimates (3)**

R. Blaheta et al. (I Geonics) **Computational (geo) micromechanics**

S. Sysala (I Geonics) **Elasto-plasticity: selected topics**

R. Blaheta et al. (I Geonics) **Identification of material parameters**

Lectures of the length of 30 or 45 minutes will be held in the **conference room of the Institute Geonics AS CR**, Studentská 1768, Ostrava Poruba.

**Details:** [www.ugn.cas.cz](http://www.ugn.cas.cz). On behalf of the organizers: R. Blaheta, T. Kozubek.

# COMPUTATIONAL MECHANICS I

Jan Valdman

- modelling of elastoplasticity using rheological models
- introduction to theory of variational inequalities and their discretization with Finite Element method
- implementation details of a time-dependent two-dimensional problem in Matlab

# Mathematical modelling of elastoplasticity

Jan Valdman

School of Engineering and Natural Sciences  
University of Iceland, Reykjavik  
email: jan.valdman@gmail.com

Ostrava, May 10-14, 2010

## Outline

- 1 Rheological models
- 2 Variational inequalities
- 3 Existence
- 4 FE Discretization
- 5 Basics of Implementation

## Explaining papers to theory and numerics:

- Carsten Carstensen, Martin Brokate, Jan Valdman, A quasi-static boundary value problem in multi-surface elastoplasticity. I: Analysis. Math. Methods Appl. Sci. 27, No.14, 1697-1710 (2004), [web link](#)
- Carsten Carstensen, Martin Brokate, Jan Valdman, A quasi-static boundary value problem in multi-surface elastoplasticity. II: Numerical solution. Math. Methods Appl. Sci. 28, No.8, 881-901 (2005), [web link](#)
- Andreas Hofinger, Jan Valdman, Numerical solution of the two-yield elastoplastic minimization problem. Computing 81, No. 1, 35-52 (2007), [web link](#)
- Peter Gruber, Jan Valdman, Solution of one-time-step problems in elastoplasticity by a Slant Newton Method. SIAM J. Scientific Computing 31, No. 2, 1558-1580 (2009), [web link](#).

Elastoplasticity solver can be downloaded at  
<http://www.mathworks.com/matlabcentral/fileexchange/authors/37756>  
as a package called 'Two-yield elastoplasticity solver'

## Further papers on a posteriori error estimates in elastoplasticity:

- Antonio Orlando, Carsten Carstensen, Jan Valdman, A convergent adaptive finite element method for the primal problem of elastoplasticity. International Journal for Numerical Methods in Engineering 67, No. 13, 1851-1887 (2006), [web link](#)
- Sergey Repin, Jan Valdman, Functional a posteriori error estimates for problems with nonlinear boundary conditions. Journal of Numerical Mathematics 16, No. 1, 51-81 (2008), [web link](#)

## The tensile test

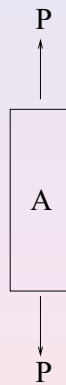


Figure: The tensile test: an increasing stress  $\sigma = P/A$  is applied to the specimen.

## The tensile test: stress-strain relation

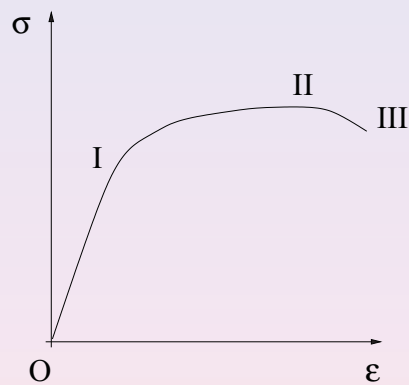
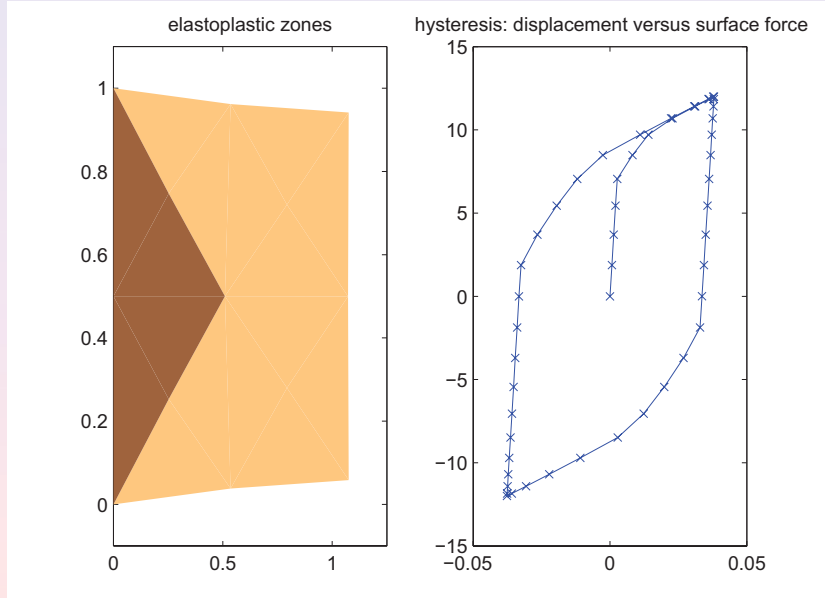


Figure: The tensile test: the resulting stress-strain relation.

- elasticity in the region  $O - I$
- plasticity with hardening after the elastic limit (point  $I$ )
- softening after necking (point  $II$ ) until fractures occur (point  $III$ )

# Time dependent 2D problem in Matlab



# Rheological elements

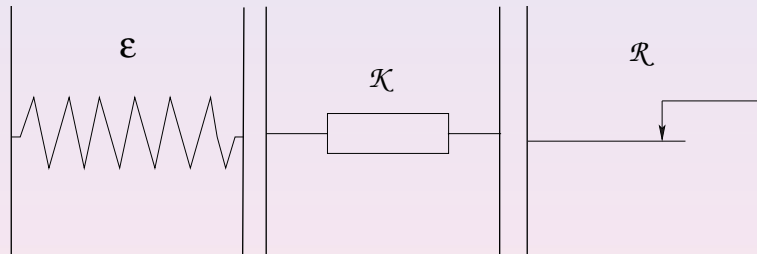


Figure: The elastic, kinematic and rigid-plastic element.

## Rheological elements

Every element is characterized by its (internal) stress and strain tensors. We denote the stress by  $\sigma$  and the strain by  $\varepsilon$ .

### The elastic element

$$\sigma = \mathbb{C}\varepsilon$$

### The kinematic element

$$\sigma = \mathcal{H}\varepsilon,$$

where  $\mathcal{H}$  is a positive definite matrix, for instance  $\mathcal{H} = h\mathbb{I}$ , where  $h > 0$  is a hardening coefficient and  $\mathbb{I}$  represents the identical matrix.

## Rheological elements

### The rigid-plastic element

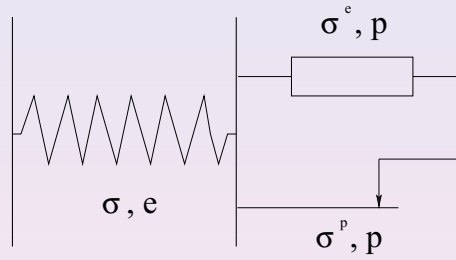
$$\begin{aligned} \sigma &\in Z \\ \langle \dot{\varepsilon}, q - \sigma \rangle &\leq 0 \quad \text{for all } q \in Z \end{aligned}$$

with a convex set  $Z \subset \mathbb{R}_{sym}^{d \times d}$ .

Example: 1D



# Kinematic hardening model



$$\begin{aligned} \varepsilon &= e + p \\ \sigma &= \sigma^e + \sigma^p \\ \sigma^e &= \mathcal{H}p \\ \sigma &= \mathbb{C}e \\ \sigma^p &\in Z \\ \langle \dot{p}, q - \sigma^p \rangle &\leq 0 \quad \text{for all } q \in Z. \end{aligned}$$

# Hysteresis property of the kinematic hardening model

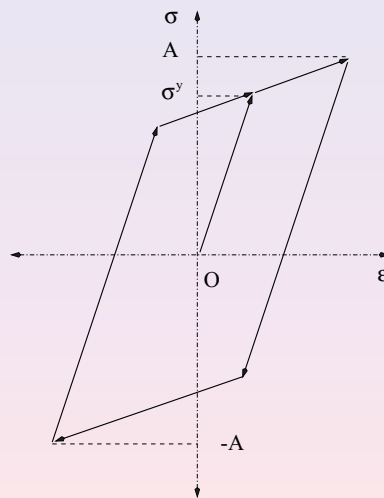


Figure: Stress-strain relation in case of linear kinematic hardening model and the cyclic stress  $\sigma = A \sin(t)$ .

## Motivation for the multi-yield model

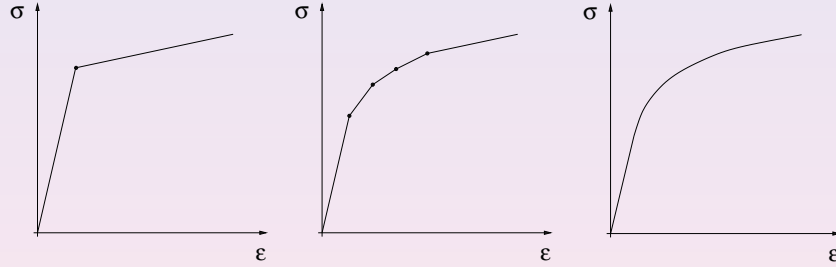
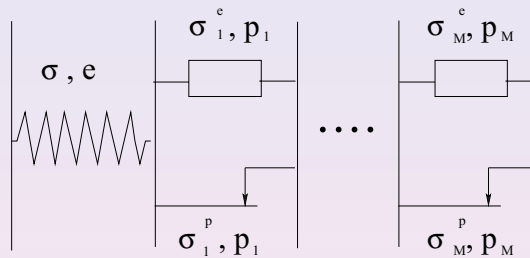


Figure: single-yield (left), multi-yield (middle) and realistic model (right) - stress-strain relation.

## The M-yield hardening model



$$\epsilon = e + p, \quad p = \sum_{r=1}^M p_r,$$

$$\sigma = \sigma_r^e + \sigma_r^p \quad \text{for all } r = 1, \dots, M,$$

$$\sigma_r^p \in Z_r,$$

$$\langle \dot{p}_r, q_r - \sigma_r^p \rangle \leq 0 \quad \text{for all } q_r \in Z_r, r = 1, \dots, M,$$

$$\sigma = \mathbb{C} e,$$

$$\sigma_r^e = \mathcal{H}_r p_r, \quad r = 1, \dots, M.$$

## Hysteresis property of the 2-yield hardening model

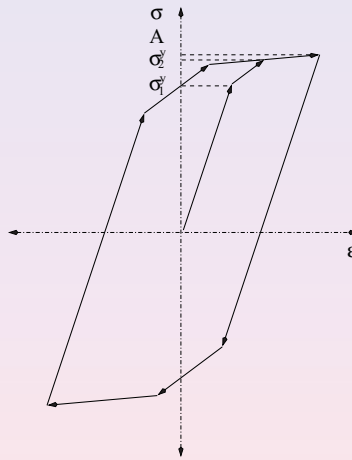


Figure: Stress-strain relation in case of two-yield model and cyclic stress  $\sigma = A \sin(t)$ .

## Books on hysteresis

- Visintin, A., Differential models of hysteresis, Springer, 1994
- Brokate, M. and Sprekels, J., Hysteresis and Phase Transitions, Springer-Verlag New York, 1996
- Krejčí, P., Hysteresis, Convexity and Dissipation in Hyperbolic Equations, GAKUTO International Series, Mathematical Sciences and Applications, 1996

## Yield criterion

## von Mises criterion

$$Z = \{\sigma \in \mathbb{R}_{sym}^{d \times d} : \|\text{dev } \sigma\|_F \leq \sigma^Y\},$$

where  $\|\cdot\|_F$  denotes the Frobenius matrix norm  $\|a\|_F^2 = a : a = \sum_{i,j=1}^d a_{ij}^2$ ,  
 $\text{dev } \sigma = \sigma - \frac{1}{d} \text{tr}(\sigma)\mathbb{I}$  is the deviatoric operator (deviator),  
 $\text{tr } \sigma = \sigma : \mathbb{I}$  is the trace operator.

## Dissipation functional

## Lemma

Let  $(\dot{p}, \sigma^p) \in \mathbb{R}_{sym}^{d \times d} \times \mathbb{R}_{sym}^{d \times d}$ . Then

$$\sigma^p \in Z, \quad \dot{p} : (\tau - \sigma^p) \leq 0 \quad \text{for all } \tau \in Z \quad (*)$$

together with  $\text{tr } \dot{p} = 0$  hold if and only if

$$\sigma^p : (q - \dot{p}) \leq \mathcal{D}(q) - \mathcal{D}(\dot{p}) \quad \forall q \in \mathbb{R}_{sym}^{d \times d}, \quad (**)$$

where  $\mathcal{D} : \mathbb{R}_{sym}^{d \times d} \rightarrow \mathbb{R} \cup \{\infty\}$ ,

$$\mathcal{D}(q) = \begin{cases} \sigma^Y \|q\| & \text{if } \text{tr } q = 0, \\ +\infty & \text{otherwise.} \end{cases}$$

Proof: together only implication  $(*) \Rightarrow (**)$ .

## Some convex analysis

## Definition (indicator function)

For any set  $Z \subset X$ , the *indicator function*  $I_Z$  of  $Z$  is defined by

$$I_Z(x) = \begin{cases} 0 & \text{if } x \in Z, \\ +\infty & \text{if } x \notin Z. \end{cases} \quad (1)$$

## Definition (subdifferential)

Let  $f$  be a convex function on  $X$ . For any  $x \in X$  the *subdifferential*  $\partial f(x)$  of  $x$  is the possibly empty subset of  $X^*$  defined by

$$\partial f(x) = \{x^* \in X^* : \langle x^*, y - x \rangle \leq f(y) - f(x) \quad \forall y \in X\}. \quad (2)$$

It means that

$$\dot{p} \in \partial I_Z(\sigma^P).$$

## Some convex analysis

## Definition (conjugate function)

For a function  $f : X \rightarrow [-\infty, \infty]$  we define the *conjugate function*  $f^* : X^* \rightarrow [-\infty, \infty]$  by

$$f^*(x^*) = \sup_{x \in X} (\langle x^*, x \rangle - f(x)). \quad (3)$$

## Lemma

Let  $X$  be a Banach space,  $f : X \rightarrow [-\infty, \infty]$  be a proper, convex, lower semicontinuous function. Then

$$x^* \in \partial f(x) \Leftrightarrow x \in \partial f^*(x^*). \quad (4)$$

Therefore,

$$\dot{p} \in \partial I_Z(\sigma^P) \Leftrightarrow \sigma^P \in \partial I_Z^*(\dot{p})$$

and

$$D(\cdot) := I_Z^*(\cdot).$$

## Equilibrium and its weak formulation

The equilibrium between external and internal forces is given by

$$\operatorname{div} \sigma(x, t) + f(x, t) = 0, \quad x \in \Omega, \quad t \in (0, T). \quad (5)$$

With the assumption of small deformations

$$\varepsilon(v) = \frac{1}{2} \left( \frac{\partial v_i}{\partial x_j} + \frac{\partial v_j}{\partial x_i} \right),$$

the variational formulation of (14) becomes (why?)

$$\int_{\Omega} \sigma : \varepsilon(v) \, dx = \int_{\Omega} f \cdot v \, dx + \int_{\Gamma_N} g \cdot v \, ds, \quad (6)$$

valid for all  $t \in [0, T]$  and all  $v \in H_D^1(\Omega)$ .

## Weak formulation of rigid-plastic elements

We express constitutive laws

$$\sigma_r^p : (q_r - \dot{p}_r) \leq \mathcal{D}_r(q_r) - \mathcal{D}_r(\dot{p}_r) \quad \forall q_r \in Q, \quad r \in I, \quad (7)$$

where (note that we only consider arguments with zero trace here)

$$\mathcal{D}_r(q_r) = \sigma_r^y \|q_r\|.$$

The integral form of (7) over  $\Omega$  is given by

$$\int_{\Omega} \sigma_r^p : (q_r - \dot{p}_r) \, dx \leq \int_{\Omega} \mathcal{D}_r(q_r) \, dx - \int_{\Omega} \mathcal{D}_r(\dot{p}_r) \, dx. \quad (8)$$

## Variational inequality

We sum the inequalities (8) over  $r$   
and subtract (6) in which we equivalently replace  $v$  by  $v - \dot{u}$   
to obtain

$$\begin{aligned} & \int_{\Omega} \sigma : (\varepsilon(v) - \sum_{r \in I} q_r) \, dx - \int_{\Omega} \sigma : (\varepsilon(\dot{u}) - \sum_{r \in I} \dot{p}_r) \, dx + \sum_{r \in I} \int_{\Omega} \sigma_r^e : (q_r - \dot{p}_r) \, dx \\ & + \sum_{r \in I} \int_{\Omega} \mathcal{D}_r(q_r) \, dx - \sum_{r \in I} \int_{\Omega} \mathcal{D}_r(\dot{p}_r) \, dx - \int_{\Omega} f \cdot (v - \dot{u}) \, dx - \int_{\Gamma_N} g \cdot (v - \dot{u}) \, ds \geq 0. \end{aligned}$$

Next, we eliminate

$$\sigma = \mathbb{C}(\varepsilon(u) - p), \quad \sigma_r^e = \mathcal{H}_r p_r.$$

## Variational inequality

We collect vectors of functions

$$w = (u, (p_r)_{r \in I}), \quad z = (v, (q_r)_{r \in I}).$$

to obtain

**Problem (BVP of quasi-static multi-surface elastoplasticity)**

For given  $\ell \in H^1(0, T; \mathcal{H}^*)$  with  $\ell(0) = 0$ ,  
find  $w \in H^1(0, T; \mathcal{H})$  with  $w(0) = 0$ , such that

$a(w(t), z - \dot{w}(t)) + \psi(z) - \psi(\dot{w}(t)) \geq \langle \ell(t), z - \dot{w}(t) \rangle$ , for all  $z \in \mathcal{H}$ ,  
holds for almost all  $t \in (0, T)$ .

## Variational inequality

A bilinear form  $a(\cdot, \cdot)$ , a linear functional  $\ell(\cdot)$  and a nonlinear functional  $\psi(\cdot)$  are defined as

$$a : \mathcal{H} \times \mathcal{H} \rightarrow \mathbb{R}, \quad a(w, z) = \int_{\Omega} \mathbb{C}(\varepsilon(u) - \sum_{r \in I} p_r) : (\varepsilon(v) - \sum_{r \in I} q_r) \, dx + \\ + \sum_{r \in I} \int_{\Omega} \mathcal{H}_r p_r : q_r \, dx,$$

$$\ell(t) : \mathcal{H} \rightarrow \mathbb{R}, \quad \langle \ell(t), z \rangle = \int_{\Omega} f(t) \cdot v \, dx + \int_{\Gamma_N} g(t) \cdot v \, ds,$$

$$\psi : \mathcal{H} \rightarrow \mathbb{R}, \quad \psi(z) = \sum_{r \in I} \int_{\Omega} \mathcal{D}_r(q_r) \, dx.$$

and  $\mathcal{H} = H_D^1(\Omega) \times \prod_{r \in I} Q$ .

## Further reading

- Glowinski, R., Lions J. L. and Trémolières R., Numerical analysis of Variational Inequalities, North-Holland, Amsterdam, 1981
- Han, W. and Reddy, B., Plasticity: Mathematical Theory and Numerical Analysis, Springer-Verlag New York, 1999



## Material assumptions

We pose the natural assumption that the elastic and hardening tensors are symmetric and positive definite,

$$\begin{aligned} \mathbb{C} \lambda &= \mathbb{C} \xi : \lambda \quad \text{for all } \xi, \lambda \in \mathbb{R}^{d \times d}, \\ \mathcal{H}_r \lambda &= \mathcal{H}_r \xi : \lambda \quad \text{for all } \xi, \lambda \in \mathbb{R}^{d \times d}, r = 1, \dots, M, \end{aligned} \quad (9)$$

and there exist constants  $c, h_r > 0$  such that

$$\begin{aligned} \mathbb{C} \xi : \xi &\geq c \|\xi\|^2 \quad \text{for all } \xi \in \mathbb{R}^{d \times d}, \\ \mathcal{H}_r \xi : \xi &\geq h_r \|\xi\|^2 \quad \text{for all } \xi \in \mathbb{R}^{d \times d}, r = 1, \dots, M. \end{aligned} \quad (10)$$

## Abstract theorem on solvability

### Theorem

Assume that (9) and (10) hold, let  $\ell \in H^1(0, T; \mathcal{H}^*)$  with  $\ell(0) = 0$ . Then there exists a unique solution  $w \in H^1(0, T; \mathcal{H})$  of BVP of quasi-static multi-surface elastoplasticity.

based on

## Abstract theorem on solvability

### Theorem (Han, Reddy, 1999)

Let  $\mathcal{H}$  be a Hilbert space,  $a : \mathcal{H} \times \mathcal{H} \rightarrow \mathbb{R}$  be a bilinear form that is symmetric, bounded, and  $\mathcal{H}$ -elliptic;  $\ell \in H^1(0, T; \mathcal{H}^*)$  with  $\ell(0) = 0$ ; and  $\psi : \mathcal{H} \rightarrow \mathbb{R}$  nonnegative, convex, positively homogeneous, and Lipschitz continuous. Then there exists a unique  $w \in H^1(0, T; \mathcal{H})$  with  $w(0) = 0$  which satisfies the variational inequality

$$a(w(t), z - \dot{w}(t)) + \psi(z) - \psi(\dot{w}(t)) \geq \langle \ell(t), z - \dot{w}(t) \rangle, \quad \text{for all } z \in \mathcal{H},$$

for almost all  $t \in (0, T)$ .

## Remark on ellipticity

To prove that

$$a(w, z) = \int_{\Omega} \mathbb{C}(\varepsilon(u) - \sum_{r \in I} p_r) : (\varepsilon(v) - \sum_{r \in I} q_r) \, dx + \sum_{r \in I} \int_{\Omega} \mathcal{H}_r p_r : q_r \, dx,$$

is elliptic, the following partial result is important:

### Problem

To determine the largest constant  $k(M)$ ,  $M \in \mathcal{N}$ , such that

$$\left( x_0 - \sum_{r=1}^M x_r \right)^2 + \sum_{r=1}^M x_r^2 \geq k(M) \sum_{r=0}^M x_r^2 \quad (11)$$

holds for all  $x_0, x_1, \dots, x_M \in \mathbb{R}$ .

## Algebraic inequality

We reformulate

$$\left(x_0 - \sum_{r=1}^M x_r\right)^2 + \sum_{r=1}^M x_r^2 = x^T A x, \quad (12)$$

where

$$A = D + a \otimes a, \quad D = \text{diag}(0, 1, \dots, 1), \quad a = (1, -1, \dots, -1). \quad (13)$$

Thus, the optimal constant  $k(M)$  is equal to the smallest eigenvalue of  $A$ !

## Algebraic inequality

The analytical computation shows

$$k(M) = \lambda_{\min} = 1 + \frac{M}{2} - \frac{1}{2} \sqrt{4M + M^2}$$

Properties:

$$\lim_{M \rightarrow \infty} k(M) = 0$$

and

$$\lim_{M \rightarrow \infty} M k(M) = 1$$

## Backward Euler scheme

In the first time step  $t_1$ , the time derivative  $\dot{x}(t_1)$  is approximated by the backward Euler method as

$$\dot{X}^1 = \frac{X^1 - X^0}{k_1},$$

where  $X^0 = 0$ . The Hilbert space  $\mathcal{H}$  is approximated by the conforming finite element (FEM) subspace

$$\mathcal{S} = \mathcal{S}_D^1(\mathcal{T}) \times \prod_{r \in I} \text{dev}(\mathcal{S}^0(\mathcal{T})_{\text{sym}}^{d \times d}),$$

which is a product space of  $\mathcal{T}$ - piecewise affine functions that are zero on  $\Gamma_D$  by

$$\mathcal{S}_D^1(\mathcal{T}) := \{v \in H_D^1(\Omega) : \forall T \in \mathcal{T}, v|_T \in \mathcal{P}_1(T)^d\}.$$

( $\mathcal{P}_1(T)$  denotes the affine functions on  $T$ ) and the space of  $\mathcal{T}$ - piecewise constant functions

$$\text{dev}(\mathcal{S}^0(\mathcal{T})_{\text{sym}}^{d \times d}) := \{a \in L^2(\Omega)^{d \times d} : \forall T \in \mathcal{T}, a|_T \in \text{dev} \mathbb{R}_{\text{sym}}^{d \times d}\}$$

## Backward Euler scheme

### The first time step problem

Find  $X^1 = (U^1, (P_r^1)_{r \in I}) := (U^1, P^1) \in \mathcal{S}$  such that

$$\langle \ell(t_1), (Y - \frac{X^1 - X^0}{k_1}) \rangle \leq a(X^1, Y - \frac{X^1 - X^0}{k_1}) + \psi(Q) - \psi(\frac{P^1 - P^0}{k_1}).$$

holds for all  $Y = (V, Q) = (V, (Q_r)_{r \in I}) \in \mathcal{S}$ .

After introducing an incremental variable  $X := (U, P) = X^1 - X^0$

and a linear functional  $L(Y) = \langle \ell(t_1), Y \rangle - a(X^0, Y)$

we obtain a one-time step incremental problem

$$L(Y - X) \leq a(X, Y - X) + \psi(Q) - \psi(P) \quad \text{for all } Y = (V, Q) \in \mathcal{S}.$$

## Introducing the energy functional

### Lemma (Equivalent Reformulations)

For each  $X = (U, P) \in \mathcal{S}$  the following three conditions (a)-(c) are equivalent:

$$(a) \quad L(Y - X) \leq a(X, Y - X) + \psi(Q) - \psi(P) \quad \text{for all } Y = (V, Q) \in \mathcal{S}.$$

$$(b) \quad L(Y - X) = a(X, Y - X) \quad \text{for all } Y = (V, P) \in \mathcal{S} \quad \text{and} \\ L(Y - X) \leq a(X, Y - X) + \psi(Q) - \psi(P) \quad \text{for all } Y = (U, Q) \in \mathcal{S}.$$

$$(c) \quad \Phi(X) = \min_{Y \in \mathcal{S}} \Phi(Y) \quad \text{with } \Phi(Y) = \frac{1}{2}a(Y, Y) + \psi(Q) - L(Y).$$

## Abreviations

The following matrix notation allows for a brief formulation of the discrete problem. Let

$$P := \begin{pmatrix} P_1 \\ \vdots \\ P_M \end{pmatrix}, P^0 := \begin{pmatrix} P_1^0 \\ \vdots \\ P_M^0 \end{pmatrix}, Q := \begin{pmatrix} Q_1 \\ \vdots \\ Q_M \end{pmatrix}, \hat{\Sigma} := \begin{pmatrix} \mathbb{C}\varepsilon(U) \\ \vdots \\ \mathbb{C}\varepsilon(U) \end{pmatrix}, \\ \hat{\Sigma}^0 := \begin{pmatrix} \mathbb{C}\varepsilon(U^0) \\ \vdots \\ \mathbb{C}\varepsilon(U^0) \end{pmatrix}, \hat{\mathbb{C}} := \begin{pmatrix} \mathbb{C} & \dots & \mathbb{C} \\ \vdots & & \vdots \\ \mathbb{C} & \dots & \mathbb{C} \end{pmatrix}, \hat{\mathcal{H}} := \begin{pmatrix} \mathcal{H}_1 & \dots & 0 \\ \vdots & & \vdots \\ 0 & \dots & \mathcal{H}_M \end{pmatrix}.$$

## Abreviations

Then there holds

$$\begin{aligned} -a(X, Y - X) &= \int_{\Omega} \left( \hat{\Sigma} - (\hat{C} + \hat{H})P \right) : (Q - P) \, dx, \\ L(Y - X) &= \int_{\Omega} \left( \hat{\Sigma}^0 - (\hat{C} + \hat{H})P^0 \right) : (Q - P) \, dx, \\ \psi(Y) &= \int_{\Omega} |Q|_{\sigma^y} \, dx. \end{aligned}$$

Since the plastic yield parameters  $\sigma_1^y, \dots, \sigma_M^y$  are positive, the expansion

$$|(Q_1, \dots, Q_M)^T|_{\sigma^y} := \sigma_1^y |Q_1| + \dots + \sigma_M^y |Q_M|$$

defines a norm in  $\mathbb{R}^{Md \times d}$ , where  $|\cdot|$  denotes the Frobenius norm.

## Coupled problem

### Problem (Discrete problem)

Given  $(U^0, P^0) \in \mathcal{S}$ , seek  $U^1 \in \mathcal{S}_D^1(\mathcal{T})$  such that for all  $V \in \mathcal{S}_D^1(\mathcal{T})$ ,

$$\int_{\Omega} \mathbb{C}(\varepsilon(U^1) - \sum_{r=1}^M P_r^1) : \varepsilon(V) \, dx - \int_{\Omega} f(t)V \, dx - \int_{\Gamma_N} gV \, dx = 0. \quad (14)$$

Here  $P = (P_1, \dots, P_M)^T = (P_1^1, \dots, P_M^1)^T - (P_1^0, \dots, P_M^0)^T$  satisfies

$$(\hat{A} - (\hat{C} + \hat{H})P) : (Q - P) \leq |Q|_{\sigma^y} - |P|_{\sigma^y} \quad (15)$$

for all  $Q = (Q_1, \dots, Q_M)^T$  with  $Q_1, \dots, Q_M \in \text{dev}(\mathcal{S}^0(\mathcal{T})_{\text{sym}}^{d \times d})$  and

$$\hat{A} := \hat{\Sigma}(U^1) + \hat{\Sigma}^0(U^0) - (\hat{C} + \hat{H})P^0.$$

## Moreau regularization

### Theorem (Moreau, 1965)

Let the function  $\mathcal{F} : \mathcal{H} \times \mathcal{H} \rightarrow \overline{\mathbb{R}}$  be defined

$$\mathcal{F}(x, y) = \frac{1}{2} \|y - x\|_{\mathcal{H}}^2 + \psi(x) \quad (16)$$

where  $\psi$  is a convex, proper and lower semi continuous mapping of  $\mathcal{H}$  into  $\overline{\mathbb{R}}$ . Then

$$F(y) := \inf_{x \in \mathcal{H}} \mathcal{F}(x, y)$$

is well defined as a functional from  $\mathcal{H}$  into  $\mathbb{R}$  and there exists a unique mapping  $\tilde{x} : \mathcal{H} \rightarrow \mathcal{H}$  such, that

$$F(y) = \mathcal{F}(\tilde{x}(y), y)$$

holds for all  $y \in \mathcal{H}$ . Moreover,  $F$  is strictly convex and Fréchet differentiable with the derivative

$$\mathcal{D}F(y) = \langle y - \tilde{x}(y), \cdot \rangle_{\mathcal{H}} \in \mathcal{H}^* \quad \forall y \in \mathcal{H}. \quad (17)$$

## Moreau regularization

Theorem of Moreau implies for elastoplasticity

### Theorem

There is a unique function

$$P = P(\varepsilon(U))$$

and the energy functional

$$\Phi(U) = \frac{1}{2} a(U, P(\varepsilon(U)); U, P(\varepsilon(U))) + \psi(P(\varepsilon(U))) - L(U)$$

is strictly convex and differentiable!

more details in

- Peter Gruber, Jan Valdman, Solution of one-time-step problems in elastoplasticity by a Slant Newton Method. SIAM J. Scientific Computing 31, No. 2, 1558-1580 (2009)

## Analysis of single-yield model (M=1)

Localization to one element  $T \in \mathcal{T}$ :

One plastic strain

$$P \in \mathbb{R}_{\text{sym}}^{2 \times 2}, \quad \text{tr } P = 0,$$

the elastic matrix  $\mathbb{C}$  with the (positive) Lamé coefficients  $\mu$  and  $\lambda$

$$\mathbb{C}P = 2\mu P + \lambda(\text{tr } P)\mathbb{I} = 2\mu P,$$

the hardening matrix  $\mathcal{H}$  with

$$\mathcal{H}P = hP,$$

the matrix norm

$$|P|_{\sigma^Y} = \sigma^Y |P|$$

and the matrix

$$A := \hat{A} := \mathbb{C}_\varepsilon(U) + \mathbb{C}_\varepsilon(U^0) - (\mathbb{C} + \mathcal{H})P^0.$$

## Analysis of single-yield model (M=1)

Lemma (Alberty, Carstensen, Zarrabi, 1999)

Given  $A \in \mathbb{R}_{\text{sym}}^{d \times d}$  and  $\sigma^Y > 0$ . There exists exactly one  $P \in \text{dev } \mathbb{R}_{\text{sym}}^{d \times d}$  that satisfies

$$\{A - (\mathbb{C} + \mathcal{H})P\} : (Q - P) \leq \sigma^Y \{|Q| - |P|\}$$

for all  $Q \in \text{dev } \mathbb{R}_{\text{sym}}^{d \times d}$ . This  $P$  is characterized as the minimiser of

$$\frac{1}{2}(\mathbb{C} + \mathcal{H})Q : Q - Q : A + \sigma^Y |Q| \quad (18)$$

(amongst trace-free symmetric  $d \times d$ -matrices) and is given by

$$P = \frac{(|\text{dev } A| - \sigma^Y)_+}{2\mu + h} \frac{\text{dev } A}{|\text{dev } A|}, \quad (19)$$

where  $(\cdot)_+ := \max\{0, \cdot\}$  denotes the non-negative part.



## Analysis of two-yield model (M=2)

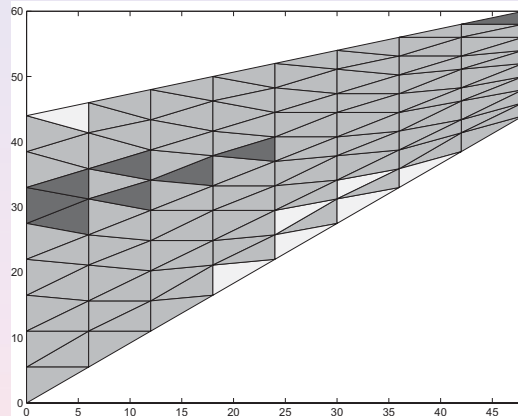


Figure: Cook's membrane problem in the first time step. The black colour shows elastic upgrade zones (where  $P_1 = P_2 = 0$ ), brown and lighter gray colours shows the first plastic upgrade ( $P_1 \neq 0, P_2 = 0$ ) and the both plastic upgrades ( $P_1 \neq 0, P_2 \neq 0$ ) zones.

## Analysis of two-yield model (M=2)

Two plastic strains  $P_1, P_2$  coupled in a generalized plastic strain

$$P = (P_1, P_2)^T.$$

The generalized elasticity matrix and the generalized hardening matrices read

$$\hat{\mathbb{C}} := \begin{pmatrix} \mathbb{C} & \mathbb{C} \\ \mathbb{C} & \mathbb{C} \end{pmatrix} \quad \text{and} \quad \hat{\mathcal{H}} := \begin{pmatrix} \mathcal{H}_1 & 0 \\ 0 & \mathcal{H}_2 \end{pmatrix},$$

the generalized loading matrix reads

$$\hat{A} = \begin{pmatrix} A_1 \\ A_2 \end{pmatrix} = \begin{pmatrix} \mathbb{C}_\varepsilon(U) \\ \mathbb{C}_\varepsilon(U) \end{pmatrix} + \begin{pmatrix} \mathbb{C}_\varepsilon(U^0) \\ \mathbb{C}_\varepsilon(U^0) \end{pmatrix} - \begin{pmatrix} \mathbb{C} + \mathcal{H}_1 & \mathbb{C} \\ \mathbb{C} & \mathbb{C} + \mathcal{H}_2 \end{pmatrix} \begin{pmatrix} P_1^0 \\ P_2^0 \end{pmatrix}$$

and the matrix norm is defined by

$$|P|_{\sigma^\gamma} = \sigma_1^\gamma |P_1| + \sigma_2^\gamma |P_2|.$$

## Analysis of two-yield model (M=2)

## Lemma

Given  $\hat{A} = (A_1, A_2)^T$ ,  $A_1, A_2 \in \mathbb{R}_{\text{sym}}^{d \times d}$ , there exists exactly one  $P = (P_1, P_2)^T$ ,  $P_1, P_2 \in \text{dev } \mathbb{R}_{\text{sym}}^{d \times d}$  that satisfies

$$(\hat{A} - (\hat{C} + \hat{H})P) : (Q - P) \leq |Q|_{\sigma^y} - |P|_{\sigma^y} \quad (20)$$

for all  $Q = (Q_1, Q_2)^T$ ,  $Q_1, Q_2 \in \text{dev } \mathbb{R}_{\text{sym}}^{d \times d}$ . This  $P$  is characterized as the minimiser of

$$f(Q) = \frac{1}{2}(\hat{C} + \hat{H})Q : Q - Q : \hat{A} + |Q|_{\sigma^y} \quad (21)$$

(amongst trace-free symmetric  $d \times d$  matrices  $Q_1, Q_2$ ).

Exact minimizer?

## Analysis of two-yield model (M=2)

We introduce the operator

$$\mathcal{F}(M, \sigma, h) := \frac{(|M| - \sigma)_+}{2\mu + h} \frac{M}{|M|}. \quad (22)$$

Algorithm (Iterative calculation of  $P_1, P_2$ )

Input  $\mu, h_1, h_2, \sigma_1^y, \sigma_2^y, \text{dev } A_1, \text{dev } A_2$  and  $\text{tol} \geq 0$ .

- 1 Set  $i := 0$  and set the initial approximation  $P_1^i = P_2^i = 0$ .
- 2 Update  $P_2^i$  via  $P_2^{i+1} = \mathcal{F}(\text{dev } A_2 - 2\mu P_1^i, \sigma_2^y, h_2)$ .
- 3 Update  $P_1^i$  via  $P_1^{i+1} = \mathcal{F}(\text{dev } A_1 - 2\mu P_2^{i+1}, \sigma_1^y, h_1)$ .
- 4 If the desired accuracy is reached, i. e., if

$$|P_1^{i+1} - P_1^i| + |P_2^{i+1} - P_2^i| \leq \text{tol} \cdot (|P_1^{i+1}| + |P_1^i| + |P_2^{i+1}| + |P_2^i|)$$

then output solution  $(P_1, P_2) = (P_1^{i+1}, P_2^{i+1})$ . Otherwise, set  $i := i + 1$  and go to step 2.

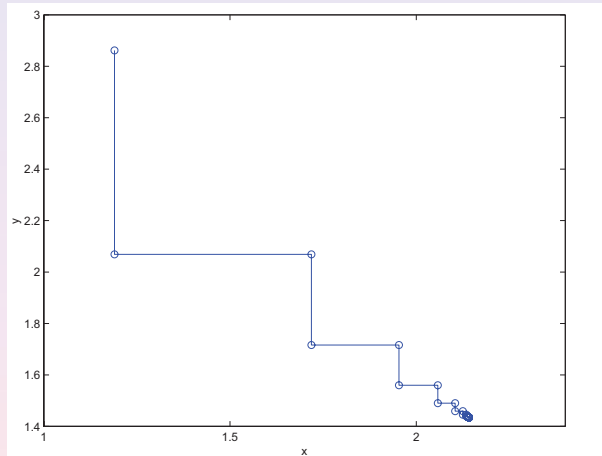
Analysis of two-yield model ( $M=2$ )

Figure: The approximations  $P_1^i = (x^i, 0; 0, -x^i)$ ,  $P_2^j = (y^j, 0; 0, -y^j)$ ,  $i = 0, \dots, 34$  computed by the iterative algorithm and displayed as the points  $(x^i, y^i)$  in the  $x - y$  coordinate system.

## Newton method

A nonlinear system of equations for  $2N$  displacement unknowns  $\mathbf{U}^1 = (U_1^1, \dots, U_{2N}^1)^T$ :

$$\mathbf{F}_i(\mathbf{U}^1) = 0 \quad \text{for all } i = 1, \dots, 2N. \quad (23)$$

We use the Newton-Raphson method for the iterative solution of (23).

## Algorithm (Newton-Raphson Method)

- (a) Choose an initial approximation  $\mathbf{U}_0^1 \in \mathbb{R}^{2N}$ , set  $k := 0$ .  
 (b) Let  $k := k + 1$ , solve  $\mathbf{U}_k^1$  from

$$D\mathbf{F}(\mathbf{U}_{k-1}^1)(\mathbf{U}_k^1 - \mathbf{U}_{k-1}^1) = -\mathbf{F}(\mathbf{U}_{k-1}^1).$$

- (c) If  $\mathbf{U}_k^1 - \mathbf{U}_{k-1}^1$  is sufficiently small then output  $\mathbf{U}_k^1$ , otherwise goto (b).

## Newton method

In order to incorporate the Dirichlet boundary conditions properly, the linear system in the step (b) is extended,

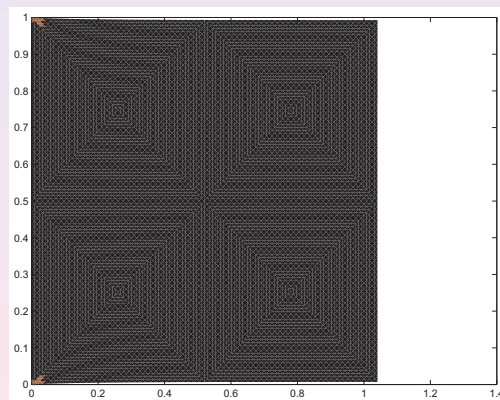
$$\begin{pmatrix} D\mathbf{F}(\mathbf{U}_{k-1}^1) & B^T \\ B & 0 \end{pmatrix} \begin{pmatrix} \mathbf{U}_k^1 - \mathbf{U}_{k-1}^1 \\ \lambda \end{pmatrix} = \begin{pmatrix} -\mathbf{F}(\mathbf{U}_{k-1}^1) \\ \mathbf{0} \end{pmatrix},$$

with some matrix  $B$  and the vector of Lagrange parameters  $\lambda$ . Here,  $D\mathbf{F}(\mathbf{U}_k^1) \in \mathbb{R}^{2N \times 2N}$  represents a sparse tangential stiffness matrix

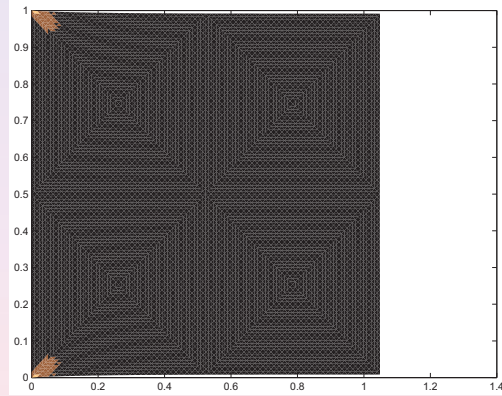
$$D\mathbf{F}(\mathbf{U})_{ij} \approx \frac{\mathbf{F}(U_1, \dots, U_j + \epsilon_j, \dots, U_{2N})_i - \mathbf{F}(U_1, \dots, U_j - \epsilon_j, \dots, U_{2N})_i}{2\epsilon_j}$$

approximated by a central difference scheme with small parameters  $\epsilon_j > 0, j = 1, \dots, 2N$ .

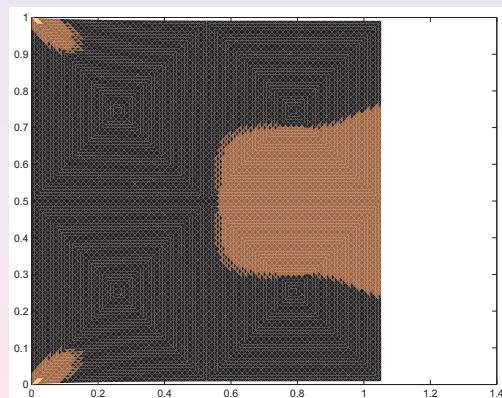
## Matlab simulations: two-yield 2D beam model



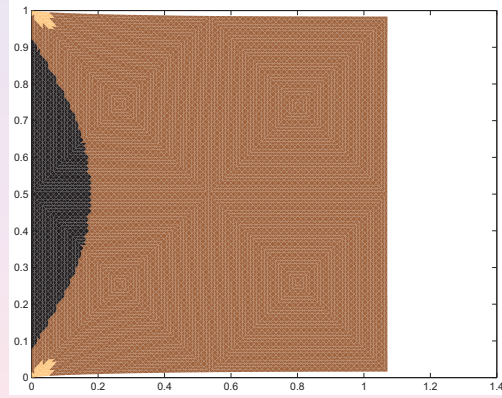
# Matlab simulations: two-yield 2D beam model



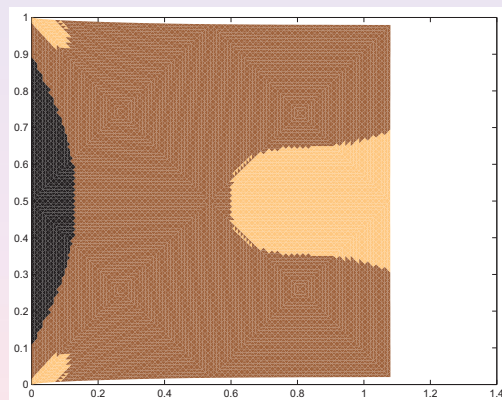
# Matlab simulations: two-yield 2D beam model



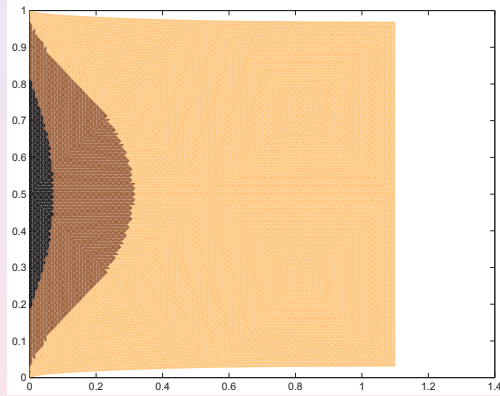
# Matlab simulations: two-yield 2D beam model



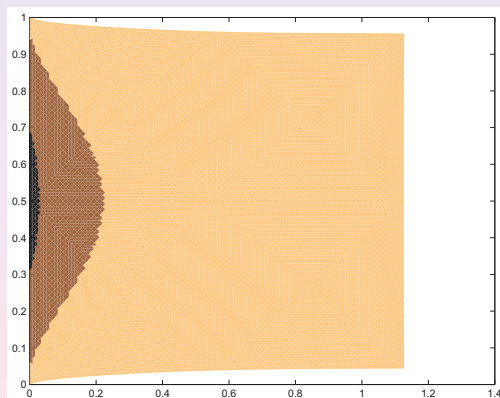
# Matlab simulations: two-yield 2D beam model



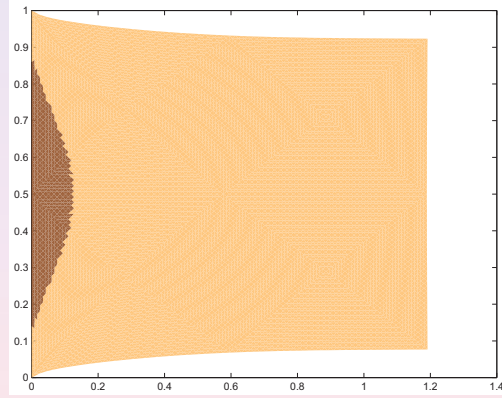
# Matlab simulations: two-yield 2D beam model



# Matlab simulations: two-yield 2D beam model



## Matlab simulations: two-yield 2D beam model



## Matlab simulations: single-yield model

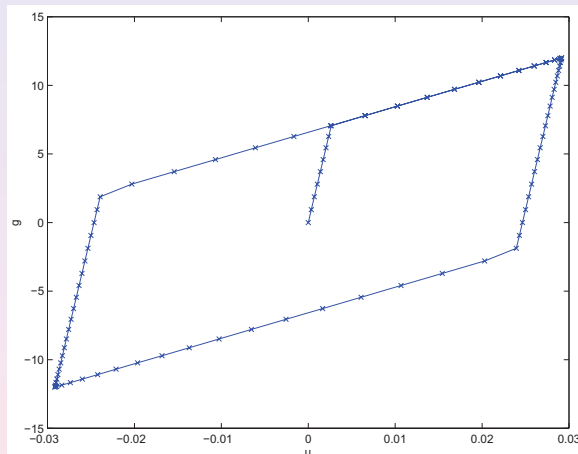


Figure: Displayed loading-deformation relation in terms of the uniform surface loading  $g_x(t)$  versus the  $x$ -displacement of the point  $(0, 1)$  for problem of the single-yield beam with 1D effects.



## Matlab simulations: two-yield model

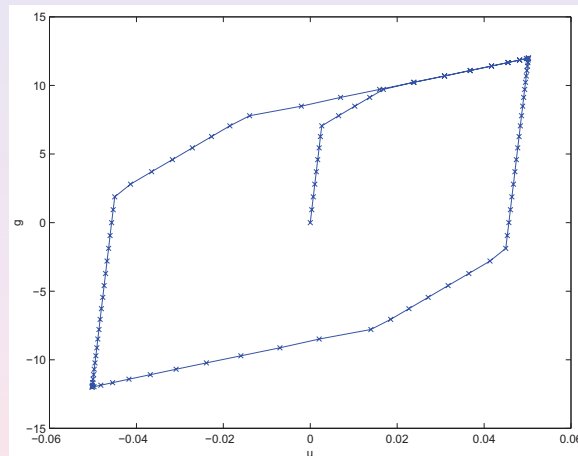


Figure: Displayed loading-deformation relation in terms of the uniform surface loading  $g_x(t)$  versus the  $x$ -displacement of the point  $(0, 1)$  for problem of the two-yield beam with 1D effects.

## Papers on Matlab Implementation

- Jochen Albery, Carsten Carstensen and Stefan A. Funken, Remarks around 50 lines of Matlab: short finite element implementation, Numerical Algorithms 20 (117), 117–137 (1999)
- Albery, Carstensen, Funken, Klose, Matlab implementation of the finite element method in elasticity, Computing 69 (3), 239 – 263 (2002)
- Carstensen C., Klose R., Elastoviscoplastic Finite Element Analysis in 100 lines of Matlab, J. Numer. Math., 10 (3), 157–192 (2002)
- Rahman T., Valdman J., Fast MATLAB assembly of FEM stiffness- and mass matrices in 2D and 3D: nodal elements, Proceedings of conference PARA 2010 (submitted)

## Computer exercises

- computation of triangulation areas
- uniform refinement in 2D
- generation of a stiffness matrix
- generation of a right-hand side
- a posteriori computation of a plasticity strain from a given stress
- alternating directions iteration over equilibrium and plasticity inequality
- extension to time-dependent problems

Thank you for your attention!

# COMPUTATIONAL MECHANICS I I

- D. Lukáš (VŠB-TU) **Parallel BEM-based methods**
- J. Valdman (U Iceland) **Aposteriori error estimates (3)**
- H. Palsson (U Iceland) **Computational fluid dynamics with OpenFOAM(2)**
- O. Axelsson (I Geonics) **Preconditioning for saddle point problems**
- M. Neytcheva (U Uppsala) **Augmented Lagrangian preconditioning**
- J. Kruis (CTU Prague) **Damage mechanics analysis with arc-length solver**
- Z. Dostál (VŠB-TU) **T-FETI based scalable algorithms for contact problems**
- O. Vlach (VŠB-TU) **Quasistatic contact problems**
- T. Kozubek (VŠB-TU) **Scalable algorithms for dynamics contact problems**
- V. Vondrák (VŠB-TU) **Efficient parallel contact shape optimization**
- R. Blaheta et al. (I Geonics) **Computational (geo) micromechanics**
- R. Blaheta et al. (I Geonics) **Identification of material parameters**
- S. Sysala (I Geonics) **Elasto-plasticity: selected topics**

# Parallel BEM–Based Methods

Workshop on Computational Mechanics II, ÚGN Ostrava, Dec. 1, 2010



D. Lukáš

Department of Applied Mathematics  
VŠB–Technical University of Ostrava, Czech Rep.

email: dalibor.lukas@vsb.cz



# Parallel BEM–Based Methods

## Outline

- Motivation: Acoustic scattering from a railway wheel
- Parallel fast boundary element method
  - Boundary element method
  - Acceleration by adaptive cross approximation
  - Parallel implementation
  - Numerical results
  - General setting
- DDM by Bramble, Pasciak, and Schatz
- BETI for contact problems

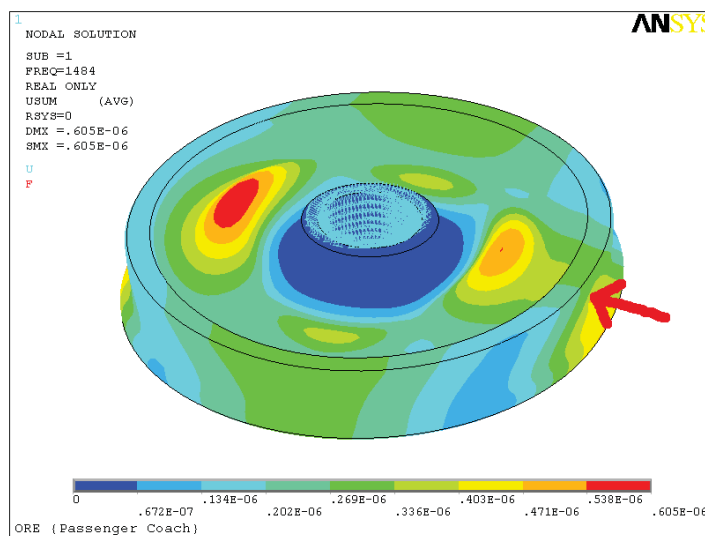
# Parallel BEM–Based Methods

## Outline

- Motivation: Acoustic scattering from a railway wheel
- Parallel fast boundary element method
  - Boundary element method
  - Acceleration by adaptive cross approximation
  - Parallel implementation
  - Numerical results
  - General setting
- DDM by Bramble, Pasciak, and Schatz
- BETI for contact problems

## Motivation: Acoustic scattering from a railway wheel

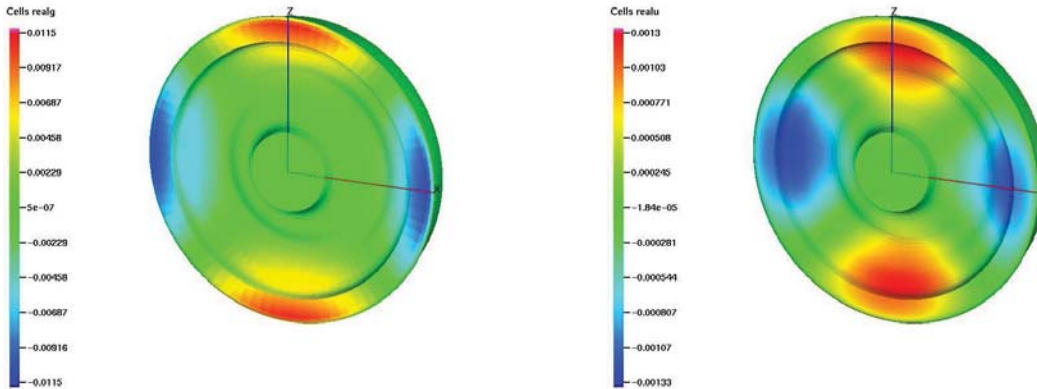
The goal: Acoustic noise elimination by profiling



a joint work with Jan Szweda, Dep. of Mechanics, VŠB-TU Ostrava

## Motivation: Acoustic scattering from a railway wheel

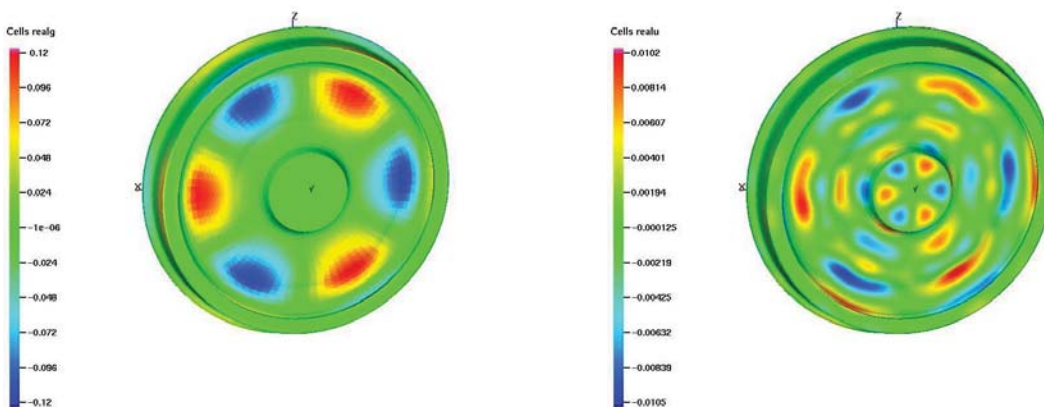
Numerical simulation on a single proc.: velocity, pressure at 341 Hz



15112 triangles, 22668 nodes,  
ACA-E assembling of  $\mathbf{K}_k$  (compr. to 12%) in 25 min, of  $\mathbf{D}_k$  (15%) in 40 min,  
142 GMRES iters. in 223 s

## Motivation: Acoustic scattering from a railway wheel

Numerical simulation on a single proc.: velocity, pressure at 2706 Hz



15112 triangles, 22668 nodes,  
ACA-E assembling of  $\mathbf{K}_k$  (compr. to 12%) in 25 min, of  $\mathbf{D}_k$  (15%) in 50 min,  
700 GMRES iters.

# Parallel BEM–Based Methods

## Outline

- Motivation: Acoustic scattering from a railway wheel
- Parallel fast boundary element method
  - Boundary element method
  - Acceleration by adaptive cross approximation
  - Parallel implementation
  - Numerical results
  - General setting
- DDM by Bramble, Pasciak, and Schatz
- BETI for contact problems

## Boundary element method

### Interior Dirichlet Laplace problem

$$\begin{aligned} -\Delta u(\mathbf{x}) &= 0, & \mathbf{x} \in \Omega \subset \mathbb{R}^3, \\ u(\mathbf{x}) &= g(\mathbf{x}), & \mathbf{x} \in \Gamma := \partial\Omega. \end{aligned}$$

### Boundary integral formulation

$$\mathbf{x} \in \Omega : \quad u(\mathbf{x}) := \int_{\Gamma} w(\mathbf{y}) \frac{1}{4\pi|\mathbf{x}-\mathbf{y}|} dS(\mathbf{y}) =: (Vw)(\mathbf{x})$$

Under some regularity assumptions,  $(Vw)(\mathbf{x})$  is continuous along  $\Gamma$ , which leads us to the (less understood) collocation method: Find  $w(\mathbf{y})$  such that

$$(Vw)(\mathbf{x}) = g(\mathbf{x}) \text{ on } \Gamma,$$

or to the well-posed Galerkin boundary integral method:

$$\text{Find } w(\mathbf{y}) \in W : \quad \langle Vw, z \rangle_{\Gamma} = \langle g, z \rangle_{\Gamma} \quad \forall z \in W,$$

where  $\langle f, z \rangle_{\Gamma} := \int_{\Gamma} f(\mathbf{x})z(\mathbf{x}) dS(\mathbf{x})$  and  $W := H^{-1/2}(\Gamma)$ .

# Boundary element method

## Boundary element method (BEM)

Triangulate the boundary  $\Gamma = \cup_{j=1}^n \overline{\gamma_j}$  and approximate  $H^{-1/2}(\Gamma)$  by piecewise constant base  $\Psi_j(\mathbf{x})$  along the triangulation. Find  $w_h(\mathbf{x}) := \sum_{j=1}^n w_j \Psi_j(\mathbf{x})$ :

$$\mathbf{A}\mathbf{w} = \mathbf{b},$$

where  $a_{ij} := \int_{\gamma_i} \int_{\gamma_j} \frac{1}{4\pi|\mathbf{x}-\mathbf{y}|} dS(\mathbf{y}) dS(\mathbf{x})$ ,  $b_i := \int_{\gamma_i} g(\mathbf{x}) dS(\mathbf{x})$ . The approximate solution then reads

$$\mathbf{x} \in \overline{\Omega} : u_h(\mathbf{x}) = \sum_{j=1}^n w_j \int_{\gamma_j} \frac{1}{4\pi|\mathbf{x}-\mathbf{y}|} dS(\mathbf{y}).$$

## Comparison to FEM

- + exterior problems: radiation conditions in the ansatz,
- + problem dimension reduced,
- expensive evaluation of singular integrals
- densely populated matrices.

# Parallel BEM–Based Methods

## Outline

- Motivation: Acoustic scattering from a railway wheel
- Parallel fast boundary element method
  - Boundary element method
  - Acceleration by adaptive cross approximation
  - Parallel implementation
  - Numerical results
  - General setting
- DDM by Bramble, Pasciak, and Schatz
- BETI for contact problems



## Acceleration by adaptive cross approximation

### Cluster geometric bisection

$C := \{\gamma_1^C, \dots, \gamma_n^C\}$  ... cluster of elements from discretization  $\{\gamma_1, \dots, \gamma_n\}$  of  $\Gamma$ ,

$\mathbf{x}^C := \frac{1}{\sum_k |\gamma_k^C|} \sum_k |\gamma_k^C| \mathbf{x}_k^C$  ... cluster centroid, where  $\mathbf{x}_k^C$  is the centroid of  $\gamma_k^C$ ,

$\mathbf{C}^C := \sum_k |\gamma_k^C| (\mathbf{x}_k^C - \mathbf{x}^C) \cdot (\mathbf{x}_k^C - \mathbf{x}^C)^T$  ... cluster covariance matrix,

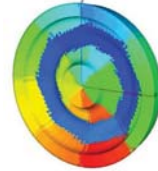
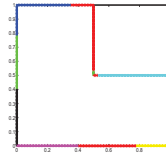
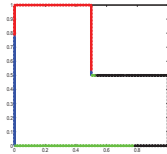
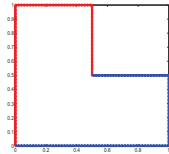
$\mathbf{n}^C$  ... a dominant eigenvector of  $\mathbf{C}^C$ .

The cluster is cutted into two subclusters by the plane  $(\mathbf{x} - \mathbf{x}^C) \cdot \mathbf{n}^C = 0$  as follows:

$C_1 := \{\gamma_k \in C : (\mathbf{x}_k^C - \mathbf{x}^C) \cdot \mathbf{n}^C \geq 0\}$  ... first subcluster,

$C_2 := \{\gamma_k \in C : (\mathbf{x}_k^C - \mathbf{x}^C) \cdot \mathbf{n}^C < 0\}$  ... second subcluster.

METIS could be an alternative.



## Acceleration by adaptive cross approximation

### Admissible pairs of clusters (quadratic complexity)

$$\min\{\text{diam } C_x, \text{diam } C_y\} \leq \eta \text{dist}(C_x, C_y), \quad \eta \in (0, 1)$$

### Stronger admissibility criterion (linear complexity)

$$\begin{aligned} \min\{\text{diam } C_x, \text{diam } C_y\} &\leq \\ 2 \min\{\text{rad } C_x, \text{rad } C_y\} &\leq \eta (|\mathbf{x}^{C_x} - \mathbf{x}^{C_y}| - \text{rad } C_x - \text{rad } C_y) \\ &\leq \eta \text{dist}(C_x, C_y), \end{aligned}$$

where  $\text{rad } C := \max_k |\mathbf{x}_k^C - \mathbf{x}^C|$ .

### Quad-tree of cluster pairs

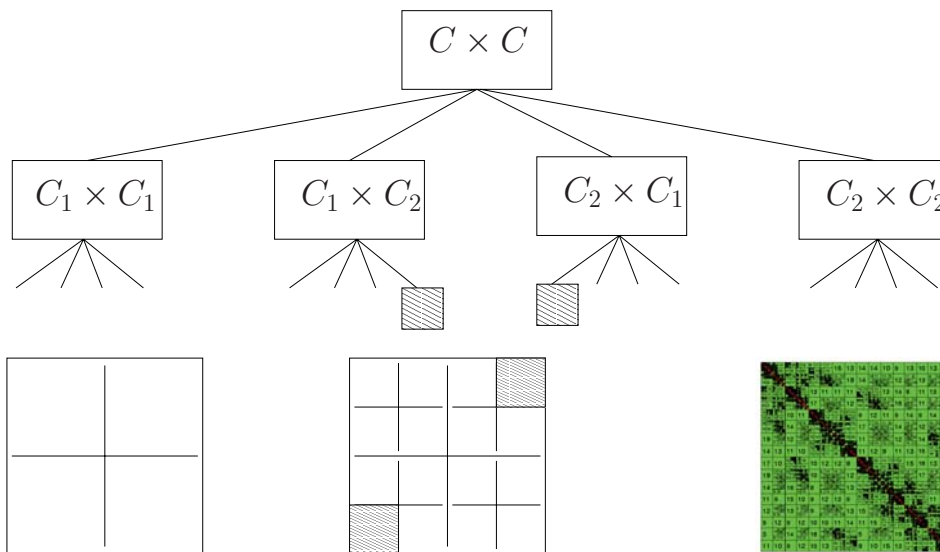
$(\{\gamma_1, \dots, \gamma_m\}, \{\gamma_1, \dots, \gamma_m\})$  is the root.

Leaves  $(C, D)$  are either admissible or  $\min\{n^C, n^D\} \leq n_{\min}$ .

Nonleaves  $(C, D)$  has four sons  $(C_1, D_1)$ ,  $(C_1, D_2)$ ,  $(C_2, D_1)$ , and  $(C_2, D_2)$ .

## Acceleration by adaptive cross approximation

Quad-tree of cluster pairs,  $\mathcal{H}$ -matrices



Nonadmissible blocks assembled as full, admissible approximated by low-rank matrices.

## Acceleration by adaptive cross approximation

Compression by singular value decomposition (SVD)

$$\mathbf{A} = \sum_{i=1}^{r:=\text{rank } \mathbf{A}} \sigma_i \mathbf{u}_i \mathbf{v}_i^T \approx \sum_{i=1}^k \sigma_i \mathbf{u}_i \mathbf{v}_i^T =: \mathbf{A}_k, \text{ where } k < r,$$

$\sigma_1 \geq \sigma_2 \geq \dots \sigma_r \geq 0 \dots$  singular values,

$(\mathbf{u}_1, \dots, \mathbf{u}_r)$  ... an orthogonal system of left singular vectors,

$(\mathbf{v}_1, \dots, \mathbf{v}_r)$  ... an orthogonal system of right singular vectors.

SVD gives the best approximation in the spectral (operator) norm:

$$\mathbf{A}_k = \arg \min_{\mathbf{M}: \text{rank } \mathbf{M} = k} \|\mathbf{A} - \mathbf{M}\|.$$

The best compression, but worse than quadratic computational complexity  $O(mnr)$ .

## Acceleration by adaptive cross approximation

### Asymptotically smooth functions

Assume  $(\mathbf{A})_{i,j} := f(\mathbf{x}_i, \mathbf{y}_j)$ , where  $\mathbf{x}_i \in C_x$ ,  $\mathbf{y}_j \in C_y$ ,  $C_x, C_y \subset \mathbb{R}^d$ .  
 $f : C_x \times C_y \rightarrow \mathbb{R}$  is asymptotically smooth if

$$\exists c_1, c_2 > 0 \exists g \leq 0 \forall \alpha \in \mathbb{N}_0^d : |\partial_{\mathbf{x}}^\alpha f(\mathbf{x}, \mathbf{y})|, |\partial_{\mathbf{y}}^\alpha f(\mathbf{x}, \mathbf{y})| \leq c_1 p! (c_2)^p |\mathbf{x} - \mathbf{y}|^{g-p}, \quad p = |\alpha|.$$

### Compression by Taylor expansion

Provided  $\text{diam } C_y \leq \text{diam } C_x$ ,  $dc_2\eta < 1$ , choose  $\mathbf{y}_0 \in C_y$  about which we expand  $f$ :

$$\mathbf{x} \in C_x, \mathbf{y} \in C_y : f(\mathbf{x}, \mathbf{y}) = \sum_{k=0}^{p-1} \frac{1}{k!} ((\mathbf{y} - \mathbf{y}_0) \partial_{\mathbf{y}} f(\mathbf{x}, \mathbf{y}_0))^k + R_p(\mathbf{x}, \mathbf{y}),$$

where

$$\begin{aligned} |R_p(\mathbf{x}, \mathbf{y})| &= \frac{1}{p!} |(\mathbf{y} - \mathbf{y}_0) \partial_{\mathbf{y}} f(\mathbf{x}, \tilde{\mathbf{y}})|^p \leq \frac{1}{p!} d^p |\mathbf{y} - \mathbf{y}_0|^p c_1 p! (c_2)^p |\mathbf{x} - \tilde{\mathbf{y}}|^{g-p} \\ &\leq c_1 d^p c_2^p \frac{\text{diam}^p C_y}{\text{dist}^p(C_x, C_y)} \text{dist}^g(C_x, C_y) \leq c_1 (dc_2\eta)^p \text{dist}^g(C_x, C_y) \rightarrow 0 \text{ as } p \rightarrow \infty. \end{aligned}$$

## Acceleration by adaptive cross approximation

### Adaptive cross approximation (ACA)

$$\begin{aligned} \mathbf{P}_{C_x} \mathbf{A} \mathbf{P}_{C_y}^T &=: \begin{pmatrix} \tilde{\mathbf{A}}_{11} & \tilde{\mathbf{A}}_{12} \\ \tilde{\mathbf{A}}_{21} & \tilde{\mathbf{A}}_{22} \end{pmatrix} \approx \begin{pmatrix} \tilde{\mathbf{A}}_{11} & \tilde{\mathbf{A}}_{12} & & \\ \tilde{\mathbf{A}}_{21} & \tilde{\mathbf{A}}_{21} & \tilde{\mathbf{A}}_{11}^{-1} & \tilde{\mathbf{A}}_{12} \end{pmatrix} = \begin{pmatrix} \tilde{\mathbf{A}}_{11} \\ \tilde{\mathbf{A}}_{21} \end{pmatrix} \left[ \tilde{\mathbf{A}}_{11}^{-1} \begin{pmatrix} \tilde{\mathbf{A}}_{11} & \tilde{\mathbf{A}}_{12} \end{pmatrix} \right] \\ &=: (\mathbf{u}_1, \dots, \mathbf{u}_r) (\mathbf{v}_1, \dots, \mathbf{v}_r)^T. \end{aligned}$$

The rank  $r := r(\varepsilon)$ , where  $\tilde{\mathbf{A}}_{11} \in \mathbb{C}^{r \times r}$ , is adaptively controlled by  $\varepsilon$  as follows:

$$\|\mathbf{u}_{k+1}\|_2 \|\mathbf{v}_{k+1}\|_2 \leq \frac{\varepsilon(1-\eta)}{1+\varepsilon} \|\mathbf{A}_k\|_F, \quad \text{where } \mathbf{A}_k := \sum_{m=1}^k \mathbf{u}_m \mathbf{v}_m^T$$

which implies, provided  $\|\mathbf{R}_{k+1}\|_F \leq \eta \|\mathbf{R}_k\|_F$ , that  $\frac{\|\mathbf{R}_k\|_F}{\|\mathbf{A}\|_F} \leq \varepsilon$ , where  $\mathbf{R}_k := \mathbf{A} - \mathbf{A}_k$ .

The pivots, stored in  $\mathbf{P}_{C_x}$ ,  $\mathbf{P}_{C_y}$ , are chosen as to maximize  $|\det \tilde{\mathbf{A}}_{11}^k|$  with a wish to minimize  $\|\mathbf{R}_k\| \equiv \|\tilde{\mathbf{A}}_{22}^k - \tilde{\mathbf{A}}_{21}^k (\tilde{\mathbf{A}}_{11}^k)^{-1} \tilde{\mathbf{A}}_{12}^k\|$ .

## Acceleration by adaptive cross approximation

ACA algorithm: an example ( $\mathbf{R}_0 := \mathbf{A}$ )

$$\begin{aligned}
 \mathbf{R}_0 &= \begin{pmatrix} 0.431 & 0.354 & 0.582 & 0.417 \\ 0.491 & 0.396 & 0.674 & 0.449 \\ 0.446 & 0.358 & 0.583 & 0.413 \\ 0.380 & 0.328 & 0.557 & 0.372 \end{pmatrix} \xrightarrow[R=\{1\}]{i_1=1, j_1=3} \frac{1}{0.582} \begin{pmatrix} 0.582 \\ 0.674 \\ 0.583 \\ 0.557 \end{pmatrix} (0.431, 0.354, 0.582, 0.417) \\
 \mathbf{R}_1 &= \begin{pmatrix} 0 & 0 & 0 & 0 \\ -0.008 & -0.014 & 0 & -0.034 \\ 0.014 & 0.003 & 0 & -0.005 \\ -0.033 & -0.011 & 0 & -0.027 \end{pmatrix} \xrightarrow[R=\{1,2\}]{i_1=2, j_1=4} \frac{1}{-0.034} \begin{pmatrix} 0 \\ -0.034 \\ -0.005 \\ -0.027 \end{pmatrix} (-0.008, -0.014, 0, -0.034) \\
 \mathbf{R}_2 &= \begin{pmatrix} 0 & 0 & 0 & 0 \\ 0 & 0 & 0 & 0 \\ 0.015 & 0.005 & 0 & 0 \\ -0.026 & 0.0004 & 0 & 0 \end{pmatrix} \xrightarrow[R=\{1,2,4\}]{i_1=4, j_1=1} \frac{1}{-0.026} \begin{pmatrix} 0 \\ 0 \\ 0.015 \\ -0.026 \end{pmatrix} (-0.026, 0.0004, 0, 0)
 \end{aligned}$$

The relative error decays as follows:  $\|\mathbf{R}_k\|_2 / \|\mathbf{A}\|_2 = 0.030, 0.016, 0.003$  for  $k = 1, 2, 3$

## Parallel BEM–Based Methods

### Outline

- Motivation: Acoustic scattering from a railway wheel
- Parallel fast boundary element method
  - Boundary element method
  - Acceleration by adaptive cross approximation
  - Parallel implementation
  - Numerical results
  - General setting
- DDM by Bramble, Pasciak, and Schatz
- BETI for contact problems

## Parallel implementation

### Master–slave model

$N$  processes, one of which is master, each stores all the nodes and triangles.

Reset sets of adm./nonadm. indices:  $\mathcal{A}_p := \emptyset$ ,  $\mathcal{N}_p := \emptyset$  for  $p = 1, 2, \dots, N$ .

Master sorts  $\mathbf{A}_i^{\text{adm}} \in \mathbb{R}^{m_i^{\text{adm}} \times n_i^{\text{adm}}}$  s.t.  $w_i^{\text{adm}} := m_i^{\text{adm}} + n_i^{\text{adm}}$

and distributes the indices to all processes so that  $\mathcal{A}_k := \mathcal{A}_k \cup \{i\}$  with

$$k := \operatorname{argmin}_{l=1,\dots,N} \sum_{j \in \mathcal{A}_l} w_j^{\text{adm}}.$$

Master sorts  $\mathbf{A}_i^{\text{non}} \in \mathbb{R}^{m_i^{\text{non}} \times n_i^{\text{non}}}$  w.r.t. weights  $w_i^{\text{non}} := m_i^{\text{non}} n_i^{\text{non}}$

and distributes the indices to all processes so that  $\mathcal{N}_k := \mathcal{N}_k \cup \{i\}$  with

$$k := \operatorname{argmin}_{l=1,\dots,N} \sum_{j \in \mathcal{N}_l} w_j^{\text{non}}.$$

Processes assemble in parallel all their admissible and nonadmissible blocks.

$$\mathbf{A} \mathbf{v} = \sum_{p=1}^N \left( \sum_{j \in \mathcal{A}_p} \mathbf{I}_j^{\text{adm}} \mathbf{U}_j^{\text{adm}} \mathbf{V}_j^{\text{adm}} \mathbf{v}_{J_j^{\text{adm}}} + \sum_{j \in \mathcal{N}_p} \mathbf{I}_j^{\text{non}} \mathbf{A}_j^{\text{non}} \mathbf{v}_{J_j^{\text{non}}} \right)$$

## Parallel BEM–Based Methods

### Outline

- Motivation: Acoustic scattering from a railway wheel
- Parallel fast boundary element method
  - Boundary element method
  - Acceleration by adaptive cross approximation
  - Parallel implementation
  - Numerical results
  - General setting
- DDM by Bramble, Pasciak, and Schatz
- BETI for contact problems

## Numerical results

$$u(\mathbf{x}) := g(\mathbf{x}) := x_1 + x_2 + x_3, \Omega := \{\mathbf{x} : |\mathbf{x}| \leq 1\}$$

$n$	err.	compr. of $\mathbf{A}$	scheduling+assembling times of $\mathbf{A}$ [s]					
			$N := 2$	$N := 4$	$N := 8$	$N := 16$	$N := 32$	$N := 46$
40	3e-4	100%	0+0	0+0	0+0	0+0	0+0	0+0
160	2.3e-4	100%	0+0	0+0	0+0	0+0	0+0	0+0
640	9.5e-5	99%	0+4	0+2	0+1	0+0	0+1	0+0
2560	4.3e-5	65%	0+43	2+23	0+12	0+6	0+3	0+3
10240	2.1e-5	27%	2+282	1+143	1+72	1+35	1+19	0+13
40960	1.1e-5	10%	46+1572	24+792	15+399	17+201	20+102	21+72
163840	6.4e-6	3%	3041+8219	1457+4162	828+2084	492+1061	409+543	397+377

$$err. := \frac{\sqrt{\langle V(u - u_h), u - u_h \rangle_\Gamma}}{\sqrt{\langle Vu, u \rangle_\Gamma}}$$

Numerically as well as parallel scalable method:  $CPU = O\left(\frac{n \log n}{N}\right)$ ,  
but  $Mem = O(N n \log n)$ .

## Parallel BEM–Based Methods

### Outline

- Motivation: Acoustic scattering from a railway wheel
- Parallel fast boundary element method
  - Boundary element method
  - Acceleration by adaptive cross approximation
  - Parallel implementation
  - Numerical results
  - General setting
- DDM by Bramble, Pasciak, and Schatz
- BETI for contact problems

## General setting

### Particular solution approach

$$\begin{aligned} -\Delta u(\mathbf{x}) &= f(\mathbf{x}) \quad , \mathbf{x} \in \Omega, \\ u(\mathbf{x}) &= g(\mathbf{x}) \quad , \mathbf{x} \in \Gamma \end{aligned}$$

is replaced by

$$\begin{aligned} -\Delta u^{\text{H}}(\mathbf{x}) &= 0 \quad , \mathbf{x} \in \Omega, \\ u^{\text{H}}(\mathbf{x}) &= g(\mathbf{x}) - u^{\text{P}}(\mathbf{x}) \quad , \mathbf{x} \in \Gamma, \end{aligned}$$

where  $-\Delta u^{\text{P}}(\mathbf{x}) = f(\mathbf{x})$ ,  $u(\mathbf{x}) = u^{\text{H}}(\mathbf{x}) + u^{\text{P}}(\mathbf{x})$ .

### Interface problem: Piecewise homogeneous material $a_i > 0$

$$\begin{aligned} -\operatorname{div}(a_i \nabla u_i(\mathbf{x})) &= f_i(\mathbf{x}) \quad , \mathbf{x} \in \Omega_i, \\ u_i(\mathbf{x}) &= g(\mathbf{x}) \quad , \mathbf{x} \in \partial\Omega_i \cap \Gamma, \\ u_i(\mathbf{x}) - u_j(\mathbf{x}) &= 0 \quad , \mathbf{x} \in \Gamma_{ij} := \partial\Omega_i \cap \partial\Omega_j \neq \emptyset, \\ a_i \frac{\partial u_i(\mathbf{x})}{\partial n} - a_j \frac{\partial u_j(\mathbf{x})}{\partial n} &= 0 \quad , \mathbf{x} \in \Gamma_{ij} \end{aligned}$$

The transmission conditions are formulated by means of boundary integral equations.

## Parallel BEM–Based Methods

### Outline

- Motivation: Acoustic scattering from a railway wheel
- Parallel fast boundary element method
  - Boundary element method
  - Acceleration by adaptive cross approximation
  - Parallel implementation
  - Numerical results
  - General setting
- DDM by Bramble, Pasciak, and Schatz
- BETI for contact problems

## DDM by Bramble, Pasciak, and Schatz '86

### Nonoverlapping domain decomposition

$$\bar{\Omega} = \bigcup_{i=1}^N \bar{\Omega}_i, \quad \Omega_i \cap \Omega_j = \emptyset \text{ for } i \neq j$$

leads to the interface problem

$$\begin{aligned} -\operatorname{div}(a_i \nabla u_i(\mathbf{x})) &= f_i(\mathbf{x}) \text{ in } \Omega_i, & u_i(\mathbf{x}) &= g(\mathbf{x}) \text{ on } \Gamma_i \cap \Gamma, \\ u_i(\mathbf{x}) - u_j(\mathbf{x}) &= 0 \text{ on } \Gamma_{ij}, & a_i \partial_n u_i(\mathbf{x}) - a_j \partial_n u_j(\mathbf{x}) &= 0 \text{ on } \Gamma_{ij}. \end{aligned}$$

### Preconditioner BPS I = particular solution + concept of corners

*Step 1.* Solve in parallel (by Multigrid-FEM):  $-\Delta u_i^P = f/a_i$  in  $\Omega_i$ ,  $u_i^P = 0$  on  $\Gamma_i$ .

*Step 2.* Solve interface problem for piecewise harmonic  $u^H(\mathbf{x})$  (by parallel ACA-BEM):

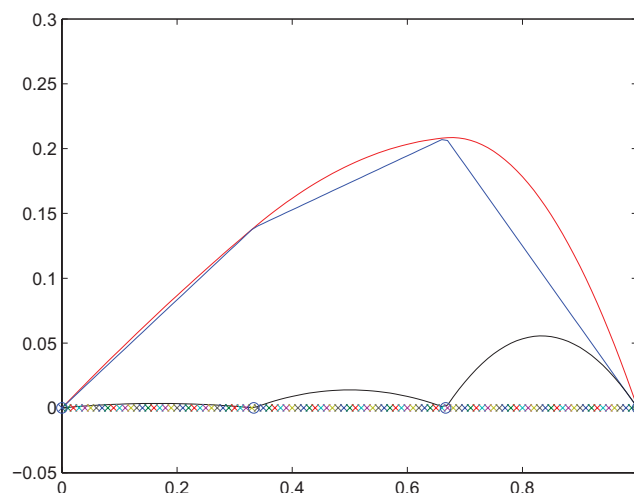
$$a_i \partial_n u_i^H - a_j \partial_n u_j^H = -(a_i \partial_n u_i^P - a_j \partial_n u_j^P) \text{ on } \Gamma_{ij}, \quad u^H = 0 \text{ on } \Gamma.$$

*Step 3.* Solve in parallel (by ACA-BEM):  $-\Delta u_i^H = 0$  in  $\Omega_i$ ,  $u_i^H = u^H$  on  $\Gamma_i$ .

Preconditioner BPS I introduces corners to decompose the interface  $\rightsquigarrow O(\log(H/h))$

## DDM by Bramble, Pasciak, and Schatz '86

$$u(\mathbf{x}) = u^H(\mathbf{x}) + u^P(\mathbf{x})$$



where  $\Omega_1 := (0, 1/3)$ ,  $\Omega_2 := (1/3, 2/3)$ ,  $\Omega_3 := (2/3, 1)$ ,  $a_1 := f_3(\mathbf{x}) := 4$ ,  $a_2 := f_2(\mathbf{x}) := 2$ ,  $a_3 := f_1(\mathbf{x}) := 1$ .



# DDM by Bramble, Pasciak, and Schatz '86

## Algebraic point of view of the FEM version

$$\mathbf{A}\mathbf{u} = \mathbf{b}$$

$I_i \dots$  interior DOFs of  $\Omega_i$ ,  $I_s \dots$  DOFs along the skeleton

$$\begin{pmatrix} \mathbf{A}_{I_1, I_1} & \mathbf{0} & \dots & \mathbf{0} & \mathbf{A}_{I_1, I_s} \\ \mathbf{0} & \mathbf{A}_{I_2, I_2} & \dots & \mathbf{0} & \mathbf{A}_{I_2, I_s} \\ \vdots & \vdots & \ddots & \vdots & \vdots \\ \mathbf{0} & \mathbf{0} & \dots & \mathbf{A}_{I_N, I_N} & \mathbf{A}_{I_N, I_s} \\ \mathbf{A}_{I_s, I_1} & \mathbf{A}_{I_s, I_2} & \dots & \mathbf{A}_{I_s, I_N} & \mathbf{A}_{I_s, I_s} \end{pmatrix} \begin{pmatrix} \mathbf{u}_{I_1}^H + \mathbf{u}_{I_1}^P \\ \mathbf{u}_{I_2}^H + \mathbf{u}_{I_2}^P \\ \vdots \\ \mathbf{u}_{I_N}^H + \mathbf{u}_{I_N}^P \\ \mathbf{u}_{I_s}^H \end{pmatrix} = \begin{pmatrix} \mathbf{b}_{I_1} \\ \mathbf{b}_{I_2} \\ \vdots \\ \mathbf{b}_{I_N} \\ \mathbf{b}_{I_s} \end{pmatrix}$$

leads to

*Step 1.*  $\mathbf{A}_{I_i, I_i} \mathbf{u}_{I_i}^P = \mathbf{b}_{I_i}$

*Step 2.*  $\mathbf{S} \mathbf{u}_{I_s}^H = \mathbf{c}$  with  $\mathbf{S} := \mathbf{A}_{I_s, I_s} - \sum_{i=1}^N \mathbf{A}_{I_s, I_i} \mathbf{A}_{I_i, I_i}^{-1} \mathbf{A}_{I_i, I_s}$ ,  $\mathbf{c} := -\sum_{i=1}^N \mathbf{A}_{I_s, I_i} \mathbf{u}_{I_i}^P$

*Step 3.*  $\mathbf{A}_{I_i, I_i} \mathbf{u}_{I_i}^H = -\mathbf{A}_{I_i, I_s} \mathbf{u}_{I_s}^H$

## Parallel BEM–Based Methods

### Outline

- Motivation: Acoustic scattering from a railway wheel
- Parallel fast boundary element method
  - Boundary element method
  - Acceleration by adaptive cross approximation
  - Parallel implementation
  - Numerical results
  - General setting
- DDM by Bramble, Pasciak, and Schatz
- BETI for contact problems

# Boundary Element Tearing and Interconnecting (BETI)

Linear case: FETI [Farhat, Roux '91], BETI [Langer, Steinbach '03]

Nonoverlapping DDM with doubled DOFs along the interface, a variant of BPS I.

Step 1.  $u^P(\mathbf{x})$  is a FEM/BEM solution to the local Neumann problems:

$$-\Delta u_i^P = f/a_i, \text{ in } \Omega_i, \quad \partial_n u_i = 0 \text{ on } \Gamma_i \quad \rightsquigarrow \quad u^P = K^+(f/a_i)$$

Step 2.  $u^H(\mathbf{x})$  is represented by Lagrange multipliers  $\lambda \in H^{-1/2}(\cup_i \Gamma_i)$ :

$$\lambda \equiv \partial_n u^H,$$

which leads to the Schur complement system with  $S := BK^+B^T$ .

Step 3. ...

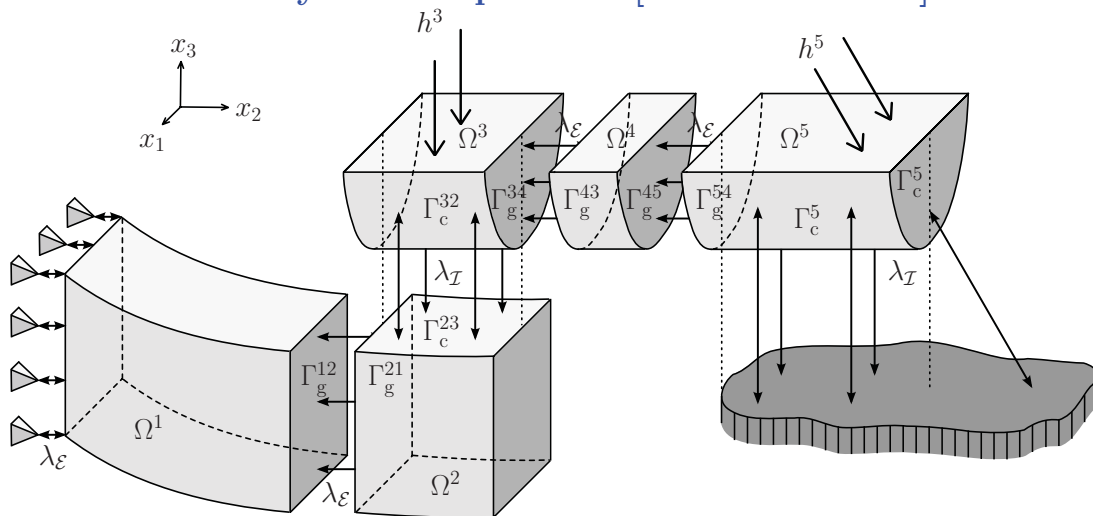
Dirichlet preconditioner [Mandel, Tezaur '96]

$S$  is preconditioned by  $\widehat{S}^{-1} := (1/2)BK_0^{-1}(1/2)B^T$ ,

where  $K_0^{-1}$  solves the local Dirichlet problems, i.e. Step 1 of BPS I.

## BETI for contact problems

TBETI for multi-body contact problem [Sadowská et al.]



In the dual the linearized nonpenetration condition translates to a simple bound  $\rightsquigarrow$

FETI/BETI  $\otimes$  MPRGP [Dostál, Schöberl '05]

# Parallel BEM–Based Methods

## References

- Steinbach, Rjasanow, Springer, 2007.
- Bebendorf, Grzhibovskis, *Math. Method. Appl. Sci.* 29:1721–1747, 2006.
- Bebendorf, Springer, 2008.
- Bramble, Pasciak, Schatz, *Math. Comp.* 47:103–134, 1986.
- Farhat, Roux, *Internat. J. Numer. Meths. Engrg.* 32:1205–1227, 1991.
- Mandel, Tezaur, *Numer. Math.* 73:473–487, 1996.
- Langer, Steinbach, *Computing* 71:205–228, 2003.
- Dostál, Schöberl, *Comput. Optim. Appl.* 30:23–44, 2005.
- Sadowská, Bouchala, Kozubek, Markopoulos, Brzobohatý, ...

# Applications of functional a posteriori error estimates to some mechanical problems

Jan Valdman

School of Engineering and Natural Sciences  
University of Iceland, Reykjavik  
email: jan.valdman@gmail.com

Ostrava, December 1-3, 2010

## Outline

- 1 Functional a posteriori error estimate for Poisson problem
- 2 Functional a posteriori error estimate for problems with nonlinear BC
- 3 Functional a posteriori error estimate for Barenblatt-Biot model
- 4 Flows in porous media
- 5 Functional a posteriori error estimate for elastoplasticity

## Literature on functional a posteriori error estimates

Theory on functional a posteriori error estimates is explained in books:

Pekka Neittaanmäki and Sergey Repin, *Reliable methods for computer simulation, Error control and a posteriori estimates*, Elsevier, New York, 2004.

Sergey Repin, *A Posteriori Estimates for Partial Differential Equations* Radon Series on Computational and Applied Mathematics, de Gruyter, 2008

Explaining papers to theory and numerics to this course:

- 1 Sergey Repin, Jan Valdman, Functional a posteriori error estimates for problems with nonlinear boundary conditions. *Journal of Numerical Mathematics* 16, No. 1, 51-81 (2008)
- 2 Jan Valdman, Minimization of Functional Majorant in A Posteriori Error Analysis based on  $H(\text{div})$  Multigrid-Preconditioned CG Method. *Advances in Numerical Analysis*, vol. 2009, Article ID 164519 (2009)
- 3 Sergey Repin, Jan Valdman, Functional a posteriori error estimates for incremental models in elasto-plasticity. *Cent. Eur. J. Math.* 7, No. 3, 506-519 (2009)
- 4 Jan Martin Nordbotten, Talal Rahman, Sergey Repin, Jan Valdman, A posteriori error estimates for approximate solutions of Barenblatt-Biot poroelastic model. *Computational Methods in Applied Mathematics* 10, No. 3, 302-315 (2010)
- 5 P. Neittaanmäki, S. I. Repin and J. Valdman, Functional a posteriori error estimates for elasticity problems with nonlinear boundary conditions. (in preparation)

## Aposteriori error estimates

### Primal problem

$$\Delta u + f = 0 \quad \text{in } \Omega, \quad u = 0 \quad \text{on } \partial\Omega$$

Let us assume that  $v$  is (numerical) approximation of  $u$ . Then it holds

### Estimate of Runge

$$\|\nabla(u - v)\|_{\Omega} \leq \|\nabla v - y^*\|_{\Omega},$$

for  $y^* \in H(\Omega, \text{div})$  satisfying

$$\text{div} y^* + f = 0 \quad \text{in } \Omega.$$

## Aposteriori error estimates

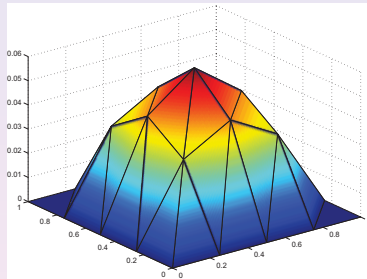
### Estimate of Repin

$$\|\nabla(u - v)\|_{\Omega} \leq \|\nabla v - y^*\|_{\Omega} + C_{\Omega} \|\text{div} y^* + f\|_{\Omega}$$

for  $y^* \in H(\Omega, \text{div})$ .  $C_{\Omega}$  is the constant in the Friedrichs' inequality

$$\|w\|_{\Omega} \leq C_{\Omega} \|\nabla w\|_{\Omega} \quad \forall w \in H_0^1(\Omega).$$

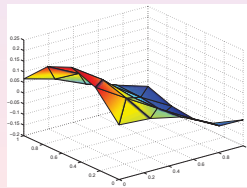
## Example: $f(x, y) = 2x(1 - x) + 2y(1 - y)$



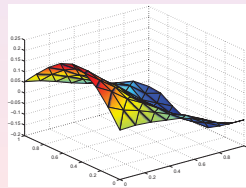
discrete solution  $v$  on coarse mesh compared to the exact solution

$$u = x(1 - x)y(1 - y)$$

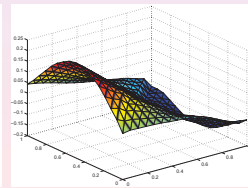
$$\text{exact error}^2 = 1.62\text{e-}03$$



$$\text{majorant} = 3.08\text{e-}03$$



$$\text{majorant} = 2.56\text{e-}03$$



$$\text{majorant} = 2.27\text{e-}03$$

## Majorant minimization problem

We have

$$\begin{aligned} & \|\nabla v - y^*\| + C_\Omega \|\text{div} y^* + f\| \\ & \leq [(1 + \beta)\|\nabla v - y^*\|^2 + (1 + \frac{1}{\beta})C_\Omega^2 \|\text{div} y^* + f\|^2]^{1/2} \end{aligned}$$

for some  $\beta > 0$ . Therefore

### Majorant minimization problem

Given  $v \in H_0^1(\Omega)$  and  $\beta > 0$ , find the minimizer  $y^* \in H(\Omega, \text{div})$  of

$$\mathcal{M}(v, y^*, \beta) := (1 + \beta)\|\nabla v - y^*\|^2 + (1 + \frac{1}{\beta})C_\Omega^2 \|\text{div} y^* + f\|^2 \rightarrow \min$$

## Majorant minimization

The minimization of the right hand side (majorant)

$$(1 + \beta) \|\nabla v - y^*\|^2 + (1 + \frac{1}{\beta}) C_{\Omega}^2 \|\operatorname{div} y^* + f\|^2 \rightarrow \min$$

leads to the linear system for the discrete solution  $y^*$ :

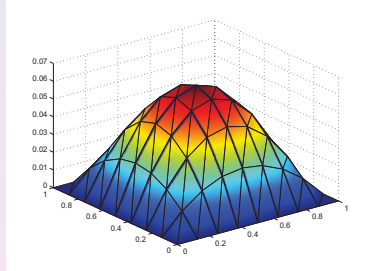
$$\left[ (1 + \beta)M + (1 + \frac{1}{\beta})C_{\Omega}^2 \operatorname{DIV} \operatorname{DIV} \right] y^* = (1 + \beta)l_1 - (1 + \frac{1}{\beta})C_{\Omega}^2 l_2,$$

where matrices  $M, \operatorname{DIV} \operatorname{DIV}$  represent the "mass" matrix and "divdiv" matrix defined by the equalities:

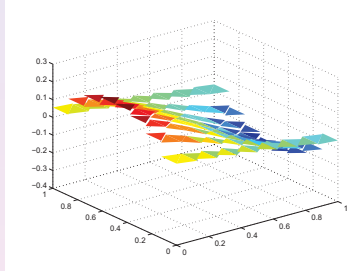
$$\int_{\Omega} uv \, dx = u^T M v, \quad \int_{\Omega} \operatorname{div} u \operatorname{div} v \, dx = u^T \operatorname{DIV} \operatorname{DIV} v$$

$$(l_1)^T y^* = (\nabla v, y^*), \quad (l_2)^T y^* = (f, \operatorname{div} y^*).$$

error<sup>2</sup>=3.24e-03



majorant=9.05e-03

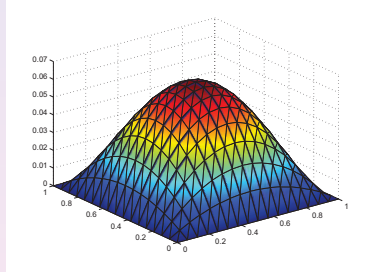


$$\mathcal{T}_2 : l_{\text{eff}} = 1.67$$

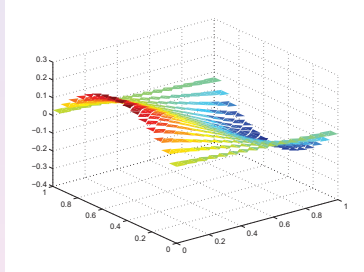
Figure: Discrete solution  $v$  (left) and  $y$ -component of the flux  $y$  (right).



error<sup>2</sup>=8.95e-04



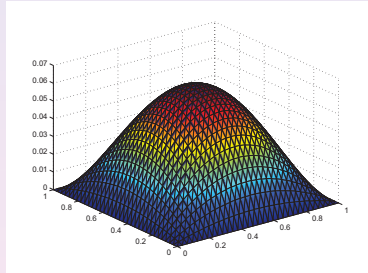
majorant=2.63e-03



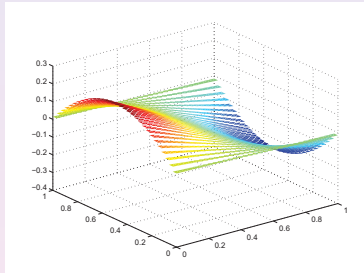
$$\mathcal{T}_3 : l_{eff} = 1.71$$

Figure: Discrete solution  $v$  (left) and  $y$ -component of the flux  $y$  (right).

error<sup>2</sup>=2.29e-04

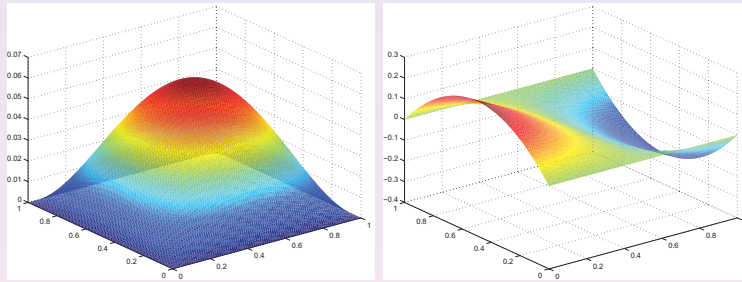


majorant=6.85e-04



$$\mathcal{T}_4 : l_{eff} = 1.72$$

Figure: Discrete solution  $v$  (left) and  $y$ -component of the flux  $y$  (right).



$\mathcal{T}_\infty$

Figure: Exact solution  $v$  (left) and  $y$ -component of the exact flux  $y$  (right).

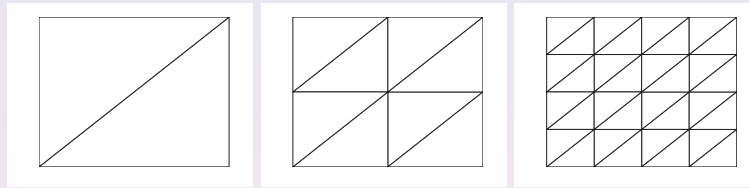
## Computational efficiency for Raviart-Thomas (RT0) elements

System matrix:  $(1 + \beta)M + (1 + \frac{1}{\beta})C_\Omega^2 DIVDIV$ ,  
 here  $\beta = 1$  for all levels.

problem size	without preconditioner	multigrid preconditioner	time in seconds (without setup)
5	1	1	0.00
16	4	4	0.00
56	14	8	0.02
208	51	12	0.04
800	129	14	0.08
3136	264	15	0.24
12416	529	15	0.85
49408	1097	16	4.08
197120	2191	16	18.21
787456	4401	16	77.22

Table: Number of iterations of the CG method using no preconditioner or the multigrid (V cycles) preconditioner with the additive smoother of Arnold, Falk and Winther for 1 smoothing step, tolerance= $1e-8$ , Matlab!

## Size of the discrete solution and of the discrete flux

Figure: Refined meshes  $\mathcal{T}_0, \mathcal{T}_1, \mathcal{T}_2$ .

The discrete solution  $v$  is a piecewise linear nodal function (P1)  
degrees of freedom on  $\mathcal{T}_0, \mathcal{T}_1, \mathcal{T}_2$ : 4, 9, 25

The discrete flux  $y$  is a lowest order Raviart Thomas function (RT0)  
degrees of freedom on  $\mathcal{T}_0, \mathcal{T}_1, \mathcal{T}_2$ : 5, 16, 56

For fine triangulations it holds:  $\text{number of edges} = \text{number of nodes} \cdot 3$

## Papers

- Jan Valdman, Minimization of Functional Majorant in A Posteriori Error Analysis based on **H(div) Multigrid-Preconditioned CG** Method. Advances in Numerical Analysis, vol. 2009, Article ID 164519 (2009)

## Problem with nonlinear BC – Classical Formulation

### Minimization problem

$$\int_{\Omega} \left( \frac{1}{2} |\nabla v|^2 - f v \right) dx + \mu \int_{\Gamma_1} |v| d\Gamma \rightarrow \min$$

among all  $v \in U := \{v \in C^2(\Omega) \cap C^1(\Omega \cup \Gamma_1) \cap C^0(\Omega \cup \Gamma_0) : v|_{\Gamma_0} = 0\}$

Note that the variation leads to

### Friction boundary condition

$$|u| \frac{\partial u}{\partial n} + \mu u = 0 \quad \text{on } \Gamma_1$$

## Problem with nonlinear bc – Classical Formulation

### Friction boundary condition

$$|u| \frac{\partial u}{\partial n} + \mu u = 0 \quad \text{on } \Gamma_1$$

Three parameter cases in our numerical examples:

- 1  $\mu \rightarrow +\infty$  - it implies the homogeneous Dirichlet boundary condition  $u|_{\Gamma_1} = 0$ .
- 2  $\mu = 0$  - it implies the homogeneous Neumann boundary condition  $\frac{\partial u}{\partial n}|_{\Gamma_1} = 0$ .
- 3  $\mu \in (0, +\infty)$  - this is a typical friction boundary condition.

## Discrete solutions of the minimization problem

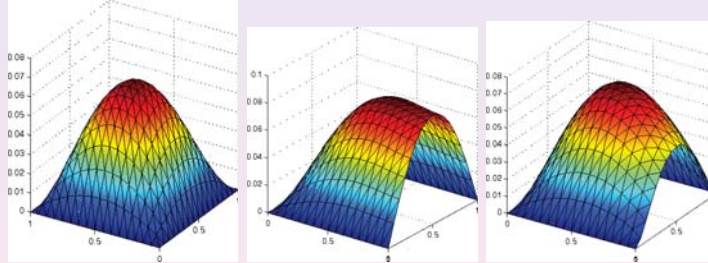


Figure:  $\mu \rightarrow \infty$  (left),  $\mu = 0$  (middle) and  $\mu = 0.1$  (right).

## Majorant estimate

Let  $u$  be an exact solution of the minimization problem and  $v$  its discrete approximation. Then it holds for all  $\alpha, \beta > 0$

Estimate

$$\frac{1}{2} \|v - u\|_a^2 \leq (1 + \beta) M_1(v, y^*) + \inf_{\xi^*} I_{\Gamma_1}(\gamma v, \delta_n y^*, \xi^*) + \frac{1}{2} \left(1 + \frac{1}{\beta}\right) (1 + \alpha) C_\Omega^2 \mathbf{R}_\Omega^2(y^*)$$

for arbitrary  $y^*$  function from the (flux) test space

$$Q_{\Gamma_1}^* := \{y^* \in Y^* \mid \operatorname{div} y^* \in L_2(\Omega), \delta_n y^* \in L_2(\Gamma_1)\} .$$

## Majorant estimate

Note that

$$M_1 = \frac{1}{2} \|\nabla v - y^*\|_{L^2(\Omega)}^2, \quad \mathbf{R}_Q(y^*) := \|\operatorname{div} y^* + f\|_{L^2(\Omega)},$$

and using the *compound functional* the boundary term is defined as

$$I_{\Gamma_1}(\gamma v, \delta_n y^*, \xi^*) := \int_{\Gamma_1} \left( j(\gamma v) + j^*(\xi^*) - (\gamma v) \xi^* + \frac{\theta}{2} |\delta_n y^* + \xi^*|^2 \right) d\Gamma,$$

where

$$\theta := \left(1 + \frac{1}{\beta}\right) \left(1 + \frac{1}{\alpha}\right) C_{\Gamma_1}^2, \quad j(\xi) = \mu|\xi|, \quad j^*(\xi^*) = \begin{cases} 0, & \text{if } |\xi^*| \leq \mu, \\ +\infty & \text{otherwise.} \end{cases}$$

## Estimate of the boundary term $\inf_{\xi^*} I_{\Gamma_1}(\gamma v, \delta_n y^*, \xi^*)$

Summary:

$$\inf_{\xi^*} I_{\Gamma_1}(\gamma v, \delta_n y^*, \xi^*) \leq \int_{\Gamma_1} (\mu|\gamma v| + \phi(\gamma v, \delta_n y^*, \mu)) d\Gamma,$$

where

$$\phi(\gamma v, \delta_n y^*, \mu) = \begin{cases} \frac{\theta}{2} (\delta_n y^* + \mu)^2 - \mu(\gamma v) & \text{if } \delta_n y^* < -\mu, \\ (-\delta_n y^*)(\gamma v) & \text{if } |\delta_n y^*| < \mu, \\ \frac{\theta}{2} (\delta_n y^* - \mu)^2 + \mu(\gamma v) & \text{if } \delta_n y^* > \mu. \end{cases}$$

Numerical results for  $\mu = 0.1$ 

N	majorant	error <sup>2</sup> /2	$l_{\text{eff}}$
25	2.9e-03	1.9e-03	1.22
81	9.0e-04	5.1e-04	1.33
289	2.7e-04	1.3e-04	1.44
1089	8.7e-05	3.3e-05	1.62
4225	2.8e-05	8.2e-06	1.87
16641	9.9e-06	1.9e-06	2.24
66049	3.9e-06	3.9e-07	3.17

Table: Majorant optimization on the same mesh.

Majorant optimized using an expensive nonlinear procedure  
- can be improved!

## Papers

S. Repin, J. Valdman, Functional A posteriori error estimates for problems with nonlinear boundary conditions, Journal of Numerical Mathematics 16 (2008), No. 1, 51-81.

## Extension to elasticity with nonlinear boundary conditions

### Friction boundary condition

Minimize the displacement  $v$  in the energy

$$\int_{\Omega} \left( \frac{1}{2} C \varepsilon(v) : \varepsilon(v) - f v \right) dx + k_{\tau} \int_{\Gamma_1} |v_{\tau}| d\Gamma$$

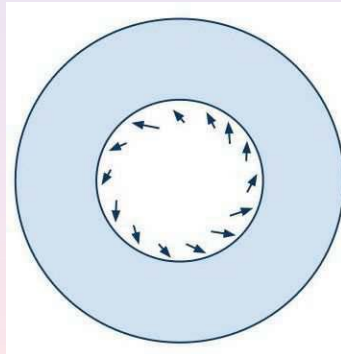
under the non-penetration condition

$$v_n = 0 \quad \text{on } \Gamma_1,$$

where  $v = (v_{\tau}, v_n)$  is decomposed in the normal and tangential components on the boundary  $\Gamma_1$ .

## Time dependent 2D symmetric problem in Matlab

polar coordinates:  $u = (u_r, u_{\phi})$



an inner radius  $a = 1$ ,  
 an outer radius  $b = 2$   
 friction parameter  $k_{\phi} = 0.02$   
 Lamé parameters  $\lambda = \mu = 1$

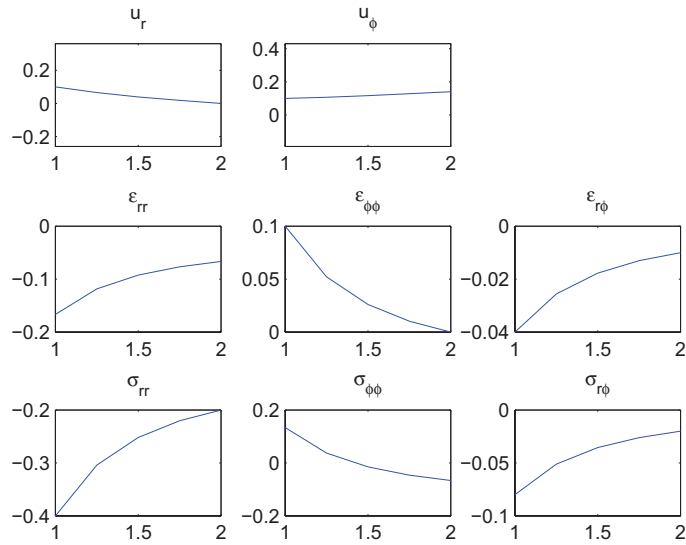
boundary conditions:

$$u_r(a) = u_{\phi}(a) = 0.1 \cos\left(\frac{t\pi}{20}\right)$$

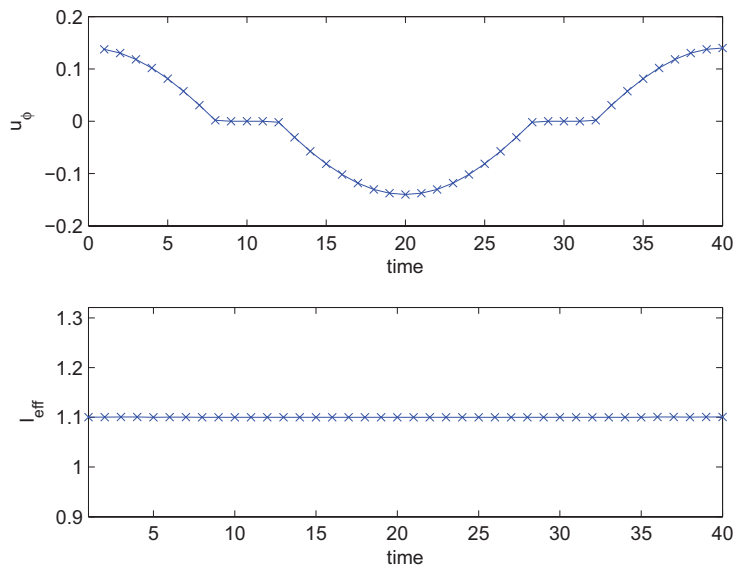
discrete times:  $t = 0, 1, 2, \dots, 40$



## Displacements, Strains, Stresses for $t_0$



## Slip testing, index of efficiency



## Papers

P. Neittaanmäki, S. I. Repin and J. Valdman, Functional a posteriori error estimates for elasticity problems with nonlinear boundary conditions. (in preparation)

Matlab solver can be downloaded at

<http://www.mathworks.com/matlabcentral/fileexchange/authors/37756>

## Mathematics model of the Barenblatt-Biot system

Barenblatt-Biot systems representing double diffusion in elastic porous media.

$$\begin{aligned} -\nabla \cdot (\mathbb{C}\varepsilon(u)) + \alpha_1 \nabla p_1 + \alpha_2 \nabla p_2 &= f(x, t) \\ c_1 \dot{p}_1 - \nabla \cdot (k_1 \nabla p_1) + \alpha_1 \nabla \cdot \dot{u} + \kappa(p_1 - p_2) &= h_1(x, t) \\ c_2 \dot{p}_2 - \nabla \cdot (k_2 \nabla p_2) + \alpha_2 \nabla \cdot \dot{u} + \kappa(p_2 - p_1) &= h_2(x, t) \end{aligned}$$

in which  $u$  is the displacement of the solid skeleton and  $p_1$  and  $p_2$  are the fluid pressures in the respective components.

Mathematical analysis of this model based on the theory of implicit evolution equations in Hilbert spaces is elaborated in

R. E. Showalter and B. Momken, *Single-phase flow in composite poroelastic media*, Math. Meth. Appl. Sci. 25 (2002), no. 2, 115–139.

## Static model

Static case of the Barenblatt-Biot system

$$\begin{aligned} -\nabla \cdot (\mathbb{C}\varepsilon(u)) + \alpha_1 \nabla p_1 + \alpha_2 \nabla p_2 &= f(x) \\ -\nabla \cdot (k_1 \nabla p_1) + \kappa(p_1 - p_2) &= h_1(x) \\ -\nabla \cdot (k_2 \nabla p_2) + \kappa(p_2 - p_1) &= h_2(x) \end{aligned}$$

Combining a functional a posteriori error estimate for an elasticity problem

$$-\nabla \cdot (\mathbb{C}\varepsilon(u)) = f - \alpha_1 \nabla p_1 - \alpha_2 \nabla p_2 \quad (1)$$

and a functional a posteriori error estimate for a double-diffusion problem

$$-\nabla \cdot (k_1 \nabla p_1) + \kappa(p_1 - p_2) = h_1(x) \quad (2)$$

$$-\nabla \cdot (k_2 \nabla p_2) + \kappa(p_2 - p_1) = h_2(x) \quad (3)$$

which describes the flow of slightly compressible fluid in a general heterogeneous medium consisting of two components.

**Problem (Variational formulation)**

Assume that  $(h_1, h_2) \in L^2(\Omega, \mathbb{R}^2)$ . Find  $\mathbf{p} = (p_1, p_2) \in H_0^1(\Omega, \mathbb{R}^2)$ , satisfying the system of variational equalities

$$\int_{\Omega} k_1 \nabla p_1 \cdot \nabla q_1 + \int_{\Omega} \kappa (p_1 - p_2) q_1 \, dx = \int_{\Omega} (h_1(x) q_1 - k_1 \nabla \bar{p} \cdot \nabla q_1) \, dx$$

$$\int_{\Omega} k_2 \nabla p_2 \cdot \nabla q_2 + \int_{\Omega} \kappa (p_2 - p_1) q_2 \, dx = \int_{\Omega} (h_2(x) q_2 - k_2 \nabla \bar{p} \cdot \nabla q_2) \, dx$$

for all testing functions  $\mathbf{q} = (q_1, q_2) \in H_0^1(\Omega, \mathbb{R}^2)$ .

Dirichlet boundary conditions assumed for simplicity!

**Problem (Abstract variational formulation)**

Find  $\mathbf{p} \in Q := H_0^1(\Omega, \mathbb{R}^2)$ , such that the equality

$$a(\mathbf{p}, \mathbf{q}) = l(\mathbf{q})$$

holds for all  $\mathbf{q} \in Q$ . The bilinear form  $a(\cdot, \cdot)$  and the linear form  $l(\cdot)$  are

$$a(\mathbf{p}, \mathbf{q}) := \int_{\Omega} (\Lambda \mathbf{p} : (\mathbb{A} \Lambda \mathbf{q}) + \mathbf{p} \cdot \mathbb{B} \mathbf{q}) \, dx,$$

$$l(\mathbf{q}) := \int_{\Omega} (h \cdot \mathbf{q} - \mathbb{C} \Lambda \mathbf{q}) \, dx,$$

where  $\Lambda \mathbf{q} := (\nabla q_1, \nabla q_2)$  and  $\mathbb{A}$ ,  $\mathbb{B}$  and  $\mathbb{C}$  are matrices formed by material dependant constants

$$\mathbb{A} := \begin{pmatrix} k_1 & 0 \\ 0 & k_2 \end{pmatrix}, \quad \mathbb{B} := \begin{pmatrix} \kappa & -\kappa \\ -\kappa & \kappa \end{pmatrix}, \quad \mathbb{C} := \begin{pmatrix} k_1 \nabla \bar{p} & 0 \\ 0 & k_2 \nabla \bar{p} \end{pmatrix}$$

and  $h$  is the right hand side vector  $h := (h_1 \ h_2)^T$ .

**Problem (Equivalent minimization problem)**

Find  $\mathbf{p} \in Q = H_0^1(\Omega, \mathbb{R}^2)$  satisfying

$$F(\mathbf{p}) + G(\Lambda \mathbf{p}) = \inf_{\mathbf{q} \in Q} \{F(\mathbf{q}) + G(\Lambda \mathbf{q})\},$$

where

$$F : Q \rightarrow \mathbb{R}, \quad F(\mathbf{q}) := \frac{1}{2} \int_{\Omega} \mathbf{q} \cdot \mathbb{B} \mathbf{q} \, dx - l(\mathbf{q}),$$

$$G : Y \rightarrow \mathbb{R}, \quad G(\Lambda \mathbf{q}) := \frac{1}{2} \int_{\Omega} \Lambda \mathbf{q} : (\mathbb{A} \Lambda \mathbf{q}) \, dx.$$

We need to find explicit forms of dual functionals

$$F^* : Q^* \rightarrow \mathbb{R}, \quad F^*(\Lambda^* \mathbb{Y}^*) := \sup_{\mathbf{q} \in Q} \{ \langle \Lambda^* \mathbb{Y}^*, \mathbf{q} \rangle - F(\mathbf{q}) \},$$

$$G^* : Y^* \rightarrow \mathbb{R}, \quad G^*(\mathbb{Y}^*) := \sup_{\Lambda \mathbf{q} \in Y} \{ \langle \mathbb{Y}^*, \Lambda \mathbf{q} \rangle - G(\Lambda \mathbf{q}) \},$$

where  $Y = Y^* := L^2(\Omega, \mathbb{R}^{2d})$ ,  $\Lambda^* \mathbb{Y}^* = (-\operatorname{div} y_1^*, -\operatorname{div} y_2^*)^T$   
and construct the corresponding compound functionals

$$D_F : Q \times Q^* \rightarrow \mathbb{R}, \quad D_F(\mathbf{q}, \Lambda^* \mathbb{Y}^*) := F(\mathbf{q}) + F^*(\Lambda^* \mathbb{Y}^*) - \langle \Lambda^* \mathbb{Y}^*, \mathbf{q} \rangle,$$

$$D_G : Y \times Y^* \rightarrow \mathbb{R}, \quad D_G(\Lambda \mathbf{q}, \mathbb{Y}^*) := G(\Lambda \mathbf{q}) + G^*(\mathbb{Y}^*) - \langle \mathbb{Y}^*, \Lambda \mathbf{q} \rangle.$$

By the the sum of  $D_F$  and  $D_G$ , we obtain the functional error majorant

$$M(\mathbf{q}, \mathbb{Y}^*) := D_F(\mathbf{q}, \Lambda^* \mathbb{Y}^*) + D_G(\Lambda \mathbf{q}, \mathbb{Y}^*), \quad (4)$$

which provides a guaranteed upper bound of the error:

$$\frac{1}{2} a(\mathbf{p} - \mathbf{q}, \mathbf{p} - \mathbf{q}) \leq M(\mathbf{q}, \mathbb{Y}^*) \quad \text{for all } \mathbb{Y}^* \in Y^*. \quad (5)$$

The majorant is fully computable and depends only on the approximation  $\mathbf{q} \in Q$  and arbitrary variable  $\mathbb{Y}^* \in Y^*$ .

## Lemma (dual functionals)

For  $k_1, k_2 > 0$  and  $\kappa > 0$ , it holds

$$G^*(\mathbb{Y}^*) = \frac{1}{2} \int_{\Omega} \mathbb{A}^{-1} \mathbb{Y}^* : \mathbb{Y}^* dx,$$

$$F^*(\Lambda^* \mathbb{Y}^*) = \begin{cases} \frac{1}{4\kappa} \int_{\Omega} (\Lambda^* \mathbb{Y}^* + h)^2 dx & \text{if } \Lambda^* y_1^* + h_1 + \Lambda^* y_2^* + h_2 = 0, \\ +\infty & \text{otherwise.} \end{cases}$$

Note that the condition

$$\Lambda^* \mathbf{Y}_1^* + h_1 + \Lambda^* \mathbf{Y}_2^* + h_2 = 0$$

is weaker than two conditions

$$\Lambda^* \mathbf{Y}_1^* + h_1 = 0, \quad \Lambda^* \mathbf{Y}_2^* + h_2 = 0,$$

which one would await from the general theory (COUPLING EFFECT!).

We obtain explicit expressions for the compound functionals

$$D_G(\Lambda \mathbf{q}, \mathbb{Y}^*) = \frac{1}{2} \int_{\Omega} \mathbb{A}(\Lambda \mathbf{q} - \mathbb{A}^{-1} \mathbb{Y}^*) : (\Lambda \mathbf{q} - \mathbb{A}^{-1} \mathbb{Y}^*) dx, \quad (6)$$

$$D_F(\mathbf{q}, \Lambda^* \mathbb{Y}^*) = \begin{cases} \frac{1}{2} \int_{\Omega} \mathbb{B} \mathbf{q} \cdot \mathbf{q} dx + \frac{1}{4\kappa} \int_{\Omega} (\Lambda^* \mathbb{Y}^* + h)^2 dx \\ \quad \text{if } \Lambda^* \mathbf{Y}_1^* + h_1 + \Lambda^* \mathbf{Y}_2^* + h_2 = 0, \\ +\infty & \text{otherwise.} \end{cases} \quad (7)$$

and let us recall that

$$M(\mathbf{q}, \mathbb{Y}^*) := D_F(\mathbf{q}, \Lambda^* \mathbb{Y}^*) + D_G(\Lambda \mathbf{q}, \mathbb{Y}^*), \quad (8)$$

provides a guaranteed upper bound of the error:

$$\frac{1}{2} a(\mathbf{p} - \mathbf{q}, \mathbf{p} - \mathbf{q}) \leq M(\mathbf{q}, \mathbb{Y}^*) \quad \text{for all } \mathbb{Y}^* \in Y^*. \quad (9)$$

## Final estimate for the coupled poro-elastic system

It holds ( $\mathbf{q}$  and  $\mathbf{v}$  are known from computations)

$$\begin{aligned} & a(\mathbf{p} - \mathbf{q}, \mathbf{p} - \mathbf{q}) + \|\varepsilon(\mathbf{u} - \mathbf{v})\|_{\mathbb{L};\Omega}^2 \\ & \leq 2\widehat{C} M_{\beta_1, \beta_2}(\mathbf{q}, \widehat{\mathbf{Y}}^*) + (1 + \beta_4 + \beta_5) \|\varepsilon(\mathbf{v}) - \mathbb{L}^{-1}\tau\|_{\mathbb{L};\Omega}^2 + \\ & \quad + \left(1 + \frac{1}{\beta_4} + \beta_6\right) C^2 \|\operatorname{div} \tau + \mathcal{F} - \alpha_1 \nabla \mathbf{q}_1 - \alpha_2 \nabla \mathbf{q}_2\|_{\Omega}^2, \end{aligned}$$

for all  $\widehat{\mathbf{Y}}^* \in Y_{div}^* := \{(\mathbf{Y}_1^*, \mathbf{Y}_2^*) \in Y^* : \Lambda^* \mathbf{Y}_1^* + \Lambda^* \mathbf{Y}_2^* \in L^2(\Omega)\}$ ,

for all  $\tau \in Q$ ,

for all  $\beta_1, \dots, \beta_6 > 0$ .

Here

$$\widehat{C} = 1 + C^2 \left(1 + \frac{1}{\beta_5} + \frac{1}{\beta_6}\right) \max \left\{ \frac{1 + \beta_3}{k_1}, \frac{1 + \beta_3}{k_2 \beta_3} \right\},$$

where  $C > 0$  satisfies Friedrichs' inequality

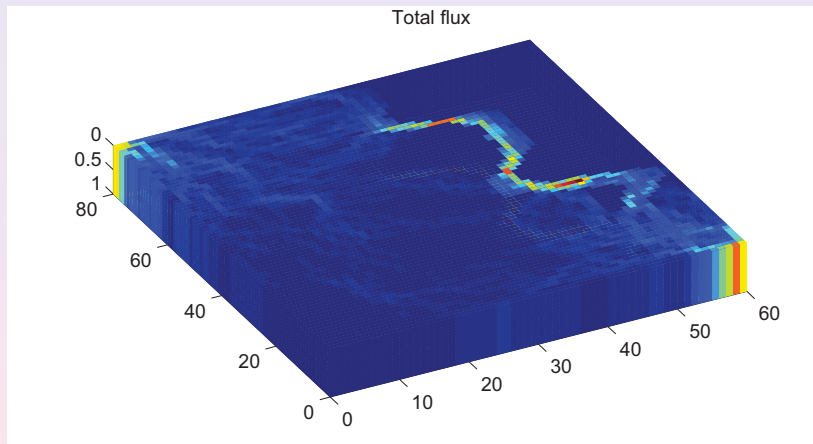
$$\|w\|_{L^2(\Omega)} \leq C \|\nabla w\|_{L^2(\Omega)}$$

valid for all  $w \in H_0^1(\Omega)$ .

## Papers

Jan Martin Nordbotten, Talal Rahman, Sergey Repin, Jan Valdman, A posteriori error estimates for approximate solutions of Barenblatt-Biot poroelastic model. Computational Methods in Applied Mathematics 10, No. 3, 302-315 (2010)

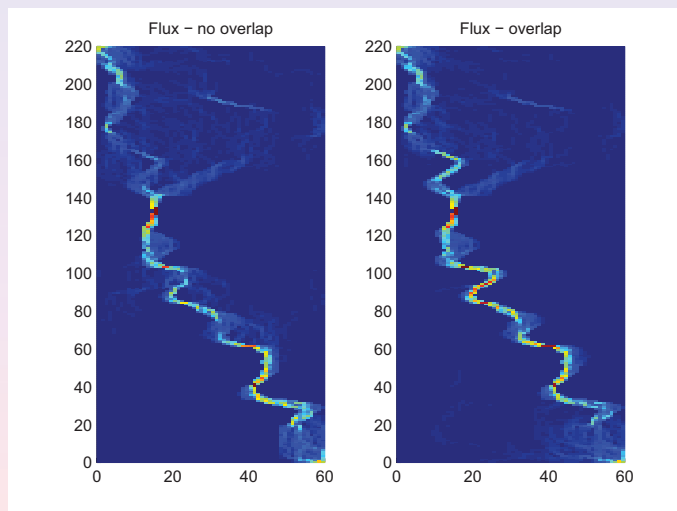
## Reservoir simulator - project with SINTEF ICT



$$v = -\lambda(\nabla p - \rho G)$$

$$\nabla \cdot v = q$$

## Variational multiscale Method (VMS):



3D Matlab solver provided by SINTEF ICT



## Similar results on multiscale methods

MSc. thesis of Sergey Alyaev on  
Adaptive Multiscale Methods Based on A Posteriori Error Estimates,  
Bergen, June 2010

## Basic estimate of the deviation from exact solution

For any  $w \in H$  it holds

$$\frac{1}{2} \| \|u - v, p - q\| \|^2 \leq \mathcal{H}(v, q) - \mathcal{H}(u, p),$$

where  $z = (u, p)$  is an exact elastoplastic solution  
and  $w = (v, q)$  is a discrete approximation.

where

$$\| \|u - v, p - q\| \| := \| \mathbb{C}(\varepsilon(u - v) - (p - q)) \|_{\mathbb{C}^{-1}}^2 + \sigma_y^2 H^2 \|q - p\|^2.$$

Note,  $H > 0$  represents a hardening parameter (done for isotropic hardening model).

## Perturbed problem

### Original problem

$$\mathcal{H}(v, q) := \frac{1}{2}a(v, q; v, q) - l(v) + \int_{\Omega} \sigma_y |q| dx$$

### Perturbed problem

$$\mathcal{H}_{\lambda}(v, q) := \frac{1}{2}a(v, q; v, q) - l(v) + \int_{\Omega} \sigma_y \lambda : q dx$$

where  $\lambda \in \Lambda := \{\lambda \in L^{\infty}(\Omega, \mathbb{R}^{d \times d}) : |\lambda| \leq 1, \text{tr}(\lambda) = 0 \text{ a. e. in } \Omega\}$ .

$$\sup_{\lambda \in \Lambda} \mathcal{H}_{\lambda}(v, q) = \mathcal{H}(v, q)$$

## Lagrangian

### Lagrangian

$$L_{\lambda}(v, q; \tau, \xi) := \int_{\Omega} \left( \tau : (\varepsilon(v) - q) - \frac{\mathbb{C}^{-1} \tau : \tau}{2} + \xi : q - \frac{|\xi|^2}{2\sigma_y^2 H^2} - fv \right) dx + \int_{\Omega} \sigma_y \lambda : q dx,$$

where  $\tau \in Q := L^2(\Omega; \mathbb{R}_{sym}^{d \times d})$ ,  $\xi \in Q_0 := \{q \in Q : \text{tr}(q) = 0 \text{ a. e. in } \Omega\}$ .

$$\sup_{\tau \in Q, \xi \in Q_0} L_{\lambda}(v, q; \tau, \xi) = \mathcal{H}_{\lambda}(v, q)$$

## First estimate

It holds for all  $\lambda \in \Lambda$

$$\mathcal{H}(u, p) = \inf_{v, q} \mathcal{H}(v, q) \geq \inf_{v, q} \mathcal{H}_\lambda(v, q) \geq \inf_{v, q} L_\lambda(v, q; \tau, \xi)$$

which yields the estimate

$$\frac{1}{2} \|\|(u - v), (p - q)\|\|^2 \leq \mathcal{H}(v, q) - \inf_{v, q} L_\lambda(v, q; \tau, \xi)$$

How to compute  $\inf_{v, q} L_\lambda(v, q; \tau, \xi)$ ?

## Majorant estimate for equilibrated fields

$$\frac{1}{2} \|\|(u - v), (p - q)\|\|^2 \leq \inf_{(\tau, \xi) \in Q_{f_\lambda}} \mathcal{M}(v, q, \tau, \xi, \lambda),$$

where

$$\begin{aligned} \mathcal{M}(v, q, \tau, \xi, \lambda) &= \frac{1}{2} \int_{\Omega} \mathbb{C}(\varepsilon(v) - q - \mathbb{C}^{-1}\tau) : (\varepsilon(v) - q - \mathbb{C}^{-1}\tau) \, dx \\ &\quad + \frac{1}{2} \int_{\Omega} \sigma_y^2 H^2 (q - \frac{1}{\sigma_y^2 H^2} \xi)^2 \, dx + \int_{\Omega} (\sigma_y |q| - \sigma_y \lambda : q) \, dx \end{aligned}$$

and

$$Q_{f_\lambda} := \{(\tau, \xi) \in Q \times Q_0 : \operatorname{div} \tau + f = 0, \tau^D = \xi + \sigma_y \lambda \text{ a. e. in } \Omega\}.$$

## Structure of Functional Majorant

$\mathcal{M}(v, q, \tau, \xi, \lambda) = 0$  if and only if

$$\tau = \mathbb{C}(\varepsilon(v) - q), \quad (10)$$

$$\operatorname{div} \tau + f = 0, \quad (11)$$

$$\lambda : q = |q|, \quad \lambda \in \Lambda, \quad (12)$$

$$\tau^D = \xi + \sigma_y \lambda, \quad (13)$$

$$\xi = \sigma_y^2 H^2 q. \quad (14)$$

These are conditions for the exact solution  $(u, p)$  of the elastoplastic minimization problem! The majorant naturally reflects properties of the original problem.

## Majorant estimate for nonequibrated fields

$$\frac{1}{2} \| \|(u - v), (p - q)\| \|^2 \leq \inf_{(\tau, \xi) \in Q_{f, \lambda}} \hat{\mathcal{M}}(v, q; \hat{\tau}, \lambda, \beta, \delta),$$

where

$$\begin{aligned} \hat{\mathcal{M}}(v, q; \hat{\tau}, \lambda, \beta, \delta) := & \frac{1}{2}(1 + \beta) \int_{\Omega} \mathbb{C}(\varepsilon(v) - q - \mathbb{C}^{-1} \hat{\tau}) : (\varepsilon(v) - q - \mathbb{C}^{-1} \hat{\tau}) \, dx \\ & + \frac{1}{2}(1 + \delta) \int_{\Omega} \frac{1}{\sigma_y^2 H^2} (\hat{\tau}^D - \zeta)^2 \, dx + \int_{\Omega} (\sigma_y |q| - \sigma_y \lambda : q) \, dx \\ & + \frac{1}{2} \left[ \left(1 + \frac{1}{\beta}\right) + \frac{C_2}{\sigma_y^2 H^2} \left(1 + \frac{1}{\delta}\right) \right] C^2 \|\operatorname{div} \hat{\tau} + f\|^2 \end{aligned}$$

and  $\hat{\tau} \in Q_{\operatorname{div}} := \{\tau \in Q : \operatorname{div} \tau \in L^2(\Omega, \mathbb{R}^d)\}$ ,  $\zeta := \sigma_y^2 H^2 q + \sigma_y \lambda$ .

## Papers

Sergey Repin, Jan Valdman,  
Functional a posteriori error estimates for incremental models in  
elasto-plasticity.  
Cent. Eur. J. Math. 7, No. 3, 506-519 (2009)

Thank you for your attention!

# Fast MATLAB assembly of FEM stiffness- and mass matrices in 2D and 3D: nodal elements

Talal Rahman, Jan Valdman

School of Engineering and Natural Sciences  
University of Iceland, Reykjavik  
email: janv@hi.is

ESCO 2010, Pilsen, 28.6. 2010

## What will be vectorized?

A stiffness matrix  $K$  and a mass matrix  $M$  defined as

$$K_{ij} = \int_{\Omega} \nabla \Phi_i \cdot \nabla \Phi_j \, dx, \quad M_{ij} = \int_{\Omega} \Phi_i \Phi_j \, dx,$$

where  $\Omega$  is the domain of computation and  $\nabla$  denotes the gradient operator,  $\Phi_i$  denote (nodal) shape functions.

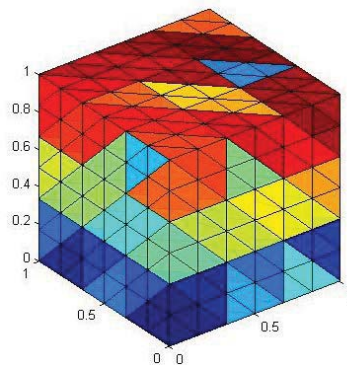


Figure: A triangulation of cube geometry.

## FEM functions of interest

We are interested in *iso-parametric* shape functions  $\Phi_j$ .

Then, the global-local element mapping reads (in 2D):

$$x = \sum_i \Phi_i(\xi, \eta) x_i, \quad y = \sum_i \Phi_i(\xi, \eta) y_i,$$

where  $(x, y)$  is a point on an element corresponding to the point  $(\xi, \eta)$  on the reference element,  $(x_i, y_i)$  are the global coordinates of the node corresponding to the shape function  $\Phi_i$ .

in 3D:

$$x = \sum_i \Phi_i(\xi, \eta, \theta) x_i, \quad y = \sum_i \Phi_i(\xi, \eta, \theta) y_i, \quad z = \sum_i \Phi_i(\xi, \eta, \theta) z_i,$$

It holds also for higher order (quadratic, cubic, etc.) shape functions!

## Examples of iso-parametric shape functions

Examples:

1.  $\Phi_1 = 1 - \xi - \eta$ ,  $\Phi_2 = \xi$ ,  $\Phi_3 = \eta$
2.  $\Phi_1 = 1 - \xi - \eta - \theta$ ,  $\Phi_2 = \xi$ ,  $\Phi_3 = \eta$ ,  $\Phi_4 = \theta$
3.  $\Phi_1 = 1 - 3\xi - 3\eta + 4\xi\eta + 2\xi^2 + 2\eta^2$ ,  $\Phi_2 = -\xi + \xi^2$ ,  $\Phi_3 = -\eta + \eta^2$ ,  
 $\Phi_4 = 4\xi\eta$ ,  $\Phi_5 = -4\xi\eta - 4\xi^2$ ,  $\Phi_6 = -4\xi\eta - 4\eta^2$

## What needs to be vectorized?

For every element  $T$  and every integration point  $IP$  we need to vectorize:

in 2D -

$$\det \begin{pmatrix} \frac{\partial x}{\partial \xi} & \frac{\partial x}{\partial \eta} \\ \frac{\partial y}{\partial \xi} & \frac{\partial y}{\partial \eta} \end{pmatrix} \quad \text{storage: number of IP} \times \text{number of T}$$
$$\begin{pmatrix} \frac{\partial x}{\partial \xi} & \frac{\partial x}{\partial \eta} \\ \frac{\partial y}{\partial \xi} & \frac{\partial y}{\partial \eta} \end{pmatrix}^{-1} \quad \text{storage: } 2 \times 2 \times \text{number of IP} \times \text{number of T}$$

Vectorizations for higher order elements **is not** more difficult!

## Concept of vectorization in Matlab - an array of matrices

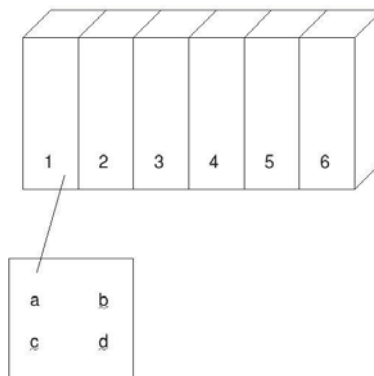


Figure: Computation of determinant (for linear elements in 2D).



## Two ways of computing determinant

1. for all elements: compute determinant of  $2 \times 2$  matrix using MATLAB command

$$\det \begin{pmatrix} a & b \\ c & d \end{pmatrix}$$

2. construct long vectors

$$a = (a_1, \dots, a_{\#T}),$$

$$b = (b_1, \dots, b_{\#T}),$$

$$c = (c_1, \dots, c_{\#T}),$$

$$d = (d_1, \dots, d_{\#T}),$$

and compute determinant using

$$a.*c - b.*d$$

## Operations on array matrices

- ▶ `smamt` ..... multiplication of scalar matrix and array of matrices
  - ▶ `aminv` ..... inversion (over first two indices) of an array of matrices
  - ▶ `amsm` ..... array of matrices times scalar matrix
  - ▶ and many more located in our vectorization library (directory)
- `sm` ..... scalar matrix, `am` ..... array of matrices, `t` ..... transpose

Example of Matlab code for computation of shape derivative:

```
for poi = 1:nop    %loop over all integration points
    %computation of Jacobian
    %inverse and determinant of Jacobian
    %computation of derivatives of shape functions

    tjac = smamt(dshape(:,:,poi),coord);

    [tjacinv,tjacdet] = aminv(tjac);

    dphi(:,:,poi,:) = amsm(tjacinv,dshape(:,:,poi));
    .....
end
```

## Our vectorization: basic features

- ▶ modularity
- ▶ reusability
- ▶ readability (still fast enough)

## Matlab code web page

Demo located at Matlab Central.

## Numerical performance in 2D: linear elements

mesh level	size of A	assembly of A time (sec)	assembly of M time (sec)
4	289	0.0047	0.0018
5	1089	0.0106	0.0053
6	4225	0.0308	0.0209
7	16641	0.1456	0.1021
8	66049	0.6662	0.4630
9	263169	2.835610	2.017507
10	1050625	11.991354	8.664730
11	4198401	50.309788	36.847517

**Table:** Times of assembly of a stiffness matrix  $A$  and a mass matrix  $M$  in 2D using  $P1$  triangular elements.

## Numerical performance in 2D: quadratic elements

mesh level	size of A	assembly of A time (sec)	assembly of M time (sec)
3	289	0.0064	0.0022
4	1089	0.0150	0.0058
5	4225	0.0471	0.0226
6	16641	0.2098	0.1045
7	66049	1.0146	0.4599
8	263169	4.4870	2.0471
9	1050625	18.2429	9.2360
10	4198401	78.0179	38.1942

Table: Times of assembly of a stiffness matrix  $A$  and a mass matrix  $M$  in 2D using  $P2$  triangular elements.

## Numerical performance in 3D: linear elements

mesh level	size of K and M	assembly of K time (sec)	assembly of M time (sec)
1	343	0.0661	0.0184
2	2197	0.1025	0.0462
3	15625	0.8524	0.4105
4	117649	7.0801	3.6764
5	912673	61.1436	33.4952

Table: Times of assembly of stiffness matrix  $A$  and mass matrix  $M$  in 3D using  $P1$  tetrahedral elements.

## Future extensions

1. rectangular elements
2. linear elasticity
3. Hdiv (Hcurl) problems

Thank you for your attention!

# Computational fluid dynamics with OpenFOAM

Halldór Pálsson

University of Iceland

Computational fluid dynamics with OpenFOAM – p. 1

## Outline

- Computational framework
- Mesh generation
- Solvers for various problems
- Numerical schemes
- Summary and conclusions

Computational fluid dynamics with OpenFOAM – p. 2

# OpenFOAM

General description:

- OpenFOAM (Field Operation And Manipulation) is a general purpose tool set for solving partial differential equations.
- It is based on a huge collection of tailor made C++ classes and programs, including advanced solvers for complex flow problems.
- It is free of use and can be tweaked and modified according to the GNU General Public License.

It is *not*:

- A fully fledged software environment, keeping track of the problem from the point of geometrical definition to presenting results.

Computational fluid dynamics with OpenFOAM – p. 3

## Ready to use software

OpenFOAM (current version is 1.7) is distributed with a large number of working programs. They can be divided into:

- Utilities for pre-processing, including mesh generation and manipulation.
- Solvers for various physical problems, flow, turbulence, heat transfer, solid mechanics, magnetohydrodynamics, e.t.c.
- Utilities for post-processing, such as calculation of derived values as well as integration and averaging of fields.

OpenFOAM has a built in support for parallel processing through the Message Passing Interface.

Computational fluid dynamics with OpenFOAM – p. 4

# The programming environment

- Based on C++, with all the advanced features included, such as
  - Object oriented programming
  - Object inheritance
  - Polymorphism and virtual objects
  - Templated classes and functions
- Divided into layers: Basic tools, containers, algorithms, solvers and utilities.
- Documented with Doxygen, giving an `html` interface for the whole software.

Computational fluid dynamics with OpenFOAM – p. 5

# Using the programming environment

## Strengths:

- Very customizable, everything can be modified and additions can be made
- Object oriented approach, resulting in a logical code structure
- Layers of complexity, e.g. specifying new PDE's without concerning parallel processing or numerical schemes

## Weaknesses:

- Lack of proper documentation with examples
- The code is huge! Difficult for new users to familiarize
- The code is constantly being changed (improved hopefully), some designs are strange/peculiar

Computational fluid dynamics with OpenFOAM – p. 6



# Using the utilities and solvers

Programs are divided into

**Utilities** for mesh generation and manipulation, data processing, etc.

**Solvers** for different problems, e.g. Laplace equation, flow, etc.

- Most programs are accompanied by files, for control. They are commonly called *dictionaries*
- Everything else is controlled by various files
- Files are stored in a well defined directory structure

Computational fluid dynamics with OpenFOAM – p. 7

## Mesh generation

Basic mesh building blocks:

- Vertices, defining face corners
- Faces, which are generally polyhedra, but should be close to planar
- Cells, which consists of four or more polyhedra faces

Mesh properties:

- The mesh structure is stored in human readable data files
- Neighbour cells share a common face, but do not need to be joined at corners (as in FEM methods)
- Faces are either interior faces (between cells) or boundary faces

Computational fluid dynamics with OpenFOAM – p. 8

# Mesh conversion

Meshes can be imported from other programs and systems, using special utilities. Possible imports are:

- Ansys mesh file, by the utility `ansysToFoam`
- Gambit (Ansys Inc.), by `gambitToFoam`
- CFX (Ansys Inc.), by `cfx4ToFoam`
- STAR-CD, by `starToFoam`
- GMSH, by `gmshToFoam`
- Tetgen, by `tetgenToFoam`
- Netgen, by `netgenNeutralToFoam`

Computational fluid dynamics with OpenFOAM – p. 9

# Meshing tools

Two tools are available as a part of OpenFOAM:

**blockMesh** A hexagonal mesher

- Simple, but primitive
- Allows curved edges and faces
- Allows a linear mesh grading between faces

**snappyHexMesh** For complex geometries

- Base mesh is needed (typically hexagonal)
- Geometry must be specified as a closed STL (Stereolithography) surface
- Grading and mesh quality can be controlled in detail

Computational fluid dynamics with OpenFOAM – p. 10

# The blockMesh program

```
FoamFile
{
  version      2.0;
  format       ascii;
  class        dictionary;
  object       blockMeshDict;
}
// ***** //

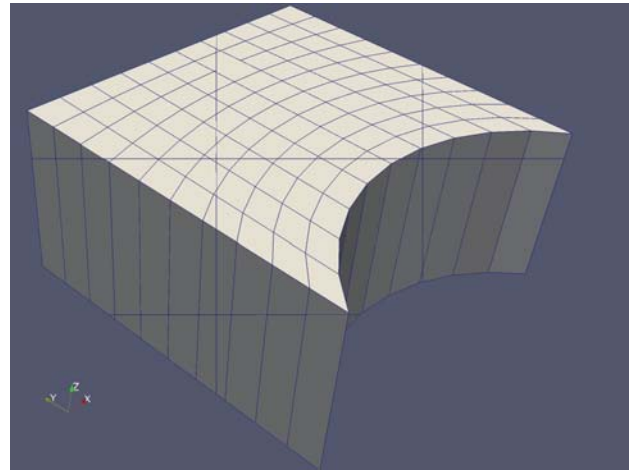
convertToMeters 1.0;

vertices
(
  (-1 -1 0) (1 -1 0) (1 1 0) (-1 1 0)
  (-1 -1 1) (1 -1 1) (1 1 1) (-1 1 1)
);

blocks
(
  hex (0 1 2 3 4 5 6 7) (10 10 1) simpleGrading (1 1 1)
);

edges
(
  arc 0 1 (0 -0.5 0)
  arc 4 5 (0 -0.5 1)
);

patches
(
  patch top ( 2 3 7 6 )
  patch bottom ( 0 1 5 4 )
  patch left ( 0 3 7 4 )
  patch right ( 1 2 6 5 )
);
// ***** //
```



Computational fluid dynamics with OpenFOAM – p. 11

## Solvers for flow problems

- Incompressible flow
  - Transient (PISO) and steady (SIMPLE)
  - Porous flow
  - Shallow water equations
- Compressible flow
  - Transient (PISO) and steady (SIMPLE)
  - Porous flow
  - Sonic flow with high Mach numbers
- Multiphase flow
  - Two phases, liquid and gas
  - Multiple phases
  - Cavitation and phase change

Computational fluid dynamics with OpenFOAM – p. 12

# Turbulence modeling

Three approaches are in general available:

- Reynolds averaged stress models (RAS or RANS)
  - About 15 common models are included ( $k - \epsilon$ ,  $k - \omega$  and others)
- Large eddy simulation (LES)
  - OpenFOAM was originally developed for LES
  - Many models (or filters) available (15-20).
- Direct numerical simulation (DNS)

Many of the solvers can use different turbulence approaches with a single switch. For an time dependent problem: Unsteady-RANS, LES, DNS, Laminar.

## Other solvers

- Basic solvers for scalar transport, Laplace equation and Poisson equation
- Heat transfer, with and without flow effects (buoyant flow)
- Combustion and particle tracking
- Electrostatics and magnetohydrodynamics (MHD)
- Structural analysis and stresses

Different solvers exist for each case, including compressible effects and turbulence.

# Numerical schemes

- The code is based on the finite volume method (FVM)
- Numerical schemes are adjusted in a single file
- Adjustments can be made while running solvers
- Schemes can be selected for each individual operator of a problem
  - Gradient, divergence and curl
  - Laplacian
  - Time derivative (first or second order)
  - Interpolation (used to calculate face values)

All schemes can be evaluated explicitly, or used to generate a linear system of equations

## Numerical schemes: Advection

Advection of field  $\psi$  where  $\phi$  is a surface flux

$$\nabla \cdot (\phi\psi) \rightarrow \text{div}(\text{phi},\text{psi})$$

A total of 51 schemes available, e.g.

- Gauss upwind
- QUICK (Quadratic)
- Cubic
- vanLeer
- MUSCL
- Various limited schemes

# Numerical schemes: Laplacian

Laplacian of a field (vector or scalar) with a coefficient

$$\nabla \cdot (\Gamma \nabla \psi) \rightarrow \text{laplacian}(\text{gamma}, \text{psi})$$

- Evaluation of gradient at faces (interpolation schemes)
- Gauss integration to evaluate the laplacian
- Limiters available for gradients
- Correction for non-orthogonal meshes

Gradients can also be evaluated with

$$\nabla \psi \rightarrow \text{grad}(\text{psi})$$

# Numerical schemes: Time integration

Two operators are available:

$$\frac{\partial \psi}{\partial t} \rightarrow \text{ddt}(\text{rho}, \text{psi})$$

$$\frac{\partial^2 \psi}{\partial t^2} \rightarrow \text{d2dt2}(\text{rho}, \text{psi})$$

Available schemes:

- Implicit Euler
- Crank Nicholson, central difference with weights
- Backward, second order difference using two time values to evaluate the third
- Steady-state, for steady problems

# An example fvSchemes file

```
ddtSchemes
{
  default          Euler;
}

gradSchemes
{
  default          Gauss linear;
}

divSchemes
{
  default          none;
  div(phi,T)      Gauss limitedLinear 1;
  div(gflux,rhok) Gauss limitedLinear 1;
}

laplacianSchemes
{
  default          none;
  laplacian((kappa|nu),p) Gauss linear corrected;
  laplacian((nu|Pr),T) Gauss linear corrected;
}

interpolationSchemes
{
  default          linear;
}
```

Computational fluid dynamics with OpenFOAM – p. 19

## Solvers for linear systems

Three iterative solvers can be used:

- Preconditioned conjugate gradients (PCG), for symmetric positive definite systems.
- Bi-conjugate gradients (PBiCG), for unsymmetric systems
- Generalized algebraic multigrid (GAMG)

Possible preconditioners are:

- Incomplete Cholesky factorization
- Incomplete LU factorization (for unsymmetric systems)
- GAMG iterations

Solvers are specified in a fvSolution file

Computational fluid dynamics with OpenFOAM – p. 20

# An example fvSolution file

```
solvers
{
  p
  {
    solver          GAMG;
    tolerance       1e-06;
    relTol          0.01;
    smoother        GaussSeidel;
    nPreSweeps      0;
    nPostSweeps     2;
    cacheAgglomeration true;
    nCellsInCoarsestLevel 10;
    agglomerator    faceAreaPair;
    mergeLevels     1;
  }
  U
  {
    solver          PBiCG;
    preconditioner  DILU;
    tolerance       1e-05;
    relTol          0.1;
  }
}

k
{
  solver          PBiCG;
  preconditioner  DILU;
  tolerance       1e-05;
  relTol          0.1;
}

epsilon
{
  solver          PBiCG;
  preconditioner  DILU;
  tolerance       1e-05;
  relTol          0.1;
}

SIMPLE
{
  nNonOrthogonalCorrectors 3;
}

relaxationFactors
{
  p          0.3;
  U          0.7;
  k          0.7;
  epsilon    0.1;
  R          0.7;
  nuTilda    0.7;
}
```

Computational fluid dynamics with OpenFOAM – p. 21

## Parallel processing

- Domain decomposition is applied:
  - Simple decomposition based on coordinate directions
  - Metis decomposition algorithm
  - Manual decomposition, based on cell selection
- Uses the openMPI system (message passing interface)
- Processes run on either shared memory systems (multicore) or distributed systems
- Easy to set up and run on clusters with queuing systems

Decomposition is controlled by a single file, `decomposeParDict`.

Computational fluid dynamics with OpenFOAM – p. 22



# Customization of solvers

## Use available source code from other solvers

```
#include "readPISOControls.H"
#include "CourantNo.H"

// Pressure-velocity PISO corrector
{
    // Momentum predictor

    fvVectorMatrix UEqn
    (
        fvm::ddt(U)
        + fvm::div(phi, U)
        + turbulence->divDevReff(U)
    );

    UEqn.relax();

    if (momentumPredictor)
    {
        solve(UEqn == -fvc::grad(p));
    }

    // Solution of the heat equation
    volScalarField kappaEff
    (
        "kappaEff",
        turbulence->nu()/Pr + turbulence->
    );
    for (int nonOrth=0; nonOrth<=nNonOrthCc
    {
        solve
        (
            fvm::ddt(T)
            + fvm::div(phi, T)
            - fvm::laplacian(kappaEff, T)
        );
    }
    runTime.write();
}
```

$$\frac{\partial \vec{U}}{\partial t} + \vec{U} \cdot \nabla \vec{U} + \nabla \cdot \bar{\tau} = -\nabla p \quad \frac{\partial T}{\partial t} + \vec{U} \nabla T - \nabla \cdot (\kappa_e \nabla T) = 0$$

Computational fluid dynamics with OpenFOAM – p. 23

# Writing utilities

## Possibilities: Boundary conditions, initial conditions, field calculations, others

```
if (fieldHeader.headerClassName() == "volScalarField")
{
    Info<< "    Reading volScalarField " << fieldName << endl;
    volScalarField field(fieldHeader, mesh);
    volVectorField grad(fvc::grad(field));

    scalar area = gSum(mesh.magSf().boundaryField()[patchi]);
    scalar sumField = 0;

    if (area > 0)
    {
        sumField = gSum
        (
            mesh.Sf().boundaryField()[patchi]
            & grad.boundaryField()[patchi]
        ) / area;
    }

    Info<< "    Average of flux of " << fieldName << " over patch "
        << patchName << '[' << patchi << ']' << " = "
        << sumField << endl;
}
}
```

Computational fluid dynamics with OpenFOAM – p. 24

# Summary

## The good things:

- A great number of solvers with many modeling options.
- Robust and fast algorithms, easily run in parallel.
- Fully customizable, for new developments or modifications.
- Solution procedures are in *batch mode* by default.
- No license fees!!!

## The bad things:

- Software basis is huge and the design is rather complex.
- No decent application for generating complex meshes.
- Documentation is adequate in some areas, very poor in others.

Computational fluid dynamics with OpenFOAM – p. 25

## Thank you for your attention

For more information visit: <http://www.openfoam.com>

Computational fluid dynamics with OpenFOAM – p. 26

# Case studies in OpenFOAM

Halldór Pálsson

University of Iceland

Case studies in OpenFOAM – p. 1

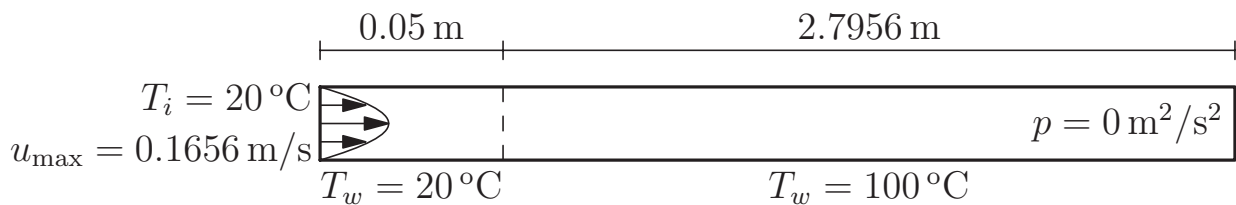
## Outline

- Laminar flow in a heated pipe
- Swirling flow for increased heat transfer
- Thermal transport in porous media
- Flow conditions around trawl doors
- Conclusions

Case studies in OpenFOAM – p. 2

# Laminar flow in a heated pipe

- Flow is laminar and steady along the whole pipe
- The wall has constant temperature at a given section, higher than the fluid temperature
- A well known problem with an analytical solution

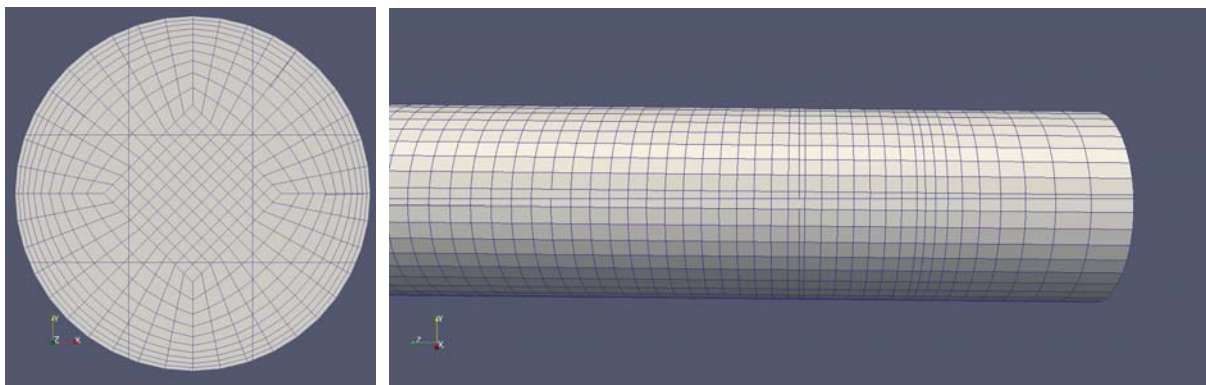


The pipe diameter is 0.05 m, the Reynolds number 319.5 and the Peclet number 223.6.

Case studies in OpenFOAM – p. 3

## Mesh generation

The mesh was generated with the `blockMesh` utility, with a total of 10 blocks, resulting initially in 105000 cells.



Note that the domain is very long in the  $z$ -direction, compared to the other two directions.

Case studies in OpenFOAM – p. 4

# Boundary conditions

- No slip conditions at the pipe walls, and a constant wall temperature.
- Pressure is constant at the outlet.
- Temperature is given at the inlet, but a parabolic laminar velocity profile must be specified.

The profile is set by a custom made utility program `laminarPipeEntrance`, based on diameter and mean velocity.

# Solvers used for computation

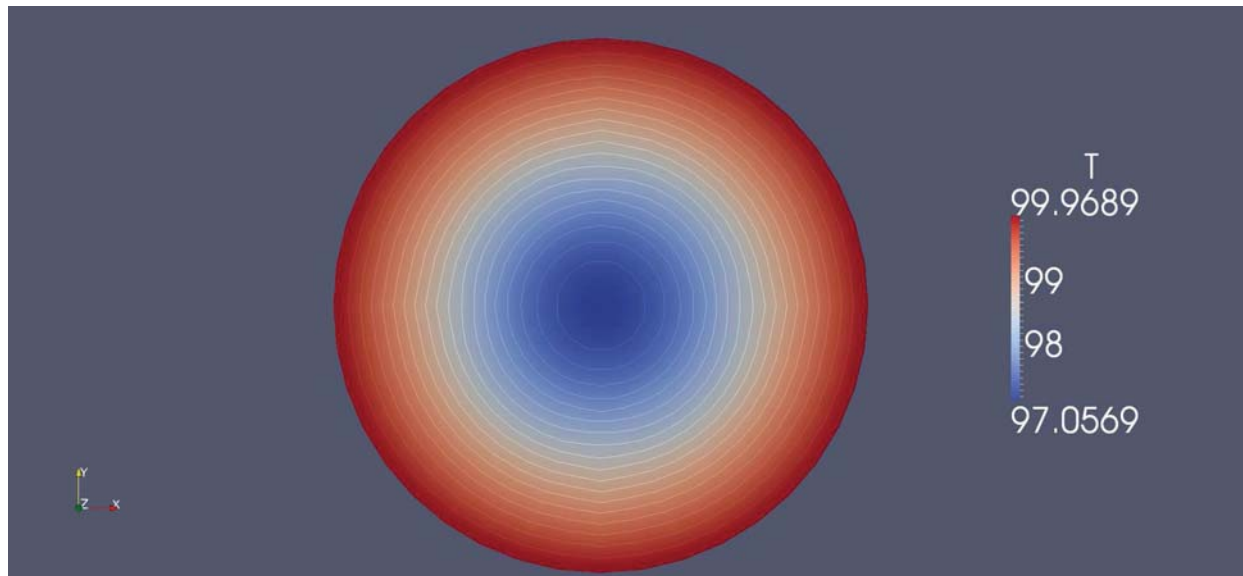
Two steps with different solvers are necessary to obtain a solution:

**For flow** The program `simpleFoam`, for steady incompressible flow with or without a RANS turbulence model

**For heat** The program `scalarTransportFoam`, for unsteady advective-diffusive heat transport with constant diffusion. The program is used in *steadyState* mode.

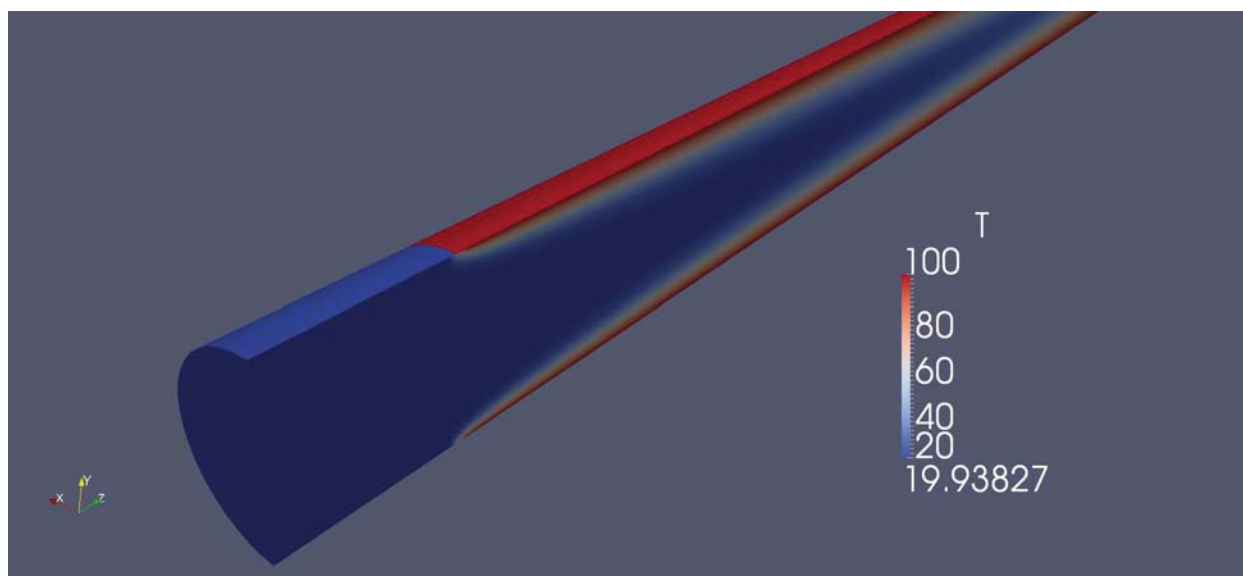
The length/diameter ratio is large (almost 56), so convergence of `simpleFoam` is slow.

# Results, exit temperature profile



Case studies in OpenFOAM – p. 7

# Results, inlet and heated wall



Note that the minimum temperature is lower than the physical minimum of 20 °C.

Case studies in OpenFOAM – p. 8

# Velocity weighted average temperature

A useful numerical value for comparison is the average temperature, weighted by velocity:

$$\bar{T} = \frac{\int_A T \vec{u} \cdot d\vec{A}}{\int_A \vec{u} \cdot d\vec{A}}$$

- Computation can be performed by using surface slices of the geometry, notably the utility `sample` in OpenFOAM.
- A dictionary has to be constructed in the `system` directory: `sampleDict`
- The result is a triangulated surface *with field values given at the corner points*

Case studies in OpenFOAM – p. 9

## Calculation for a single triangle

Each triangle is defined by closed loop of three vectors,  $\vec{v}_1$ ,  $\vec{v}_2$  and  $\vec{v}_3$ . Area is given by

$$\vec{A} = \frac{(\vec{v}_2 - \vec{v}_1) \times (\vec{v}_3 - \vec{v}_1)}{2}$$

velocity flux by

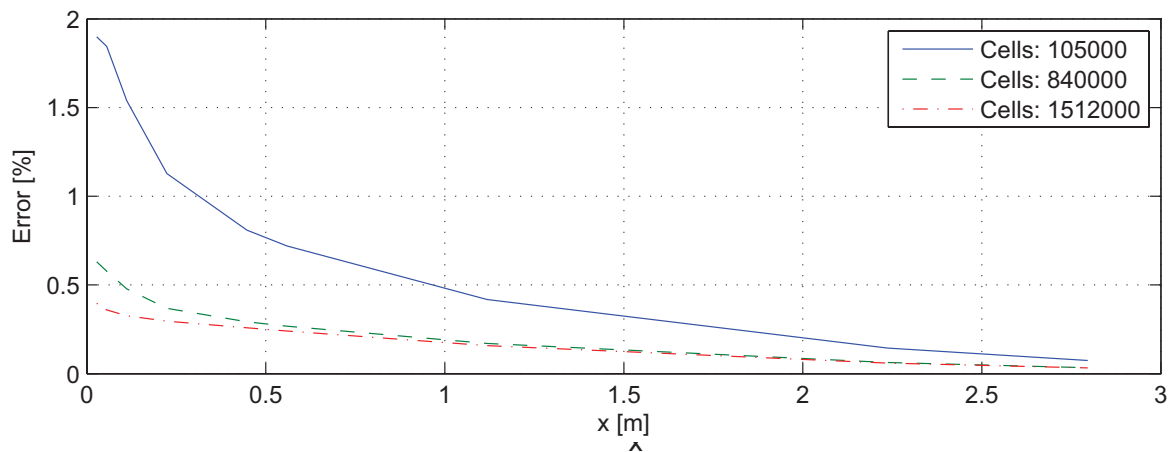
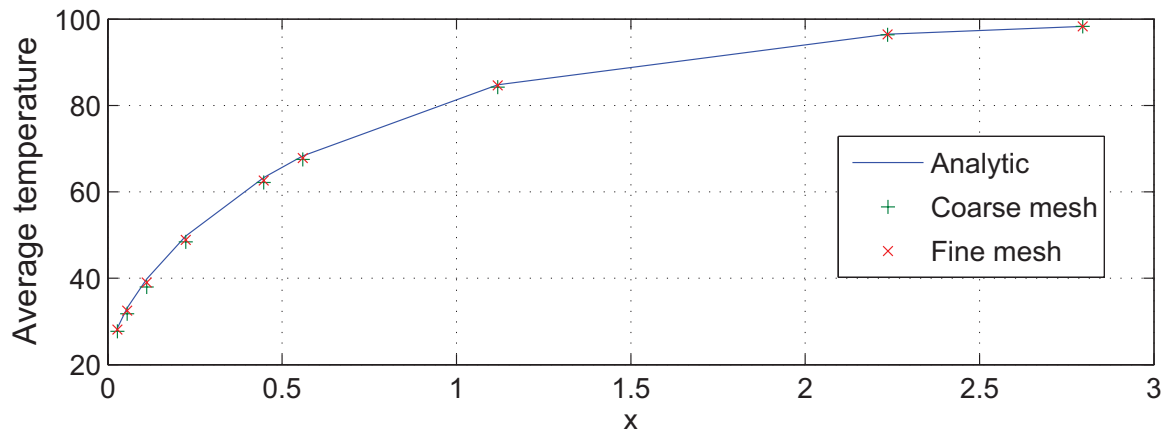
$$\hat{u} = \int_A \vec{u} \cdot d\vec{A} = \frac{(\vec{u}_1 + \vec{u}_2 + \vec{u}_3)}{3} \cdot \vec{A}$$

and temperature weighted flux by

$$\hat{T} = \int_A T \vec{u} \cdot d\vec{A} = \frac{1}{12} \begin{bmatrix} \vec{A} \cdot \vec{u}_1 & \vec{A} \cdot \vec{u}_2 & \vec{A} \cdot \vec{u}_3 \end{bmatrix} \begin{bmatrix} 2 & 1 & 1 \\ 1 & 2 & 1 \\ 1 & 1 & 2 \end{bmatrix} \begin{bmatrix} T_1 \\ T_2 \\ T_3 \end{bmatrix}$$

Case studies in OpenFOAM – p. 10

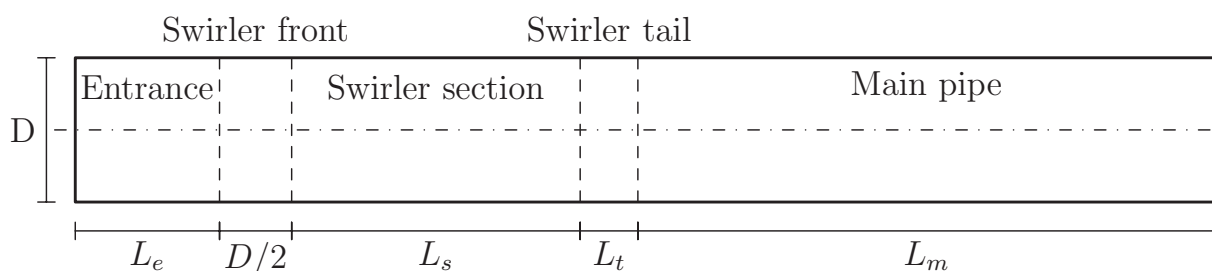
# Comparison with theory



Case studies in OpenFOAM – p. 11

# Induced swirling flow in a pipe

- A pipe is modeled, including a swirler device in one section
- The entrance is laminar, no heating takes place yet
- The flow model is steady state with realizable  $k - \epsilon$  turbulence modeling.
- The model geometry is dictated by a set of parameters, specified in the dictionary file `swirlerDict`

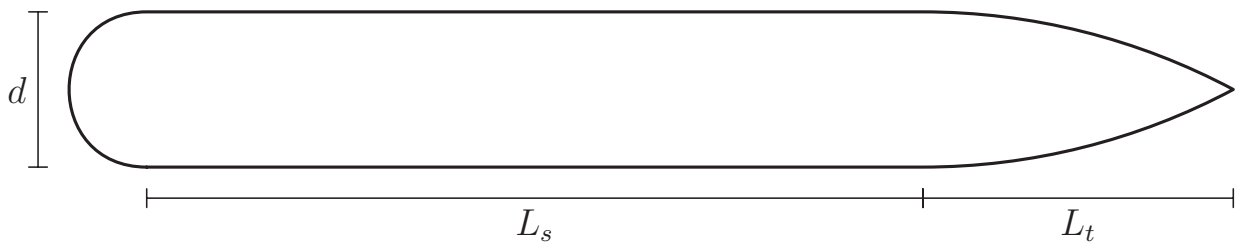


Case studies in OpenFOAM – p. 12



# Swirl device geometry

- The device consists of a narrow cylinder in the pipe center
- Thin fins or baffles connect the cylinder to the pipe, in the  $L_s$  section
- The fins are twisted along the axis, to direct flow into a swirling motion



Case studies in OpenFOAM – p. 13

## Strategy for mesh generation

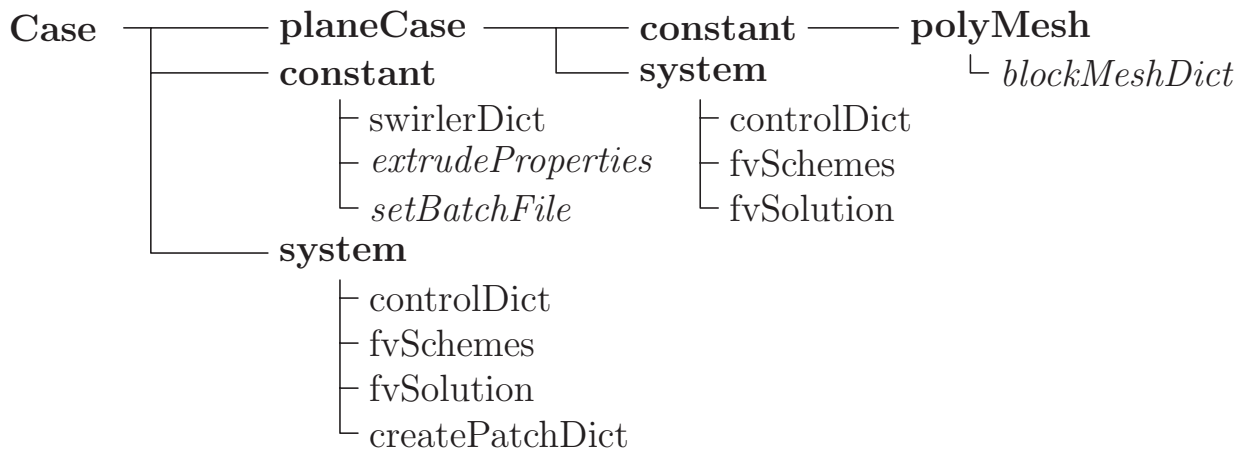
Three observations are used:

1. The pipe and the center piece are axi-symmetric in shape, so it is natural to use this symmetry to simplify the model generation.
2. The fins are distributed equally in the angular direction around the centerpiece, making it possible to identify their position in the axi-symmetric setup.
3. The fins are twisted along the length of the pipe, which can be performed in modeling terms with a coordinate transform, based on axial location.

Case studies in OpenFOAM – p. 14

# File structure in OpenFOAM

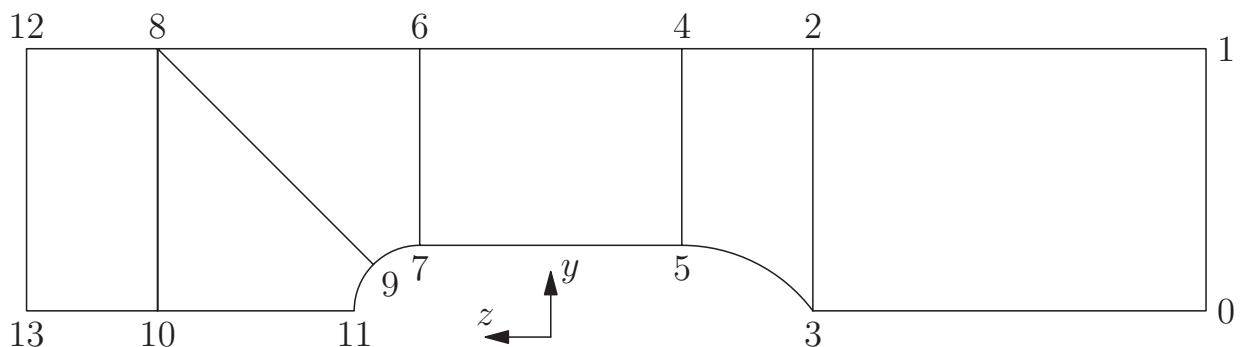
- A set of directories and files have to be generated
- The slanted ones are generated by the custom utility `swirlerMesh`
- Others are made/copied by the user



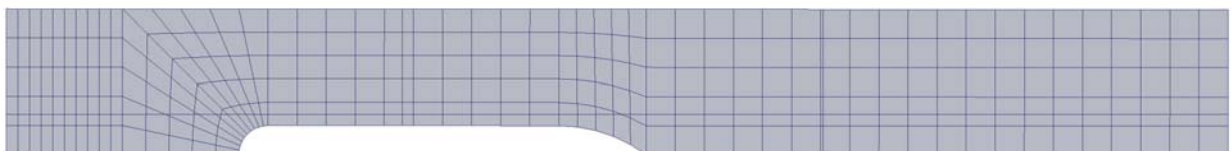
Case studies in OpenFOAM – p. 15

## An axi-symmetrical cross section

The `blockMesh` utility is used to create a mesh, based on the following vertex and block definitions



Resulting in a planar mesh



Case studies in OpenFOAM – p. 16

# Extrusion for generating a volume

- The utility `extrudeMesh` is used to rotate the plane around the  $z$ -axis
- Controlled by a dictionary `constant/extrudeProperties`, generated by `swirlerMesh`
- Specifications are:
  - Extrude type, *wedge*
  - Number of cells in extrusion direction
  - Rotation axis, position and direction
  - Rotation angle. If  $360^\circ$  then end planes are connected.

Case studies in OpenFOAM – p. 17

## Specifying boundaries

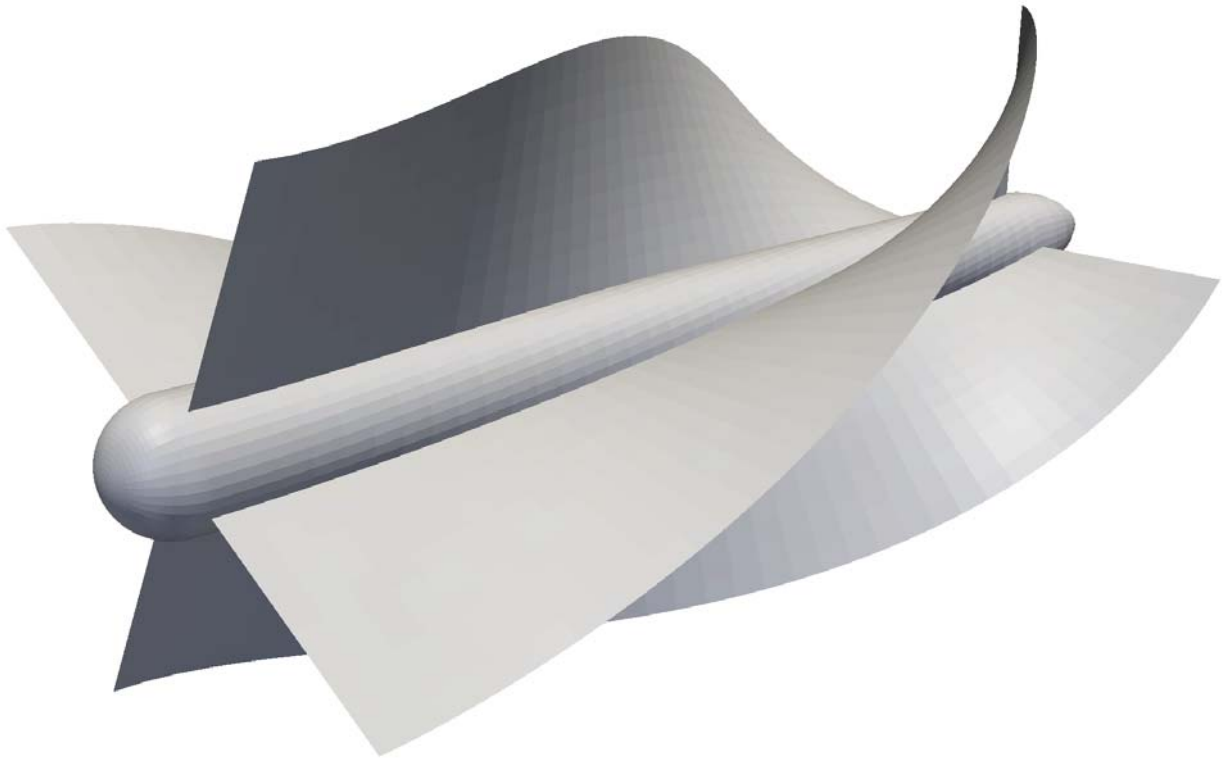
Boundaries involve *inlet*, *outlet*, *pipe wall*, *centerpiece* and *fins*. The generation procedure is:

1. Divide boundary, using utility `autoPatch` 45. The parameter 45 is a *feature angle*
2. Use utility `setSet` to select internal faces that will become fins, based on `constant/setBatchFile`
3. Transform face sets into face zones, using utility `setsToZones`
4. Create fins with utility `createBaffles`. A face set and a name of a new boundary patch must be given
5. Redefine boundary patch names and clean up all boundary definitions, using utility `createPatch` which uses the dictionary `system/createPatchDict`

Case studies in OpenFOAM – p. 18

# Twisting the mesh

The mesh is twisted along a predefined curve.



Case studies in OpenFOAM – p. 19

## Mesh generation summary

In the whole, the following commands must be executed, e.g. as a script.

```
swirlerMesh
blockMesh -case planeCase
extrudeMesh
autoPatch 45 -overwrite
setSet -noVTK -batch constant/setBatchFile
setsToZones -noFlipMap
createBaffles baffles otherSide -overwrite
createPatch -overwrite
twistMesh
```

Case studies in OpenFOAM – p. 20

# Boundary conditions

There are three types of boundary conditions used in the model:

- No-slip conditions at walls, using turbulent wall functions.
- Constant pressure at the outlet.
- Given laminar velocity profile at the inlet, computed with a custom utility `laminarSwirlerEntrance`

$$u_z(x, y) = -2\bar{u} \left( 1 - \frac{2\sqrt{x^2 + y^2}}{D} \right)$$

They are specified in the directory `0` as files `p`, `U`, `k` and `epsilon`

Case studies in OpenFOAM – p. 21

## Results: Pressure

The whole pipe:



A cut through the center, around the fins:



Case studies in OpenFOAM – p. 22

# Results: Velocity

Velocity magnitude:

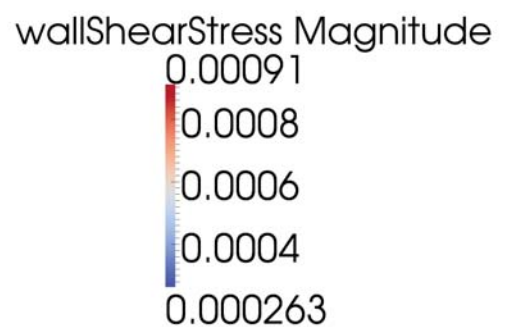


Velocity in  $x$ -direction, showing swirling:

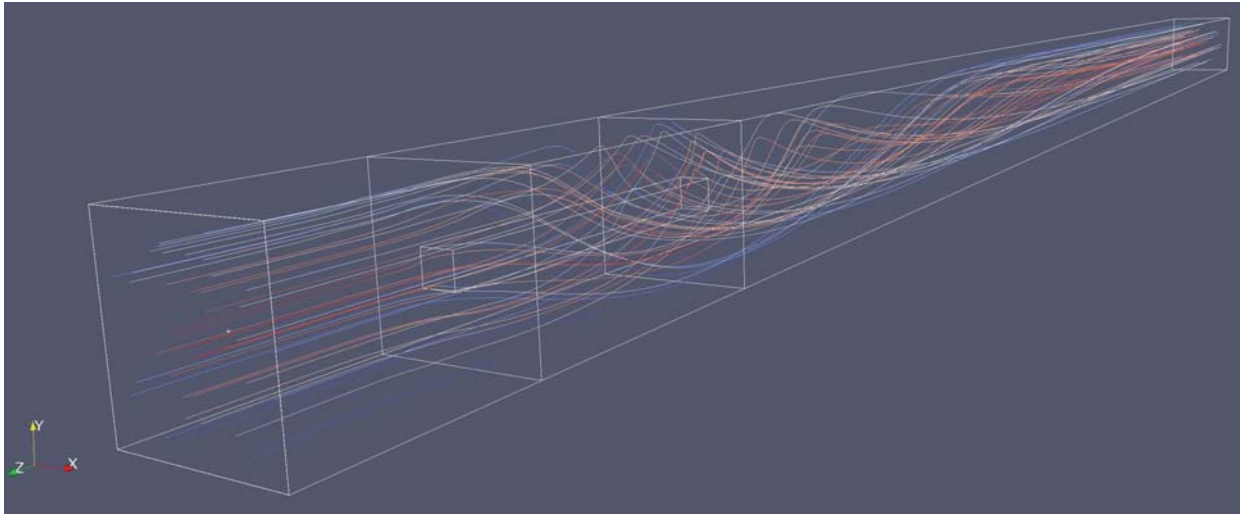


# Results: Wall shear stress

Shear stress at walls, computed with `wallShearStress`



# Results: Streamlines



Case studies in OpenFOAM – p. 25

## Heat flow in porous media

The Darcy equation

$$\vec{q} = -\frac{\bar{k}}{\mu} (\nabla p + \rho \vec{g})$$

The heat equation

$$\frac{\partial T}{\partial t} + \vec{q} \cdot \nabla T = \frac{k}{\rho_0 c} \nabla^2 T$$

The Boussinesq approximation

$$\rho = \rho_0 (1 - \beta(T - T_0))$$

Continuity of flow

$$\nabla \cdot \vec{q} = 0$$

Case studies in OpenFOAM – p. 26

# Dimensionless variables

Dimensionless temperature is defined as

$$\theta = \frac{T - T_0}{T_1 - T_0}$$

the dimensionless pressure as

$$\phi = \frac{\rho_0 c \kappa}{\mu k} (p + \rho_0 g L z)$$

and the dimensionless time as

$$\tau = \left( \frac{k}{\rho_0 c L^2} \right) t$$

Case studies in OpenFOAM – p. 27

## The Darcy-Lapwood system

By introduction the dimensionless field variables the heat equation becomes

$$\frac{\partial \theta}{\partial \tau} = \nabla \cdot ((\nabla \phi - \text{Ra} \theta \vec{z}) \theta + \nabla \theta)$$

and the continuity requirement is then

$$\nabla \cdot (\nabla \phi - \text{Ra} \theta \vec{z}) = 0$$

with the dimensionless porous Rayleigh number defined as

$$\text{Ra} = \frac{\rho_0^2 c g \beta (T_1 - T_0) \kappa L}{\mu k}$$

Case studies in OpenFOAM – p. 28



# A customized solver code

```
while (runTime.loop())
{
    Info<< "Time = " << runTime.timeName() << nl << endl;

    # include "readPISOControls.H"
    # include "CourantNo.H"

    for (int nonOrth=0; nonOrth<=nNonOrthCorr; nonOrth++)
    {
        fvScalarMatrix pEqn
        (
            // Darcy equation for porous flow
            fvm::laplacian(kappa / nu, p) + kappa / nu * fvc::div(gflux, rhok)
        );

        // Set reference pressure and solve Darcy equation
        pEqn.setReference(pRefCell, pRefValue);
        pEqn.solve();

        // Update velocity field and flux
        U = -kappa / nu * (fvc::grad(p) + rhok * g);
        phi = fvc::interpolate(U) & mesh.Sf();

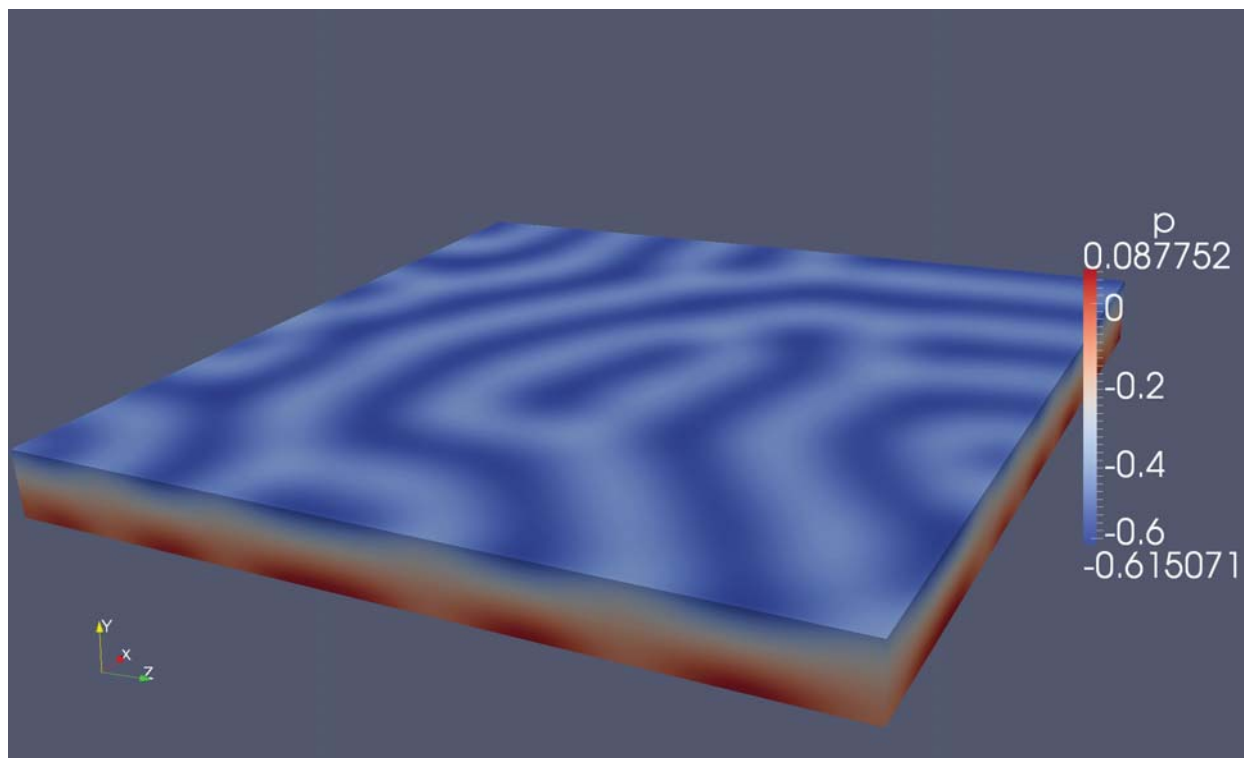
        solve
        (
            // Solve heat transport equation
            fvm::ddt(T) + fvm::div(phi, T) - fvm::laplacian(nu / Pr, T)
        );

        // Update kinematic density, based on Boussinesq approximation
        rhok = 1.0 - beta*(T - TRef);
    }

    runTime.write();
}
```

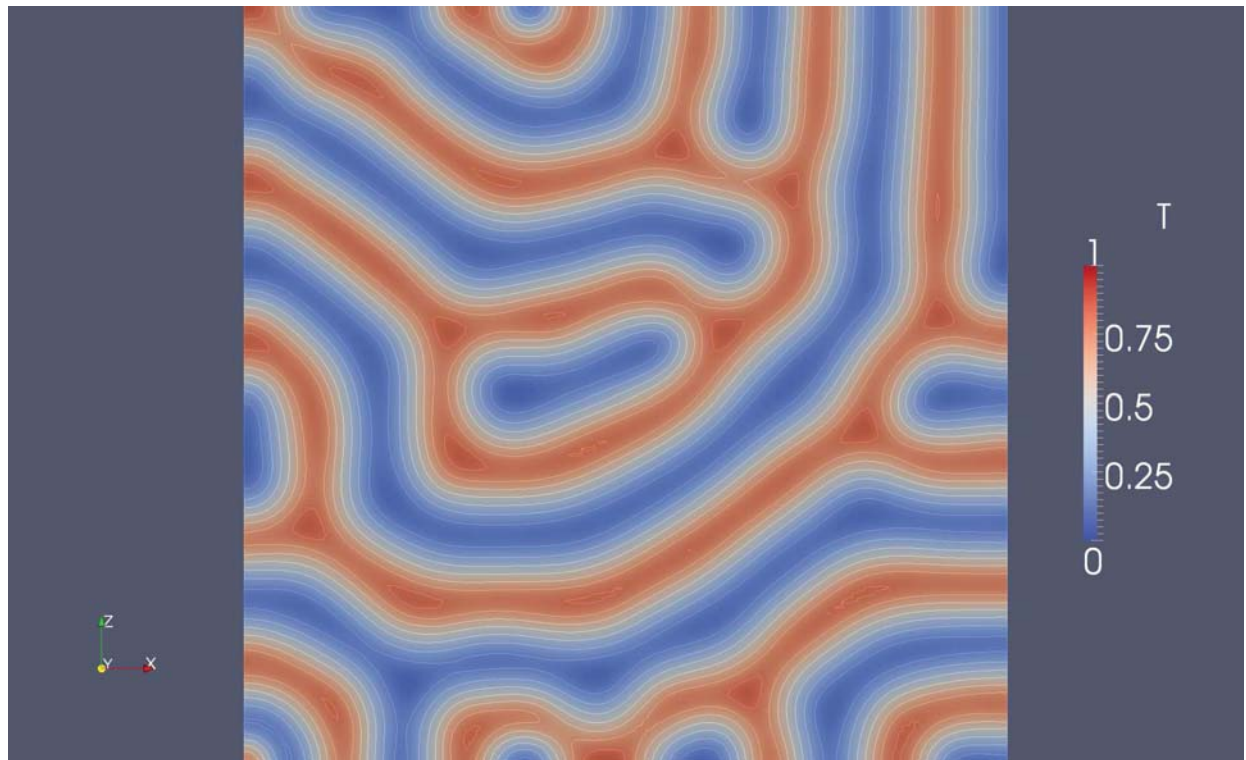
Case studies in OpenFOAM – p. 29

## Results for $Ra = 100$ , pressure



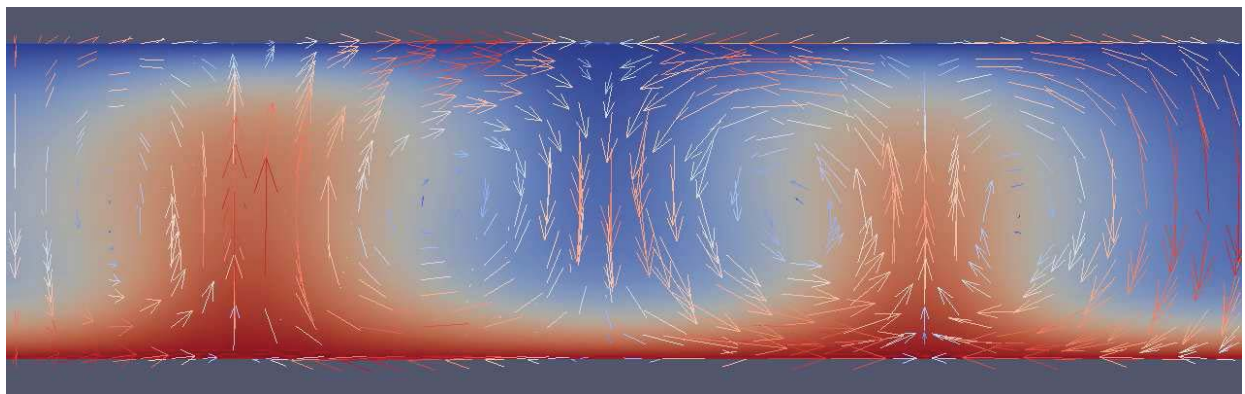
Case studies in OpenFOAM – p. 30

# Results for $Ra = 100$ , temperature



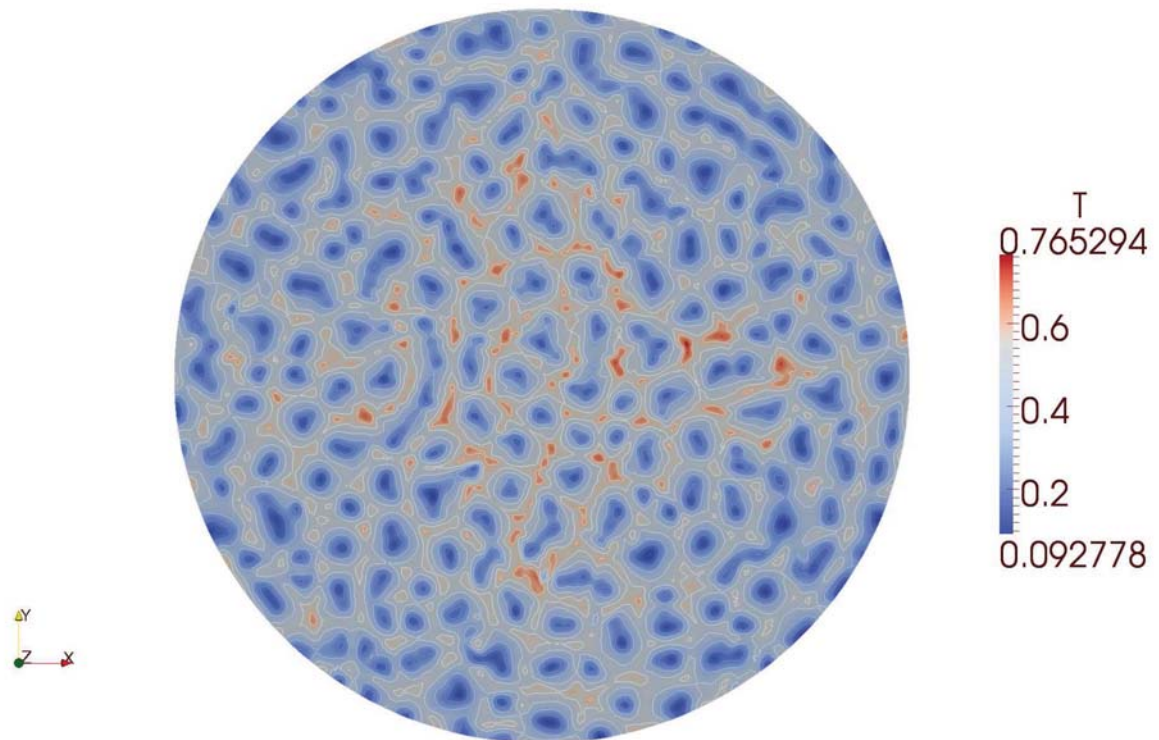
Case studies in OpenFOAM – p. 31

# Results for $Ra = 100$ , continued



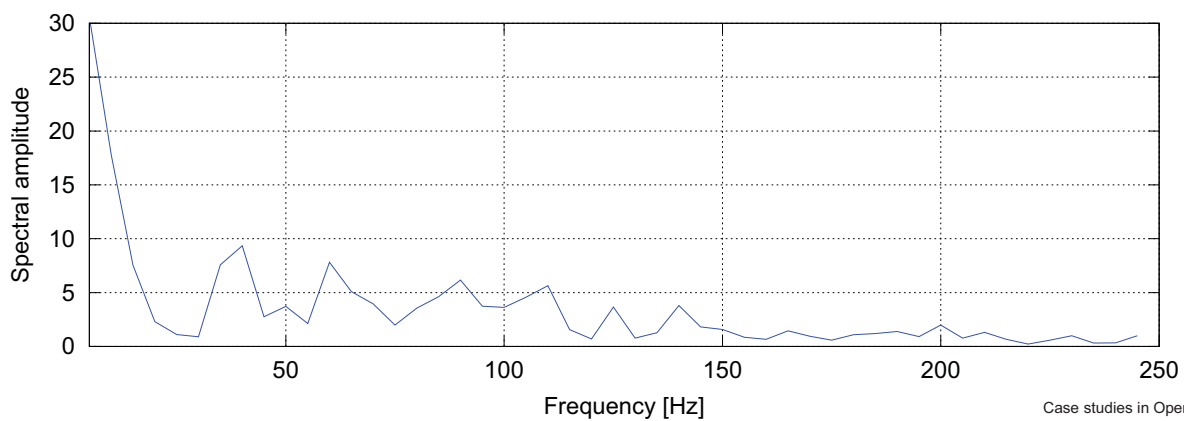
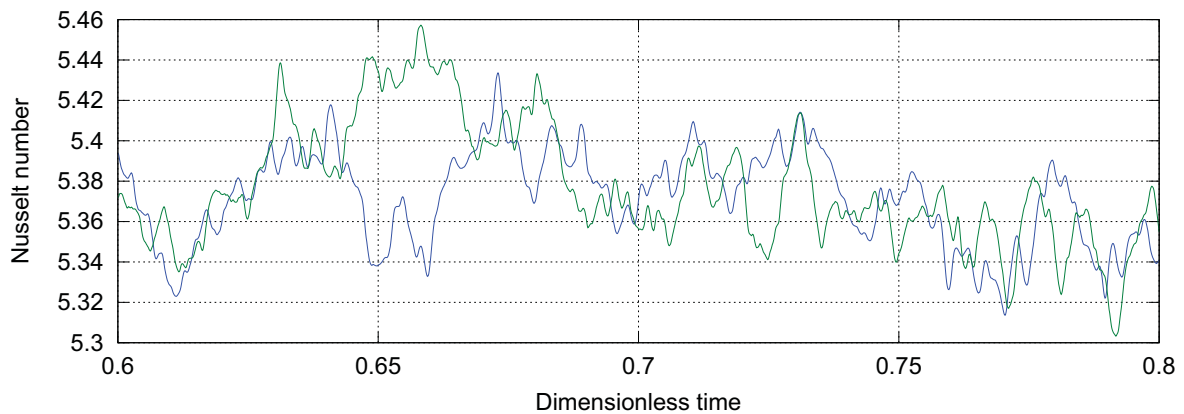
Case studies in OpenFOAM – p. 32

# Results for $Ra = 500$ , temperature



Case studies in OpenFOAM – p. 33

# Dimensionless flux from top and bottom



Case studies in OpenFOAM – p. 34

# Conclusion

- Both simple and complex geometries can be meshed, using the tools included
- When needed, customized programs can be written, but that can be quite demanding because of the complexity of the programming environment
- Standard flow problems, as well as customized problems can be solved with relative ease, using parallel processing when appropriate
- Visualization of results is performed in `paraview`, but further calculations can be performed with builtin libraries or custom programs
- Results compared to theory are generally accurate, but some care must be taken when calculating derivatives of fields

# *On preconditioning of matrices in two-by-two block form*

Owe Axelsson

Institute of Geonics, AS CR, Ostrava, The Czech Republic

Department of Information Technology, Uppsala University, Sweden

---

Institute of Geonics, Ostrava, December 1-3, 2010



Owe Axelsson, Owe.Axelsson@it.uu.se – p. 1/48

*This talk is based on the following three papers:*

- Owe Axelsson: Preconditioners for regularized saddle point matrices; in preparation.
- Owe Axelsson, Maya Neytcheva: A general approach to analyze preconditioners for two-by-two block matrices; submitted to NLA.
- Owe Axelsson, Radim Blaheta: Preconditioning of matrices partitioned in  $2 \times 2$  block form: eigenvalue estimates and Schwarz DD for mixed FEM, Numer. Linear Algebra Appl. 17(2010), pp. 787–810.

Owe Axelsson, Owe.Axelsson@it.uu.se – p. 2/48

## *Plan of the talk:*

- Introduction: Some examples of practical problems where saddle point matrices arise
- Preconditioners for saddle point problems and regularized saddle point problems
- A general approach to construct and control the accuracy of preconditioners for matrices in two-by-two block form
- Some numerical illustrations

Owe Axelsson, Owe.Axelsson@it.uu.se - p. 3/48

## *Introduction*

Matrices in  $2 \times 2$  block form

$$A = \begin{bmatrix} A_{11} & A_{12} \\ A_{21} & A_{22} \end{bmatrix}$$

arise naturally in several applications.

Owe Axelsson, Owe.Axelsson@it.uu.se - p. 4/48

## Examples:

- Flows in porous media, modelled by Darcy's equations,

$$\begin{aligned}K^{-1}\mathbf{u} + \nabla p &= 0 \quad \text{in } \Omega \\ \nabla \cdot \mathbf{u} &= f \quad \text{in } \Omega,\end{aligned}$$

where  $\mathbf{u} \cdot \mathbf{n} = q_1$  on  $\partial\Omega_D$ ,  $p = q_2$  on  $\partial\Omega_N$ .

- Mixed FEM for elliptic problems
- The elasticity equations for nearly incompressible materials can be formulated in a variational form (due to Hermann) as

$$\begin{aligned}\frac{1}{\nu}a(\mathbf{u}, \mathbf{v}) + b(\mathbf{v}, p) &= \frac{1}{2\nu\mu} \int_{\Gamma} (\mathbf{g}, \mathbf{v}) d\Omega \quad \forall \mathbf{v} \in \mathbf{V}, \\ b(\mathbf{u}, q) - (1 - 2\nu)(p, q) &= 0 \quad \forall q \in \mathbf{H}.\end{aligned}$$

Here  $a(\mathbf{u}, \mathbf{v}) = \sum_{i,j} \int_{\Omega} \epsilon_{i,j}(\mathbf{u}) \epsilon_{i,j}(\mathbf{v}) d\Omega$  is a  $H^1$ -elliptic form (Korn's inequality) with strains  $\epsilon_{i,j}$  and displacements  $\mathbf{u}$ , and  $b(\mathbf{u}, p) = \int_{\Omega} \text{div}(\mathbf{u}) p d\Omega$ , where  $p$  denotes the pressure function. The material parameter  $\nu$  ( $\nu < 1/2$ ), called Poisson ratio, becomes  $\nu = 1/2$  for incompressible materials.

Owe Axelsson, Owe.Axelsson@it.uu.se - p. 5/48

## Saddle point matrices

The above problems can be formulated as constrained optimization problems and lead to saddle point matrices in the form

$$\begin{bmatrix} A_{11} & A_{12} \\ A_{21} & 0 \end{bmatrix} = \begin{bmatrix} M & B^T \\ B & 0 \end{bmatrix}$$

or some regularized form thereof.

Owe Axelsson, Owe.Axelsson@it.uu.se - p. 6/48



## Nonsymmetric saddle point problems

Nonsymmetric saddle point problems arise, e.g., in the numerical solution of steady Navier–Stokes equations which are often solved via a sequence of linearized problems, referred to as the Oseen problem:

$$\begin{aligned} -\nu\Delta\mathbf{u} + (\mathbf{w} \cdot \nabla)\mathbf{u} + \nabla p &= \mathbf{f} \quad \text{in } \Omega \\ \nabla \cdot \mathbf{u} &= 0 \quad \text{in } \Omega \\ \mathbf{u} &= \mathbf{g} \quad \text{on } \partial\Omega \end{aligned}$$

Here  $\nu > 0$  is the kinematic viscosity coefficient,  $\Delta$  is the Laplace operator and  $\mathbf{w}$  is the current approximation of the velocity vector  $\mathbf{u}$ ;  $\mathbf{f} : \Omega \rightarrow \mathfrak{R}^d$  is the given force field and  $\mathbf{g} : \partial\Omega \rightarrow \mathfrak{R}^d$  the given boundary data.

The problem is to find the velocity field  $\mathbf{u} : \Omega \rightarrow \mathfrak{R}^d$  and pressure variable  $p : \Omega \rightarrow \mathfrak{R}$ .

The FEM discretization leads here to a saddle point matrix with a non-selfadjoint operator  $M$ .

Owe Axelsson, Owe.Axelsson@it.uu.se – p. 7/48

## Preconditioners and the CBS constant

Block diagonal preconditioners are easy to handle but in general not sufficiently accurate. For instance, for an spd matrix for the generalized eigenvalue problem,

$$\lambda \begin{bmatrix} A_{11} & 0 \\ 0 & A_{22} \end{bmatrix} \begin{bmatrix} x \\ y \end{bmatrix} = \begin{bmatrix} A_{11} & A_{12} \\ A_{21} & A_{22} \end{bmatrix} \begin{bmatrix} x \\ y \end{bmatrix}$$

it holds  $1 - \gamma \leq \lambda \leq 1 + \gamma$ ,

where  $\gamma = \rho(A_{11}^{-1}A_{12}A_{22}^{-1}A_{21})$ , the so-called CBS constant, which can be seen to measure the relative strength of the off-diagonal blocks.

Here  $\gamma < 1$  but in many ill-conditioned problems  $\gamma$  can take values very close to unit value which leads to large condition numbers  $(1 + \gamma)/(1 - \gamma)$ .

Similarly, for the Schur complement matrix  $S_2 = A_{22} - A_{21}A_{11}^{-1}A_{12}$ , it holds

$$(1 - \gamma^2)A_{22} \leq S_2 \leq A_{22} \quad (\text{inequalities in a positive semidefinite sense}).$$

The above relations are of particular interest when a finite element mesh is separated in 'coarse' and 'fine' mesh nodes. Then, with the use of [hierarchical basis functions](#),  $A_{22}$  becomes the coarse mesh matrix.

Owe Axelsson, Owe.Axelsson@it.uu.se – p. 8/48



## Preconditioners and the CBS constant, cont.

More accurate approximations can be constructed by use of an approximate block matrix factorization in the form

$$P = \begin{bmatrix} I_1 & 0 \\ A_{21}C_{11} & I_2 \end{bmatrix} \begin{bmatrix} \tilde{A}_{11} & 0 \\ 0 & S \end{bmatrix} \begin{bmatrix} I_1 & B_{11}A_{12} \\ 0 & I_2 \end{bmatrix}.$$

Here  $B_{11}, C_{11}$  are some sparse approximations of  $A_{11}^{-1}$  (possibly one of them is a zero block) and  $\tilde{A}_{11}^{-1}$  denotes an approximation, often only implicitly defined by use of inner iterations to solve the arising systems with matrix  $A_{11}$ . Finally,  $S$  denotes a nonsingular approximation of  $S_2$ .

To measure the accuracy of such approximations a more generally applicable measure ( $\sigma$ ) than the CBS constant will be used. This measure can be controlled by the choice of the approximations  $B_{11}, C_{11}$ .

In the talk we present first some comprehensible results for clustering of eigenvalues for preconditioning of saddle point matrices and discuss then shortly some new results for the general matrix factorization method.

Owe Axelsson, Owe.Axelsson@it.uu.se – p. 9/48

## Efficient preconditioning for saddle point matrices

Given: a possibly nonsymmetric, real valued saddle point matrix in the form

$$\mathcal{M} = \begin{bmatrix} M & B^T \\ C & 0 \end{bmatrix},$$

where  $M$  has order  $n \times n$  and  $B, C$  have orders  $m \times n$ ,  $m \leq n$ .

Next:

- We give assumptions to enable to state that  $\mathcal{M}$  is nonsingular
- If they do not hold, we consider a regularization of  $\mathcal{M}$  to make the regularized matrix nonsingular.

For both cases we present efficient preconditioners for which a strong clustering of the eigenvalues of the preconditioned matrix take place.

Owe Axelsson, Owe.Axelsson@it.uu.se – p. 10/48

## Preconditioning for a nonsingular saddle point matrix

The construction of the preconditioner is based on the following assumption.

Let  $\mathcal{R}(A)$  denote the range of an operator (A).

### Assumption 1

(i) There exists a nonsingular matrix  $W$  (possibly  $W = I$ ) such that  $\widetilde{M} = M + B^T W^{-1} C$  is nonsingular. Note that this implies in particular that  $\mathcal{N}(C) \cap \mathcal{N}(M) = \emptyset$ ,  $\mathcal{N}(B) \cap \mathcal{N}(M^T) = \emptyset$ .

(ii) The intersection of  $\mathcal{N}(C)$  with the one-to-one transformation of  $\mathcal{R}(B^T)$  with  $\widetilde{M}^{-1}$ , denoted  $\widetilde{\mathcal{R}}(B^T)$ , includes only the trivial vector, that is,  $\mathcal{N}(C) \cap \widetilde{\mathcal{R}}(B^T) = \emptyset$ .

(iii) Matrix  $B$  has full rank. Note that if  $C = B$ , then this condition implies  $\mathcal{N}(B) \cap \mathcal{R}(B^T) = \emptyset$ , i.e. condition (ii) holds.

Owe Axelsson, Owe.Axelsson@it.uu.se – p. 11/48

## Preconditioning for a nonsingular saddle point matrix, cont.

**Lemma 1** Under Assumption 1 it follows that  $\mathcal{M}$  is nonsingular.

**Proof** The homogeneous system

$$\begin{bmatrix} M & B^T \\ C & 0 \end{bmatrix} \begin{bmatrix} x \\ y \end{bmatrix} = \begin{bmatrix} 0 \\ 0 \end{bmatrix} \quad (1)$$

implies that  $Mx + B^T y = 0$  and  $Cx = 0$ . Then  $B^T W^{-1} Cx = 0$  so  $(M + B^T W^{-1} C)x + B^T y = \widetilde{M}x + B^T y = 0$ , or  $x = -\widetilde{M}^{-1} B^T y$ . But then  $x$  belongs to a one-to-one transformation of  $\mathcal{R}(B^T)$  and, since  $x \in \mathcal{N}(C)$ , by Assumption 1, it follows that  $x = 0$ . Then  $B^T y = 0$  so, since  $B$  has full rank, it follows that  $y = 0$ . Hence the homogeneous system (1) has only the trivial solution. ■

Owe Axelsson, Owe.Axelsson@it.uu.se – p. 12/48

## Preconditioning for a nonsingular saddle point matrix, cont.

For the nonsingular matrix  $\mathcal{M}$  it turns out that the preconditioner  $\begin{bmatrix} M & \alpha B^T \\ 0 & -W \end{bmatrix}$ ,  $\alpha = 2$ , can be very efficient in clustering the eigenvalues of the preconditioned matrix.

The corresponding generalized eigenvalue problem,

$$\lambda \begin{bmatrix} M & 2B^T \\ 0 & -W \end{bmatrix} \begin{bmatrix} x \\ y \end{bmatrix} = \begin{bmatrix} M & B^T \\ C & 0 \end{bmatrix} \begin{bmatrix} x \\ y \end{bmatrix} \quad (2)$$

implies  $\lambda y = -W^{-1}Cx$ . Since both matrices in (2) are nonsingular, it follows that  $\lambda \neq 0$ .

Hence  $y = -\lambda^{-1}W^{-1}Cx$  and from the first equation in (2) it follows that

$$(\lambda - 1)Mx = \left(-\lambda + 2 - \frac{1}{\lambda}\right)B^TW^{-1}Cx, \text{ or}$$

$$\lambda(\lambda - 1)Mx = -(\lambda - 1)^2B^TW^{-1}Cx. \quad (3)$$

It follows that if  $x \in \mathcal{N}(C)$  or  $x \in \mathcal{N}(B)$ , then  $\lambda = 1$ .

Owe Axelsson, Owe.Axelsson@it.uu.se – p. 13/48

## Preconditioning for a nonsingular saddle point matrix, cont.

Likewise, if  $x \in \mathcal{N}(M)$  (i.e., then  $x \notin \mathcal{N}(C)$ ), then  $\lambda = 1$ . The dimension of  $\mathcal{N}(C)$  is at least  $n - m$ . Assume that the dimension of  $\mathcal{N}(M)$  equals  $\nu$  (it is seen from assumptions made that  $\nu < m$ ). Then the multiplicity of eigenvalues  $\lambda = 1$  equals  $n - m + \nu$ .

If  $x \notin \mathcal{N}(M) \cup \mathcal{N}(B) \cup \mathcal{N}(C)$ , then  $\lambda \neq 1$  and it follows from (3) that

$$\lambda Mx = -(\lambda - 1)B^TW^{-1}Cx, \text{ or}$$

$$\lambda \widetilde{M}x = B^TW^{-1}Cx, \quad x \neq 0, \quad (4)$$

where we recall that  $\widetilde{M} = M + B^TW^{-1}C$ .

We will use a matrix  $W$  involving a parameter  $r$  in the form  $\frac{1}{r}W$ , where  $r > 0$  and  $W$  is nonsingular. Then (4) takes the form

$$\lambda(M + rB^TW^{-1}C)x = rB^TW^{-1}Cx, \quad x \neq 0. \quad (5)$$

The above implies that for eigenvalues  $\lambda \neq 1$ , it holds  $\lambda = \lambda_r \rightarrow 1$  as  $r \rightarrow \infty$ .

This shows that all eigenvalues cluster at the unit value as  $r \rightarrow \infty$ .

Owe Axelsson, Owe.Axelsson@it.uu.se – p. 14/48

## Preconditioning for a nonsingular saddle point matrix, cont.

We collect the results in a theorem.

**Theorem 1** *Let Assumption 1 hold. Then the preconditioned matrix*

$$\begin{bmatrix} M & 2B^T \\ 0 & -W_r \end{bmatrix}^{-1} \begin{bmatrix} M & B^T \\ C & 0 \end{bmatrix}, \text{ where } W_r = \frac{1}{r}W,$$

has eigenvalues  $\lambda = 1$  of multiplicity at least  $n - m + \nu$ , where  $\nu$  ( $\nu \leq m$ ) is the dimension of  $\mathcal{N}(M)$ . The remaining eigenvalues satisfy  $\lambda = \lambda_r \rightarrow 1$  as  $r \rightarrow \infty$ .

If  $C = B$  and  $M = M^T$ , then

$$\frac{1}{1 + \mu_1/r} \leq \lambda \leq \frac{1}{1 - \mu_0/r},$$

where  $\mu_0, \mu_1$  are the extreme eigenvalues of

$$Mx = \mu B^T W^{-1} Bx, \quad x \notin \mathcal{N}(B).$$

Owe Axelsson, Owe.Axelsson@it.uu.se – p. 15/48

## Preconditioning for a regularized saddle point matrix

The matrix  $M_r = M + rB^T W^{-1} C$  can be said to be a regularized form of  $M$ . The corresponding regularized saddle point matrix takes the form

$$\widetilde{\mathcal{M}}_r = \begin{bmatrix} M_r & B^T \\ C & 0 \end{bmatrix}.$$

Note that the regularized and unregularized systems,

$$\widetilde{\mathcal{M}}_r \begin{bmatrix} x \\ y \end{bmatrix} = \begin{bmatrix} f \\ 0 \end{bmatrix} \quad \text{and} \quad \mathcal{M} \begin{bmatrix} x \\ y \end{bmatrix} = \begin{bmatrix} f \\ 0 \end{bmatrix}$$

have the same (unique if  $\mathcal{M}$  is nonsingular) solution. However, depending on the choice of  $W$ , applying actions of  $\widetilde{\mathcal{M}}_r$  can be costly.

Owe Axelsson, Owe.Axelsson@it.uu.se – p. 16/48

## Preconditioning for a regularized saddle point matrix, cont.

Instead we shall only use such a regularized form, where  $M$  is replaced by  $M_{r_0}$ , in the preconditioner to  $\mathcal{M}$ . Here  $M_{r_0} = M + r_0 B^T W^{-1} C$ , and  $r_0 < r$ , where  $r$  is another method parameter.

In addition, the above regularization does not handle the case where  $\mathcal{M}$  is singular, due to a rank deficient matrix  $B$ . We replace then the zero (2,2) block in the matrix, and in its preconditioner with  $-W_r = -\frac{1}{r}W$ .

This means that the matrix  $\mathcal{M}$  is perturbed with the matrix  $\begin{bmatrix} 0 & 0 \\ 0 & -W_r \end{bmatrix}$ . We assume that  $r$  takes sufficiently large values so that the corresponding perturbation of the solution is negligible or, otherwise, we can use some steps of a defect-correction method to correct for this perturbation.

From the corresponding block matrix factorization,

$$\mathcal{M}_r = \begin{bmatrix} M & B^T \\ C & -W_r \end{bmatrix} = \begin{bmatrix} M_r & B^T \\ 0 & -\frac{1}{r}W \end{bmatrix} \begin{bmatrix} I_1 & 0 \\ -rW^{-1}C & I_2 \end{bmatrix},$$

it follows that  $\mathcal{M}_r$  is nonsingular if and only if  $M_r = M + rB^T W^{-1}C$  is nonsingular.

Owe Axelsson, Owe.Axelsson@it.uu.se – p. 17/48

## Preconditioning for a regularized saddle point matrix, cont.

We make now the following assumption.

**Assumption 2** The matrix  $M_r = M + rB^T W^{-1}C$  is nonsingular for all  $r \geq r_0$  for some  $r_0 > 0$ .

The preconditioner to  $\mathcal{M}_r$  will be taken as  $\begin{bmatrix} M_{r_0} & B^T \\ 0 & -W_r \end{bmatrix}$ , where  $W_r = \frac{1}{r}W$  and the corresponding generalized eigenvalue problem takes the form

$$\lambda \begin{bmatrix} M_{r_0} & B^T \\ 0 & -W_r \end{bmatrix} \begin{bmatrix} x \\ y \end{bmatrix} = \begin{bmatrix} M & B^T \\ C & -W_r \end{bmatrix} \begin{bmatrix} x \\ y \end{bmatrix},$$

or

$$(\lambda - 1) \begin{bmatrix} M_{r_0} & B^T \\ 0 & -W_r \end{bmatrix} \begin{bmatrix} x \\ y \end{bmatrix} = \begin{bmatrix} -r_0 B^T W^{-1} C x \\ C x \end{bmatrix}.$$

It follows that  $\lambda = 1$  for any eigenvector  $\begin{bmatrix} x \\ y \end{bmatrix}$  in the form  $x \in \mathcal{N}(C)$ ,  $y \in \mathbb{R}^m$ .

Owe Axelsson, Owe.Axelsson@it.uu.se – p. 18/48

## Preconditioning for a regularized saddle point matrix, cont.

We collect the results in the next theorem.

**Theorem 2** Assume that  $M + rB^T W^{-1}C$  is nonsingular for all  $r \geq r_0, r_0 > 0$ . Then the preconditioned matrix

$$\begin{bmatrix} M_{r_0} & B^T \\ 0 & -W_r \end{bmatrix}^{-1} \begin{bmatrix} M & B^T \\ C & -W_r \end{bmatrix}$$

has eigenvalues  $\lambda = 1$  of multiplicity at least  $n - m$ . As  $r_0 \rightarrow \infty$ , the remaining eigenvalues cluster about the point  $r/r_0$ .

( $W_r = 1/rW$ )

Owe Axelsson, Owe.Axelsson@it.uu.se - p. 19/48

## Two-by-two block matrices

We present now a general algebraic approach to construct, analyze and control the accuracy of preconditioners for matrices in two-by-two block form.

This includes symmetric and nonsymmetric matrices, as well as indefinite matrices.

The general form of a matrix in two-by-two block form is:

$$A = \begin{bmatrix} A_{11} & A_{12} \\ A_{21} & A_{22} \end{bmatrix}$$

We assume here that both

- $A_{11}$
  - $S_2(A) = A_{22} - A_{21}A_{11}^{-1}A_{12}$  (the Schur complement)
- are nonsingular, which implies that  $A$  is also nonsingular.

Owe Axelsson, Owe.Axelsson@it.uu.se - p. 20/48

## General form: approximate block matrix factorization

A general form of an approximate block factorization of the matrix  $A$  takes the form

$$P = \begin{bmatrix} I_1 & 0 \\ A_{21}C_{11} & I_2 \end{bmatrix} \begin{bmatrix} \tilde{A}_{11} & 0 \\ 0 & S \end{bmatrix} \begin{bmatrix} I_1 & B_{11}A_{12} \\ 0 & I_2 \end{bmatrix}.$$

- $B_{11}$  and  $C_{11}$  are approximations of  $A_{11}^{-1}$  (possibly zero matrices but normally sparse and given on explicit form)
- $\tilde{A}_{11}^{-1}$  denotes some approximation of  $A_{11}^{-1}$ , often only implicitly defined via inner iterations
- $S$  is a nonsingular approximation of  $S_2$ .

When we use inner iterations, the preconditioner at each outer iteration step becomes variable. In such a case, the outer iteration method must, in general, be some form of a generalized conjugate gradient method, such as GCG, GMRES or the modified Least Squares GMRES method.

Owe Axelsson, Owe.Axelsson@it.uu.se – p. 21/48

$$P = \begin{bmatrix} I_1 & 0 \\ A_{21}C_{11} & I_2 \end{bmatrix} \begin{bmatrix} \tilde{A}_{11} & 0 \\ 0 & S \end{bmatrix} \begin{bmatrix} I_1 & B_{11}A_{12} \\ 0 & I_2 \end{bmatrix}$$

Further, we consider the special but important case when only one of  $B_{11}$  and  $C_{11}$  equals zero. In this case,  $P$  is block-triangular and if, say,  $B_{11} = 0$ , then  $P$  takes the form

$$P = \begin{bmatrix} \tilde{A}_{11} & 0 \\ A_{21} & S \end{bmatrix}.$$

This corresponds to the choice  $C_{11} = \tilde{A}_{11}^{-1}$  and  $B_{11} = 0$  above. Note that the computational expense of this preconditioner is essentially the same as for the block-diagonal preconditioner but, as we shall see, it can be much more efficient.

The rate of convergence of preconditioned conjugate gradient methods depends on the distribution of eigenvalues of  $P^{-1}A$ , which we now estimate.

In the analysis, we introduce a scalar

$$\sigma$$

which plays a role similar to the CBS constant  $\gamma$ , or rather to

$$\gamma^2/(1 - \gamma^2)$$

but is of relevance not only for symmetric and positive definite matrices. As we shall see,  $\sigma = 1$  for indefinite problems on saddle point form, but for other types of problems it is important that  $C_{11}$  (and/or  $B_{11}$ ) is a sufficiently accurate preconditioner to limit the upper bound of  $\sigma$  to a viable value.

Owe Axelsson, Owe.Axelsson@it.uu.se - p. 23/48

$$A = \begin{bmatrix} A_{11} & A_{12} \\ A_{21} & A_{22} \end{bmatrix}; P = \begin{bmatrix} I_1 & 0 \\ A_{21}C_{11} & I_2 \end{bmatrix} \begin{bmatrix} \tilde{A}_{11} & 0 \\ 0 & S \end{bmatrix} \begin{bmatrix} I_1 & B_{11}A_{12} \\ 0 & I_2 \end{bmatrix}$$

**Proposition 1** Let  $A, C$  be defined as above. Then  $P^{-1}A$  is similarly equivalent to (i.e. the eigenvalues of  $P^{-1}A$  equal those of) the matrix

$$\left( \begin{bmatrix} I_1 & 0 \\ 0 & I_2 \end{bmatrix} + \begin{bmatrix} (\tilde{A}_{11}^{-1}A_{11} - I_1) & 0 \\ 0 & (S^{-1}S_2 - I_2) \end{bmatrix} \right) \times \\ \left( \begin{bmatrix} I_1 & 0 \\ 0 & I_2 \end{bmatrix} + \begin{bmatrix} 0 & 0 \\ \tilde{A}_{21} & 0 \end{bmatrix} \right) \left( \begin{bmatrix} I_1 & 0 \\ 0 & I_2 \end{bmatrix} + \begin{bmatrix} 0 & \tilde{A}_{12} \\ 0 & 0 \end{bmatrix} \right)$$

where  $\tilde{A}_{12} = (I_1 - B_{11}A_{11})A_{11}^{-1}A_{12}$ ,  $\tilde{A}_{21} = S_2^{-1}A_{21}(I_1 - C_{11}A_{11})$ .

**Proof** Use the similarity transformation  $\begin{bmatrix} I_1 & B_{11}A_{11} \\ 0 & I_2 \end{bmatrix} P^{-1}A \begin{bmatrix} I_1 & -B_{11}A_{11} \\ 0 & I_2 \end{bmatrix}$ . ■

Owe Axelsson, Owe.Axelsson@it.uu.se - p. 24/48



The limit case:  $\tilde{A}_{11}^{-1} = A_{11}^{-1}$ ,  $S = S_2$

Note that in this case we do not need to assume that  $I + G$  is diagonalizable.

**Proposition 2** Consider  $P$  with  $\tilde{A}_{11} = A_{11}$  and  $S = S_2$ . Then, for the generalized eigenvalue problem  $A\mathbf{x} = \lambda P\mathbf{x}$  there is a multiple eigenvalue  $\lambda = 1$  for eigenvectors  $x = [x_1, x_2]^T$ , where

$$x_1 \in \ker(A_{21}(I_1 - C_{11}A_{11})), \quad x_2 \in \ker((I_1 - B_{11}A_{11})A_{11}^{-1}A_{12}).$$

The remaining eigenvalues equal  $\lambda = 1 + \frac{1}{2}\zeta(1 \pm \sqrt{1 + 4/\zeta})$  for  $\zeta$  being any nonzero eigenvalue of the matrix product  $\tilde{A}_{12}\tilde{A}_{21}$ , where  $\tilde{A}_{12} = (I_1 - B_{11}A_{11})A_{11}^{-1}A_{12}$  and  $\tilde{A}_{21} = S_2^{-1}A_{21}(I_1 - C_{11}A_{11})$ .

Owe Axelsson, Owe.Axelsson@it.uu.se - p. 25/48

The limit case:  $\tilde{A}_{11}^{-1} = A_{11}^{-1}$ ,  $S = S_2$

**Proposition 2 (cont.)**

If  $C_{11} = B_{11}$ ,  $A$  is symmetric and  $S_2$  is positive definite, then the eigenvalues  $\zeta$  are real and positive, and we obtain

$$\lambda_{\max} = 1 + \frac{1}{2}\sigma(1 + \sqrt{1 + 4/\sigma}), \quad \lambda_{\min} = \frac{\sqrt{1 + 4/\sigma} - 1}{\sqrt{1 + 4/\sigma} + 1},$$

where  $\sigma = \rho(\tilde{A}_{12}\tilde{A}_{21})$  and  $0 < \zeta \leq \sigma$ . In the general case of nonsymmetric matrices, letting  $\sigma = \|\tilde{A}_{12}\tilde{A}_{21}\|$ , then for the absolute values of the eigenvalues it holds that  $\lambda_{\min} \leq |\lambda| \leq \lambda_{\max}$ .

The value of  $\sigma$  can be large if  $B_{11}$  and  $C_{11}$  are less accurate approximations of  $A_{11}^{-1}$ .

Owe Axelsson, Owe.Axelsson@it.uu.se - p. 26/48

When  $A_{22}$  is nonsingular, a more visible connection between the measures

$$\gamma = \rho(A_{11}^{-1}A_{12}A_{22}^{-1}A_{21}) \quad \text{and}$$

$\sigma = \rho((I_1 - B_{11}A_{11})A_{11}^{-1}A_{12}S_2^{-1}A_{21}(I_1 - C_{11}A_{11}))$  can be established. Using the Sherman-Morrison-Woodbury formula for the matrix product  $Q = A_{11}^{-1}A_{12}S_2^{-1}A_{21}$ , which is a factor in  $\sigma$ , it holds

$$\begin{aligned} Q &= A_{11}^{-1}A_{12} \left( A_{22} - A_{21}A_{11}^{-1}A_{12} \right)^{-1} A_{21} \\ &= A_{11}^{-1}A_{12} \left[ A_{22}^{-1} + A_{22}^{-1}A_{21} \left( A_{11} - A_{12}A_{22}^{-1}A_{21} \right)^{-1} A_{12}A_{22}^{-1} \right] A_{21} \\ &= A_{11}^{-1}A_{12}A_{22}^{-1}A_{21} + A_{11}^{-1}A_{12}A_{22}^{-1}A_{21}(I_1 - A_{11}^{-1}A_{12}A_{22}^{-1}A_{21})^{-1}A_{11}^{-1}A_{12}A_{22}^{-1}A_{21} \\ &= \Gamma + \Gamma(I_1 - \Gamma)^{-1}\Gamma \\ &= \Gamma(I_1 - \Gamma)^{-1}, \end{aligned}$$

where  $\Gamma = A_{11}^{-1}A_{12}A_{22}^{-1}A_{21}$ .

**Proposition 3** Assume that  $A$  is symmetric and positive definite,  $C_{11} = B_{11}$ ,  $\tilde{A}_{11} = A_{11}$  and  $S = S_2$ . Let  $\sigma = \rho(\tilde{A}_{12}\tilde{A}_{21})$ , where  $\tilde{A}_{12}$ ,  $\tilde{A}_{21}$  are defined in Proposition 1. Then

$$\sigma \leq \frac{\gamma^2}{1 - \gamma^2} \|I_1 - B_{11}A_{11}\|^2. \quad (6)$$

## Block-diagonal preconditioners for saddle point matrices

The block-diagonal preconditioner  $P = \begin{bmatrix} A_{11} & 0 \\ 0 & S_2 \end{bmatrix}$ , however, is directly applicable for saddle point problems, where  $A_{22} = 0$ . In this case  $S_2 = -A_{21}A_{11}^{-1}A_{12}$  and

$$\sigma = \mp \rho(A_{11}^{-1}A_{12}S^{-1}A_{21}) = \begin{cases} -1 & \text{if } S = S_2 \\ +1 & \text{if } S = -S_2 \end{cases}$$

This implies the next proposition.

**Proposition 4** Let  $A = \begin{bmatrix} A_{11} & A_{12} \\ A_{21} & 0 \end{bmatrix}$  be symmetric, where  $A_{11}$  and  $S_2 = -A_{21}A_{11}^{-1}A_{12}$

are nonsingular (i.e.,  $A_{21}$  has full rank). Then the preconditioned matrix  $P^{-1}A$ , where

$$P = \begin{bmatrix} A_{11} & 0 \\ 0 & S \end{bmatrix}, \text{ has eigenvalues } \lambda = \begin{cases} 1 \pm \sqrt{5}, & \text{if } S = -S_2 \\ 1 \pm i\sqrt{3}, & \text{if } S = S_2 \end{cases}$$

There are only three eigenvalues of  $P^{-1}A$ , the unit value plus either of the two eigenvalue pairs given above.

Owe Axelsson, Owe.Axelsson@it.uu.se – p. 29/48

## Block-triangular preconditioners

Clearly, the optimal balance to get the smallest total computational cost, including the costs for the inner iterations and for the Schur complement matrix, is problem dependent, i.e., must be analyzed for each separate type of problem.

The most efficient form of the preconditioner is in general of block-tridiagonal form. If we let  $C_{11} = \tilde{A}_{11}^{-1}$  and, for simplicity, let  $B_{11} = 0$  then it takes the form

$$P = \begin{bmatrix} \tilde{A}_{11}^{-1} & 0 \\ A_{21} & S_2 \end{bmatrix}$$

and

$$\sigma = \|A_{11}^{-1}A_{12}S_2^{-1}A_{21}(I_1 - \tilde{A}_{11}^{-1}A_{11})\|.$$

Here we can control the value of  $\sigma$ , and make it arbitrarily small, by making a sufficient number of inner iterations in solving the arising systems with matrix  $A_{11}$ .

Owe Axelsson, Owe.Axelsson@it.uu.se – p. 30/48

## *Approximations of Schur complement matrices*

For ill-conditioned problems, for example when the LBB – stability condition is violated, one can use some form of regularization of the problem. This is similar to the use of a penalized or augmented Lagrangian method for general constrained optimization

problems. For instance, if the given saddle point matrix has the form  $\mathcal{A} = \begin{bmatrix} A & B^T \\ B & 0 \end{bmatrix}$ ,

then the matrix for the regularized problem (which actually has the same solution) has the form

$$\mathcal{A}_r = \begin{bmatrix} A + rB^T B & B^T \\ B & 0 \end{bmatrix},$$

where  $r$  can be a large penalization parameter.

As has been shown in an earlier works, here the Schur complement matrix approaches the value  $\frac{1}{r}I_2$ , where  $I_2$  is an identity matrix, so there is no need to precondition the Schur complements in the outer iteration method. In the ideal case, using a block-diagonal preconditioner, there will only be three to four outer iterations for large values of the parameter  $r$ .

Owe Axelsson, Owe.Axelsson@it.uu.se – p. 31/48

## *How to solve with the modified pivot block?*

However, here the difficulty is left to the solution of the pivot block matrix.

This can be handled by some form of a domain decomposition and Schwarz alternating iteration method, for instance.

The major intention of this presentation is to introduce the eigenvalue analysis and the handling of various arising matrices, using methods such as Schwarz alternating iteration method will therefore not be taken up further here.

Owe Axelsson, Owe.Axelsson@it.uu.se – p. 32/48

## Numerical illustrations

**Problem 1 (Convection-diffusion problem)** Find  $u$  satisfying the equation

$$\begin{aligned} -\varepsilon \Delta u + (\mathbf{b} \cdot \nabla) u &= f(x, y) \text{ in } \Omega \\ u(x, y) &= g(x, y) \text{ on } \Gamma_D, \quad \frac{\partial u}{\partial n} = 0 \text{ on } \Gamma_N, \end{aligned}$$

where  $\Omega = [0, 1]^2$ ,  $\Gamma_D \cup \Gamma_N = \partial\Omega$  and  $\Gamma_D \cap \Gamma_N = \emptyset$  and  $0 < \varepsilon \leq 1$ .

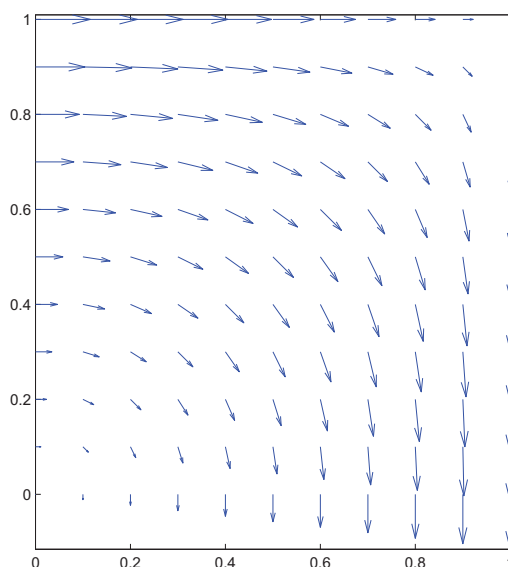
We choose  $\mathbf{b} = \begin{bmatrix} 2y(1-x^2) \\ -2x(1-y^2) \end{bmatrix}$ , which represents a quarter of a vortex flow, centered at the origin, visualized in the following figure. The boundary

conditions are of inhomogeneous Dirichlet type on  $x = 0$ ,  $x = 1$ ,  $y = 1$  and of homogeneous Neumann type on  $y = 0$ .

The problem is discretized using piece-wise linear conforming finite elements. (Within this setting we do not consider very strongly convection dominated problems.)

Owe Axelsson, Owe.Axelsson@it.uu.se – p. 33/48

## Numerical illustrations: test problem 1



The vector  $\mathbf{b}$  in Problem 1

## Numerical illustrations: test problem 2

**Problem 2 (Moving interface problem)** Simulation of a moving interface with a constant speed by using the Cahn-Hilliard equation, written in the form of a coupled system of two partial differential equations:

$$\begin{aligned}
 \eta - \Psi'(C) + \alpha\Delta C &= 0, & x \in \Omega, & t > 0 \\
 -\beta\Delta\eta + \frac{\partial C}{\partial t} + (\mathbf{b} \cdot \nabla)C &= 0, & x \in \Omega, & t > 0 \\
 \frac{\partial C}{\partial \mathbf{n}} = 0, \quad \frac{\partial \eta}{\partial \mathbf{n}} &= 0, & x \in \partial\Omega, & t > 0, \\
 C(x, 0) &= C_0(x) & x \in \Omega.
 \end{aligned} \tag{7}$$

Here the unknown function  $C$  (the concentration) is a continuous scalar variable that describes the diffusive interface profile. It has constant value in each phase,  $\pm 1$ , and changes rapidly but in a continuous manner from one to the other in an interface strip of certain thickness. The function  $\Psi$  is a double-well function with two minima at  $\pm 1$ , corresponding to the two stable phases. The variable  $\eta = \Psi'(C) - \alpha\Delta C$  is the so-called chemical potential.  $\alpha, \beta$  are constant and positive problem parameters.

Owe Axelsson, Owe.Axelsson@it.uu.se - p. 35/48

## Numerical illustrations: test problem 2

For the particular test problem we use  $\Psi(C) = \frac{1}{4}(C + 1)^2(C - 1)^2$ . The domain of definition is  $\Omega = [-1, 1] \times [0, 1]$  and the initial position of the front is at  $x = 0$ . The velocity vector  $\mathbf{b} = [1, 0]$ , i.e., the front is moving to the right with time.

The problem is discretized in time using a backward Euler implicit time-stepping method and in space - by linear FEM for both variables on a triangular grid. As is seen from (7), the problem is nonlinear and within each time step we use Newton's method to solve it.

Here we are interested primarily in the solution of the corresponding Jacobian matrix equation. The linear system to be solved during each nonlinear iteration has the following form.

$$\begin{bmatrix} M & -J - \alpha K \\ \beta \Delta t_k K & M + \Delta t_k W \end{bmatrix} \begin{bmatrix} \eta \\ \mathbf{c} \end{bmatrix} = \begin{bmatrix} \mathbf{0} \\ \mathbf{f} \end{bmatrix} \tag{8}$$

where  $J$  is the part of the Jacobian, which corresponds to the nonlinear term  $\Psi'(C)$ . Here,  $K, M$  and  $W$  are the stiffness, mass and convection matrices, respectively.

There are several problem parameters involved in (7). For the numerical experiments we have used  $\beta = 1/Pe$ , where  $Pe = 300$  is the Peclet number,  $\alpha$  is the square of the so-called Cahn number, chosen in this case as 0.1.

Owe Axelsson, Owe.Axelsson@it.uu.se - p. 36/48

**Problem 1:** we impose a  $2 \times 2$  block structure by considering two consecutive (nested) refinements of the computational domain.

We consider some given mesh, referred to as 'coarse' and perform one regular refinement (in this case, into four congruent triangles), to obtain a 'fine' mesh. In this way, the degrees of freedom on the fine mesh is split into two non-intersecting classes, imposing the desired block two-by-two structure of the matrix on the fine level. We note, that the finite elements on the coarse mesh can be seen as macro-elements on the fine mesh and, by the same ordering, the corresponding macro-element stiffness matrix is also of block two-by-two form.

Owe Axelsson, Owe.Axelsson@it.uu.se – p. 37/48

All numerical experiments are performed in `Matlab`. The chosen size of the test matrices is not very large since the theoretical bounds, to be illustrated, involve matrix functions, which are costly to compute exactly, such as the value of  $\gamma$  computed as  $\rho(A_{11}^{-1}A_{12}A_{22}^{-1}A_{21})$ , and the value of  $\sigma$ , computed as  $\rho(\tilde{A}_{12}\tilde{A}_{21})$  or  $\|\tilde{A}_{12}\tilde{A}_{21}\|$ .

We test the effect of three different approximations of  $A_{11}^{-1}$ , namely,  $C_{11}^{(1)}$ ,  $C_{11}^{(2)}$  and  $C_{11}^{(3)}$ . The first two are computed as  $C_{11}^{(i)} = (L^{(i)}U^{(i)})^{-1}$ , where  $L^{(i)}U^{(i)}$ ,  $i = 1, 2$  is an incomplete factorization of  $A_{11}$  with a drop tolerance  $\tau_1 = 0.01$ ,  $\tau_2 = 0.001$  and  $\tau_3 = 0.0001$ . The LU-factors are computed using the `Matlab` function `luinc(A11,  $\tau_i$ )` or `cholinc` for spd matrices.

The matrix  $C_{11}^{(3)}$  is constructed only in the setting of Problem 1 as a sparse approximate inverse of  $A_{11}$  as follows. First we compute an element-by-element approximation of  $A_{11}^{-1}$  as

$$C_{11}^{(3,1)} = \sum_{\ell=1}^M \left( A_{11,E}^{(\ell)} \right)^{-1}.$$

Owe Axelsson, Owe.Axelsson@it.uu.se – p. 38/48

Clearly,  $C_{11}^{(3,1)}$  is sparse and cheap to obtain. In order to improve the quality of  $C_{11}^{(3,1)}$  as an approximation of  $A_{11}^{-1}$ , we compute a sparse additive correction,  $C_{11}^{(3,2)}$ , to it, such that the following Frobenius norm is minimized

$$\|I_1 - (C_{11}^{(3,1)} + C_{11}^{(3,2)})A_{11}\|_{A_{11}^{-1}} \quad (9)$$

Then we let  $C_{11}^{(3)} = C_{11}^{(3,1)} + C_{11}^{(3,2)}$ . Here,  $C_{11}^{(3,1)}$  has the sparsity pattern of  $A_{11}$  and  $C_{11}^{(3,2)}$  has the sparsity pattern of the error matrix  $I_1 - C_{11}^{(3,1)}A_{11}$ .

The matrix  $B_{11}$  is chosen to be either zero or equal to  $C_{11}$ , as indicated in the tables.

Owe Axelsson, Owe.Axelsson@it.uu.se - p. 39/48

Size	$\gamma$	$\sigma$	$\delta$	$eig(P^{-1}A)$			$\ I_1 - C_{11}A_{11}\ $
				$\lambda_{min}$	$\lambda_{max}$	$cond(P^{-1}A)$	
$C_{11}^{(3)}$							
1089	0.9969	4.3717	4.6552	0.1610	6.211	38.573	0.1714
4225	0.9992	18.956	20.003	0.0478	20.91	437.45	0.1745
$C_{11}^{(1)} = chol(A_{11}, 0.01)$							
1089	0.9969	0.1353	0.2639	0.6937	1.442	2.0784	0.0408
4225	0.9992	0.6183	1.1652	0.4642	2.154	4.6402	0.0421
$C_{11}^{(2)} = chol(A_{11}, 0.001)$							
1089	0.9969	0.0023	0.0049	0.9530	1.049	1.1010	0.0056
4225	0.9992	0.0106	0.0218	0.9024	1.108	1.2282	0.0058
$C_{11}^{(2)} = chol(A_{11}, 0.0001)$							
1089	0.9969	1.64e-5	5.21e-5	0.9960	1.0041	1.008	0.0006
4225	0.9992	7.82e-5	0.00023	0.9912	1.0089	1.018	0.0006

Problem 1,  $\mathbf{b} = \mathbf{0}$ ,  $\varepsilon = 1$ :  $\tilde{A}_{11} = A_{11}$ ,  $S = S_2$ ,  $B_{11} = C_{11}$   
 $\delta = \frac{\gamma^2}{1-\gamma^2} \|I - B_{11}A_{11}\| \|I - C_{11}A_{11}\|$ ,  $\gamma^2 = \rho(A_{11}^{-1}A_{12}A_{22}^{-1}A_{21})$

Owe Axelsson, Owe.Axelsson@it.uu.se - p. 40/48



Size	$\gamma$	$\sigma$	$\delta$	$eig(P^{-1}A)$				$\ I_1 - C_{11}A_1$
				$\lambda_{min}^{est}$	$\lambda_{min}$	$\lambda_{max}$	$\lambda_{max}^{est}$	
$C_{11}^{(3)}, B_{11} = 0$								
1089	0.9944	20.517	27.872	0.0445	0.0445	22.472	22.472	0.1570
4225	0.9987	88.397	119.39	0.0111	0.0111	90.386	90.386	0.1601
$C_{11}^{(1)} = chol(A_{11}, 0.01), B_{11} = 0$								
1089	0.9944	3.8784	7.233	0.1753	0.1753	5.7031	5.7031	0.04075
4225	0.9987	17.357	31.41	0.0518	0.0518	19.305	19.305	0.04210
$C_{11}^{(2)} = chol(A_{11}, 0.001), B_{11} = 0$								
1089	0.9944	0.4263	0.9326	0.5263	0.5263	1.8999	1.8999	0.00525
4225	0.9987	1.9173	4.0879	0.2745	0.2745	3.6428	3.6428	0.00548
$C_{11}^{(2)} = chol(A_{11}, 0.0001), B_{11} = 0$								
1089	0.9944	0.0399	0.1078	0.8193	0.8193	1.2206	1.2206	0.00061
4225	0.9987	1.9173	4.0879	0.2745	0.2745	3.6428	3.6428	0.00548
$C_{11}^{(2)} = chol(A_{11}, 0.0001), B_{11} = C_{11}$								
1089	0.9944	2.07e-5	6.548e-5	0.9955	0.9955	1.0046	1.0046	0.00061
4225	0.9987	8.53e-5	0.0003	0.9908	0.9908	1.0093	1.0093	0.00060

Problem 1,  $\mathbf{b} = [1, 0]$ ,  $\varepsilon = 1$ :  $\tilde{A}_{11} = A_{11}$ ,  $S = S_2$ ,  
 $\delta = \frac{\gamma^2}{1-\gamma^2} \|I - B_{11}A_{11}\| \|I - C_{11}A_{11}\|$ ,  $\gamma^2 = \rho(A_{11}^{-1}A_{12}A_{22}^{-1}A_{21})$

Owe Axelsson, Owe.Axelsson@it.uu.se - p. 41/48

Next, we apply the two-level preconditioner  $P$  in a multilevel setting. We test with the matrices from Problem 1, where on each level  $C_{11}$  is computed as  $C_{11}^{(3)}$  and  $B_{11} = C_{11}$ . The multilevel construction requires an approximation of the Schur complement. For this test we have used the element-by-element technique, where on each level local Schur complements are computed exactly and summed up in a FEM manner. In other words, we compute

$$S_E^{(\ell)} = A_{22,E}^{(\ell)} - A_{22,E}^{(\ell)}(A_{11,E}^{(\ell)})^{-1}A_{12,E}^{(\ell)} \quad \text{and let} \quad S = \sum_{\ell} S_E^{(\ell)}.$$

The so-obtained matrices  $S_E^{(\ell)}$  play the role of the element matrices on the coarser levels so that the construction can be repeated recursively. We see, that on the coarser levels the value of  $\sigma$  decreases as well as the condition number of the preconditioned system  $P^{-1}A$ . We also see that the eigenvalue bounds are quite tight.

Owe Axelsson, Owe.Axelsson@it.uu.se - p. 42/48

size( $A/A_{11}/S$ )	$\gamma$	$\sigma$	$eig(P^{-1}A)$			$\ I_1 - C_{11}A_{11}\ $
			$\lambda_{min}$	$\lambda_{max}$	$cond(P^{-1}A)$	
$\varepsilon = 1$						
5 levels of refinement						
1089/800/289	0.9944	3.8919	0.1749	5.717	32.684	0.15702
289/208/ 81	0.9725	0.57897	0.4754	2.1036	4.4251	0.13464
81/ 56/ 25	0.8779	0.071477	0.7660	1.3055	1.7042	0.10544
25/ 16/ 9	0.5480	0.002499	0.9513	1.0513	1.1051	0.05545
9/ 5/ 4	0.0468	0	1	1	1	0.00568
6 levels of refinement						
4225/3136/1089	0.9987	17.170	0.0523	19.118	365.48	0.16005
1089/ 800/289	0.9934	2.8380	0.2164	4.6216	21.359	0.14355
289/ 208/81	0.9703	0.5008	0.4997	2.0011	4.0043	0.12842
81/ 56/25	0.8729	0.0644	0.7765	1.2879	1.6587	0.10128
25/ 16/9	0.5395	0.0023	0.9536	1.0486	1.0996	0.05306
9/ 5/4	0.0529	0	1	1	1	0.00506

Problem 1:  $\tilde{A}_{11} = A_{11}, S = S_2, C_{11}^{(3)}, B_{11} = C_{11}$

Owe Axelsson, Owe.Axelsson@it.uu.se - p. 43/48

size( $A/A_{11}/S$ )	$\gamma$	$\sigma$	$eig(P^{-1}A)$			$\ I_1 - C_{11}A_{11}\ $
			$\lambda_{min}$	$\lambda_{max}$	$cond(P^{-1}A)$	
$\varepsilon = 0.01$						
5 levels of refinement						
1089/800/289	0.9966	2.5871	0.22948	4.3576	18.9886	0.17364
289/208/ 81	0.9814	0.023764	0.85727	1.1665	1.3607	0.062409
81/ 56/ 25	0.8945	0.000125	0.98887	1.0113	1.0226	0.009115
25/ 16/ 9	0.5862	8.05e-10	0.99997	1	1.0001	1.7279e-5
9/ 5/ 4	3.81e-8	0	1	1	1	0
6 levels of refinement						
4225/3136/1089	0.9986	3.7184	0.1806	5.5378	30.668	0.1452
1089/ 800/289	0.9958	0.2972	0.5835	1.7137	2.9367	0.0909
289/ 208/81	0.9785	0.0096	0.9065	1.1031	1.2169	0.0282
81/ 56/25	0.8996	2.63e-5	0.9949	1.0051	1.0103	0.0010
25/ 16/9	0.6278	2.60e-12	1	1	1	1.06e-6
9/ 5/4	0	0	1	1	1	0

Problem 1:  $\tilde{A}_{11} = A_{11}, S = S_2, C_{11}^{(3)}, B_{11} = C_{11}$

Owe Axelsson, Owe.Axelsson@it.uu.se - p. 44/48

Problem 2:

The next table contains results for matrices arising from Problem 2. It is well known that a high quality approximation of the mass matrix is its diagonal and therefore we set

$$\tilde{A}_{11} = B_{11} = C_{11} = (\text{diag}(A_{11}))^{-1} \text{ and } S = A_{22} - A_{21}(\text{diag}(A_{11}))^{-1}A_{12}.$$

We include the iteration counts to solve one system with the Jacobian matrix with a block-factorized preconditioner and with a block-triangular preconditioner (the case when  $B_{11} = 0$ ). Systems with  $\tilde{A}_{11}$  and with  $S$  are solved by a direct method. In this example the system matrix is not symmetric and not positive definite in general. We see, that the value of  $\gamma$  is larger than 1 and nearly doubles when we refine the mesh once, while  $\sigma$  is less than 1 and its increase is much less pronounced and even stabilizes. We include also the numerically estimated two-norm of the error matrices  $\|I_1 - C_{11}A_{11}\|$  and  $\|I_1 - S^{-1}S_2\|$ , which illustrate the effect on approximation of the inverse of  $A_{11}$  (the mass matrix in this case) by the inverse of its diagonal.

Size	$\gamma$	$B_{11} = C_{11}$				$B_{11} = 0$	
		$\sigma$	$\delta$	$\rho(I_1 - C_{11}A_{11})$	$\rho(I_1 - S^{-1}S_2)$	it	it
$C_{11} = \text{diag}(A_{11})^{-1}$							
578	0.7069	0.371	0.99869	1	0.9961	12	22
2178	0.7071	0.555	0.99968	1	0.9991	13	22
8450	-	-	-	-	-	14	23
33282	-	-	-	-	-	14	23
132098	-	-	-	-	-	14	23
$C_{11} = C_{11}^{(3)}$							
578	0.7069	0.0444	0.171	0.4133	0.2646	8	14
2178	0.7071	0.0453	0.179	0.4232	0.2697	8	14
8450	-	-	-	-	-	8	14
33282	-	-	-	-	-	8	14
132098	-	-	-	-	-	8	14

Problem 2: Iteration counts for the block-factorized and the block upper-triangular preconditioners; values of  $\gamma$ ,  $\delta$  and  $\sigma$  computed for the small-sized tests;  $\Delta t = h^2$

## *Conclusions*

- A general form of approximate block factorizations for matrices on two-by-two block form has been presented.
- A new parameter ( $\sigma$ ) to measure the quality of the corresponding preconditioner has been introduced. This replaces the previously commonly used parameter, the CBS constant  $\gamma$ . The latter is fixed for the given matrix, i.e., does not depend on the preconditioner and, furthermore, is applicable only for symmetric positive definite problems.
- A problem with the parameter  $\sigma$  is that it can not be computed locally, as the parameter  $\gamma$  can. However, its upper bound involves  $\gamma^2/(1 - \gamma^2)$ , which can be computed locally, and the additional factors in  $\sigma$  can be approximated by its values on local subdomains.
- By involving inner iterations, one can get arbitrarily accurate preconditioners or, at least in the limit, of a form leading to just two or three conjugate gradients iterations.
- For matrices on saddle point form, one can use a form of regularization which implies that the Schur complement approaches a multiple of the identity matrix, i.e., there is then no need to devise some other approximations of the Schur complement matrix.
- Several of the results have been illustrated by numerical tests.

*Thank you for your attention!*



UPPSALA  
UNIVERSITET

## On an augmented Lagrangian-based preconditioning of Oseen type problems

Maya Neytcheva

Division of Scientific Computing  
Department of Information Technology  
Uppsala University, Sweden

*Joint work with He Xin and Stefano Serra*



Institute of Geonics  
Ostrava

Maya Neytcheva, IT, Uppsala University maya@it.uu.se – p. 1/41



UPPSALA  
UNIVERSITET

## Large scale problems in Statistics

Plan of the talk:

- Saddle point matrices, preconditioning, Oseen's problem
- The augmented Lagrangian technique - two approaches
- Do we, indeed, avoid the need to approximate a Schur complement matrix?
- On the approximation of FEM mass matrices
- Numerical experiments

## Motivation: multiphase flow

Processes, modelled by the (convective) Cahn-Hilliard equ.:

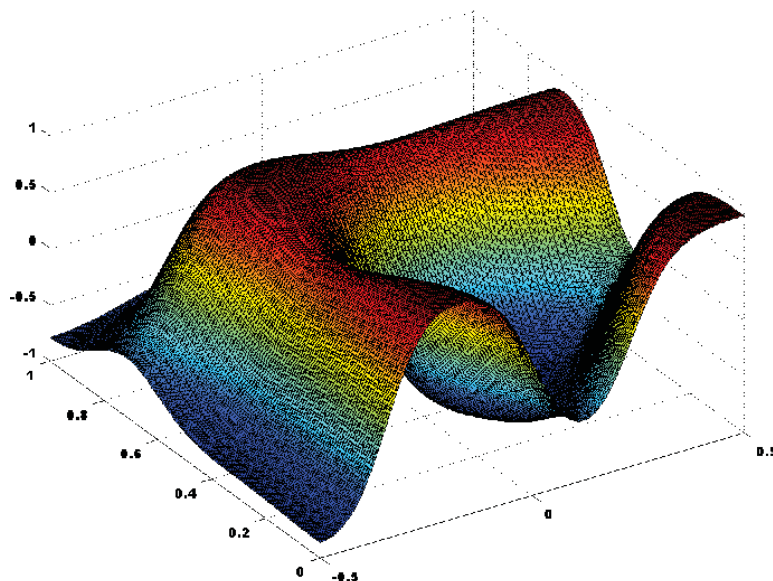
$$\frac{\partial C}{\partial t} + (\mathbf{u} \cdot \nabla)C = \nabla \cdot [\kappa(C)\nabla (\Psi'(C) - \epsilon^2\Delta C)].$$

Above,  $\mathbf{u}$  is the velocity vector, obtained as a solution of the time-dependent Navier-Stokes (N-S) equation:

$$\rho \frac{\partial \mathbf{u}}{\partial t} + (\rho \mathbf{u} \cdot \nabla) \mathbf{u} = -\nabla p + \nabla \cdot [\mu(\nabla) \mathbf{u} + \nabla \mathbf{u}^T] - \eta \nabla C + F.$$

Here  $p$  is the pressure,  $\rho$  and  $\mu(\mathbf{x})$  are the density and viscosity, correspondingly, and  $F$  is the force term. The term  $\eta \nabla C$ , where  $\eta = \Psi'(C) - \epsilon^2 \Delta C$ , gives the coupling with C-H and represents the surface tension force in a potential form.

## Motivation: multiphase flow



## Oseen's problem:

$$\begin{aligned} -\nu \Delta \mathbf{u} + (\mathbf{w} \cdot \nabla) \mathbf{u} + \nabla p &= \mathbf{f} \quad \text{in } \Omega, \\ \operatorname{div} \mathbf{u} &= 0 \quad \text{in } \Omega, \end{aligned}$$

subject to suitable boundary conditions on  $\partial\Omega$ .

$\nu > 0$  - the kinematic viscosity coefficient, assumed to be constant.

$\Delta$  - the Laplace operator in  $\mathbb{R}^d$

$\nabla$  - the gradient operator

$\operatorname{div}$  - the divergence operator.

The first equation - conservation of momentum

the second equation - incompressibility condition

The (wind) vector  $\mathbf{w}$  is an approximation of the velocity at a previous iteration step, so it is updated at every nonlinear iteration.

## The discrete linear system:

$$\begin{bmatrix} A & B^T \\ B & O \end{bmatrix} \begin{bmatrix} \mathbf{u}_h \\ \mathbf{p}_h \end{bmatrix} = \begin{bmatrix} \mathbf{f} \\ \mathbf{g} \end{bmatrix} \quad \text{or} \quad \mathcal{A} \mathbf{x} = \mathbf{b},$$

where  $\mathbf{u}_h$  is the discrete velocities vector,  $\mathbf{p}_h$  is the discrete pressure vector and  $\mathbf{x}^T = [\mathbf{u}_h^T \ \mathbf{p}_h^T]$ .

The matrix  $A$  is the discretized convection-diffusion operator (**nonsymmetric**).

The matrix  $B$  is the (negative) divergence matrix and  $B^T$  is the gradient matrix.

## How to precondition $\begin{bmatrix} A & B^T \\ B & O \end{bmatrix}$ ?

$$\begin{bmatrix} A_{11} & A_{12} \\ A_{21} & A_{22} \end{bmatrix} = \begin{bmatrix} I_1 & 0 \\ A_{21}A_{11}^{-1} & I_2 \end{bmatrix} \begin{bmatrix} A_{11} & 0 \\ 0 & S_2 \end{bmatrix} \begin{bmatrix} I_1 & A_{11}^{-1}A_{12} \\ 0 & I_2 \end{bmatrix}$$

$$S_2 = A_{22} - A_{21}A_{11}^{-1}A_{12}$$

$$\mathcal{M}_F = \begin{bmatrix} \tilde{A} & O \\ B & S \end{bmatrix} \begin{bmatrix} I_1 & \tilde{A}^{-1}B^T \\ O & I_2 \end{bmatrix}$$

$$\mathcal{M}_D = \begin{bmatrix} \tilde{A} & O \\ 0 & S \end{bmatrix}, \quad \mathcal{M}_L = \begin{bmatrix} \tilde{A} & O \\ B & S \end{bmatrix}, \quad \mathcal{M}_U = \begin{bmatrix} \tilde{A} & B^T \\ 0 & S \end{bmatrix}$$

## How to approximate the Schur complement

$$BA^{-1}B^T?!$$

- (1) Pressure mass matrix  $M_p$
- (2) The pressure convection-diffusion (PCD) preconditioner

$$S_{PCD}^{-1} = \tilde{M}_p^{-1} A_p L_p^{-1},$$

- (3) The BFBt preconditioner

$$S_{BFBt}^{-1} = (B\hat{M}_u^{-1}B^T)^{-1}B\hat{M}_u^{-1}A\hat{M}_u^{-1}B^T(B\hat{M}_u^{-1}B^T)^{-1},$$

- (4) Element-by-element Schur complement

$$S_{EBE} = \sum_e S_{2,e} = \sum_e A_{22,e} - A_{21,e}A_{11,e}^{-1}A_{12,e}$$



## How to avoid approximating the Schur complement?

Augmented Lagrangian technique:

Approach 1: Consider a regularized linear system (*not consistent* with the original one),

$$\begin{bmatrix} A & B^T \\ B & -\frac{1}{r}W \end{bmatrix} \begin{bmatrix} \mathbf{u}_h \\ \mathbf{p}_h \end{bmatrix} = \begin{bmatrix} \mathbf{f} \\ \mathbf{g} \end{bmatrix} \quad \text{or} \quad \bar{\mathcal{A}}\mathbf{x} = \mathbf{b},$$

for some large enough scalar parameter  $r$  and some spd matrix  $W$ . Systems of this form are obtained via various stabilization techniques.

$$\mathcal{A} = \begin{bmatrix} A & B^T \\ B & 0 \end{bmatrix}, \quad \bar{\mathcal{A}} = \begin{bmatrix} A & B^T \\ B & -\frac{1}{r}W \end{bmatrix}$$

$$\bar{\mathcal{A}} = \begin{bmatrix} I_1 & -rB^TW^{-1} \\ 0 & I_2 \end{bmatrix} \begin{bmatrix} A + rB^TW^{-1}B & 0 \\ 0 & -\frac{1}{r}W \end{bmatrix} \begin{bmatrix} I_1 & 0 \\ -rW^{-1}B & I_2 \end{bmatrix}$$

$$\mathcal{M}_L = \begin{bmatrix} A + rB^TW^{-1}B & 0 \\ B & -\frac{1}{r}W \end{bmatrix} \quad \text{or} \quad \mathcal{M}_U = \begin{bmatrix} A + rB^TW^{-1}B & B^T \\ 0 & -\frac{1}{r}W \end{bmatrix}$$

- good candidates to precondition the matrix  $\bar{\mathcal{A}}$  and, for large values of  $r$ , for  $\mathcal{A}$  itself. » b

$$A = \begin{bmatrix} A & B^T \\ B & 0 \end{bmatrix}$$

**Approach 2:** Transform the original system into an *equivalent* one:

$$\begin{bmatrix} A + rB^TW^{-1}B & B^T \\ B & 0 \end{bmatrix} \begin{bmatrix} \mathbf{u}_h \\ \mathbf{p}_h \end{bmatrix} = \begin{bmatrix} \hat{\mathbf{f}} \\ \mathbf{g} \end{bmatrix}$$

where  $\hat{\mathbf{f}} = \mathbf{f} + rB^TW^{-1}B \mathbf{g}$ .

NOTE: the transformation holds for any value of  $r$ , including  $r = 1$  or  $r \ll 1$ , and there is more freedom in choosing the (nonsingular) matrix  $W$ .

$$\tilde{A} = \begin{bmatrix} A + rB^TW^{-1}B & B^T \\ B & 0 \end{bmatrix}, \quad \tilde{A}\mathbf{v} = \lambda\mathcal{M}_L\mathbf{v}$$

$$\mathcal{M}_L^{-1}\tilde{A} = \begin{bmatrix} I & (A + rB^TW^{-1}B)^{-1}B^T \\ 0 & rW^{-1}B(A + rB^TW^{-1}B)^{-1}B^T \end{bmatrix}.$$

Apply Sherman-Morrison-Woodbury's formula to  $(A + rB^TW^{-1}B)^{-1}$ :

$$rW^{-1}B(A + rB^TW^{-1}B)^{-1}B^T = rQ - rQ(I + rQ)^{-1}rQ,$$

where  $Q = W^{-1}BA^{-1}B^T$ . » f

$$\mathcal{M}_L^{-1} \tilde{\mathcal{A}} = \begin{bmatrix} I & (A + rB^T W^{-1} B)^{-1} B^T \\ 0 & rW^{-1} B (A + rB^T W^{-1} B)^{-1} B^T \end{bmatrix}.$$

**Lemma 1** Let the matrices  $\tilde{\mathcal{A}}$  and  $\mathcal{M}_L$  be defined above, and let  $\mu$  be any eigenvalue of  $BA^{-1}B^T \mathbf{w} = \mu W \mathbf{w}$ . Let  $\delta$  be an eigenvalue of the matrix  $\tilde{Q} \equiv rQ - rQ(I + rQ)^{-1}rQ$ , where  $Q = W^{-1}BA^{-1}B^T$ . Then the following holds:

The matrices  $Q$  and  $\tilde{Q}$  have the same eigenvectors and the eigenvalues of  $\tilde{Q}$  are equal to

$$\delta = \frac{r\mu}{1 + r\mu} = \frac{1}{1 + \frac{1}{r\mu}}.$$

When  $r \rightarrow \infty$  all nonzero eigenvalues of the eigenproblem  $\tilde{\mathcal{A}} \mathbf{v} = \lambda \mathcal{M}_L \mathbf{v}$  converge to 1.

**Consider now the modified pivot block in**

$$\begin{bmatrix} A + rB^T W^{-1} B & B^T \\ B & 0 \end{bmatrix} :$$

How to solve systems with  $\hat{A} = A + rB^T W^{-1} B$ ?

$$A + rB^T W^{-1} B = (I + rB^T W^{-1} B A^{-1}) A$$



## We notice, that

$Q = W^{-1}BA^{-1}B^T$  and  $Q = B^TW^{-1}BA^{-1}$   
have the same spectra.



## We notice, that

$Q = W^{-1}BA^{-1}B^T$  and  $Q = B^TW^{-1}BA^{-1}$   
have the same spectra.

$$Q = W^{-1}BA^{-1}B^T \quad \rightarrow \quad Q = B^TW^{-1}BA^{-1}$$

## We notice, that

$Q = W^{-1}BA^{-1}B^T$  and  $Q = B^TW^{-1}BA^{-1}$   
have the same spectra.

$$Q = W^{-1}BA^{-1}\overset{\circlearrowleft}{B^T} \longrightarrow Q = \overset{\circlearrowright}{B^T}W^{-1}BA^{-1}$$

**Lemma 4** Let  $X$  and  $Y$  be two general matrices,  $X \in \mathbb{C}^{n \times m}$  and  $Y \in \mathbb{C}^{m \times n}$ . Then the spectra of the products  $XY$  and  $YX$  are identical up to some additional zero eigenvalues of multiplicity  $(\max(n, m) - \min(n, m))$ .

»skip proof

## $XY$ and $YX$ have the same spectra

**Proof:**

(a) Let  $X$  and  $Y$  be square, i.e.,  $n = m$ .

(a1) Let  $X$  be nonsingular. Then  $XY$  is spectrally equivalent to  $YX$  because of the trivial equality  $XY = X(YX)X^{-1}$ .



## $XY$ and $YX$ have the same spectra

- (a2) Let both  $X$  and  $Y$  be singular. We consider the Schur decomposition of  $X$ ,  $X = UTU^*$ , where  $U$  is unitary and  $T$  is upper triangular with diagonal elements equal to the eigenvalues of  $X$ . Clearly, at least one diagonal entry in  $T$  is zero. Let  $\varepsilon > 0$  and construct  $T_\varepsilon$  as following

$$(T_\varepsilon)_{ij} = \begin{cases} T_{ij} & \text{for } i \neq j; \\ T_{ii} & \text{if } T_{ii} \neq 0; \\ \varepsilon & \text{if } T_{ii} = 0. \end{cases}$$

Let  $X_\varepsilon = UT_\varepsilon U^*$ . Clearly  $X_\varepsilon$  is nonsingular and  $\|X - X_\varepsilon\| < \varepsilon$ .

Due to (a1), there holds that the spectrum of  $X_\varepsilon Y$  coincides with that of  $Y X_\varepsilon$  as well as their characteristic polynomials, i.e.,  $P(X_\varepsilon Y) = P(Y X_\varepsilon)$ . Using the fact that the matrices are continuous functions of their entries and so are the coefficients of their characteristic polynomials, letting  $\varepsilon \rightarrow 0$  we obtain that

$$P(XY) = P(YX).$$



## $XY$ and $YX$ have the same spectra

- (b) Let now  $n \neq m$ , and for convenience assume that  $n > m$ . Augmenting  $X$  and  $Y$  to square matrices by adding  $(n - m)$  columns, respectively rows,

$$\tilde{X} = \begin{bmatrix} X & 0 \end{bmatrix}, \quad \tilde{Y} = \begin{bmatrix} Y \\ 0 \end{bmatrix},$$

$$\tilde{X}\tilde{Y} = XY,$$

$$\tilde{Y}\tilde{X} = \begin{bmatrix} Y \\ 0 \end{bmatrix} \begin{bmatrix} X & 0 \end{bmatrix} = \begin{bmatrix} YX & 0 \\ 0 & 0 \end{bmatrix}.$$

By (i2) we know that the spectrum of  $\tilde{X}\tilde{Y}$  is equal to  $\tilde{Y}\tilde{X}$ , which in its turn coincides with the spectrum of  $YX$  augmented with  $(n - m)$  zero eigenvalues.

## Two condition number indicators:

$$\kappa \left( A^{-1}(A + rB^T W^{-1}B) \right) = |1 + r\mu| \quad \kappa \left( \mathcal{M}_L^{-1} \tilde{\mathcal{A}} \right) = |1 + 1/(r\mu)|$$

Try to balance the two constraints, for instance, by minimizing the quantity

$$\left( |1 + r\mu|^p + |1 + 1/r\mu|^p \right)^{1/p},$$

A direct computation shows that, independently of  $p$ ,  $r\mu$  should be  $O(1)$  and since we want  $r$  to be also  $O(1)$ , we conclude that  $\mu = O(1)$ , i.e.,  $W$  should approximate well the negative Schur complement of the original system,  $BA^{-1}B^T$ . More specifically, the minimum is attained for real positive  $\mu$  and for  $p = 1$  the global minimum over the positive complex half plane is attained when  $r\mu = 1$ .

## Outcome:

The above reasonings, although appearing to be trivial, show that the attempts to approximate the modified pivot block  $A + rB^T W^{-1}B$  with matrices or computational procedures, which perform reasonably well for small values of  $r$ , ultimately destroy the outer convergence rate.

Thus, the weight of the product  $B^T W^{-1}B$  is significant and cannot be neglected:

- either find a good approximation of the Schur complement,
- or
- solve the modified block very accurately.

## The influence of $r$ on the outer and the inner convergence rates:

Size	$r = \nu$	$r = 1$	$r = 1/\nu$	$r = 1000$
$\nu = 1$				
578	15(10)	15(10)	15(10)	2(42)
2178	15(10)	15(10)	15(10)	2(51)
8450	15(11)	15(11)	15(11)	2(53)
$\nu = 0.1$				
578	28(3)	16(11)	4(38)	2(54)
2178	29(3)	15(13)	4(44)	2(66)
8450	26(3)	14(14)	4(45)	2(71)
$\nu = 0.01$				
578	58(3)	49(11)	5(65)	3(76)
2178	83(3)	47(14)	4(115)	2(135)
8450	106(3)	45(18)	4(154)	2(179)

Outer(inner) iterations as functions of  $\nu$  and  $r$

«< conclude

COMPUTATIONAL MECHANICS II, December 1-3, 2010, Ostrava

Maya Neytcheva, IT, Uppsala University maya@it.uu.se – p. 21/41

Mass matrices



## The finite element matrices

$$M = \sum_{k=1}^{n_E} R_k^T M_k R_k.$$

Here  $R_k$  are the standard Boolean matrices which prescribe the local-to-global correspondence of the degrees of freedom. The matrix  $M$  is symmetric, positive definite.

For some special FEM discretizations  $M$  is diagonal.  
(Example: nonconforming FEM)

For the conforming FEM discretization  $M$  is a sparse matrix.

Tasks:

- How to approximate  $M^{-1}$ ?
- How to measure how good the approximation is?

## Known results:

I. Fried, Bounds on the spectral and maximum norms of the finite element stiffness, flexibility and mass matrices. *International Journal of Solids and Structures*, 9 (1973), 1013–1034.

A.J. Wathen, Realistic eigenvalue bounds for the Galerkin mass matrix, *IMA Journal of Numerical Analysis* 7 (1987), 449-457.

I. Fried and M. Coleman, Improvable bounds on the largest eigenvalue of a completely positive finite element flexibility matrix *Journal of Sound and Vibration*, (283) 2005, pp. 487-494

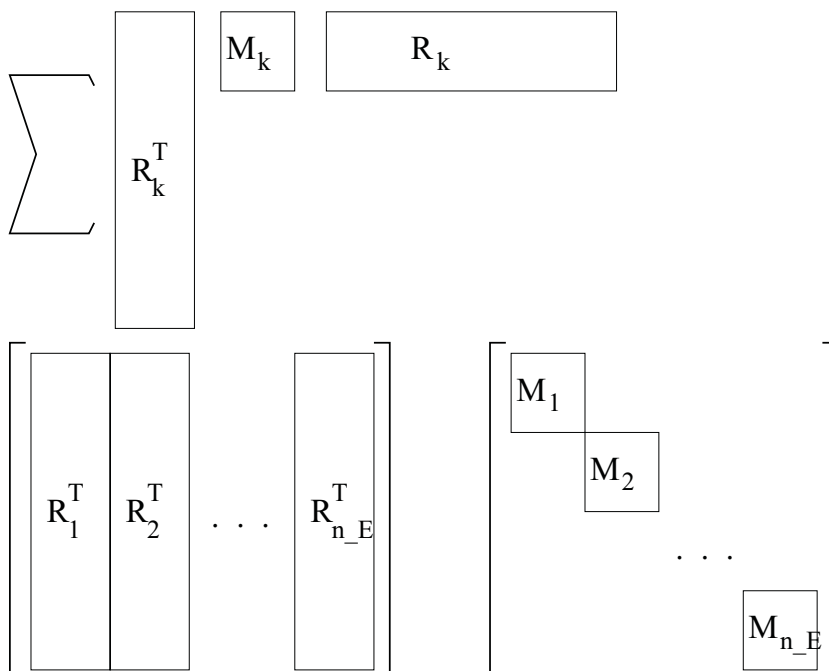
## An element-by-element representations

$$M = \sum_{k=1}^{n_E} R_k^T M_k R_k.$$

$$M = R^T \text{diag}(M_k) R,$$

where  $R^T = [R_1^T, \dots, R_{n_E}^T]$ .

$$M = \sum_{k=1}^{n_E} R_k^T M_k R_k, \quad M = R^T \text{diag}(M_k) R$$



# Estimating the eigenvalues of $M$ via the eigenvalues of the element stiffness matrices $M_k$

I. Fried:

$$\min_{k=1, \dots, n_E} (\lambda_{\min}(M_k)) \leq \lambda(M) \leq p_{\max} \max_{k=1, \dots, n_E} (\lambda_{\max}(M_k))$$

where  $p_{\max}$  is the degree of the graph of the mesh (the maximum number of elements around any nodal points).

# How to approximate $M^{-1}$

Denote:

$D_M$  the (pointwise) diagonal of  $M$

$D_M^{-1}$   $inv(D_M)$

$L_M$  the lumped mass matrix

$\widehat{M}^{-1}$  the element-by-element sparse approximate inverse of  $M^{-1}$ :

$$\widehat{M}^{-1} = \sum_{k=1}^{n_E} R_k^T M_k^{-1} R_k$$

$D_{\widehat{M}}^{-1}$  the diagonal of  $\widehat{M}^{-1}$

$$\kappa(D_M^{-1}M)$$

Recall:  $M = R^T \text{diag}(M_k)R$ .

Let  $\lambda$  be an eigenvalue of  $D_M^{-1}M$ .

Using Rayleigh quotient:

$$\min_{\mathbf{x} \neq \mathbf{0}} \frac{\mathbf{x}^T M \mathbf{x}}{\mathbf{x}^T D_M \mathbf{x}} \leq \lambda \leq \max_{\mathbf{x} \neq \mathbf{0}} \frac{\mathbf{x}^T M \mathbf{x}}{\mathbf{x}^T D_M \mathbf{x}}$$

$$\min_{\mathbf{x} \neq \mathbf{0}} \frac{\mathbf{x}^T L^T \text{diag}(M_k) L \mathbf{x}}{\mathbf{x}^T L^T \text{diag}(D_{M_k}) L \mathbf{x}} \leq \lambda \leq \max_{\mathbf{x} \neq \mathbf{0}} \frac{\mathbf{x}^T L^T \text{diag}(M_k) L \mathbf{x}}{\mathbf{x}^T L^T \text{diag}(D_{M_k}) L \mathbf{x}}$$

$$\min_{\mathbf{y} \neq \mathbf{0}} \frac{\mathbf{y}^T \text{diag}(M_k) \mathbf{y}}{\mathbf{y}^T \text{diag}(D_{M_k}) \mathbf{y}} \leq \lambda \leq \max_{\mathbf{y} \neq \mathbf{0}} \frac{\mathbf{y}^T \text{diag}(M_k) \mathbf{y}}{\mathbf{y}^T \text{diag}(D_{M_k}) \mathbf{y}}$$

$$\min_e \lambda_{\min}(D_k^{-1}M_k) \leq \lambda \leq \max_e \lambda_{\min}(D_k^{-1}M_k)$$

## Some particular element matrices

Element	$\lambda_{\min}$	$\lambda_{\max}$	$\kappa(D_M^{-1}M)$
Arbitrary linear triangles	1/2	2	4
Bilinear rectangles	1/4	9/4	9
Arbitrary linear tetrahedra	1/2	5/2	5
Rectangular trilinear bricks	1/8	27/8	27

## Straightforward consequence: $\theta$ -method

For parabolic problems:

$$(M + \theta\Delta tK)U^{n+1} = (M - (1 - \theta)\Delta tK)U^n$$

$$M + \theta\Delta tK = L^T (\text{diag}(M_e + \theta\Delta tK_e)) L$$

## Can we do better?

Consider the element-by-element idea:

$$M_k = \frac{\alpha_k}{12} \begin{bmatrix} 2 & 1 & 1 \\ 1 & 2 & 1 \\ 1 & 1 & 2 \end{bmatrix}, \quad \lambda(M_k) = \frac{\alpha_k}{12} [1, 1, 4]$$

$$D_{M_k^{-1}} M_k = \frac{3}{4} \begin{bmatrix} 2 & 1 & 1 \\ 1 & 2 & 1 \\ 1 & 1 & 2 \end{bmatrix}, \quad \lambda(D_{M_k^{-1}} M_k) = \frac{3}{4} [1, 1, 4]$$

Thus,  $\kappa(D_{\widehat{M}^{-1}} M) \leq 4$ ,  $\kappa(\widehat{M}^{-1} D_{\widehat{M}^{-1}}^{-1}) \leq 4$  and  $\kappa(\widehat{M}^{-1} M) \leq 16$ .

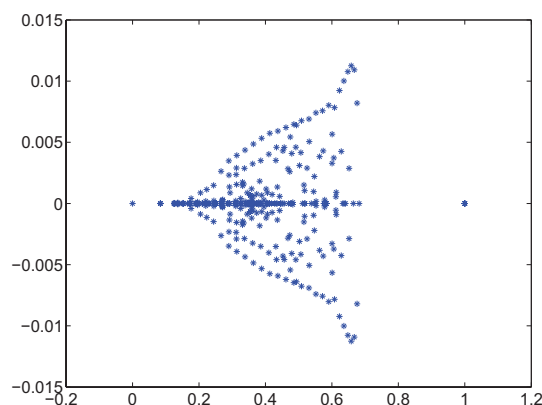
## Preconditioners, involving mass matrices:

Stationary Navier-Stokes:

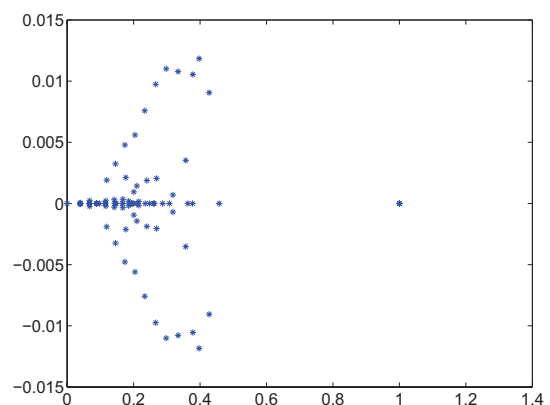
$$\tilde{A} = \begin{bmatrix} A + \gamma B^T M^{-1} B & B^T \\ B & 0 \end{bmatrix}$$

$$\mathcal{M} = \begin{bmatrix} A + \gamma B^T M^{-1} B & 0 \\ B & -\frac{1}{\gamma} M \end{bmatrix}$$

$$\begin{bmatrix} A + \gamma B^T M^{-1} B & 0 \\ B & -\frac{1}{\gamma} M \end{bmatrix}^{-1} \begin{bmatrix} A + \gamma B^T M^{-1} B & B^T \\ B & 0 \end{bmatrix}$$



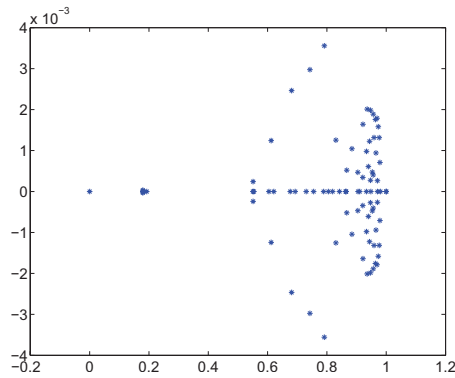
(a)  $D_M^{-1}$



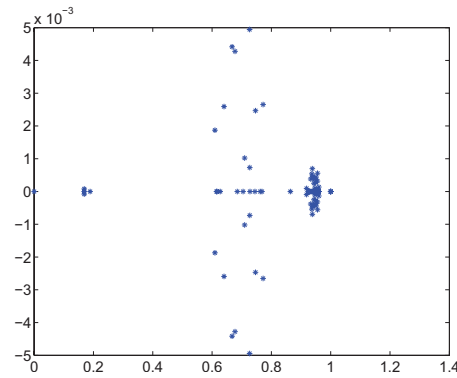
(b)  $L_M^{-1}$

The spectrum of  $\mathcal{M}_L^{-1} \tilde{A}, \gamma = 1, \nu = 1$

$$\begin{bmatrix} A + \gamma B^T M^{-1} B & 0 \\ B & -\frac{1}{\gamma} M \end{bmatrix}^{-1} \begin{bmatrix} A + \gamma B^T M^{-1} B & B^T \\ B & 0 \end{bmatrix}$$



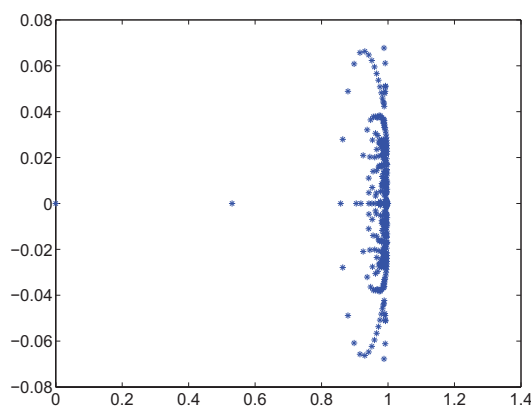
(c)  $D_{\widehat{M}^{-1}}$



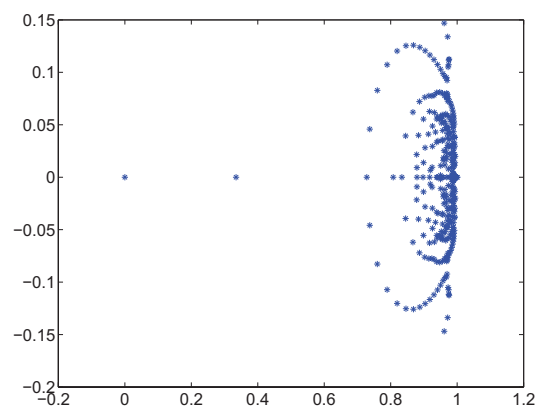
(d)  $\widehat{M}^{-1}$

The spectrum of  $\mathcal{M}_L^{-1} \widetilde{\mathcal{A}}, \gamma = 1, \nu = 1$

$$\begin{bmatrix} A + \gamma B^T M^{-1} B & 0 \\ B & -\frac{1}{\gamma} M \end{bmatrix}^{-1} \begin{bmatrix} A + \gamma B^T M^{-1} B & B^T \\ B & 0 \end{bmatrix}$$



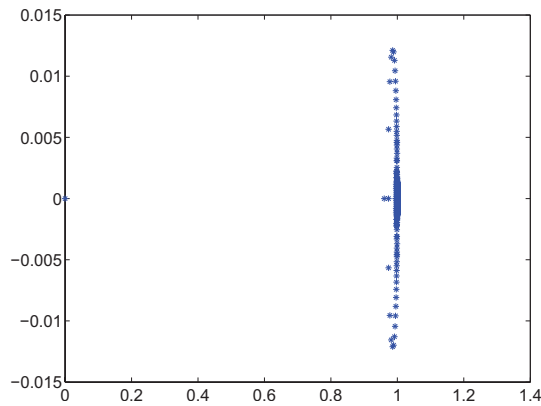
(e)  $D_M^{-1}$



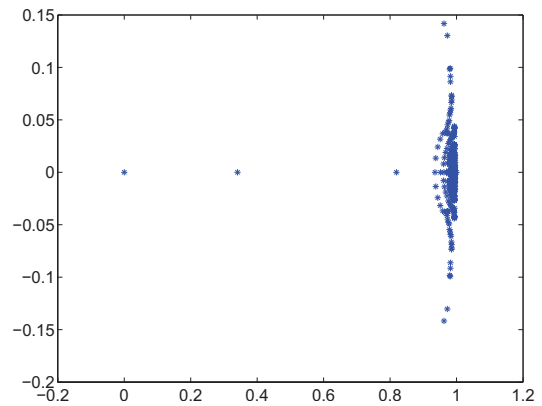
(f)  $L_M^{-1}$

The spectrum of  $\mathcal{M}_L^{-1} \widetilde{\mathcal{A}}, \gamma = 1, \nu = 1/320$

$$\begin{bmatrix} A + \gamma B^T M^{-1} B & 0 \\ B & -\frac{1}{\gamma} M \end{bmatrix}^{-1} \begin{bmatrix} A + \gamma B^T M^{-1} B & B^T \\ B & 0 \end{bmatrix}$$



(g)  $D_{\widehat{M}^{-1}}$



(h)  $\widehat{M}^{-1}$

The spectrum of  $\mathcal{M}_L^{-1} \tilde{\mathcal{A}}$ ,  $\gamma = 1$ ,  $\nu = 1/320$

## Cahn-Hilliard equation:

$$\frac{\partial C}{\partial t} + (\mathbf{u} \cdot \nabla) C = \nabla \cdot [\kappa(C) \nabla (\Psi'(C) - \epsilon^2 \Delta C)]$$

$$\begin{aligned} \eta - \Psi'(C) + \epsilon^2 \Delta C &= 0, & (\mathbf{x}, t) \in \Omega_T \equiv \Omega \times (0, T) \\ \nabla \cdot [\kappa(C) \nabla \eta] - \frac{\partial C}{\partial t} - (\mathbf{u} \cdot \nabla) C &= 0, & (\mathbf{x}, t) \in \Omega_T \end{aligned}$$

$$\begin{bmatrix} \theta M & -\theta J(\mathbf{c}) - \theta \epsilon^2 K \\ \theta \kappa \Delta t_k K & M + \theta \Delta t_k W \end{bmatrix}.$$





What about

$$\|I - \widehat{M}^{-1}M\|_F$$

or

$$\|I - D_M^{-1}M\|_F$$



To conclude:

- In the context of the augmented Lagrangian technique, we still need a reasonably good approximation of the Schur complement matrix  $BA^{-1}B^T$ .
- It remains an open problem how to solve systems of the type  $A + rB^TW^{-1}B$ .
- There are very good quality diagonal approximations of the inverse of the mass matrix.  
 $\|I - \widehat{M}^{-1}M\|$  can be further improved using Frobenius norm minimization techniques.



UPPSALA  
UNIVERSITET

Thank you for your attention!

Czech Technical University in Prague  
Faculty of Civil Engineering  
Department of Mechanics

# Damage Analysis and Arc-Length Methods

Jaroslav Kruis

---

1. 12. – 3. 12. 2010

Institute of Geonics AS CR

Ostrava

CTU

Damage, Arc-length Method

J. Kruis

---

## Outline

- Damage
  - uniaxial case
  - mesh-adjusted softening modulus
  - multiaxial case
- Non-linear equations
- Arc-length method
  - spherical and cylindrical method
  - linearized method
  - original method

---

1. 12. – 3. 12. 2010

Institute of Geonics AS CR

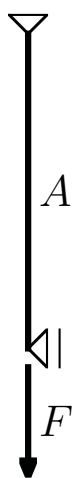
Ostrava

# Damage

The theory of damage describes the evolution between the virgin state and macroscopic crack initiation.

The phenomenon of damage represents surface discontinuities in the form of microcracks, or volume discontinuities in the form of cavities.

## Uniaxial Case



$A$	area of cross section of bar
$\tilde{A}$	area of undamaged part of cross section
$A_d$	area of damaged part of cross section
$\sigma = \frac{F}{A}$	apparent stress
$\tilde{\sigma} = \frac{F}{\tilde{A}}$	effective stress
$\varepsilon$	strain

areas of cross section

$$A = \tilde{A} + A_d$$

damage parameter

$$\omega = \frac{A_d}{A} \quad \omega \in \langle 0; 1 \rangle$$

$$F = \tilde{\sigma} \tilde{A} = \sigma A \quad \Rightarrow \quad \sigma = \frac{A - A_d}{A} \tilde{\sigma}$$

effective stress

$$\tilde{\sigma} = \frac{1}{1 - \omega} \sigma$$

## Principles of Equivalence

### Principle of Strain Equivalence–The Effective Stress Concept

The strain associated with a damaged state under the applied stress  $\sigma$  is equivalent to the strain associated with the undamaged state under the effective stress  $\tilde{\sigma}$ .

$$\left. \begin{array}{l} \tilde{\sigma} = E \tilde{\varepsilon} = E \varepsilon \\ \sigma = \tilde{E} \varepsilon \end{array} \right\} \frac{\tilde{\sigma}}{E} = \frac{\sigma}{\tilde{E}} \Rightarrow \frac{\tilde{E}}{E} = 1 - \omega$$

### Principle of Stress Equivalence–The Effective Strain Concept

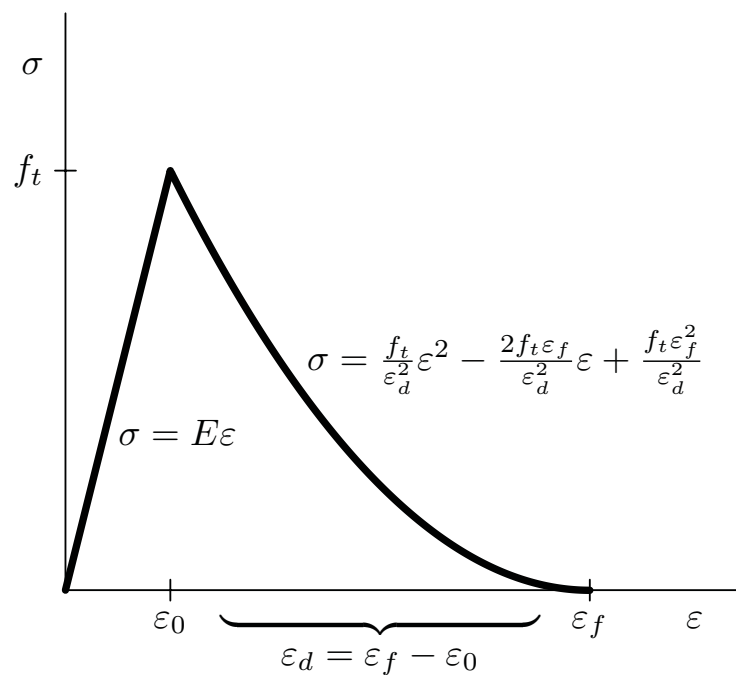
The stress associated with a damaged state under the applied strain  $\varepsilon$  is equivalent to the stress associated with the undamaged state under the effective strain  $\tilde{\varepsilon}$ .

$$\left. \begin{array}{l} \tilde{\varepsilon} = \frac{\tilde{\sigma}}{E} = \frac{\sigma}{E} \\ \varepsilon = \frac{\sigma}{\tilde{E}} \end{array} \right\} \tilde{\varepsilon}E = \tilde{E}\varepsilon \Rightarrow \frac{E}{\tilde{E}} = \frac{1}{1 - \omega}$$

### Principle of Elastic Energy Equivalence

$$\left. \begin{array}{l} \tilde{\sigma} = E\tilde{\varepsilon} \\ \tilde{W} = \frac{1}{2}\tilde{\sigma}\tilde{\varepsilon} \\ \sigma = \tilde{E}\varepsilon \\ W = \frac{1}{2}\sigma\varepsilon \end{array} \right\} \tilde{\sigma}\tilde{\varepsilon} = \sigma\varepsilon \Rightarrow \sqrt{\frac{\tilde{E}}{E}} = 1 - \omega$$

### Stress–Strain Diagram



1. 12. – 3. 12. 2010

Institute of Geonics AS CR

Ostrava

CTU

Damage, Arc-length Method

J. Kruis

$$\sigma = (1 - \omega)E\epsilon = (1 - g(\epsilon))E\epsilon$$

$$g(\epsilon) = 1 - \frac{\sigma}{E\epsilon}$$

stress-strain diagram with linear and quadratic functions

$$\epsilon \in \langle 0; \epsilon_0 \rangle \quad \sigma = E\epsilon$$

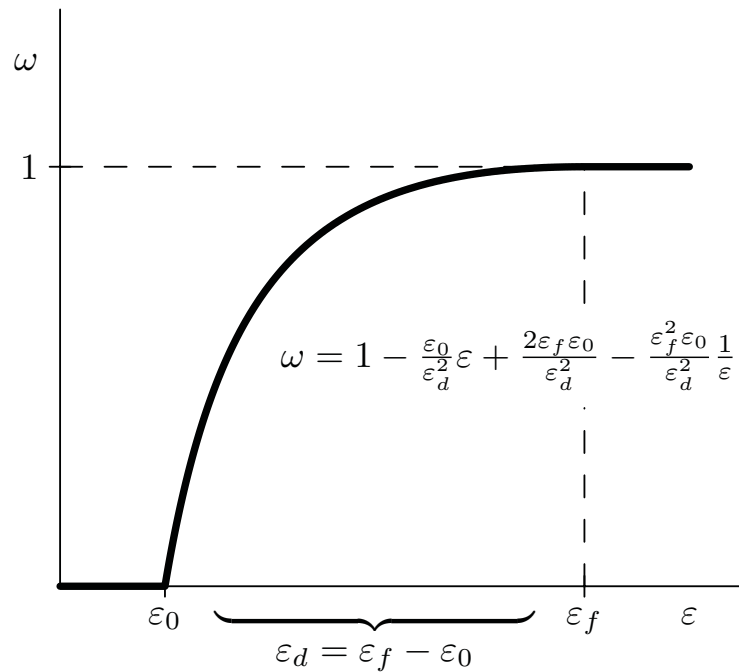
$$\epsilon \in \langle \epsilon_0; \epsilon_f \rangle \quad \sigma = \frac{f_t}{\epsilon_d^2}\epsilon^2 - \frac{2f_t\epsilon_f}{\epsilon_d^2}\epsilon + \frac{f_t\epsilon_f^2}{\epsilon_d^2}$$

$$\omega = 1 - \frac{\epsilon_0}{\epsilon_d^2}\epsilon + \frac{2\epsilon_f\epsilon_0}{\epsilon_d^2} - \frac{\epsilon_f^2\epsilon_0}{\epsilon_d^2} \frac{1}{\epsilon}$$

1. 12. – 3. 12. 2010

Institute of Geonics AS CR

Ostrava



loading function - specifies the elastic domain

$$f(\varepsilon, \kappa) = \varepsilon - \kappa \leq 0$$

$\kappa$  is the largest strain ever reached in the history

$$f(\varepsilon, \kappa) \leq 0, \quad \dot{\kappa} \geq 0, \quad \dot{\kappa} f(\varepsilon, \kappa) = 0$$

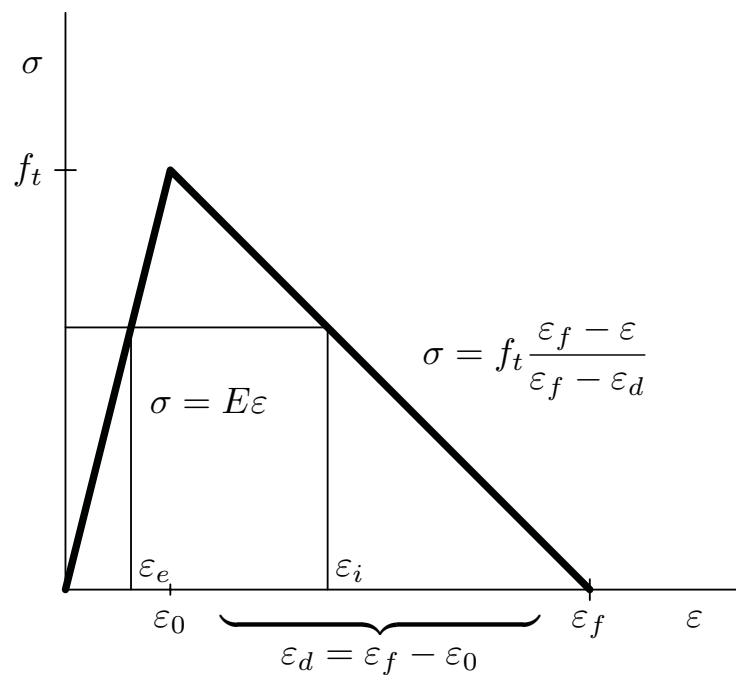
$$f(\varepsilon, \kappa) < 0, \quad \dot{\kappa} = 0 \quad \text{elastic state}$$

$$f(\varepsilon, \kappa) = 0, \quad \dot{\kappa} = 0 \quad \text{neutral loading, damage does not grow}$$

$$f(\varepsilon, \kappa) = 0, \quad \dot{\kappa} > 0 \quad \text{damage grows}$$



## Mesh-Adjusted Softening Modulus



1. 12. – 3. 12. 2010

Institute of Geonics AS CR

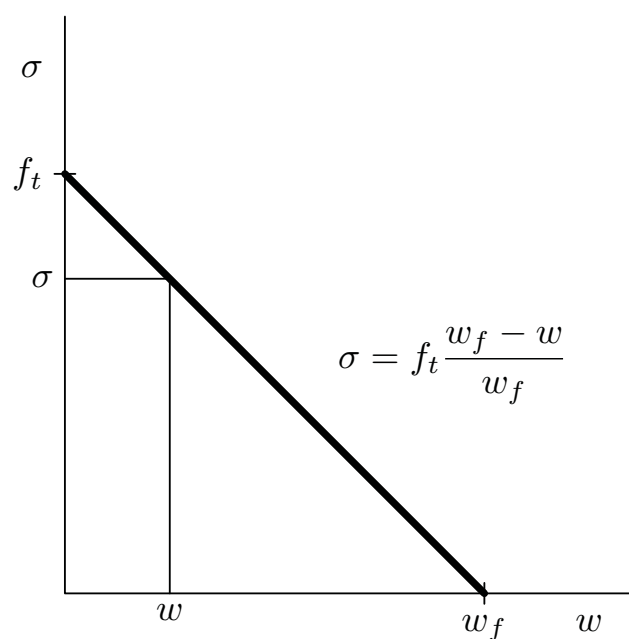
Ostrava

CTU

Damage, Arc-length Method

J. Kruis

## Traction–Separation Law



1. 12. – 3. 12. 2010

Institute of Geonics AS CR

Ostrava

elongation of the bar

$$u = h\varepsilon_i + (l - h)\varepsilon_e = \varepsilon_f h + \sigma \left( \frac{l - h}{E} + \frac{\varepsilon_0 - \varepsilon_f}{f_t} h \right)$$

the traction-separation law

$$\sigma = f(w) = f_t \frac{w_f - w}{w_f}$$

where  $w$  is the crack opening and  $\sigma$  is the stress normal to the crack  
cracking strain

$$\sigma = (1 - \omega)E\varepsilon = E(\varepsilon - \omega\varepsilon) = E(\varepsilon - \varepsilon_c) = E\varepsilon_e$$

$$\varepsilon_c = \omega\varepsilon$$

the crack opening

$$w = h\varepsilon_c = h\omega\varepsilon$$

$$(1 - \omega)E\varepsilon = f_t \left( 1 - \frac{h\omega\varepsilon}{w_f} \right)$$

$$w_f = h\varepsilon_f$$

$$\omega = 1 - \frac{\varepsilon_0}{\varepsilon} \frac{w_f - \varepsilon h}{w_f - \varepsilon_0 h} = 1 - \frac{\varepsilon_0}{\varepsilon} \frac{\varepsilon_f - \varepsilon}{\varepsilon_f - \varepsilon_0}$$

exponential traction–separation law

$$(1 - \omega)E\varepsilon = f_t e^{-\frac{w}{w_f}} = f_t e^{-\frac{h\omega\varepsilon}{w_f}}$$

numerical solution

## Multiaxial Case

strain components

$$\varepsilon_{ij} = \frac{1}{2} \left( \frac{\partial u_i}{\partial x_j} + \frac{\partial u_j}{\partial x_i} \right)$$

strain tensor

$$\begin{pmatrix} \varepsilon_{xx} & \varepsilon_{xy} & \varepsilon_{xz} \\ \varepsilon_{yx} & \varepsilon_{yy} & \varepsilon_{yz} \\ \varepsilon_{zx} & \varepsilon_{zy} & \varepsilon_{zz} \end{pmatrix}$$

strain vector

$$\boldsymbol{\varepsilon}^T = (\varepsilon_{xx}, \varepsilon_{yy}, \varepsilon_{zz}, 2\varepsilon_{yz}, 2\varepsilon_{zx}, 2\varepsilon_{xy})$$

loading function

$$f(\boldsymbol{\varepsilon}, \kappa) = \hat{\varepsilon}(\boldsymbol{\varepsilon}) - \kappa \leq 0$$

$\hat{\varepsilon}(\boldsymbol{\varepsilon})$  is the equivalent strain

evolution law

$$\omega = \omega(\kappa)$$

### Equivalent Strains

strain norm

$$\hat{\varepsilon} = \sqrt{\varepsilon_{xx}^2 + \varepsilon_{yy}^2 + \varepsilon_{zz}^2 + 2(\varepsilon_{yz}^2 + \varepsilon_{zx}^2 + \varepsilon_{xy}^2)}$$

$$\hat{\varepsilon} = \frac{1}{\sqrt{1 - 2\nu^2}} \sqrt{\varepsilon_{xx}^2 + \varepsilon_{yy}^2 + \varepsilon_{zz}^2 + 2(\varepsilon_{yz}^2 + \varepsilon_{zx}^2 + \varepsilon_{xy}^2)}$$

energy norm

$$\hat{\varepsilon} = \sqrt{\frac{\boldsymbol{\varepsilon}^T \mathbf{D} \boldsymbol{\varepsilon}}{E}}$$

Mazar's norm

$$\hat{\varepsilon} = \sqrt{\langle \varepsilon_\alpha \rangle \langle \varepsilon_\alpha \rangle} \quad \varepsilon_\alpha \text{ are the principal strains}$$

isotropic damage

$$\tilde{\sigma} = \frac{1}{1 - \omega} \sigma$$

asymmetric effective stress

$$\tilde{\sigma} = \sigma (\mathbf{I} - \Omega)^{-1}$$

symmetric part of the asymmetric effective stress

$$\tilde{\sigma} = \frac{1}{2} (\sigma (\mathbf{I} - \Omega)^{-1} + (\mathbf{I} - \Omega)^{-1} \sigma)$$

$$\tilde{\sigma} = (\mathbf{I} - \Omega)^{-\frac{1}{2}} \sigma (\mathbf{I} - \Omega)^{-\frac{1}{2}}$$

## Non-linear System of Algebraic Equations

body occupies a domain

$\Omega \in R^3$  with a boundary  $\Gamma$

the boundary is split

$\Gamma = \Gamma_u \cup \Gamma_t \quad (\Gamma_u \cap \Gamma_t = \emptyset)$

the displacement field

$\mathbf{u} : \Omega \rightarrow R^3$

the strain field

$\boldsymbol{\varepsilon} : \Omega \rightarrow R^6$

the stress field

$\boldsymbol{\sigma} : \Omega \rightarrow R^6$

the body forces

$\mathbf{b} : \Omega \rightarrow R^3$

the surface traction

$\mathbf{t} : \Gamma_t \rightarrow R^3$

equilibrium condition

$$\forall \mathbf{x} \in \Omega : \partial \boldsymbol{\sigma} + \mathbf{b} = \mathbf{0}$$

boundary conditions

$$\forall \mathbf{x} \in \Gamma_u : \mathbf{u} = \mathbf{0}$$

$$\forall \mathbf{x} \in \Gamma_t : \boldsymbol{\sigma} \mathbf{n} = \mathbf{t}$$

strain–displacement relationship

$$\boldsymbol{\varepsilon} = \partial^T \mathbf{u}$$

constitutive law

$$\boldsymbol{\sigma} = \boldsymbol{\sigma}(\boldsymbol{\varepsilon}) = \boldsymbol{\sigma}(\mathbf{u})$$

$$\int_{\Omega} \boldsymbol{\varphi}^T \partial \boldsymbol{\sigma} d\Omega + \int_{\Omega} \boldsymbol{\varphi}^T \mathbf{b} d\Omega = \mathbf{0}$$

$$- \int_{\Omega} \boldsymbol{\sigma}^T \partial \boldsymbol{\varphi} d\Omega + \int_{\Gamma_t} \boldsymbol{\varphi}^T \boldsymbol{\sigma} \mathbf{n} d\Gamma + \int_{\Omega} \boldsymbol{\varphi}^T \mathbf{b} d\Omega = \mathbf{0}$$

finite element discretization

$$\mathbf{u} = \mathbf{N} \mathbf{d}$$

$$\boldsymbol{\varphi} = \mathbf{N} \mathbf{p}$$

$$\mathbf{B} = \partial \mathbf{N}$$

$$- \mathbf{p}^T \int_{\Omega} \mathbf{B}^T \boldsymbol{\sigma} d\Omega + \mathbf{p}^T \int_{\Gamma_t} \mathbf{N}^T \mathbf{t} d\Gamma + \mathbf{p}^T \int_{\Omega} \mathbf{N}^T \mathbf{b} d\Omega = \mathbf{0}$$

notation

$$\mathbf{f}^{int} = \int_{\Omega} \mathbf{B}^T \boldsymbol{\sigma}(\mathbf{d}) d\Omega$$

$$\mathbf{f}^{ext} = \int_{\Gamma_t} \mathbf{N}^T \mathbf{t} d\Gamma + \int_{\Omega} \mathbf{N}^T \mathbf{b} d\Omega$$

equilibrium condition

$$\boxed{\mathbf{f}_{int}(\mathbf{d}) = \mathbf{f}_{ext}}$$

## Arc-length Method

equilibrium condition

$$\mathbf{f}_{int}(\mathbf{d}) = \mathbf{f}_c + \lambda \mathbf{f}_p$$

residual – the vector of unbalanced forces

$$\mathbf{r}(\mathbf{d}, \lambda) = \mathbf{f}_c + \lambda \mathbf{f}_p - \mathbf{f}_{int}(\mathbf{d})$$

equilibrium

$$\mathbf{r}(\mathbf{d}, \lambda) = \mathbf{0}$$

assumption

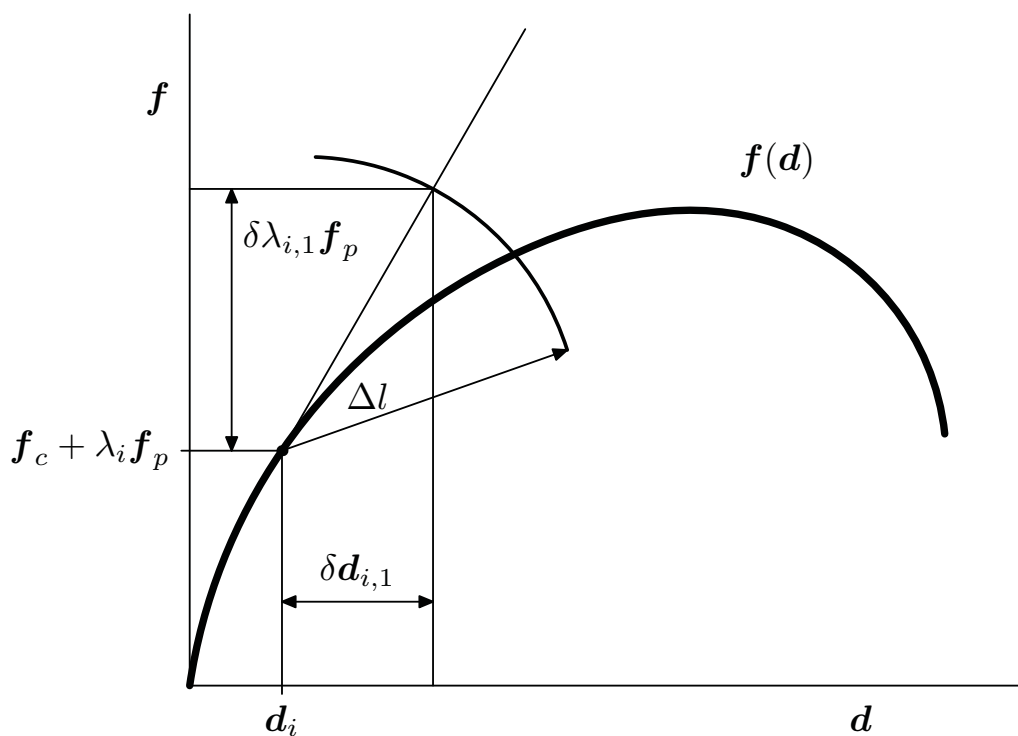
the vector  $\mathbf{d}_i$  and the parameter  $\lambda_i$  are known and  $\mathbf{r}(\mathbf{d}_i, \lambda_i) = \mathbf{0}$

$$\mathbf{r}(\mathbf{d}_{i+1}, \lambda_{i+1}) = \mathbf{r}(\mathbf{d}_i, \lambda_i) + \frac{\partial \mathbf{r}(\mathbf{d}_i, \lambda_i)}{\partial \mathbf{d}} \delta \mathbf{d}_i + \frac{\partial \mathbf{r}(\mathbf{d}_i, \lambda_i)}{\partial \lambda} \delta \lambda_i$$

$$\frac{\partial \mathbf{r}(\mathbf{d}_i, \lambda_i)}{\partial \mathbf{d}} = -\mathbf{K}_i$$

$$\frac{\partial \mathbf{r}(\mathbf{d}_i, \lambda_i)}{\partial \lambda} = \mathbf{f}_p$$

$$\mathbf{r}(\mathbf{d}_{i+1}, \lambda_{i+1}) = -\mathbf{K}_{i,0} \delta \mathbf{d}_{i,1} + \mathbf{f}_p \delta \lambda_{i,1} = \mathbf{0}$$





assumption

$$\exists \mathbf{v}_{i,1} : \quad \delta \mathbf{d}_{i,1} = \delta \lambda_{i,1} \mathbf{v}_{i,1}$$

$$\delta \lambda_{i,1} \mathbf{K}_{i,0} \mathbf{v}_{i,1} = \delta \lambda_{i,1} \mathbf{f}_p \quad \Rightarrow \quad \mathbf{v}_{i,1} = \mathbf{K}_{i,0}^{-1} \mathbf{f}_p$$

the length of arc

$$(\delta \mathbf{d}_{i,1})^T \delta \mathbf{d}_{i,1} + \psi^2 (\delta \lambda_{i,1})^2 \mathbf{f}_p^T \mathbf{f}_p = (\Delta l)^2$$

$$(\delta \lambda_{i,1})^2 \mathbf{v}_{i,1}^T \mathbf{v}_{i,1} + \psi^2 (\delta \lambda_{i,1})^2 \mathbf{f}_p^T \mathbf{f}_p = (\Delta l)^2$$

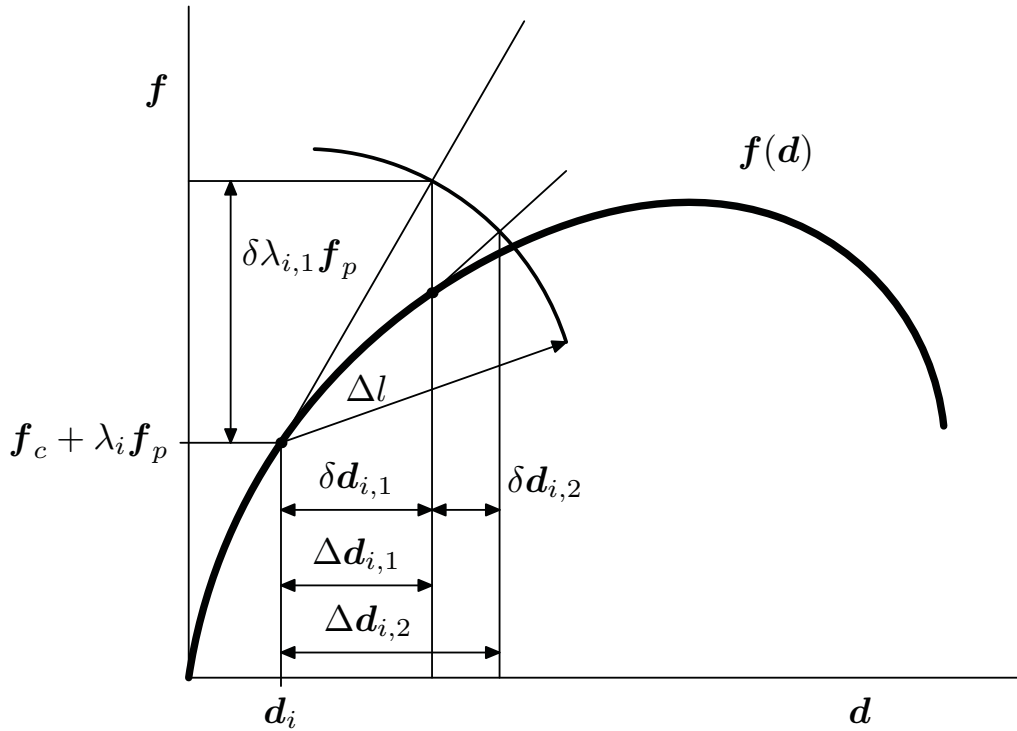
$$\delta \lambda_{i,1} = \pm \frac{\Delta l}{\sqrt{\mathbf{v}_{i,1}^T \mathbf{v}_{i,1} + \psi^2 \mathbf{f}_p^T \mathbf{f}_p}}$$

$$\mathbf{r}(\mathbf{d}_i + \delta \mathbf{d}_{i,1}, \lambda_i + \delta \lambda_{i,1}) = \mathbf{f}_c + (\lambda_i + \delta \lambda_{i,1}) \mathbf{f}_p - \mathbf{f}_{int}(\mathbf{d}_i + \delta \mathbf{d}_{i,1}) \neq \mathbf{0}$$

$$\mathbf{r}_{i,1} = \mathbf{r}(\mathbf{d}_i + \delta \mathbf{d}_{i,1}, \lambda_i + \delta \lambda_{i,1})$$

$$\mathbf{r}(\mathbf{d}_{i+1}, \lambda_{i+1}) = \mathbf{r}_{i,1} - \mathbf{K}_{i,1} \delta \mathbf{d}_{i,2} + \mathbf{f}_p \delta \lambda_{i,2} = \mathbf{0}$$

$$\begin{aligned} \mathbf{r}(\mathbf{d}_{i+1}, \lambda_{i+1}) &= \mathbf{f}_c + (\lambda_i + \delta \lambda_{i,1}) \mathbf{f}_p - \mathbf{f}_{int}(\mathbf{d}_i + \delta \mathbf{d}_{i,1}) - \\ &- \mathbf{K}_{i,1} \delta \mathbf{d}_{i,2} + \mathbf{f}_p \delta \lambda_{i,2} = \mathbf{0} \end{aligned}$$



1. 12. – 3. 12. 2010

Institute of Geonics AS CR

Ostrava

CTU

Damage, Arc-length Method

J. Kruis

$$\Delta d_{i,j} = \Delta d_{i,j-1} + \delta d_{i,j} \quad (\Delta d_{i,1} = \delta d_{i,1})$$

$$\Delta \lambda_{i,j} = \Delta \lambda_{i,j-1} + \delta \lambda_{i,j} \quad (\Delta \lambda_{i,1} = \delta \lambda_{i,1})$$

$$\begin{aligned} \mathbf{r}(d_{i+1}, \lambda_{i+1}) &= \mathbf{f}_c + (\lambda_i + \delta \lambda_{i,1}) \mathbf{f}_p - \mathbf{f}_{int}(d_i + \delta d_{i,1}) - \\ &- \mathbf{K}_{i,1} \delta d_{i,2} + \mathbf{f}_p \delta \lambda_{i,2} = \mathbf{0} \end{aligned}$$

$$\mathbf{K}_{i,1} \delta d_{i,2} = \mathbf{f}_c + (\lambda_i + \Delta \lambda_{i,1}) \mathbf{f}_p - \mathbf{f}_{int}(d_i + \Delta d_{i,1}) + \mathbf{f}_p \delta \lambda_{i,2}$$

auxiliary systems of equations

$$\mathbf{K}_{i,1} \mathbf{u}_{i,2} = \mathbf{f}_c + (\lambda_i + \Delta \lambda_{i,1}) \mathbf{f}_p - \mathbf{f}_{int}(d_i + \Delta d_{i,1})$$

$$\mathbf{K}_{i,1} \mathbf{v}_{i,2} = \mathbf{f}_p$$

1. 12. – 3. 12. 2010

Institute of Geonics AS CR

Ostrava

$$\delta \mathbf{d}_{i,2} = \mathbf{u}_{i,2} + \delta \lambda_{i,2} \mathbf{v}_{i,2}$$

the length of arc

$$\|\Delta \mathbf{d}_{i,2} + \mathbf{u}_{i,2} + \delta \lambda_{i,2} \mathbf{v}_{i,2}\|^2 + \psi^2 \|\Delta \lambda_{i,1} \mathbf{f}_p + \delta \lambda_{i,2} \mathbf{f}_p\|^2 = (\Delta l)^2$$

$$a_1 = \mathbf{v}_{i,2}^T \mathbf{v}_{i,2} + \psi^2 \mathbf{f}_p^T \mathbf{f}_p$$

$$a_2 = 2\mathbf{v}_{i,2}^T (\Delta \mathbf{d}_{i,1} + \mathbf{u}_{i,2}) + 2\Delta \lambda_{i,1} \psi^2 \mathbf{f}_p^T \mathbf{f}_p$$

$$a_3 = (\Delta \mathbf{d}_{i,1} + \mathbf{u}_{i,2})^T (\Delta \mathbf{d}_{i,1} + \mathbf{u}_{i,2}) + (\Delta \lambda_{i,1})^2 \psi^2 \mathbf{f}_p^T \mathbf{f}_p - (\Delta l)^2$$

the length of arc

$$a_1 (\delta \lambda_{i,2})^2 + a_2 (\delta \lambda_{i,2}) + a_3 = 0$$

### Algorithm of the Arc-length Method

$$\lambda_0 = 0, \mathbf{d}_0 = \mathbf{0}$$

For  $i = 0, 1, 2, \dots$

$$\Delta \lambda_{i,0} = 0, \Delta \mathbf{d}_{i,0} = \mathbf{0}, \mathbf{r}_{i,0} = \mathbf{0}$$

For  $j = 0, 1, 2, \dots$

$$\mathbf{u}_{i,j+1} = \mathbf{K}_{i,j}^{-1} \mathbf{r}_{i,j}$$

$$\mathbf{v}_{i,j+1} = \mathbf{K}_{i,j}^{-1} \mathbf{f}_p$$

$$a_1 = \mathbf{v}_{i,j+1}^T \mathbf{v}_{i,j+1} + \psi^2 \mathbf{f}_p^T \mathbf{f}_p$$

$$a_2 = 2\mathbf{v}_{i,j+1}^T (\Delta \mathbf{d}_{i,j} + \mathbf{u}_{i,j+1}) + 2\Delta \lambda_{i,j} \psi^2 \mathbf{f}_p^T \mathbf{f}_p$$

$$a_3 = \|\Delta \mathbf{d}_{i,j} + \mathbf{u}_{i,j+1}\|^2 + (\Delta \lambda_{i,j})^2 \psi^2 \mathbf{f}_p^T \mathbf{f}_p - (\Delta l)^2$$

$$a_1 (\delta \lambda_{i,j+1})^2 + a_2 (\delta \lambda_{i,j+1}) + a_3 = 0 \Rightarrow \delta \lambda_{i,j+1}$$

$$\delta \mathbf{d}_{i,j+1} = \mathbf{u}_{i,j+1} + \delta \lambda_{i,j+1} \mathbf{v}_{i,j+1}$$

$$\Delta \mathbf{d}_{i,j+1} = \Delta \mathbf{d}_{i,j} + \delta \mathbf{d}_{i,j+1}$$

$$\Delta \lambda_{i,j+1} = \Delta \lambda_{i,j} + \delta \lambda_{i,j+1}$$

$$\mathbf{r}_{i,j+1} = \mathbf{f}_c + (\lambda_i + \Delta \lambda_{i,j}) \mathbf{f}_p - \mathbf{f}_{int}(\mathbf{d}_i + \Delta \mathbf{d}_{i,j})$$

if  $\|\mathbf{r}_{i,j+1}\| < \varepsilon$ , stop

$$\lambda_{i+1} = \lambda_i + \Delta \lambda_i$$

$$\mathbf{d}_{i+1} = \mathbf{d}_i + \Delta \mathbf{d}_i$$

### Selection of the Roots $\delta\lambda_{i,j+1}$

$$\Delta \mathbf{d}_{i,j+1} = \Delta \mathbf{d}_{i,j} + \delta \mathbf{d}_{i,j+1}$$

$$\Delta \lambda_{i,j+1} = \Delta \lambda_{i,j} + \delta \lambda_{i,j+1}$$

$$\cos \theta = \frac{\Delta \mathbf{d}_{i,j+1}^T \Delta \mathbf{d}_{i,j}}{(\Delta l)^2} \rightarrow \max$$

$$\cos \theta = \frac{1}{(\Delta l)^2} \Delta \mathbf{d}_{i,j}^T (\Delta \mathbf{d}_{i,j} + \mathbf{u}_{i,j+1} + \delta \lambda_{i,j+1} \mathbf{v}_{i,j+1})$$

$$a_4 = \Delta \mathbf{d}_{i,j}^T (\Delta \mathbf{d}_{i,j} + \mathbf{u}_{i,j+1})$$

$$a_5 = \Delta \mathbf{d}_{i,j}^T \mathbf{v}_{i,j+1}$$

$$\cos \theta = \frac{a_4 + \delta \lambda_{i,j+1} a_5}{(\Delta l)^2}$$

## Linearized Arc-length Method

the length of arc

$$l(\Delta \mathbf{d}, \Delta \lambda) = \Delta \mathbf{d}^T \Delta \mathbf{d} + \psi^2 (\Delta \lambda)^2 \mathbf{f}_p^T \mathbf{f}_p - (\Delta l)^2 = 0$$

$$\frac{\partial l(\Delta \mathbf{d}, \Delta \lambda)}{\partial \Delta \mathbf{d}} = 2\Delta \mathbf{d}^T$$

$$\frac{\partial l(\Delta \mathbf{d}, \Delta \lambda)}{\partial \Delta \lambda} = 2\psi^2 \Delta \lambda \mathbf{f}_p^T \mathbf{f}_p$$

$$l_{i,j} = l(\Delta \mathbf{d}_{i,j}, \Delta \lambda_{i,j})$$

$$l_{i,j+1} = l_{i,j} + 2\Delta \mathbf{d}_{i,j}^T \delta \mathbf{d}_{i,j+1} + 2\psi^2 \Delta \lambda_{i,j} \delta \lambda_{i,j+1} \mathbf{f}_p^T \mathbf{f}_p = 0$$

$$\begin{aligned} l_{i,j+1} &= l_{i,j} + 2\Delta \mathbf{d}_{i,j}^T (\mathbf{u}_{i,j+1} + \delta \lambda_{i,j+1} \mathbf{v}_{i,j+1}) + \\ &+ 2\psi^2 \Delta \lambda_{i,j} \delta \lambda_{i,j+1} \mathbf{f}_p^T \mathbf{f}_p = 0 \end{aligned}$$

$$\delta \lambda_{i,j+1} = \frac{-\frac{1}{2}l_{i,j} - \Delta \mathbf{d}_{i,j}^T \mathbf{u}_{i,j+1}}{\Delta \mathbf{d}_{i,j}^T \mathbf{v}_{i,j+1} + \psi^2 \Delta \lambda_{i,j} \mathbf{f}_p^T \mathbf{f}_p}$$

the length of arc

$$l(\Delta \mathbf{d}, \Delta \lambda) = \Delta \mathbf{d}^T \Delta \mathbf{d} + \psi^2 (\Delta \lambda)^2 \mathbf{f}_p^T \mathbf{f}_p - (\Delta l)^2 = 0$$

$$\begin{aligned} l_{i,j+1} &= l_{i,j} + 2\Delta \mathbf{d}_{i,j}^T (\mathbf{u}_{i,j+1} + \delta \lambda_{i,j+1} \mathbf{v}_{i,j+1}) + \\ &+ 2\psi^2 \Delta \lambda_{i,j} \delta \lambda_{i,j+1} \mathbf{f}_p^T \mathbf{f}_p = 0 \end{aligned}$$

force residual

$$\mathbf{r}_{i,j+1} = \mathbf{r}_{i,j} + \frac{\partial \mathbf{r}_{i,j}}{\partial \mathbf{d}} \delta \mathbf{d}_{i,j+1} + \frac{\partial \mathbf{r}_{i,j}}{\partial \lambda} \delta \lambda_{i,j+1}$$

$$\mathbf{r}_{i,j+1} = \mathbf{r}_{i,j} - \mathbf{K}_{i,j} \delta \mathbf{d}_{i,j+1} + \mathbf{f}_p \delta \lambda_{i,j+1} = \mathbf{0}$$

$$\begin{pmatrix} \mathbf{K}_{i,j} & -\mathbf{f}_p \\ \Delta \mathbf{d}_{i,j}^T & 2\psi^2 \Delta \lambda_{i,j} \mathbf{f}_p^T \mathbf{f}_p \end{pmatrix} \begin{pmatrix} \delta \mathbf{d}_{i,j+1} \\ \delta \lambda_{i,j+1} \end{pmatrix} = \begin{pmatrix} \mathbf{r}_{i,j} \\ -l_{i,j} \end{pmatrix}$$

## Conclusions

- isotropic, orthotropic, anisotropic damage model
- mesh adjusted softening modulus
- spherical, cylindrical, linearized arc-length methods
- efficient implementation



# Optimal QP algorithms and scalable algorithms for nonlinear problems of mechanics

Zdeněk Dostál  
and colleagues

3.12.2010  
CM-II  
Ostrava



**With**

Tomáš Kozubek  
Alex Markopoulos  
Tomáš Brzobohatý  
Marie Sadovská  
Vít Vondrák  
Jiří Bouchala  
Petr Vodstrčil

...







## Outline

1. Motivation, optimal algorithms
2. TFETI/TBETI for contact problems as application of duality
3. Linear and subsymmetric separable QPQC (SMALSE)
4. Optimal algorithms for bound constrained QP (MPEGP)
5. Application to the contact problems



## Scalable algorithms

An algorithm is *numerically scalable* if  
the cost of the solution  $\sim$  number of unknowns

(for unconstrained QP problems multigrid –  
Fedorenko 60s, FETI Farhat and Roux 90s)

An algorithm enjoys *parallel scalability* if  
the time of the solution  $\sim$  1/number of processors

(for unconstrained QP problems Farhat and Roux  
FETI 1991)





## Challenges

- Identify the active constraints for free
- Get rate of convergence independent of conditioning of constraints
- Use only preconditioners that preserve bound constraints
- Get an initial approximation which is near the solution, i.e.

$$\|\hat{\mathbf{u}} - \mathbf{u}^0\| \leq C\|\mathbf{f}\|, \mathbf{u}^0 \text{ feasible}$$



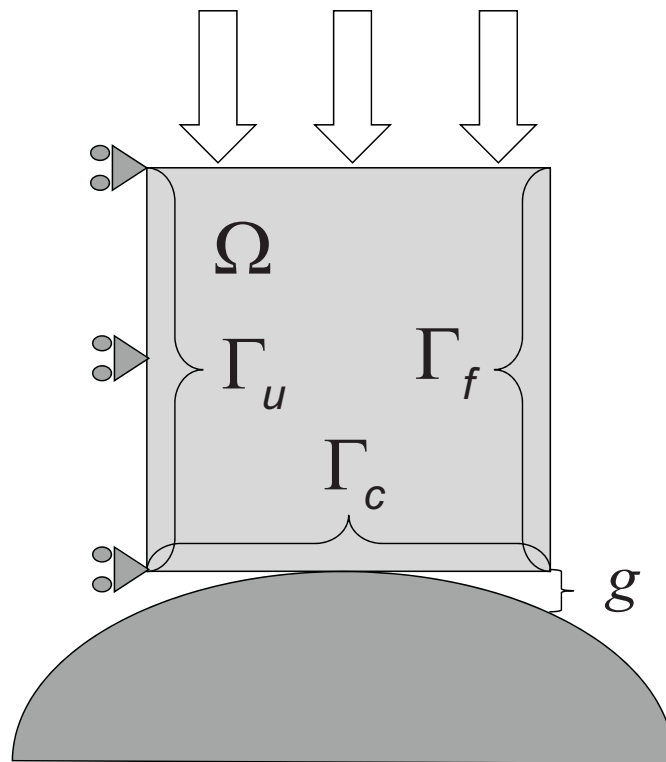
## Key observation

- In dual, there is a well defined **subspace with the solution** that can be used as a coarse grid

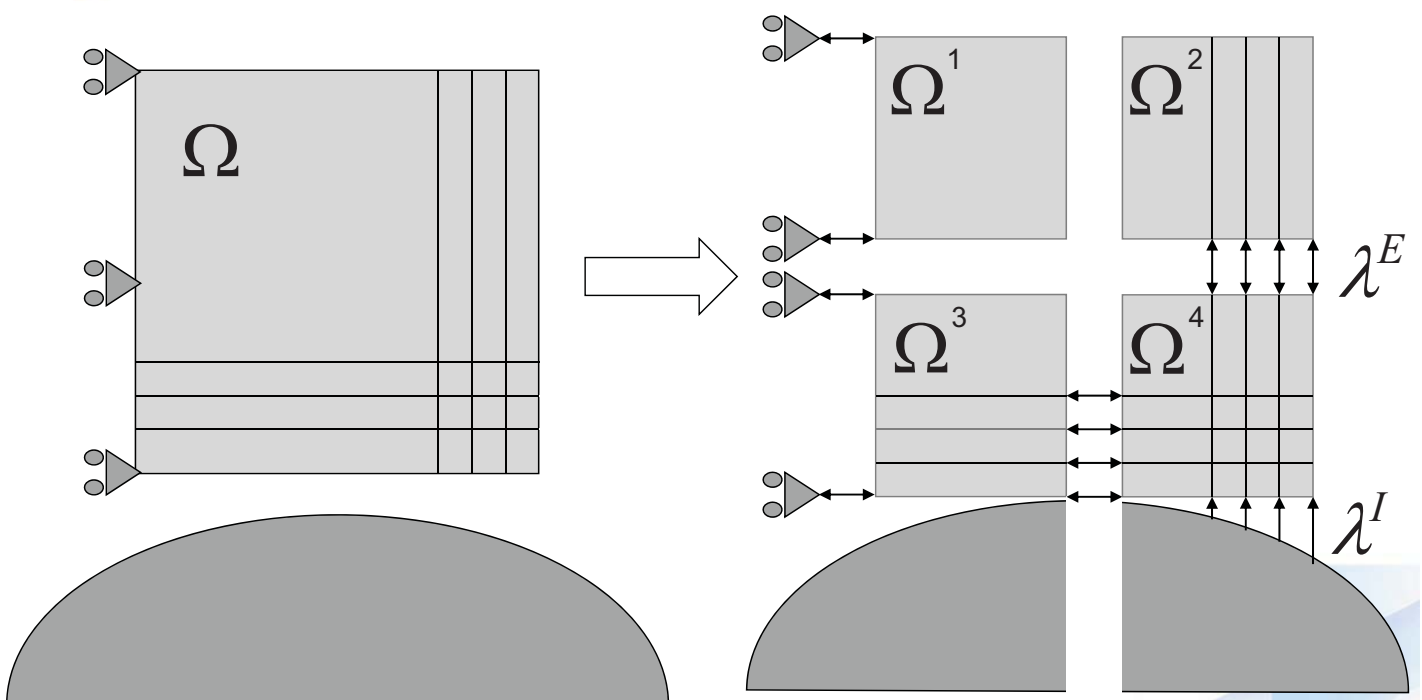




## Contact problem

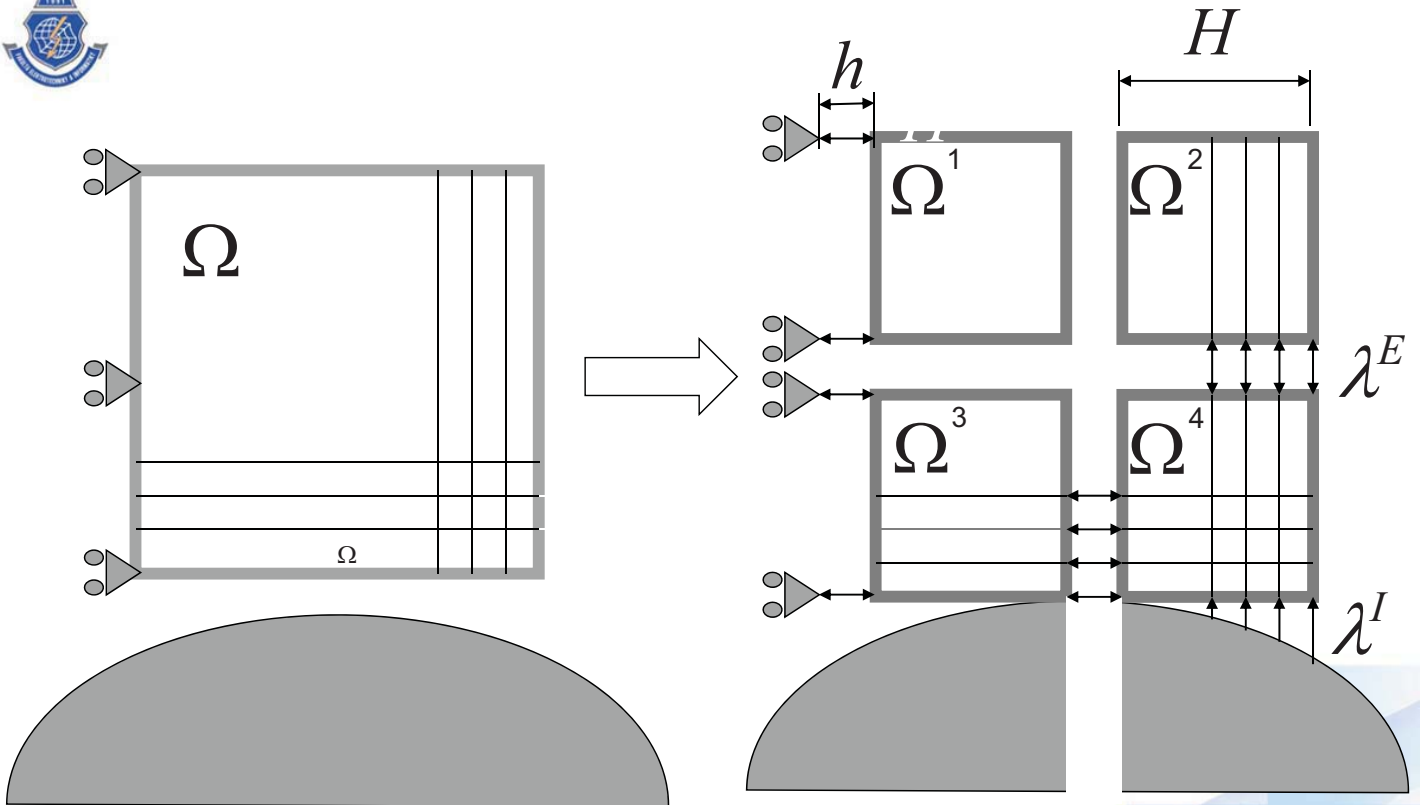


## TFETI (AF FETI) domain decomposition





## TBETI (AF BETI) domain decomposition



Linear problems Langer and Steinbach Computing 2003

Variational inequalities Bouchala, Z.D., Sadowská Computing 2008, 2009



## Stiffness matrices TFETI

$$\mathbf{K} = \begin{bmatrix} \mathbf{K}^1 & & \\ & \ddots & \\ & & \mathbf{K}^s \end{bmatrix} \quad (\text{positive semidefinite}) \quad \mathbf{f} = \begin{bmatrix} \mathbf{f}^1 \\ \vdots \\ \mathbf{f}^s \end{bmatrix}$$

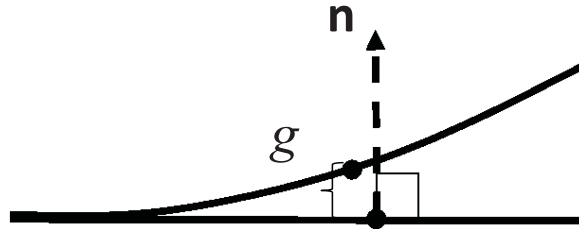
$$\text{Ker } \mathbf{K}^j = \begin{bmatrix} y_i & 1 & 0 \\ -x_i & 0 & 1 \end{bmatrix} \quad (\text{in 2D})$$

$$\text{Ker } \mathbf{K}^j = \begin{bmatrix} 0 & -z_i & y_i & 1 & 0 & 0 \\ z_i & 0 & -x_i & 0 & 1 & 0 \\ -y_i & x_i & 0 & 0 & 0 & 1 \end{bmatrix} \quad (\text{in 3D})$$





## Discretized non-penetration



$$\mathbf{B}^I = \left[ \dots (\mathbf{n}^i)^T \dots (\mathbf{n}^k)^T \dots \right], \quad \mathbf{n}^i = -\mathbf{n}^k$$

$$\Rightarrow \text{non-penetration} : \mathbf{B}^I \mathbf{u} \leq \mathbf{g}^I$$



## Discretized frictionless problem

$$J(\mathbf{u}) = \frac{1}{2} \mathbf{u}^T \mathbf{K} \mathbf{u} - \mathbf{f}^T \mathbf{u} \quad (\text{convex})$$

$$\text{gluing} : \mathbf{B}^E \mathbf{u} = \mathbf{o}$$

$$\text{non-penetration} : \mathbf{B}^I \mathbf{u} \leq \mathbf{g}$$

$$\mathcal{K}_h = \left\{ \mathbf{u} : \mathbf{B}^E \mathbf{u} = \mathbf{o} \quad \text{and} \quad \mathbf{B}^I \mathbf{u} \leq \mathbf{g} \right\}$$

$$(P_h) \quad \text{Find} \quad \min J_h(\mathbf{u}) \quad \text{s.t.} \quad \mathbf{u} \in \mathcal{K}_h$$





## Dual formulation

Convexity of  $L(\cdot, \lambda)$  and gradient argument :

$$\nabla L(\cdot, \lambda) = \mathbf{K}\mathbf{u} - \mathbf{f} + \mathbf{B}^T \lambda = \mathbf{o}$$

$\mathbf{R}$  full rank matrix,  $\text{Im}\mathbf{R} = \text{Ker}\mathbf{K}$

Solvable for  $\mathbf{f} - \mathbf{B}^T \lambda \in \text{Im}\mathbf{K} \Leftrightarrow \mathbf{R}^T(\mathbf{f} - \mathbf{B}^T \lambda) = \mathbf{o}$

$\mathbf{K}^+$  generalized inverse  $\mathbf{K}\mathbf{K}^+\mathbf{K} = \mathbf{K}$

$$\begin{aligned} (\text{D}_h) \text{ Find } & \min \lambda^T \mathbf{B}\mathbf{K}^+\mathbf{B}\lambda - \lambda^T (\mathbf{B}\mathbf{K}^+\mathbf{f} - \mathbf{c}) \\ \text{s.t. } & \lambda^I \geq \mathbf{o}, \quad \mathbf{R}^T(\mathbf{f} - \mathbf{B}^T \lambda) = \mathbf{o} \end{aligned}$$



## FETI notation and homogenization



Notation :

$$\mathbf{F} = \mathbf{B}\mathbf{K}^+\mathbf{B}^T$$

$$\mathbf{G} = \mathbf{R}^T\mathbf{B}^T$$

$$\hat{\mathbf{d}} = \mathbf{B}\mathbf{K}^+\mathbf{f} - \mathbf{c}$$

$$\mathbf{e} = \mathbf{R}^T\mathbf{f}$$

$$\begin{aligned} & \frac{1}{2} \lambda^T \mathbf{F}\lambda - \lambda^T \hat{\mathbf{d}} \rightarrow \min \\ \text{s.t. } & \lambda^I \geq \mathbf{o} \quad \text{and} \quad \mathbf{G}\lambda = \mathbf{e} \end{aligned}$$

Homogenization:

$$\mathbf{G}\bar{\lambda} = \mathbf{e} \quad \lambda = \mu + \bar{\lambda}$$

$$\mathbf{G}\lambda = \mathbf{e} \quad \Leftrightarrow \quad \mathbf{G}\mu = \mathbf{o}$$

$$\lambda^I \geq \mathbf{o} \quad \Leftrightarrow \quad \mu^I \geq -\bar{\lambda}^I$$

$$\begin{aligned} (\text{FETI}_h) & \quad \frac{1}{2} \lambda^T \mathbf{F}\lambda - \lambda^T \hat{\mathbf{d}} \rightarrow \min \\ \text{s.t. } & \lambda^I \geq -\bar{\lambda}^I \quad \text{and} \quad \mathbf{G}\lambda = \mathbf{o} \end{aligned}$$





## More on homogenization

How to choose  $\bar{\lambda}$  so that we are able to find  $\lambda^0 \geq \bar{\lambda}$  so that

$$\|\lambda^0 - \hat{\lambda}\| \leq C\|\mathbf{d}\|, \quad C \text{ independent of } h \text{ and } H ?$$

(i) Lemma : If the problem is coercive, then there is  $\bar{\lambda}$  such that

$$\lambda = \mathbf{0} \quad \text{satisfies} \quad \lambda^I \geq -\bar{\lambda}^I$$

(ii) Use  $\bar{\lambda}$  which solves  $\min \frac{1}{2} \|\lambda\|^2$  s.t.  $\lambda^I \geq \mathbf{0}$  and  $\mathbf{G}\lambda = \mathbf{e}$

In our experiments  $\bar{\lambda} = \mathbf{G}^T (\mathbf{G}\mathbf{G})^{-1} \mathbf{e}$



## Natural coarse grid projectors

$$\mathbf{Q} = \mathbf{G}^T (\mathbf{G}\mathbf{G}^T)^{-1} \mathbf{G}$$

$$\mathbf{P} = \mathbf{I} - \mathbf{Q}$$

$$\text{Im } \mathbf{Q} = \text{Im } \mathbf{G}^T$$

$$\text{Im } \mathbf{P} = \text{Ker } \mathbf{G}$$

$$\begin{aligned} (\text{FETI-NCG}_h) \quad & \frac{1}{2} \lambda^T \mathbf{P}\mathbf{F}\mathbf{P}\lambda - \lambda^T \mathbf{P}\mathbf{d} + \frac{\rho}{2} \lambda^T \mathbf{Q}\lambda \quad \rightarrow \quad \min \\ & \text{s.t. } \lambda^I \geq -\bar{\lambda}^I \quad \text{and} \quad \mathbf{G}\lambda = \mathbf{0} \end{aligned}$$

$$\rho \approx \|\mathbf{F}\|$$





## Optimal estimates

Theorem : Let there be positive constants  $B_1, B_2$  such that for any discretization parameter  $h$  and  $H$

$$B_1 \leq \lambda_{\min}(\mathbf{B}\mathbf{B}^T) \leq \lambda_{\max}(\mathbf{B}\mathbf{B}^T) \leq B_2$$

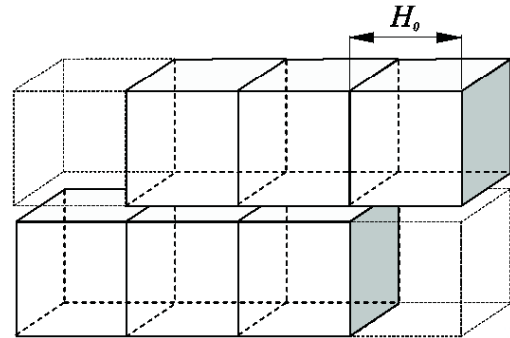
Let the elements and subdomains have regular shape and size.

Then

$$C_1 \leq \lambda_{\min}(\mathbf{F} | \text{Im}\mathbf{F})$$

$$\|\mathbf{F}\| \leq C_2 \frac{H}{h}$$

$$\kappa(\mathbf{F} | \text{Im}\mathbf{F}) \leq C_2 \frac{H}{h}$$



ETI: Farhat, Mandel, Roux 1994

ETI: Bouchala, Z.D., Sadowská 2009, based on Langer and Steinbach 2003



## Discretized Tresca problem

$$J_h(\mathbf{u}) = \frac{1}{2} \mathbf{u}^T \mathbf{K} \mathbf{u} - \mathbf{f}^T \mathbf{u} + j_h(\mathbf{u}) \quad (\text{convex})$$

$$j_h(\mathbf{u}) = \sum_{i=1}^m \psi_i \|\mathbf{T}_i \mathbf{u}\| \quad (\text{non-differentiable})$$

$$\text{gluing : } \mathbf{B}^E \mathbf{u} = \mathbf{o}$$

$$\text{non-penetration : } \mathbf{B}^I \mathbf{u} \leq \mathbf{g}$$

$$\mathcal{K}_h = \left\{ \mathbf{u} : \mathbf{B}^E \mathbf{u} = \mathbf{o} \quad \text{and} \quad \mathbf{B}^I \mathbf{u} \leq \mathbf{g} \right\}$$

$$(P_h) \quad \text{Find} \quad \min J_h(\mathbf{u}) \quad \text{s.t.} \quad \mathbf{u} \in \mathcal{K}_h$$







## Dissipative terms in 2D and 3D

2D:

$$j_h(\mathbf{u}) = \sum_{i=1}^m \psi_i \|\mathbf{T}_i \mathbf{u}\| = \sum_{i=1}^m \max_{|\tau_i| \leq \psi_i} \tau_i \mathbf{T}_i \mathbf{u}$$

3D:

$$j_h(\mathbf{u}) = \sum_{i=1}^m \psi_i \|\mathbf{T}_i \mathbf{u}\| = \sum_{i=1}^m \max_{\|\tau_i\| \leq \psi_i} \tau_i \mathbf{T}_i \mathbf{u}$$



## Mixed formulation (3D)



$$\begin{aligned} L_h(\mathbf{u}, \lambda) &= \frac{1}{2} \mathbf{u}^T \mathbf{K} \mathbf{u} - \mathbf{u}^T \mathbf{f} + \lambda_N^T (\mathbf{B}^I \mathbf{u} - \mathbf{c}) + \lambda_E^T \mathbf{B}^E \mathbf{u} + \sum_{i=1}^m \tau_i^T \mathbf{T}_i \mathbf{u} \\ &= J_h(\mathbf{u}) + \lambda^T \mathbf{B} \mathbf{u} \end{aligned}$$

$$\mathbf{B} = \begin{bmatrix} \mathbf{B}^N \\ \mathbf{T} \\ \mathbf{B}^E \end{bmatrix}, \quad \lambda = \begin{bmatrix} \lambda_N \\ \tau \\ \lambda_E \end{bmatrix}, \quad \Lambda = \Lambda(\psi) = \{ \lambda : \lambda_N \geq \mathbf{0} \text{ and } \|\tau_i\| \leq \psi_i \}$$

$$(M_h) \quad \text{Find } \min_{\mathbf{u}} \max_{\lambda \in \Lambda} L_h(\mathbf{u}, \lambda) = \max_{\lambda \in \Lambda} \min_{\mathbf{u}} L_h(\mathbf{u}, \lambda)$$



2 sets of variables



differentiable problem





## Duality and natural coarse grid projectors

$$\mathbf{Q} = \mathbf{G}^T (\mathbf{G}\mathbf{G}^T)^{-1} \mathbf{G}$$

$$\text{Im } \mathbf{Q} = \text{Im } \mathbf{G}^T$$

$$\mathbf{P} = \mathbf{I} - \mathbf{Q}$$

$$\text{Im } \mathbf{P} = \text{Ker } \mathbf{G}$$

$$\begin{aligned} (\text{TFETI-NCG}_h) \quad & \frac{1}{2} \lambda^T \mathbf{P}\mathbf{F}\mathbf{P}\lambda - \lambda^T \mathbf{P}\mathbf{d} \rightarrow \min \\ & \text{s.t. } \lambda \in \Lambda \quad \text{and} \quad \mathbf{G}\lambda = \mathbf{o} \end{aligned}$$



## Bound and equality constrained problems

For  $i \in \mathcal{T}$  let

$$f_i(\mathbf{x}) = \frac{1}{2} \mathbf{x}^T \mathbf{A}_i \mathbf{x} - \mathbf{b}_i^T \mathbf{x}$$

$$\Omega_i = \{ \mathbf{x} : \mathbf{x} \geq \mathbf{c}_i \text{ and } \mathbf{B}_i \mathbf{x} = \mathbf{o} \}, \quad \|\mathbf{B}_i\| \leq C_0$$

$$\mathbf{A}_i = \mathbf{A}_i^T$$

$$C_1 \|\mathbf{x}\|^2 \leq \mathbf{x}^T \mathbf{A}_i \mathbf{x} \leq C_2 \|\mathbf{x}\|^2, \quad \mathbf{o} \in \Omega_i$$

$$(\text{QPBE}_i) \quad \text{Find } \min_{\Omega_i} f_i(\mathbf{x})$$



Challenge: Find an approximate solution in  $O(1)$  iterations!!!

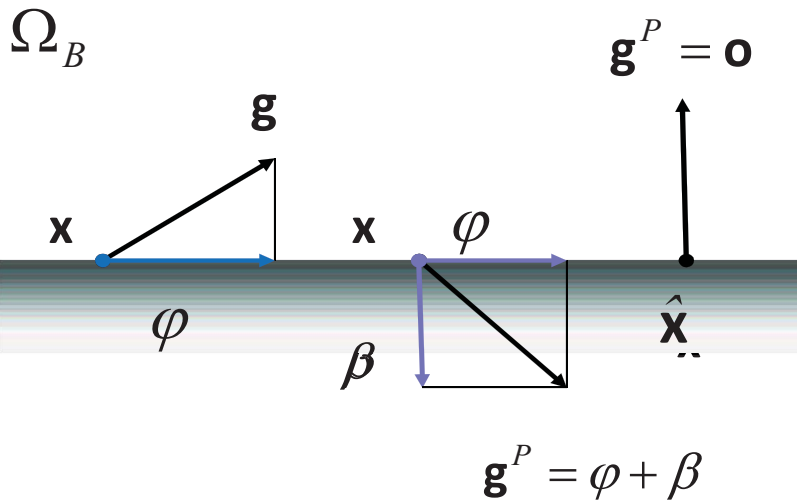


## Augmented Lagrangian and gradient

$$L(\mathbf{x}, \mu, \rho) = f(\mathbf{x}) + \mu^T \mathbf{B}\mathbf{x} + \frac{1}{2} \|\mathbf{B}\mathbf{x}\|^2$$

$$\mathbf{g}(\mathbf{x}, \mu, \rho) = \nabla_{\mathbf{x}} L(\mathbf{x}, \mu, \rho)$$

$$\mathbf{g}^P = \mathbf{g}^P(\mathbf{x}, \mu, \rho) = \varphi(\mathbf{x}, \mu, \rho) + \beta(\mathbf{x}, \mu, \rho)$$



## Algorithm SMALBE-M



Step 0  $\beta < 1, \rho > 0, M_0 > 0, \eta > 0, \mu^0$

{Approximate solution of bound constrained problem}

Step 1 Find  $\mathbf{x}^k$  such that  $\|\mathbf{g}^P(\mathbf{x}^k, \mu^k, \rho)\| \leq \min\{M_k \|\mathbf{B}\mathbf{x}^k\|, \eta\}$

{Test}

Step 2 if  $\|\mathbf{g}^P(\mathbf{x}^k, \mu^k, \rho)\|$  and  $\|\mathbf{B}\mathbf{x}^k\|$  are small then  $\mathbf{x}^k$  is solution

{Update Lagrange multipliers}

Step 3  $\mu^{k+1} = \mu^k + \rho \mathbf{B}\mathbf{x}^k$

{Update  $M_k$ }

Step 4 If  $L(\mathbf{x}^k, \mu^k, \rho) \leq L(\mathbf{x}^{k-1}, \mu^{k-1}, \rho) + \frac{\rho}{2} \|\mathbf{B}\mathbf{x}^k\|$

then  $M_{k+1} = \beta M_k$

else  $M_{k+1} = M_k$

Step 5  $k = k + 1$  and return to Step 1



## Basic relations for SMALBE

Theorem: Let  $\mathbf{x}^k, \mu^k, \rho$  be generated by SMALBE - M. Then

(i) If  $\rho \geq M_k^2 / \lambda_{\min}(\mathbf{A})$  then

$$L(\mathbf{x}^k, \mu^k, \rho) \geq L(\mathbf{x}^{k-1}, \mu^{k-1}, \rho) + \frac{\rho}{2} \|\mathbf{B}\mathbf{x}^k\|^2$$

(ii) There is  $C$  such that

$$\sum_{k=1}^{\infty} \frac{\rho}{2} \|\mathbf{B}\mathbf{x}^k\|^2 \leq C$$

Z.D. SINUM 2005, Computing 2006



## Optimality of SMALBE

Corollary: Let  $\mathbf{x}^k, \mu^k, M_k$  be generated by SMALBE - M,  $\varepsilon > 0$ .

Then:

(i)  $M_k^2 \geq \min\{M_0^2, \rho \lambda_{\min}(\mathbf{A})\}$

(ii) SMALBE - M generates  $\mathbf{x}^k$  that satisfies

$$\|\mathbf{g}_i^P(\mathbf{x}^k)\| \leq \varepsilon \|\mathbf{b}_i\| \quad \text{and} \quad \|\mathbf{B}_i \mathbf{x}^k\| \leq \varepsilon \|\mathbf{b}_i\|$$

at  $O(1)$  outer iterations

Z.D. SINUM 2005, Z.D. Computing 2006, Z.D. book 2009





## Bound constrained problems

For  $i \in \mathcal{T}$  let

$$f_i(\mathbf{x}) = \frac{1}{2} \mathbf{x}^T \mathbf{A}_i \mathbf{x} - \mathbf{b}_i^T \mathbf{x}$$

$$\Omega_i = \{ \mathbf{x} : \mathbf{x} \geq \mathbf{c}_i \}, \quad \|\mathbf{c}_i^+\| \leq C_0$$

$$\mathbf{A}_i = \mathbf{A}_i^T$$

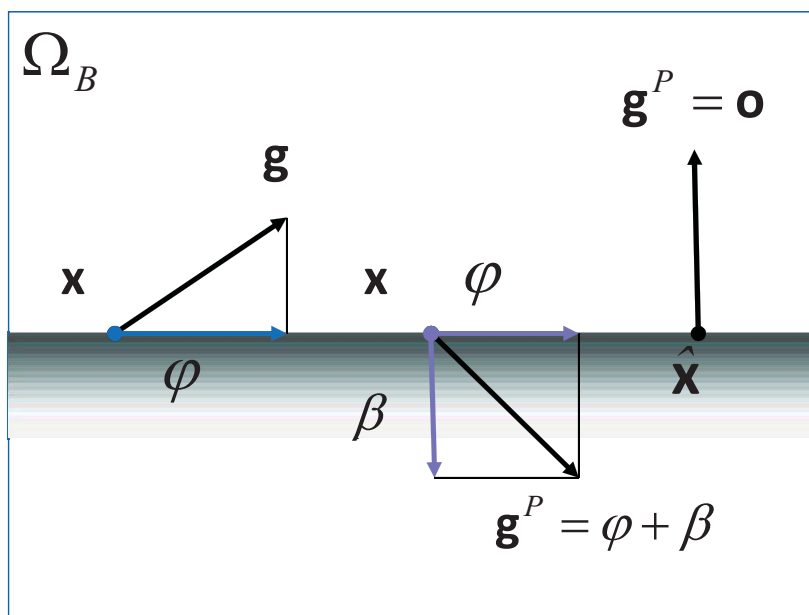
$$C_1 \|\mathbf{x}\|^2 \leq \mathbf{x}^T \mathbf{A}_i \mathbf{x} \leq C_2 \|\mathbf{x}\|^2,$$

$$(\text{QPB}_i) \quad \text{Find} \quad \min_{\Omega_i} f_i(\mathbf{x})$$

Challenge: Find an approximate solution in  $O(1)$  iterations!!!

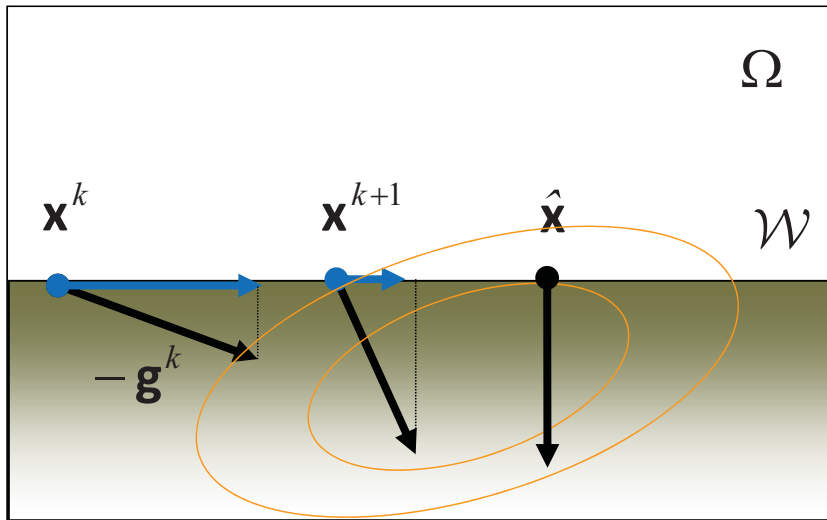


## Bound constraints: Splitting of the gradient and KKT

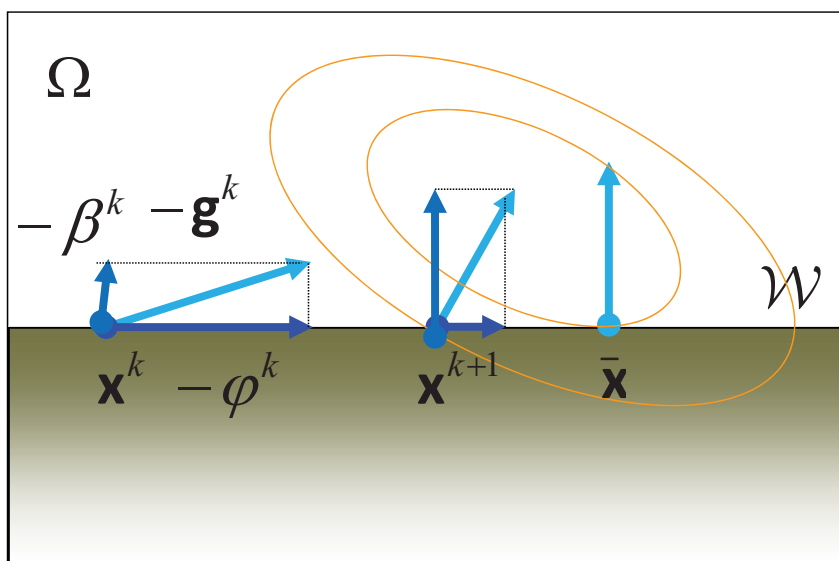




## Active set strategy in the face with the solution



## When to leave the face?

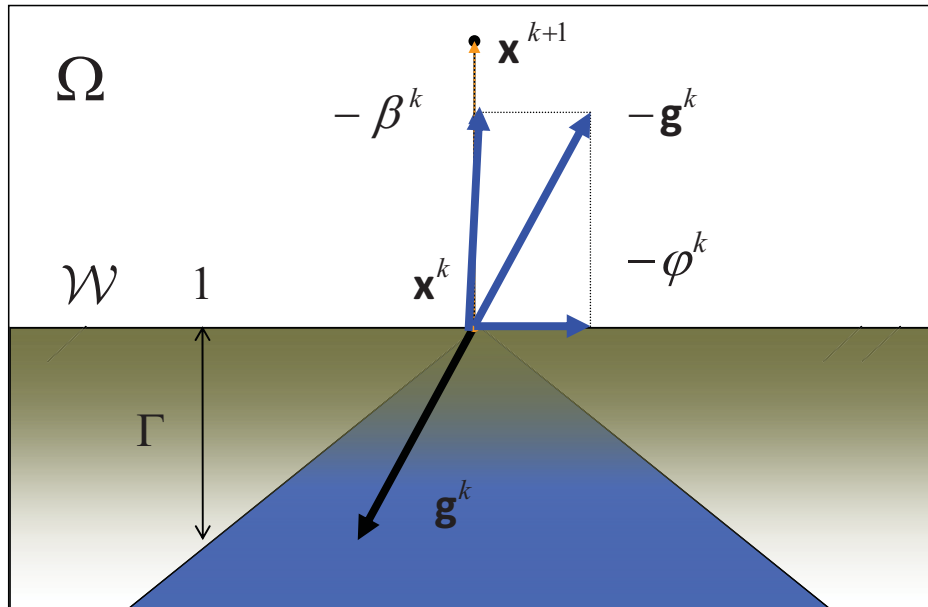




## Proportioning

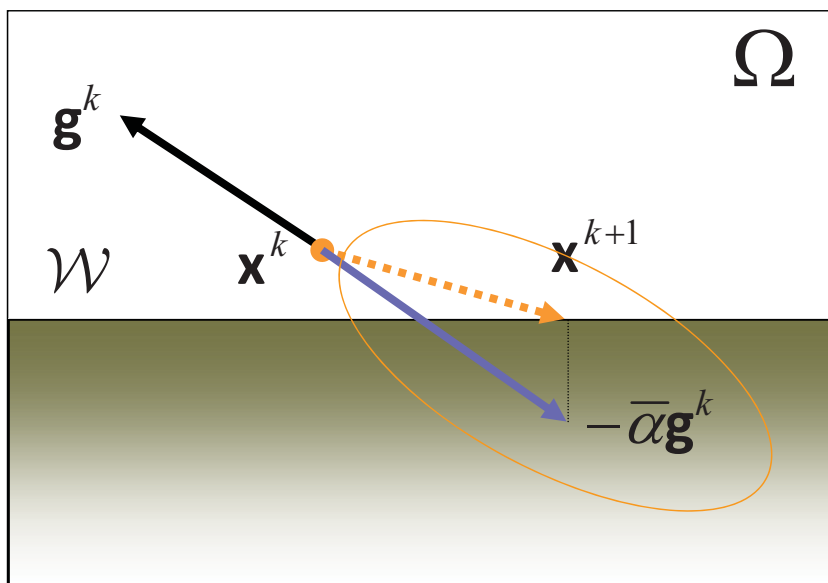
$\mathbf{x}$  not proportional:  $\Gamma^2 \tilde{\varphi}^T(x) \varphi(x) \leq \|\beta(x)\|^2$

Reduction of the active set for non-proportional iterations



## How to expand the face? Reduced gradient projection with superrelaxation

$$\mathbf{x}^{k+1} = P_{\Omega}(\mathbf{x}^k - \bar{\alpha} \varphi^k), \quad \bar{\alpha} \in (0, 2\|\mathbf{A}\|^{-1})$$





## Effect of reduced gradient projection

$\mathbf{x}^{k+1} = P_{\Omega_S}(\mathbf{x}^k - \bar{\alpha}\varphi^k)$ , proportional

$\alpha \in (0, \|A\|^{-1}]$  Schöberl, 1998:

$$f(\mathbf{x}^{k+1}) - f(\hat{\mathbf{x}}) \leq \left(1 - \frac{\alpha\lambda_{\min}}{2 + 2\Gamma^2}\right) (f(\mathbf{x}^k) - f(\hat{\mathbf{x}}))$$

Superrelaxation,

$\hat{\alpha} = \min\{\alpha, 2\|A\|^{-1} - \alpha\}$ ,  $\alpha \in (0, \|A\|^{-1}]$ , Z.D., 2008:

$$f(\mathbf{x}^{k+1}) - f(\hat{\mathbf{x}}) \leq \left(1 - \frac{\hat{\alpha}\lambda_{\min}}{2 + 2\Gamma^2}\right) (f(\mathbf{x}^k) - f(\hat{\mathbf{x}}))$$



## Conjugate gradient step

$$\mathbf{x}^{k+1} = \mathbf{x}^k - \alpha_{\text{cg}} \mathbf{p}_j, \quad \mathbf{p}_0 = \varphi_i(\mathbf{x}^k)$$

If  $\|\varphi(\mathbf{x}^k)\| \geq \Gamma \|\beta(\mathbf{x}^k)\|$ ,  $\Gamma > 0$

then

$$f(\mathbf{x}^{k+1}) - f(\hat{\mathbf{x}}) \leq \left(1 - \frac{\hat{\alpha}\lambda_{\min}}{2 + 2\Gamma^2}\right) (f(\mathbf{x}^k) - f(\hat{\mathbf{x}}))$$





## Algorithm MPRGP



{Initialization}

Step 0  $\mathbf{x}^0 \geq \mathbf{c}, \Gamma > 0, \bar{\alpha} \in (0, 2\|\mathbf{A}\|^{-1}]$

{Proportioning}

Step 1 If

$$\Gamma^2 \tilde{\varphi}(\mathbf{x}^k)^T \varphi(\mathbf{x}^k) < \|\beta(\mathbf{x}^k)\|^2$$

then define  $\mathbf{x}^{k+1}$  by minimization in the direction  $-\beta(\mathbf{x}^k)$

{Conjugate gradient step}

Step 2 if  $\mathbf{x}^k$  is proportional, then generate  $\mathbf{x}^{k+1}$  by trial CG step

{Projection}

Step 3 If  $\mathbf{x}^{k+1} \geq \mathbf{c}$ , then use it,

$$\text{else } \mathbf{x}^{k+1} = (\mathbf{x}^k - \bar{\alpha} \varphi(\mathbf{x}^k))^+$$

Z.D., Schöberl COA 2005, book 2009



## Rate of convergence of MPRGP

Theorem: Let  $\mathbf{x}^k$  be generated with  $\Gamma > 0, \hat{\Gamma} = \max\{\Gamma, \Gamma^{-1}\}, \bar{\alpha} \in (0, 2\|\mathbf{A}\|^{-1})$

Then :

(i) The R - linear rate of convergence in the energy norm is given by

$$\|\mathbf{x}^k - \hat{\mathbf{x}}\|_{\mathbf{A}} \leq \eta^k (f(\mathbf{x}^0) - f(\hat{\mathbf{x}})) \quad \text{with} \quad \eta = 1 - \frac{\bar{\alpha} \lambda_{\min}}{2 + 2\hat{\Gamma}^2}$$

(ii) The R - linear rate of convergence of the projected gradient is given by

$$\|\mathbf{g}^P(\mathbf{x}^k)\| \leq 2a\eta^k (f(\mathbf{x}^0) - f(\hat{\mathbf{x}})) \quad \text{with} \quad a = \frac{\bar{\alpha}^{-1} \lambda_{\min}^{-1}}{\eta(1-\eta)}$$

Z.D., Schoeberl COA 2005, Z.D. book 2009





## Optimality of MPRGP

Theorem :

Let  $\Gamma > 0$ ,  $0 < \alpha < 2C_2^{-1}$ ,  $\bar{\mathbf{x}}_i$  solution of (QPB<sub>*i*</sub>)

For  $i \in \mathcal{T}$  let  $\{\mathbf{x}_i^k\}$  be generated by MPRGP

with  $\alpha$  and  $\Gamma$ . Then  $\mathbf{x}_i^k$  that satisfy

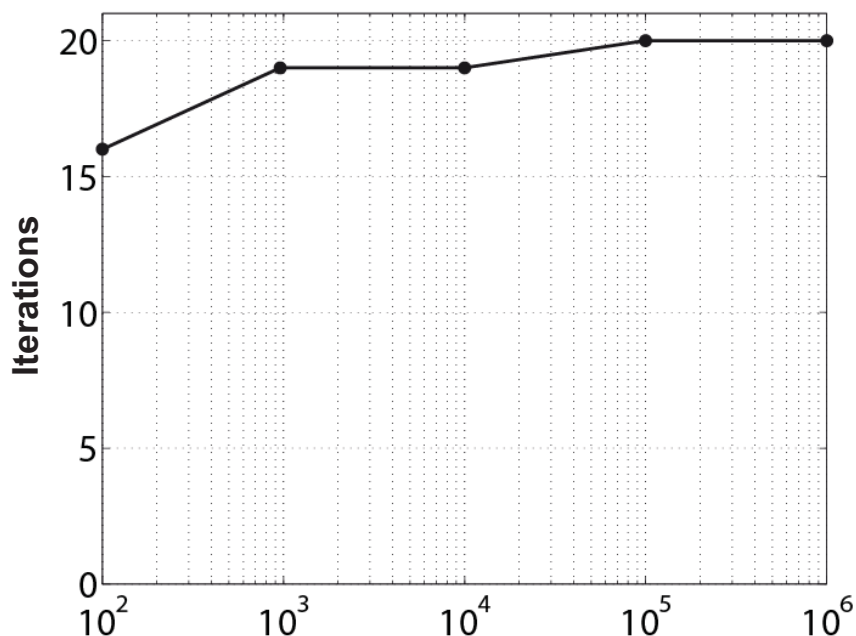
$$\|\mathbf{x}_i^k - \bar{\mathbf{x}}_i\| \leq \varepsilon \|\mathbf{b}_i\| \quad \text{and} \quad \|\mathbf{g}^P(\mathbf{x}_i^k)\| \leq \varepsilon \|\mathbf{b}_i\|$$

can be find in  $O(1)$  iterations



## Optimality for bound constrained problems

String system on Winkler support, bound constraints, cond=5





## Optimality results SMABE/MPRGP

Theorem : Let  $\hat{\mathbf{x}}_i$  be the solution of (QPBE<sub>i</sub>) generated with  $\Gamma > 0$ ,  $\bar{x} \in (0, 2C_2^{-1})$ ,  $\rho > 0$ ,  $M > 0$ . Let  $\varepsilon > 0$ .

Then  $\mathbf{x}_i^k$  that satisfies

$$\|\mathbf{x}_i^k - \hat{\mathbf{x}}_i\| \leq \varepsilon \|\mathbf{b}\| \quad \text{and} \quad \|\mathbf{g}^P(\mathbf{x}_i^k)\| \leq \varepsilon \|\mathbf{b}\|$$

s found at

O(1) matrix - vector multiplications

For bound constrained problems Z.D. Computing 2006, Z.D. book 2009,  
application to scalar problems TFETI Z.D., Horák SINUM 2007  
application to scalar problems TBETI Bouchal, Z.D., Sadowská Computing 2008  
Generalization to separable subsymmetric constraints Z.D., Kozubek 2010



## Optimality of TFETI with SMALBE/MPRGP

Theorem : Let  $\hat{\mathbf{x}}_h$  be the solution of (TFETI - NCG<sub>h</sub>) and  $\varepsilon > 0$ .

Then  $\mathbf{x}_h^k$  that satisfies

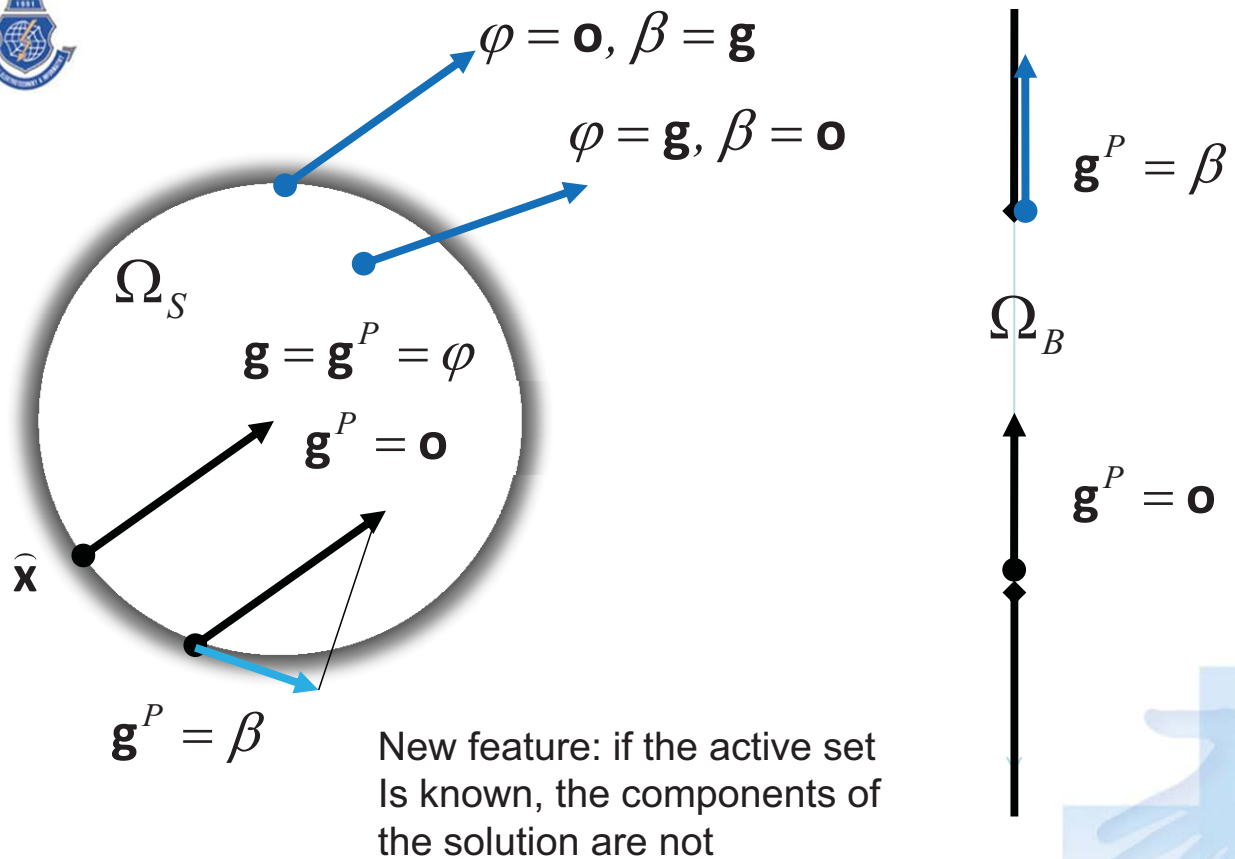
$$\|\mathbf{B}_h \mathbf{x}_h^k\| \leq \varepsilon \|\mathbf{b}_h\| \quad \text{and} \quad \|\mathbf{g}^P(\mathbf{x}_h^k)\| \leq \varepsilon \|\mathbf{b}_h\|$$

is found at

O(1) matrix - vector multiplications

Scalability no friction FETI Z.D., Kozubek, Brzobohatý, Markopoulos 2009  
Scalability no friction BETI Bouchala, Z.D., Sadowská 2008  
Scalability 2D friction Z.D., Kozubek, Brzobohatý, Markopoulos, Horyl 2010  
Scalability 3D friction Z.D., Kozubek, Brzobohatý, Markopoulos, Horyl 2010

# Separable spheric and elliptic constraints



## Effect of gradient projection

$\mathbf{x}^{k+1} = P_{\Omega_S}(\mathbf{x}^k - \bar{\alpha} \varphi^k)$ , proportional  
 $\alpha \in (0, \|A\|^{-1}]$  Schöberl, 1998:

$$f(\mathbf{x}^{k+1}) - f(\hat{\mathbf{x}}) \leq \left(1 - \frac{1}{2} \alpha \lambda_{\min}\right) (f(\mathbf{x}^k) - f(\hat{\mathbf{x}}))$$

Superrelaxation,

$\hat{\alpha} = \min\{\alpha, 2\|A\|^{-1} - \alpha\}$ ,  $\alpha \in (0, \|A\|^{-1}]$  Z.D., Kozubek 2010:

$$f(\mathbf{x}^{k+1}) - f(\hat{\mathbf{x}}) \leq \left(1 - \frac{1}{2} \hat{\alpha} \lambda_{\min}\right) (f(\mathbf{x}^k) - f(\hat{\mathbf{x}}))$$



## Algorithm MPGP



{Initialization}

Step 0  $\mathbf{x}^0 \geq \mathbf{c}, \Gamma > 0, \bar{\alpha} \in (0, 2\|\mathbf{A}\|^{-1}]$

{Proportioning}

Step 1 If

$$\Gamma \|\varphi(\mathbf{x}^k)\| < \|\beta(\mathbf{x}^k)\|^2$$

then define  $\mathbf{x}^{k+1}$  by gradient projection

{Conjugate gradient step}

Step 2 if  $\mathbf{x}^k$  is proportional, then generate  $\mathbf{x}^{k+1}$  by trial CG step

{Projection}

Step 3 If  $\mathbf{x}^{k+1} \geq \mathbf{c}$ , then use it,

$$\text{else } \mathbf{x}^{k+1} = P_{\Omega}(\mathbf{x}^k - \bar{\alpha}\varphi(\mathbf{x}^k))$$

Z.D., Kozubek 2010



## Rate of convergence of MPGP

Theorem: Let  $\mathbf{x}^k$  be generated with  $\Gamma > 0, \bar{\alpha} \in (0, 2\|\mathbf{A}\|^{-1})$

Then :

(i) The R - linear rate of convergence in the energy norm is given by

$$\|\mathbf{x}^k - \hat{\mathbf{x}}\|_{\mathbf{A}} \leq \eta^k (f(\mathbf{x}^0) - f(\hat{\mathbf{x}})) \quad \text{with} \quad \eta = 1 - \frac{\bar{\alpha}\lambda_{\min}}{2 + 2\Gamma^2}$$

(ii) The R - linear rate of convergence of the projected gradient is given by

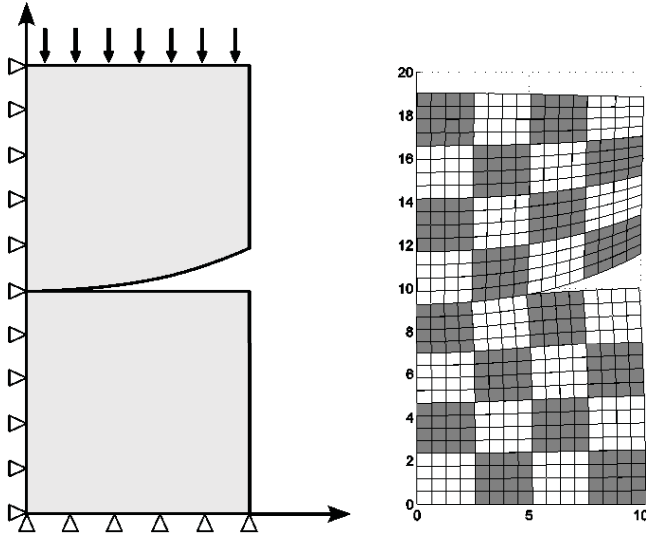
$$\|\mathbf{g}^P(\mathbf{x}^k)\| \leq 2a\eta^k (f(\mathbf{x}^0) - f(\hat{\mathbf{x}})) \quad \text{with} \quad a = \frac{\bar{\alpha}^{-1}\lambda_{\min}^{-1}}{\eta(1-\eta)}$$

Z.D., Kozubek 20102005, Z.D. book 2009





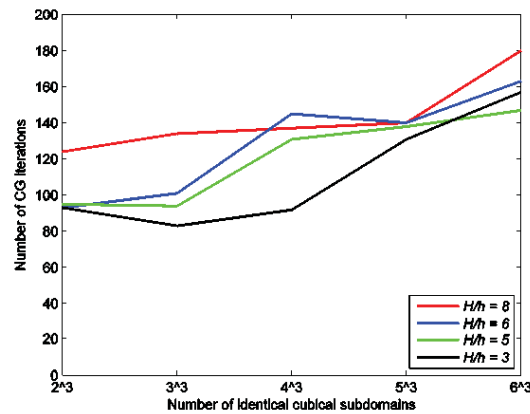
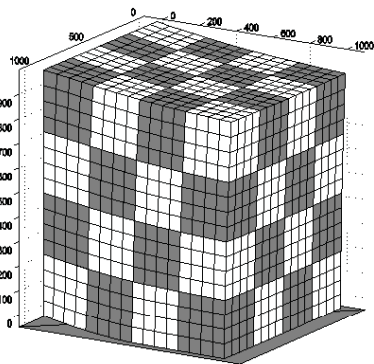
# Scalability TFETI – Hertz 2D



Primal dimension	Dual dimension	Subdomains	Null space	Matrix-vector	Time (sec)
40000	6000	2	6	45	10
640000	11200	32	96	88	78
10240000	198400	512	1536	134	1300



# Scalability TBETI – no friction 3D



Primal dimension	Dual dimension	Subdomains	Null space	Matrix-vector
11712	5023	8	48	130
93696	43441	64	192	137
316224	63275	396	1068	133





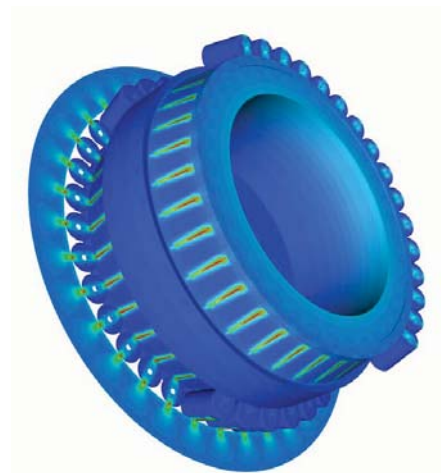
## Roler bearing of wind generator



## Decomposition and solution of roler bearing of wind generator



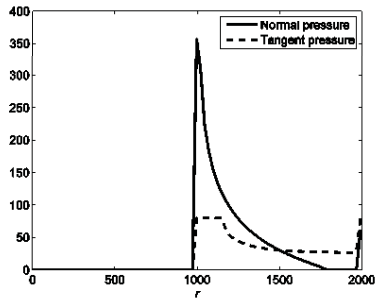
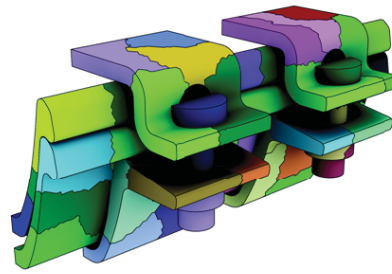
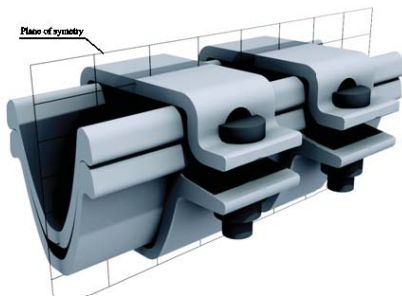
<b>Bodies</b>	73
Subdomains	700
Primal variables	2,73 M
Dual variables	459,8 k
Iterations	4270



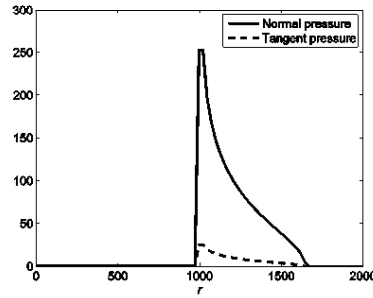




# Applications: yielding clamped connection



Tresca



Coulomb

1592853 primal, 216604 dual, 250 subdomains,  
1922 Hessian multiplications, 5100 sec/24 CPU

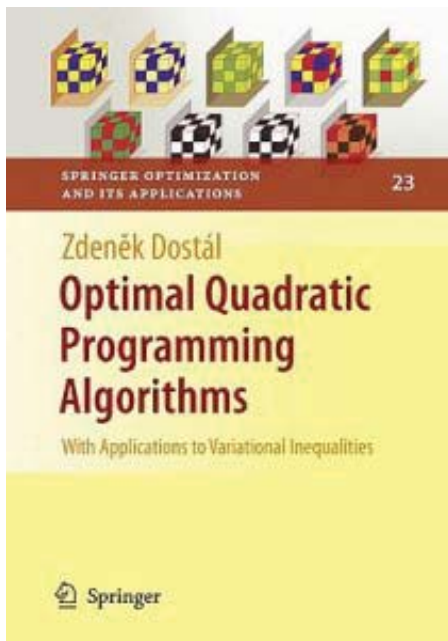


Table of Contents - Preface.

## Part I. Background

1. Linear Algebra.- 2. Optimization.

## Part II. Algorithms

3. CG for Unconstrained Minimization  
4. Equality Constrained Minimization  
5. Bound Constrained Minimization  
6. Bound and Equality Constrained Minimization

## Part III. Applications to Variational Inequalities

7. Solution of a Coercive Variational Inequality by FETI-DP method  
8. Solution to a Semicoercive Variational Inequality by TFETI Method.- References.- Index.







## Conclusions

- Total FETI/BETI is powerful tool for the solution of contact problem
- Natural coarse grid is a unique way how to get coarse grid to the contact interface
- Well conditioned convex QP and QPQC problems can be solved with optimal complexity
- Theory covers 2D and 3D frictionless contact problems and contact problems with a given (Tresca) friction
- MatSol (Kozubek et al.) is a great tool for the solution of contact problems
- MatSol often outperforms commercial solvers by orders



# T-FETI domain decomposition method for quasistatic contact problems with Coulomb friction

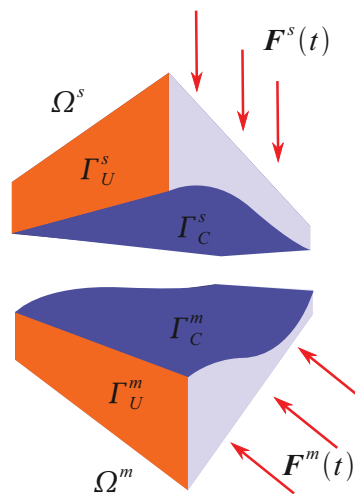
O. Vlach

KAM VŠB-TU, Ostrava  
oldrich.vlach2@vsb.cz

COMPUTATIONAL MECHANICS II 2.12.2010



## Geometry of the problem



$$\Omega = \Omega^m \cup \Omega^s \quad \partial\Omega^p = \bar{\Gamma}_U^p \cup \bar{\Gamma}_F^p \cup \bar{\Gamma}_C^p \quad p \in \{m, s\}$$



## Classical formulation

( $\forall p \in \{m, s\}$ )

equilibrium equations:

$$\frac{\partial \sigma_{ij}(\mathbf{u}^p)}{\partial x_j} + F_i^p = 0 \quad \text{in } \Omega^p \times (0, T)$$

linear Hooke's law, small deformations :

$$\sigma_{ij}(\mathbf{u}^p) = c_{ijkl} \varepsilon_{kl}(\mathbf{u}^p) \quad \varepsilon_{kl}(\mathbf{u}^p) = \frac{1}{2} \left( \frac{\partial u_k^p}{\partial x_l} + \frac{\partial u_l^p}{\partial x_k} \right)$$

classical boundary conditions:

$$\mathbf{u}^p = \mathbf{0} \quad \text{on } \Gamma_U^p \times (0, T)$$

$$\mathbf{T}(\mathbf{u}^p) := \sigma(\mathbf{u}^p) \mathbf{n}^p = \mathbf{P}^p \quad \text{on } \Gamma_F^p \times (0, T)$$

initial condition:

$$\mathbf{u}^p(0) = \mathbf{u}_0^p \quad \text{in } \Omega^p$$

Navigation icons: back, forward, search, etc.

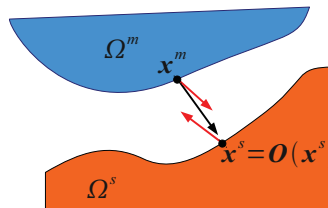
## Classical formulation

contact mapping:

$$\mathbf{O} : \Gamma_C^m \rightarrow \Gamma_C^s \quad \mathbf{n}^m \parallel (\mathbf{x}^m - \mathbf{O}(\mathbf{x}^m))$$

action - reaction:

$$(\sigma(\mathbf{u}^m(\mathbf{x}^m)) - \sigma(\mathbf{u}^s(\mathbf{O}(\mathbf{x}^m)))) \cdot \mathbf{n}^m = \mathbf{0} \quad \text{on } \Gamma_C^m \times (0, T)$$



Navigation icons: back, forward, search, etc.

## Classical formulation

notation:

$$\begin{aligned} [u_n](\mathbf{x}^m) &:= (\mathbf{u}^m(\mathbf{x}^m) - \mathbf{u}^s(\mathbf{O}(\mathbf{x}^m))) \cdot \mathbf{n}^m & T_n &:= \sigma_{ij} n_i^m n_j^m \\ [\mathbf{u}_t](\mathbf{x}^m) &:= (\mathbf{u}^m(\mathbf{x}^m) - \mathbf{u}^s(\mathbf{O}(\mathbf{x}^m))) - [u_n] \mathbf{n}^m & \mathbf{T}_t &:= \mathbf{T} - T_n \mathbf{n}^m \\ c(\mathbf{x}^m) &:= (\mathbf{O}(\mathbf{x}^m) - \mathbf{x}^m) \quad \dots \text{ gap} \end{aligned}$$

unilateral conditions:

$$[u_n] \leq c, \quad T_n \leq 0, \quad ([u_n] - c) T_n = 0 \quad \text{on } \Gamma_C^m \times (0, T_0);$$

Coulomb's law of friction:

$$\begin{aligned} [\dot{\mathbf{u}}_t](\mathbf{x}^m) = \mathbf{0} &\Rightarrow \|\mathbf{T}_t(\mathbf{x}^m)\| \leq -\mathcal{F} T_n(\mathbf{x}^m) \\ [\dot{\mathbf{u}}_t](\mathbf{x}^m) \neq \mathbf{0} &\Rightarrow \mathbf{T}_t(\mathbf{x}^m) = \mathcal{F} T_n(\mathbf{x}^m) \frac{[\dot{\mathbf{u}}_t](\mathbf{x}^m)}{\|[\dot{\mathbf{u}}_t](\mathbf{x}^m)\|}, \quad \mathbf{x}^m \in \Gamma_C^m \times (0, T_0) \end{aligned}$$

## Weak formulation

Notation

$$\begin{aligned} V &= \prod_{p \in \{m, s\}} \{v^p \in H^1(\Omega^p) \mid v^p = 0 \text{ on } \Gamma_U^p\}, \quad \mathbb{V} = V^3 \\ \mathbb{K} &= \{\mathbf{v} \in \mathbb{V} \mid [v_n] \leq c \text{ a.e. on } \Gamma_C^m\} \\ H^{1/2}(\Gamma_C^m) &= V|_{\Gamma_C^m} \quad (\text{trace space on } \Gamma_C^m \text{ of functions from } V) \\ H^{-1/2}(\Gamma_C^m) &= (H^{1/2}(\Gamma_C^m))' \quad (\text{the dual of } H^{1/2}(\Gamma_C^m)) \\ H_-^{-1/2}(\Gamma_C^m) &\dots \quad (\text{cone of non-positive elements of } H^{-1/2}(\Gamma_C^m)) \\ \langle \cdot, \cdot \rangle &\dots \quad \text{duality pairing between } H^{-1/2}(\Gamma_C^m) \text{ and } H^{1/2}(\Gamma_C^m) \end{aligned}$$

## Weak formulation

### Notation

$$\mathbf{u}, \mathbf{v} \in \mathbb{V}, \quad \lambda_n \in H^{-1/2}(\Gamma_C^m)$$

$$a(\mathbf{u}, \mathbf{v}) := \sum_{p \in \{m, s\}} \int_{\Omega^p} \sigma_{ij}(\mathbf{u}^p) \varepsilon_{ij}(\mathbf{v}^p) dx$$

$$j(\lambda_n, \mathbf{v}) := -\langle \mathcal{F} \lambda_n, \|\dot{\mathbf{v}}_t\| \rangle$$

$$L(t)(\mathbf{v}) := \sum_{p \in \{m, s\}} \int_{\Omega^p} \mathbf{F}(t) \cdot \mathbf{v} dx + \int_{\Gamma_F^p} \mathbf{P}(t) \cdot \mathbf{v} ds$$

where

$$\mathbf{F} \in W^{1,2}(0, T, \prod_{p \in \{m, s\}} (L^2(\Omega^p))^3)$$

$$\mathbf{P} \in W^{1,2}(0, T, \prod_{p \in \{m, s\}} (L^2(\Gamma_F^p))^3)$$

## Weak formulation

$$\left. \begin{aligned} & \text{Find } \mathbf{u} \in W^{1,2}(0, T, \mathbb{V}), \lambda_n \in W^{1,2}(0, T, H^{-1/2}(\Gamma_C^m)) : \\ & \mathbf{u}(t) \in \mathbb{K} \quad \text{for a.a. } t \in (0, T), \quad \mathbf{u}(0) = \mathbf{u}_0 \text{ in } \Omega \\ & a(\mathbf{u}(t), \mathbf{v} - \dot{\mathbf{u}}(t)) + j(\lambda_n(t), \mathbf{v}) - j(\lambda_n(t), \dot{\mathbf{u}}(t)) \geq L(t)(\mathbf{v} - \dot{\mathbf{u}}(t)) \\ & \quad + \langle \lambda_n(t), [\mathbf{v}_n - \dot{\mathbf{u}}_n(t)] \rangle \quad \forall \mathbf{v} \in \mathbb{V} \text{ and for a.a. } t \in (0, T) \\ & \langle \lambda_n(t), z_n - ([u_n(t)] - c) \rangle \geq 0 \quad \forall z \in \mathbb{K} \end{aligned} \right\} (\mathcal{P})$$

where  $\mathbf{u}_0 \in \mathbb{K}$  is such that

$$a(\mathbf{u}_0, \mathbf{v} - \mathbf{u}_0) + j(\lambda_{n0}, \mathbf{v} - \mathbf{u}_0) \geq L(0)(\mathbf{v} - \mathbf{u}_0) \quad \forall \mathbf{v} \in \mathbb{K}, \quad \lambda_0 = T_n(\mathbf{u}_0)|_{\Gamma_C^m}.$$

It holds:

$$\lambda_n = T_n(\mathbf{u})|_{\Gamma_C^m}$$

Theorem ( [ Rocca R. and Coccu M. 01 ] )

If  $\text{supp } \mathcal{F} \subset \Gamma_c$  and  $\mathcal{F}$  is sufficiently small, then  $(\mathcal{P})$  has at least one solution.

## Time discretization

$\Delta t = T/n \dots$  time step,

- $t_i = i\Delta t, u^i := u(t_i)$
- $\dot{\mathbf{u}}^{i+1} \approx \frac{\Delta^{i+1}\mathbf{u}}{\Delta t}$ , where  $\Delta^{i+1}\mathbf{u} := \alpha\mathbf{u}^{i+1} + \beta\mathbf{u}^i + \gamma\mathbf{u}^{i-1}$ ,  
 $\alpha = \frac{3}{2}, \beta = -2, \gamma = \frac{1}{2}$  ( $\alpha = 1, \beta = -1, \gamma = 0$ )
- set  $\mathbf{w} := \mathbf{u}^i + \Delta t\mathbf{v} \in \mathbb{V}$
- for simplicity we write  $\mathbf{u}$  instead  $\mathbf{u}^{i+1}$  and  $\mathbf{v}$  instead  $\mathbf{u}^i$
- skip index  $i$

## Time discretization

At each time step we obtain the following **implicit VI**:

$$\left. \begin{aligned} & \text{Find } (\mathbf{u}, \lambda_n) \in \mathbb{V} \times H^{-1/2}(\Gamma_C^m) \text{ such, that} \\ & \left. \begin{aligned} & a(\mathbf{u}, \mathbf{w} - \mathbf{u}) + j(\lambda_n, \mathbf{w} - \mathbf{v}) - j(\lambda_n, \mathbf{u} - \mathbf{v}) \geq \\ & L(\mathbf{w} - \mathbf{u}) + \langle \lambda_n, [w_n - u_n] \rangle \quad \forall \mathbf{w} \in \mathbb{V} \\ & \langle \mu_n - \lambda_n, [u_n] - c \rangle \geq 0 \quad \forall \mu_n \in H^{-1/2}(\Gamma_C^m) . \end{aligned} \right\} \quad (\mathcal{Q}) \end{aligned}$$

( $\mathcal{Q}$ ) is nothing else than the **static** contact problem with the following Coulomb friction law:

$$\begin{aligned} \|\mathbf{T}_t(\mathbf{x})\| &\leq -\mathcal{F}T_n(\mathbf{x}), \\ [\mathbf{u}_t](\mathbf{x}) \neq [\mathbf{v}_t](\mathbf{x}) &\Rightarrow \mathbf{T}_t(\mathbf{x}) = \mathcal{F}T_n(\mathbf{x}) \frac{[\mathbf{u}_t(\mathbf{x})] - [\mathbf{v}_t(\mathbf{x})]}{\|[\mathbf{u}_t(\mathbf{x})] - [\mathbf{v}_t(\mathbf{x})]\|} \\ &\mathbf{x} \in \Gamma_C^m \times (0, T). \end{aligned}$$

## Fixed-point formulation of $(\mathcal{Q})$

Let  $g \in H_{-}^{-1/2}(\Gamma_{\mathcal{C}}^m)$ ,  $\mathbf{v} \in \mathbb{K}$  be given and define the auxiliary problem:

$$\left. \begin{aligned} & \text{Find } \mathbf{u} := \mathbf{u}(g) \in \mathbb{V}, \lambda_n := \lambda_n(g) \in H_{-}^{-1/2}(\Gamma_{\mathcal{C}}^m) \text{ such that} \\ & a(\mathbf{u}, \mathbf{w} - \mathbf{u}) + j(g, \mathbf{w} - \mathbf{v}) - j(g, \mathbf{u} - \mathbf{v}) \geq \\ & \quad L(\mathbf{w} - \mathbf{u}) + \langle \lambda_n, [w_n - u_n] \rangle \quad \forall \mathbf{w} \in \mathbb{V} \\ & \langle \mu_n - \lambda_n, [u_n] - c \rangle \geq 0 \quad \forall \mu_n \in H_{-}^{-1/2}(\Gamma_{\mathcal{C}}^m). \end{aligned} \right\} (\mathcal{Q}(g))$$

Define the mapping  $\Phi : H_{-}^{-1/2}(\Gamma_{\mathcal{C}}^m) \mapsto H_{-}^{-1/2}(\Gamma_{\mathcal{C}}^m)$  by:

$$\Phi(g) = \lambda_n, \quad g \in H_{-}^{-1/2}(\Gamma_{\mathcal{C}}^m).$$

$(\mathbf{u}, \lambda_n)$  solves  $(\mathcal{Q})$  iff  $\lambda_n$  is a **fixed-point** of  $\Phi$ :

$$\Phi(\lambda_n) = \lambda_n.$$

## Solution strategy: the method of successive approximations

Let  $\lambda_n^{(0)} \in H_{-}^{-1/2}(\Gamma_{\mathcal{C}}^m)$  be given,  $k := 1$ ;

if  $\lambda_n^{(k)} \in H_{-}^{-1/2}(\Gamma_{\mathcal{C}}^m)$ ,  $k \geq 1$  is known,

solve  $(\mathcal{Q}(\lambda_n^{(k)}))$  and set  $\lambda_n^{(k+1)} := \lambda_n$ ,

where  $(\mathbf{u}, \lambda_n)$  is a solution of  $(\mathcal{Q}(\lambda_n^{(k)}))$ ;

$k := k + 1$ ;

repeat until stopping criterion

## Mixed formulation of $(Q(g))$

Let

$$\Lambda_n = H_-^{-1/2}(\Gamma_C^m)$$

$$\Lambda_t(g) = \{\boldsymbol{\mu}_t \in (L^2(\Gamma_C^m))^2 \mid \|\boldsymbol{\mu}_t\| \leq -\mathcal{F}g \text{ a.e. on } \Gamma_C^m\}, \quad g \in L^2(\Gamma_C^m)$$

Mixed formulation of  $(Q(g))$  reads as follows:

$$\left. \begin{array}{l} \text{Find } (\mathbf{u}, \lambda_n, \boldsymbol{\lambda}_t) \in \mathbb{V} \times \Lambda_n \times \Lambda_t(g) \text{ such that} \\ a(\mathbf{u}, \mathbf{w}) = L(\mathbf{w}) + \langle \lambda_n, [w_n] \rangle + \langle \boldsymbol{\lambda}_t, [\mathbf{w}_t] \rangle \quad \forall \mathbf{w} \in \mathbb{V} \\ \langle \mu_n - \lambda_n, [u_n] \rangle \geq \langle \mu_n - \lambda_n, c \rangle \quad \forall \mu_n \in \Lambda_n \\ \langle \boldsymbol{\mu}_t - \boldsymbol{\lambda}_t, [\mathbf{u}_t] \rangle \geq \langle \boldsymbol{\mu}_t - \boldsymbol{\lambda}_t, [\mathbf{v}_t] \rangle \quad \forall \boldsymbol{\mu}_t \in \Lambda_t(g) \end{array} \right\} (\mathcal{M}(g))$$

It holds:

- $\mathbf{u} \in \mathbb{K}$  solves  $(Q(g))$ ;
- $\lambda_n = T_n(\mathbf{u})|_{\Gamma_C^m}$ ,  $\boldsymbol{\lambda}_t = \mathbf{T}_t(\mathbf{u})|_{\Gamma_C^m}$  on  $\Gamma_C^m$ .

## T-FETI domain decomposition method

$$\bar{\Omega} = \bigcup_{i=1}^s \bar{\Omega}_i; \quad \Omega_i \cap \Omega_j = \emptyset, \quad i \neq j; \quad \text{we skip indices } m, n \text{ for now}$$

$\Gamma_{ij} := \partial\Omega_i \cap \partial\Omega_j$  ... a common part of  $\Omega_i$  and  $\Omega_j$ ,  $i \neq j$ , if  $\text{meas}_2 \Gamma_{ij} > 0$

$\Gamma_{uk} := \partial\Omega_k \cap \Gamma_u$  ... a common part of  $\Omega_k$  and  $\Gamma_u$  if  $\text{meas}_2 \Gamma_{uk} > 0$ ,

$\Gamma_{cl} := \partial\Omega_l \cap \Gamma_c$  ... a common part of  $\Omega_l$  and  $\Gamma_c$  if  $\text{meas}_2 \Gamma_{cl} > 0$ ,

Let

$$\mathcal{I} := \{(i, j) \mid \text{meas}_2 \Gamma_{ij} > 0, \quad i < j\}, \quad \mathcal{D} := \{k \mid \text{meas}_2 \Gamma_{uk} > 0\}$$

$$\mathcal{C} := \{l \mid \text{meas}_2 \Gamma_{cl} > 0\}$$

$$\mathbb{W} := \{\mathbf{v} \in (L^2(\Omega))^3 \mid \mathbf{v}|_{\Omega_i} \in (H^1(\Omega_i))^3, \quad i = 1, \dots, s\} = \prod_{i=1}^s (H^1(\Omega_i))^3$$

$$\mathbf{v} \in \mathbb{V} \Leftrightarrow \left\{ \begin{array}{l} \mathbf{v} \in \mathbb{W} \\ [\mathbf{v}]_{ij} := (\mathbf{v}_i - \mathbf{v}_j)|_{\Gamma_{ij}} = \mathbf{0} \quad \forall (i, j) \in \mathcal{I} \\ \mathbf{v}|_{\Gamma_{uk}} = \mathbf{0} \quad \forall k \in \mathcal{D} \end{array} \right\} \text{ realized by Lagrange mult.}$$



## T-FETI domain decomposition method

Define the trace spaces

$$Y_{ij} := (H^{1/2}(\Gamma_{ij}))^3 = (H^1(\Omega_i))_{|\Gamma_{ij}}^3 = (H^1(\Omega_j))_{|\Gamma_{ij}}^3, \quad (i,j) \in \mathcal{I};$$

$$Y_k := (H^{1/2}(\Gamma_{uk}))^3 = (H^1(\Omega_k))_{|\Gamma_{uk}}^3, \quad k \in \mathcal{D}$$

Then

$$\mathbf{v} \in \mathbb{V} \Leftrightarrow \begin{cases} \mathbf{v} \in \mathbb{W} \\ \langle \boldsymbol{\mu}_{ij}, [\mathbf{v}]_{ij} \rangle = \mathbf{0} & \forall \boldsymbol{\mu}_{ij} \in (Y_{ij})' & \forall (i,j) \in \mathcal{I} \\ \langle \boldsymbol{\mu}_k, \mathbf{v}|_{\Gamma_{uk}} \rangle = \mathbf{0} & \forall \boldsymbol{\mu}_k \in (Y_k)' & \forall k \in \mathcal{D}, \end{cases}$$

or denoting

$$\Lambda_\Gamma := \prod_{(i,j) \in \mathcal{I}} (Y_{ij})', \quad \Lambda_d := \prod_{k \in \mathcal{D}} (Y_k)'$$

$$\mathbf{v} \in \mathbb{V} \Leftrightarrow \begin{cases} \mathbf{v} \in \mathbb{W} \\ \langle \boldsymbol{\mu}_\Gamma, [\mathbf{v}] \rangle := \sum_{(i,j) \in \mathcal{I}} \langle \boldsymbol{\mu}_{ij}, [\mathbf{v}]_{ij} \rangle = \mathbf{0} & \forall \boldsymbol{\mu}_\Gamma \in \Lambda_\Gamma \\ \langle \boldsymbol{\mu}_d, \mathbf{v} \rangle := \sum_{k \in \mathcal{D}} \langle \boldsymbol{\mu}_k, \mathbf{v}|_{\Gamma_{uk}} \rangle = \mathbf{0} & \forall \boldsymbol{\mu}_d \in \Lambda_d \end{cases}$$

## T-FETI domain decomposition method

T-FETI formulation of  $(\mathcal{M}(g))$ :

$$\left. \begin{aligned} & \text{Find } (\mathbf{u}, \lambda_n, \boldsymbol{\lambda}_t, \boldsymbol{\lambda}_\Gamma, \boldsymbol{\lambda}_d) \in \mathbb{W} \times \tilde{\Lambda}_n \times \Lambda_t(g) \times \Lambda_\Gamma \times \Lambda_d \text{ s.t.} \\ & \sum_{i=1}^s a_i(\mathbf{u}, \mathbf{w}) = \sum_{i=1}^s L_i(\mathbf{w}) + \langle \lambda_n, [w_n] \rangle + \\ & \quad \langle \boldsymbol{\lambda}_t, [\mathbf{w}_t] \rangle + \langle \boldsymbol{\lambda}_\Gamma, [\mathbf{w}]_\Gamma \rangle + \langle \boldsymbol{\lambda}_d, \mathbf{w}_d \rangle \\ & \langle \mu_n - \lambda_n, [u_n] \rangle \geq 0 \\ & \langle \boldsymbol{\mu}_t - \boldsymbol{\lambda}_t, [\mathbf{u}_t] \rangle \geq \langle \boldsymbol{\mu}_t - \boldsymbol{\lambda}_t, [\mathbf{v}_t] \rangle \\ & \langle \boldsymbol{\mu}_\Gamma, [\mathbf{u}]_\Gamma \rangle = \mathbf{0} \\ & \langle \boldsymbol{\mu}_d, \mathbf{u}_d \rangle = \mathbf{0} \end{aligned} \right\} (\mathcal{TM}(g))$$

$$\begin{aligned} & \forall \mathbf{w} \in \mathbb{W} \\ & \forall \mu_n \in \tilde{\Lambda}_n \\ & \forall \boldsymbol{\mu}_t \in \Lambda_t(g) \\ & \forall \boldsymbol{\mu}_\Gamma \in \Lambda_\Gamma \\ & \forall \boldsymbol{\mu}_d \in \Lambda_d. \end{aligned}$$

where  $\tilde{\Lambda}_n := \prod_{l \in \mathcal{C}} H^{-1/2}(\Gamma_{cl})$ .

## Discretization

Let  $\Omega$  be a polyhedral domain and  $\mathcal{T}_i$  be a partition of  $\bar{\Omega}_i$  into tetrahedrons,  $i = 1, \dots, s$ , such that  $\mathcal{T}_i|_{\Gamma_{ij}} = \mathcal{T}_j|_{\Gamma_{ij}}$  for all  $(i, j) \in \mathcal{I}$ .

$$\mathbb{X}_i = \{v \in (C(\bar{\Omega}_i))^3 \mid v|_T \in (P_1(T))^3 \quad \forall T \in \mathcal{T}_i\}, \quad \mathbb{X} = \prod_{i=1}^s \mathbb{X}_i$$

We use **algebraic** Lagrange multipliers.

Denote

$$\begin{aligned} \{x_q^{ij}\}_{q=1}^{d_{ij}} & \dots \text{ nodes of } \mathcal{T}_i \text{ on } \bar{\Gamma}_{ij}, & (i, j) \in \mathcal{I}; \\ \{y_q^k\}_{q=1}^{d_k} & \dots \text{ nodes of } \mathcal{T}_k \text{ on } \bar{\Gamma}_{uk}, & k \in \mathcal{D}; \\ \{z_q^l\}_{q=1}^{d_l} & \dots \text{ nodes of } \mathcal{T}_l \text{ on } \bar{\Gamma}_{cl} \setminus \bar{\Gamma}_u, & l \in \mathcal{I}^c; \end{aligned}$$

## Discretization

$$\mathbb{A}_n = \{\mu_n \mid \mu_n = \sum_{l \in \mathcal{I}^c} \sum_{q=1}^{d_l} \mu_q^l \delta_{z_q^l}, \mu_q^l \leq 0\}$$

$$[\mu_n, v_n] := \sum_{l \in \mathcal{I}^c} \sum_{q=1}^{d_l} \mu_q^l v_n(z_q^l) \quad \forall v \in \mathbb{X};$$

$$[\mu_n, v_n] \geq 0 \quad \forall \mu_n \in \mathbb{A}_n \quad \Leftrightarrow \quad v_n(z_q^l) \leq 0 \quad \forall l \in \mathcal{I}^c, \quad q = 1, \dots, d_l$$

$$\mathbb{A}_t(\mathbf{g}) = \{\mu_t \mid \mu_t = \sum_{l \in \mathcal{I}^c} \sum_{q=1}^{d_l} \mu_q^l \delta_{z_q^l}, \mu_q^l \in \mathbb{R}^2, \|\mu_q^l\| \leq (\mathcal{F}g_q^l)(z_q^l)\}$$

where  $\delta_{z_q^l}$  is the Dirac function at  $z_q^l$ .

$$[\mu_t, v_t] := \sum_{l \in \mathcal{I}^c} \sum_{q=1}^{d_l} \sum_{k=1}^2 \mu_{qk}^l v_{tk}(z_q^l), \quad v_t = (v_{t1}, v_{t2})$$

## Discretization

$$\Lambda_\Gamma = \{ \mu_\Gamma \mid \mu_\Gamma = \sum_{(i,j) \in \mathcal{I}} \sum_{q=1}^{d_{ij}} \mu_q^{ij} \delta_{x_q^{ij}}, \mu_q^{ij} \in \mathbb{R}^3 \}$$

$$\Lambda_d = \{ \mu_d \mid \mu_d = \sum_{k \in \mathcal{D}} \sum_{q=1}^{d_k} \mu_q^k \delta_{y_q^k}, \mu_q^k \in \mathbb{R}^3 \}$$

$$[\mu_d, \mathbf{v}] := \sum_{k \in \mathcal{D}} \sum_{q=1}^{d_k} \sum_{l=1}^3 \mu_{ql}^k v_l(y_q^k)$$

$$[\mu_d, \mathbf{v}] = 0 \quad \forall \mu_d \in \Lambda_d \quad \Leftrightarrow \quad v_l(y_q^k) = 0 \quad \forall k \in \mathcal{D}, q = 1, \dots, d_k, l = 1, 2, 3$$

$$\begin{aligned} \mathbb{W} &\sim \mathbb{X}; & \tilde{\Lambda}_n &\sim \Lambda_n; & \Lambda_t(\mathbf{g}) &\sim \Lambda_t(\mathbf{g}) \\ \Lambda_\Gamma &\sim \Lambda_\Gamma; & \Lambda_d &\sim \Lambda_d \end{aligned}$$

## Algebraic formulation of the mixed problem

$$\left. \begin{aligned} & \text{Find } (\mathbf{u}, \boldsymbol{\lambda}) \in \mathbb{R}^p \times \tilde{\Lambda}(\mathbf{g}) \text{ such that} \\ & \mathbf{K}\mathbf{u} = \mathbf{f} + \mathbf{B}^\top \boldsymbol{\lambda} \\ & (\boldsymbol{\mu} - \boldsymbol{\lambda})^\top \mathbf{B}\mathbf{u} \geq (\boldsymbol{\mu} - \boldsymbol{\lambda})^\top \mathbf{z} \quad \forall \boldsymbol{\mu} \in \tilde{\Lambda}(\mathbf{g}) \end{aligned} \right\} \quad (\mathbf{M}(\mathbf{g}))$$

where

$$\begin{aligned} \tilde{\Lambda}(\mathbf{g}) &= \mathbb{R}_-^{m_n} \times \Lambda_t(\mathbf{g}) \times \mathbb{R}^{m_r + m_d} \\ \Lambda_t(\mathbf{g}) &= \{ (\boldsymbol{\mu}_a^\top, \boldsymbol{\mu}_b^\top)^\top \in \mathbb{R}^{2m_n} \mid \|(\mu_{ai}, \mu_{bi})\| \leq \mathcal{F}_i g_i \quad \forall i = 1, \dots, m_n \} \\ \boldsymbol{\mu} &= (\boldsymbol{\mu}_n^\top, \boldsymbol{\mu}_t^\top, \boldsymbol{\mu}_\Gamma^\top, \boldsymbol{\mu}_d^\top)^\top \\ \mathbf{z} &= (\mathbf{c}^\top, (\mathbf{T}\mathbf{v})^\top, \mathbf{0}^\top, \mathbf{0}^\top)^\top \\ \mathbf{B} &= (\mathbf{N}^\top, \mathbf{T}, \mathbf{B}_\Gamma^\top, \mathbf{B}_d^\top)^\top \end{aligned}$$

### Remark

Note that  $\mathbf{K}$  is *block-diagonal* where all diagonal blocks are *singular*.

## Dual algebraic formulation

We eliminate  $\mathbf{u}$  from  $(\mathbf{M}(\mathbf{g}))_1$ :

$$\mathbf{u} = \mathbf{K}^\dagger(\mathbf{f} + \mathbf{B}^\top \boldsymbol{\lambda}) + \mathbf{R}\boldsymbol{\alpha} ,$$

where  $\mathbf{K}^\dagger$  is a generalized inverse of  $\mathbf{K}$ , columns of  $\mathbf{R} \in \mathbb{R}^{p \times l}$  span  $\ker \mathbf{K}$  and  $\boldsymbol{\alpha} \in \mathbb{R}^l$ .

## Dual algebraic formulation

$$\left. \begin{array}{l} \text{Find } \boldsymbol{\lambda} \in \boldsymbol{\Lambda}(\mathbf{g}) \text{ such that} \\ S(\boldsymbol{\lambda}) \leq S(\boldsymbol{\mu}) \quad \forall \boldsymbol{\mu} \in \boldsymbol{\Lambda}(\mathbf{g}) \end{array} \right\}$$

where

$$S(\boldsymbol{\mu}) = \frac{1}{2} \boldsymbol{\mu}^\top \mathbf{F} \boldsymbol{\mu} - \boldsymbol{\mu}^\top \mathbf{h}$$

$$\boldsymbol{\Lambda}(\mathbf{g}) = \{ \boldsymbol{\mu} \in \tilde{\boldsymbol{\Lambda}}(\mathbf{g}) \mid \mathbf{G} \boldsymbol{\mu} = \mathbf{e} \}$$

$$\mathbf{F} = \mathbf{B} \mathbf{K}^\dagger \mathbf{B}^\top, \quad \mathbf{h} = \mathbf{z} - \mathbf{B} \mathbf{K}^\dagger \mathbf{f}$$

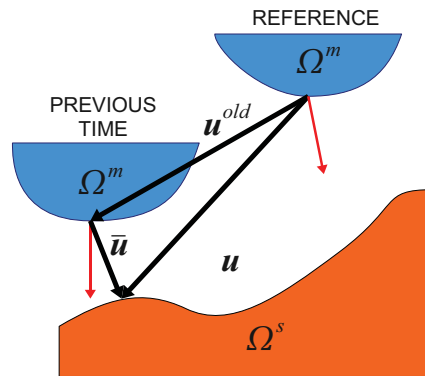
$$\mathbf{G} = \mathbf{R}^\top \mathbf{B}^\top, \quad \mathbf{e} = -\mathbf{R}^\top \mathbf{f}$$

### Remark

*This quadratic programming problem with separable simple and quadratic constraints is solved by the algorithm MPPG.*

## Correction of contact mapping

$$\bar{\mathbf{N}}\bar{\mathbf{u}} \leq \bar{\mathbf{c}} \wedge \mathbf{u} = \bar{\mathbf{u}} + \mathbf{u}^{old} \Rightarrow \bar{\mathbf{N}}\mathbf{u} \leq \bar{\mathbf{c}} + \bar{\mathbf{N}}\bar{\mathbf{u}}$$



## Model example

$$\Omega = (0, 3) \times (0, 1) \times (0, 1) [m].$$

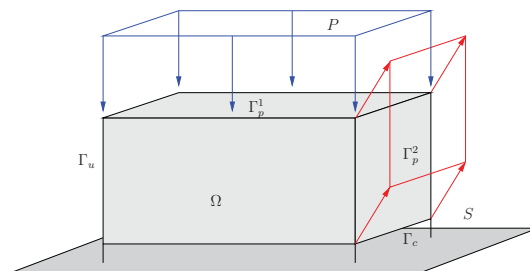
$$\text{Young's modulus } E = 2.119e5 [Pa],$$

$$\text{Poisson's ratio } \sigma = 0.277$$

50 timesteps

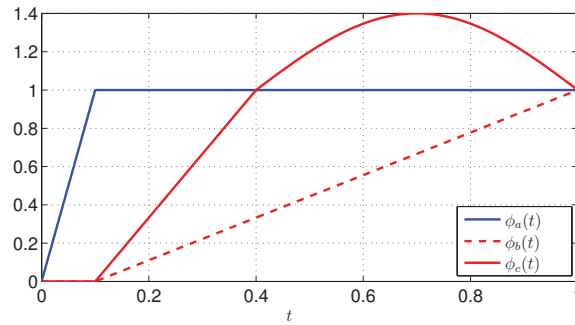
$$P(t) = \phi_a(t) \begin{pmatrix} 0 \\ 0 \\ 3 \end{pmatrix} 1e1 \quad \text{on } \Gamma_p^1$$

$$P(t) = \phi_x(t) \begin{pmatrix} 0.9 \\ 0 \\ 1.5 \end{pmatrix} 1e1 \quad \text{on } \Gamma_p^2, x \in \{b, c\}.$$

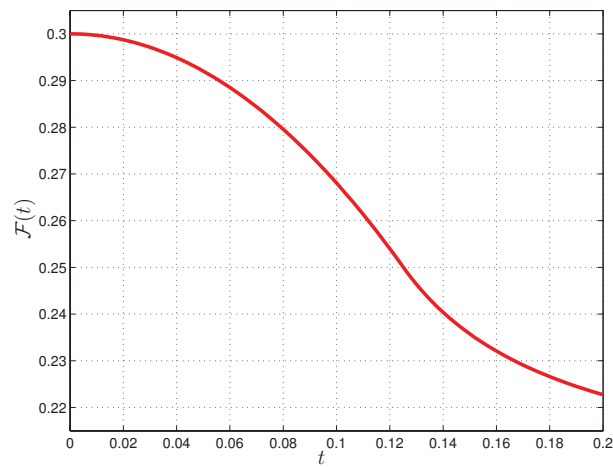


Loading history (characterized by  $\phi_x : [0, 1] \rightarrow \mathbb{R}^1$ )

$$\phi_x(t) := \begin{cases} \phi_b(t) \dots & \text{monotone loading} \\ \phi_c(t) \dots & \text{nonmonotone loading} \end{cases}$$



Coefficient of friction  $\mathcal{F}(\|\dot{\mathbf{u}}_t\|)$

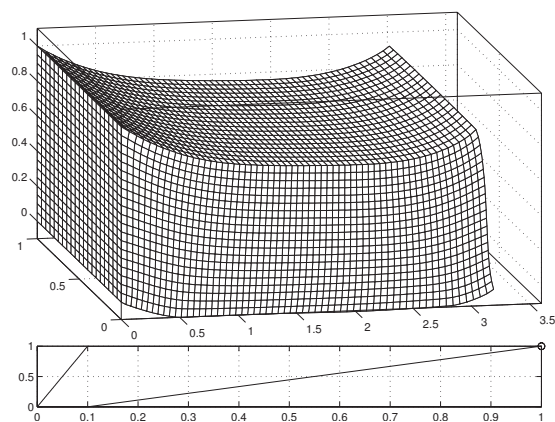


## Dependence on $h$

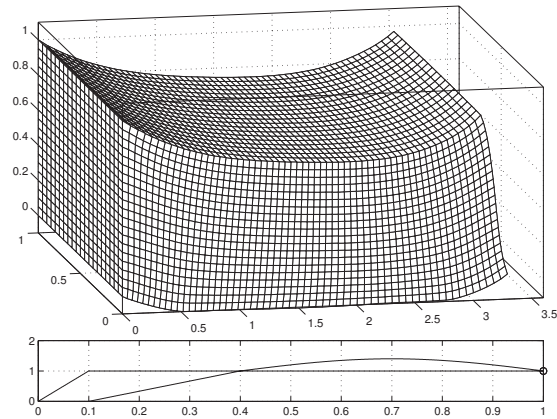
$n_s, n_p, n_d$  ... number of subdomains, primal and dual variables  
 $it$  ... number of fixed point iterations (sum for all time steps)  
 $n_m$  ... dual matrix multiplication  
 time [s] ... CPU time

$n$	$n_s$	$n_p$	$n_d$	$it$	$n_m$	time [s]
1	3	1944	594	254/234	24903/30353	2.8e2/3.4e2
2	24	15552	5652	257/237	32554/38562	2.5e3/3.4e3
4	192	124416	48816	256/238	43013/54067	3.0e4/3.5e4
5	648	419904	168804	257/239	53631/69620	1.1e5/1.5e5

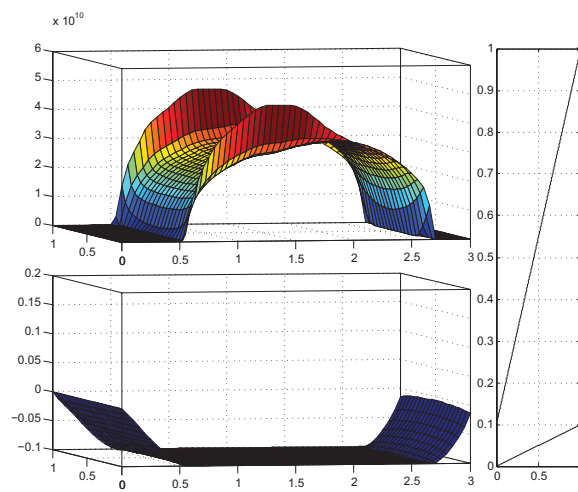
## Deformation



## Deformation

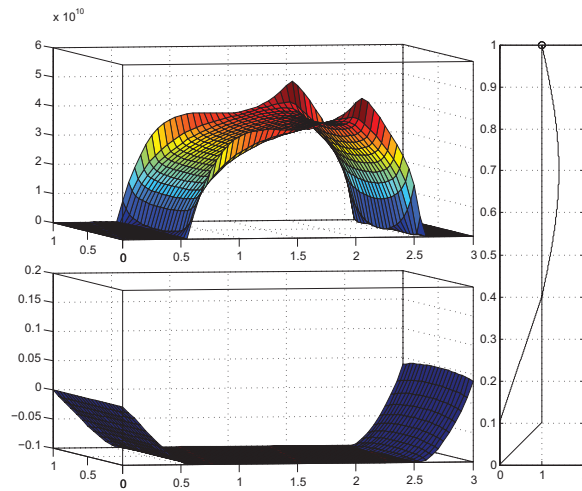


## Normal contact stress $-T_n$ and displacement $-u_n$

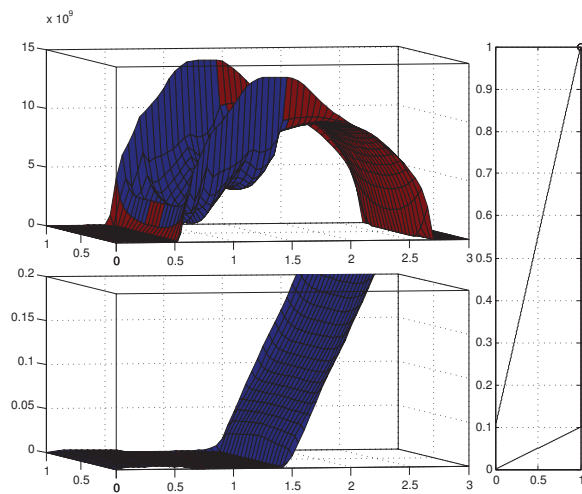




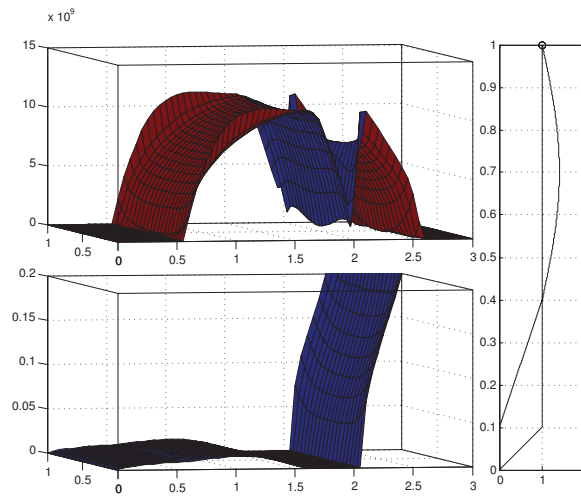
Normal contact stress  $-T_n$  and displacement  $-u_n$



Norms of tangential stress  $\|T_t\|$  and velocity  $\|\dot{u}_t\|$



## Norms of tangential stress $\|T_t\|$ and velocity $\|\dot{u}_t\|$



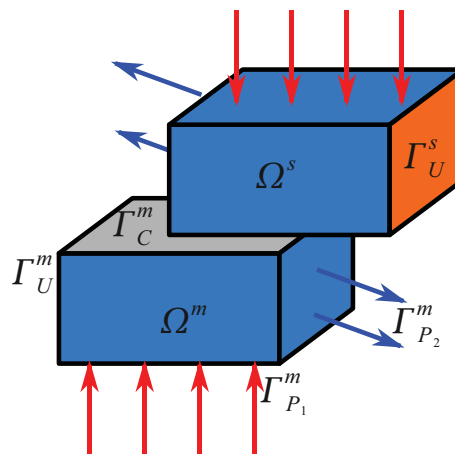
### Model example

$$\Omega^m = (0, 2) \times (-0.05, 1.05) \times (0, 1) \quad \Omega^s = \left(\frac{2}{3}, \frac{8}{3}\right) \times (0, 1) \times (1.1, 2.1).$$

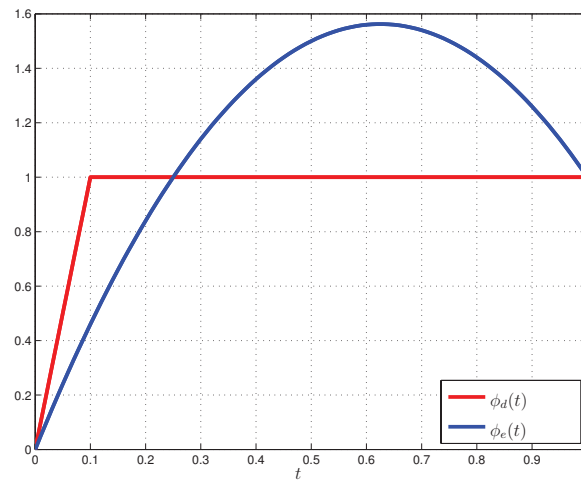
$$E^m = E^s = 5e4, \quad \sigma^m = 0.277, \quad \sigma^s = 0.35$$

$$\left. \begin{aligned} P(t) &= \phi_d(t)(0, 0, 2)1e3 && \text{on } \Gamma_{P_1}^m \\ P(t) &= \phi_e(t)(3, 0, -1)1e3 && \text{on } \Gamma_{P_2}^m \end{aligned} \right\}$$

and symmetric on  $\Gamma$   
10 timesteps



## Loading history

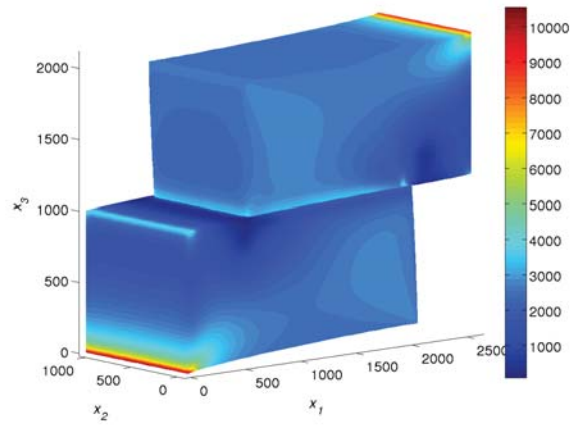


## Dependence on $h$

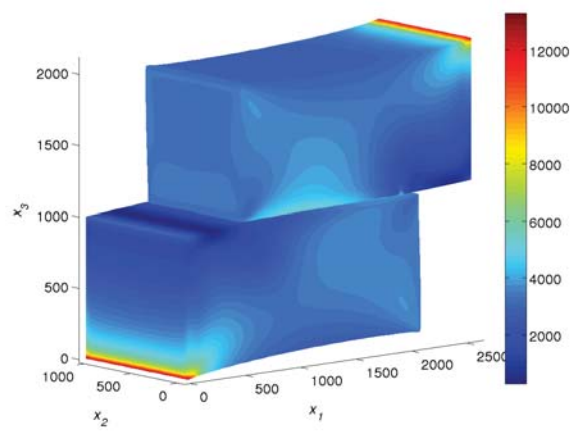
$n_s, n_p, n_d$  ... number of subdomains, primal and dual variables  
 $it$  ... number of fixed point iterations (sum for all time steps)  
 $n_m$  ... dual matrix multiplication  
 time [s] ... CPU time

$n$	$n_s$	$n_p$	$n_d$	$it$	$n_m$	time [s]
1	4	4116	798	119	1851	3.5e1
2	32	32928	9336	138	4353	3.2e2
3	108	111132	34809	163	5930	1.2e3
4	256	263424	86301	195	7440	3.1e3

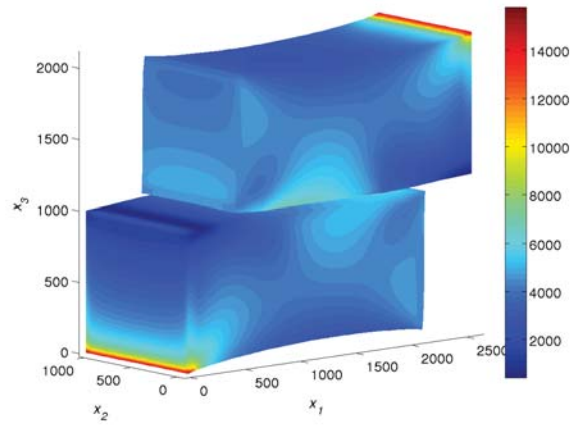
## Deformation



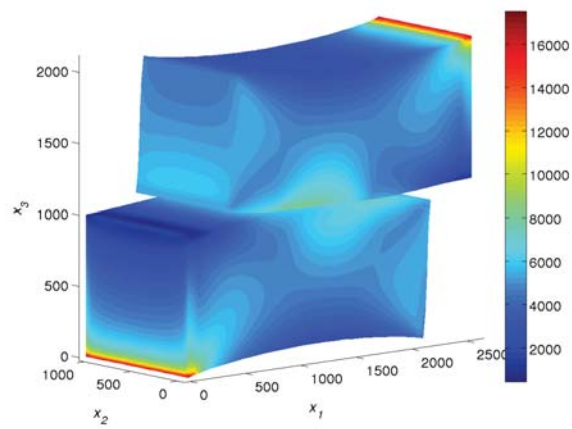
## Deformation



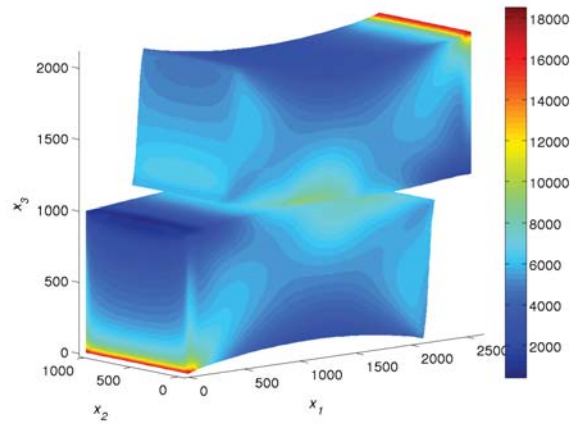
## Deformation



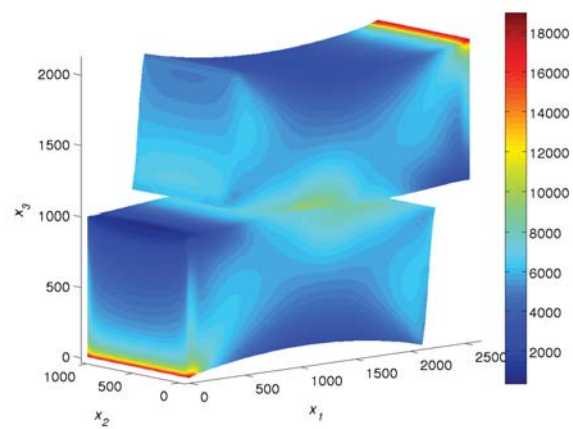
## Deformation



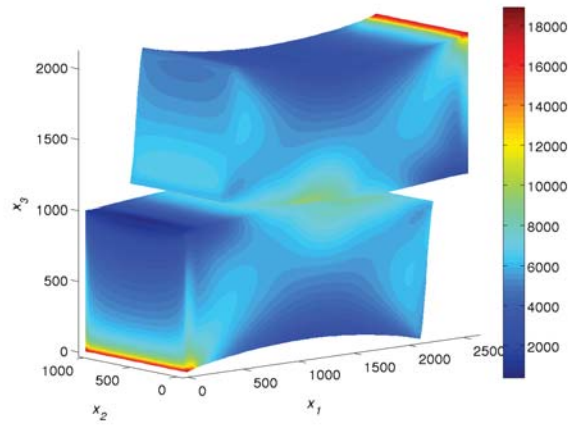
## Deformation



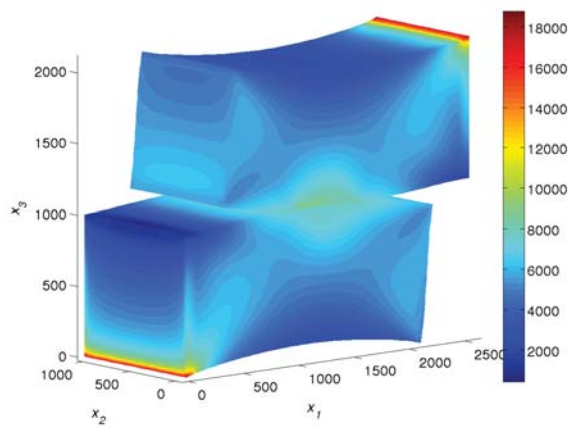
## Deformation



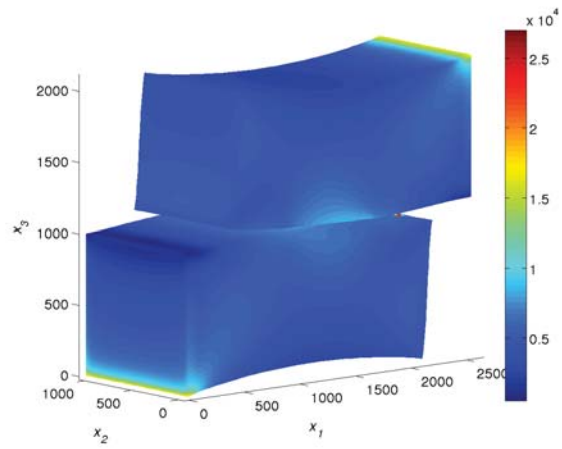
## Deformation



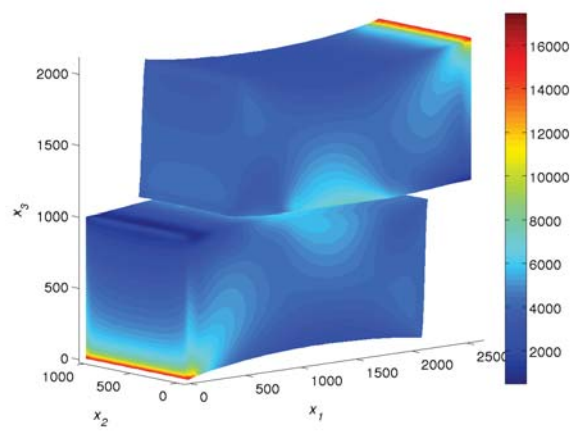
## Deformation



## Deformation

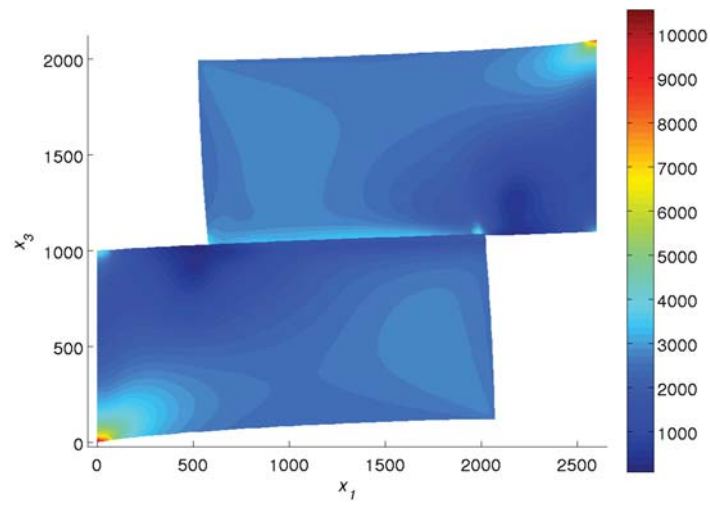


## Deformation

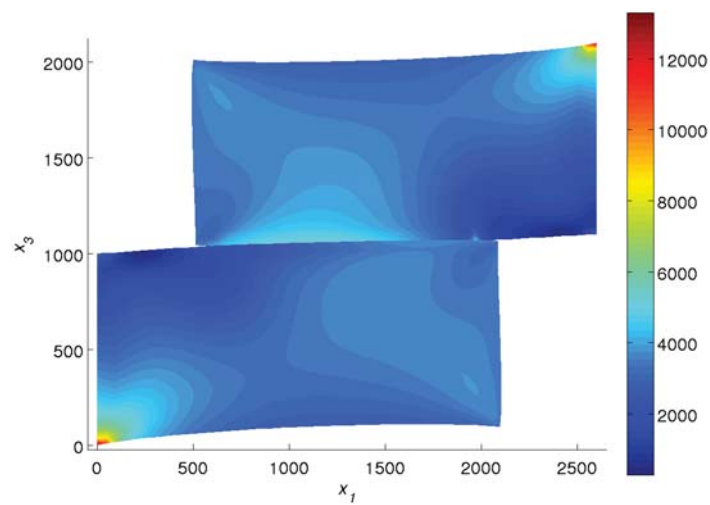




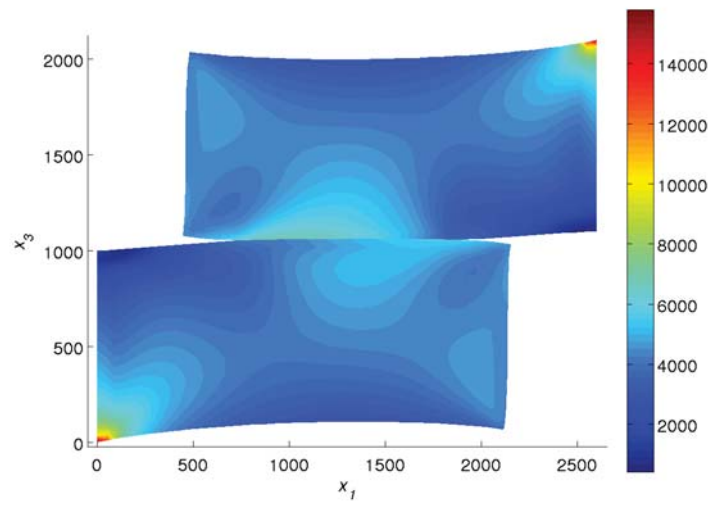
## Deformation



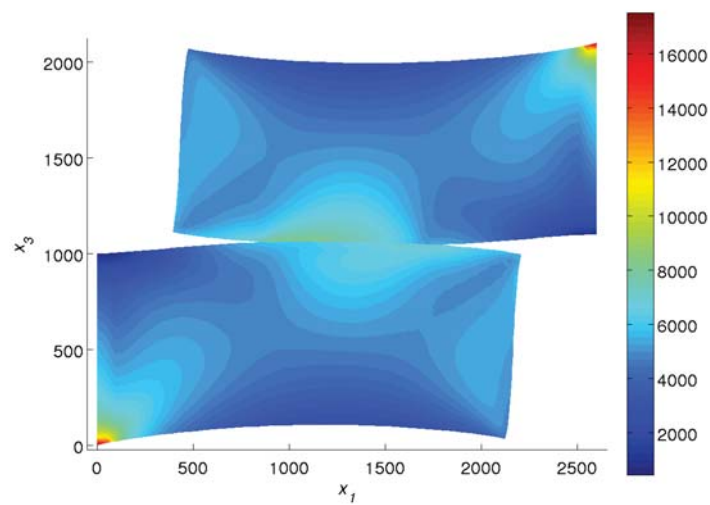
## Deformation



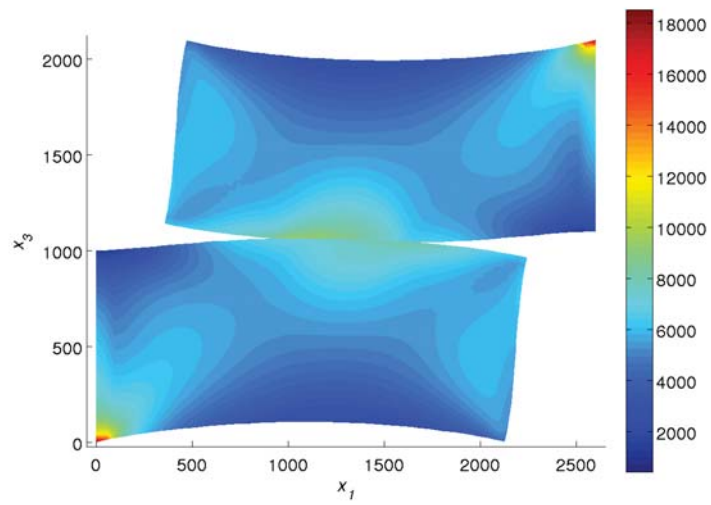
## Deformation



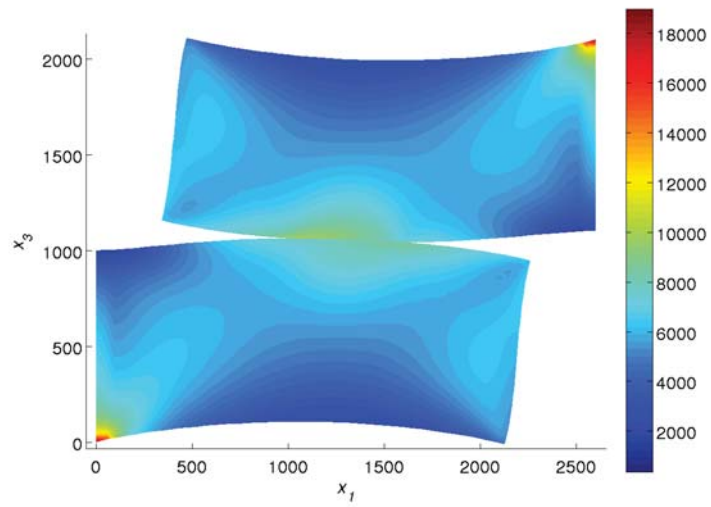
## Deformation



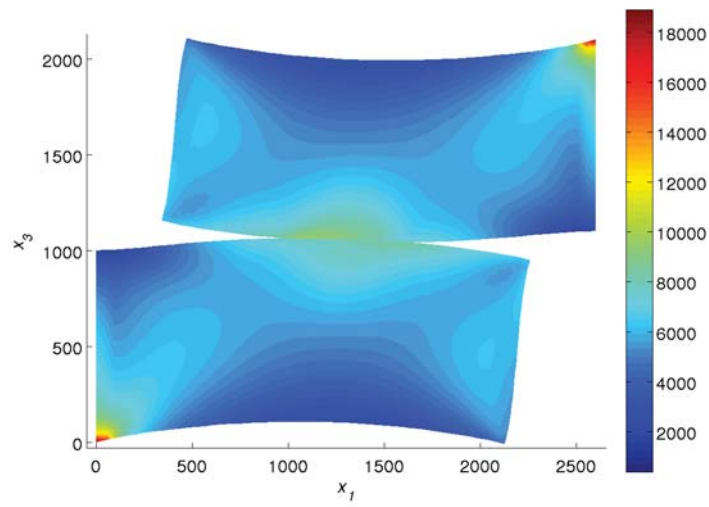
## Deformation



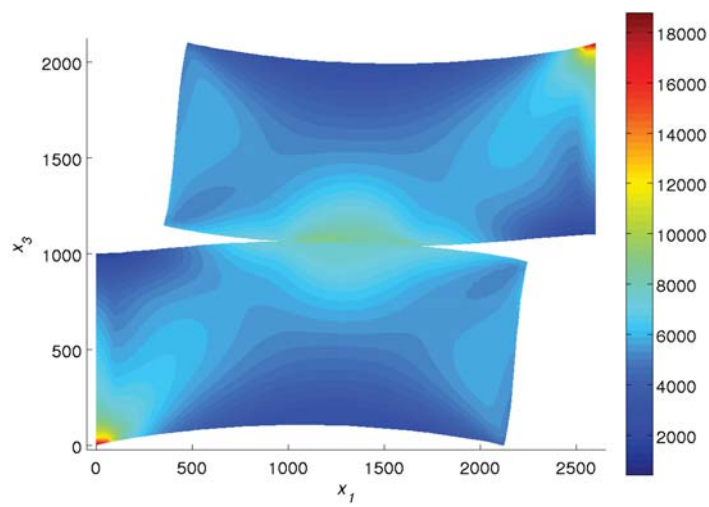
## Deformation



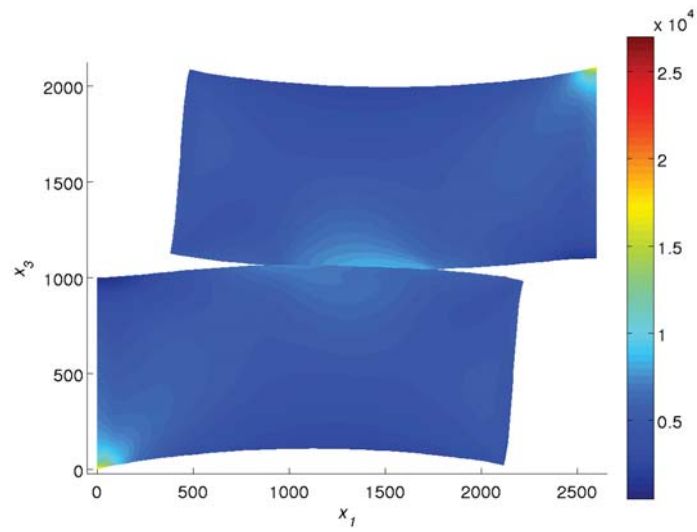
## Deformation



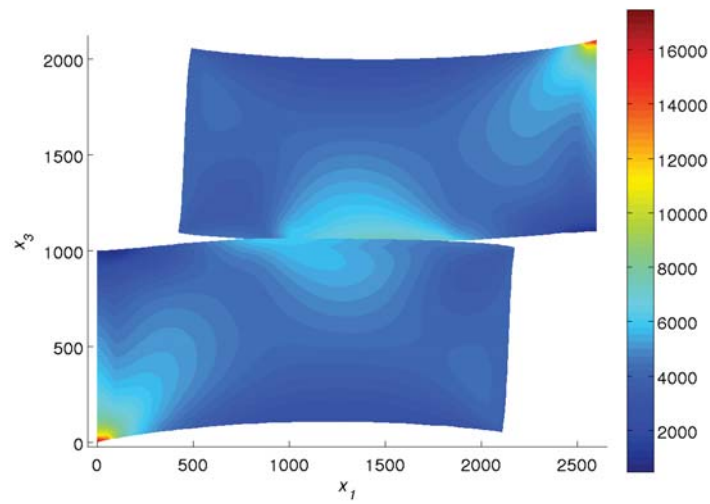
## Deformation



## Deformation



## Deformation



# Numerically and Parallel Scalable FETI Based Algorithms for Contact Problems of Mechanics and Their Powerful Ingredients

T. Kozubek,

Z. Dostál, T. Brzobohatý, A. Markopoulos,  
R. Kučera, V. Vondrák, M. Sadowská



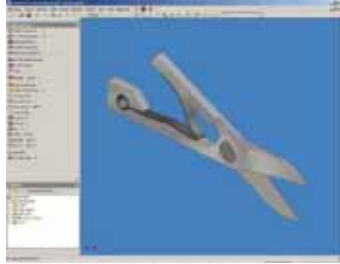
Department of Applied Mathematics  
VSB-Technical University of Ostrava  
Czech Republic



## Outline

1. MatSol – Matlab Library with scalable solvers based on FETI(BETI)
2. Optimal TFETI(TBETI) based algorithm for contact problems
3. Main ingredients of TFETI(TBETI)
  1. Parallel implementation
  2. Pseudoinverse stabilization
  3. Fixing rigid body motions
  4. Domain decomposition correction
  5. Contact direction correction
4. Benchmarks
5. Dynamics

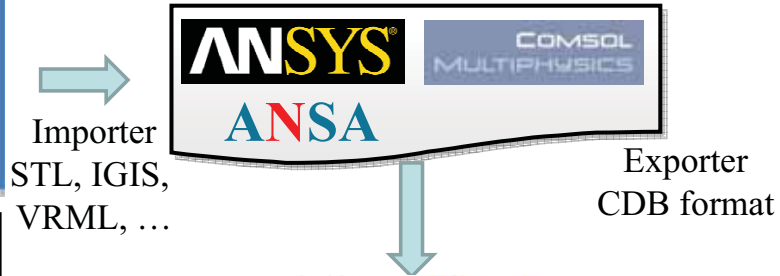
Geometry modeling



**CAD System Integration**

- Autodesk Inventor
- CATIA
- Pro/ENGINEER
- Solid Edge
- SolidWorks
- Unigraphics

**Problem specification and mesh gen.**  
(problem type, material parameters, initial and boundary conditions, ...)



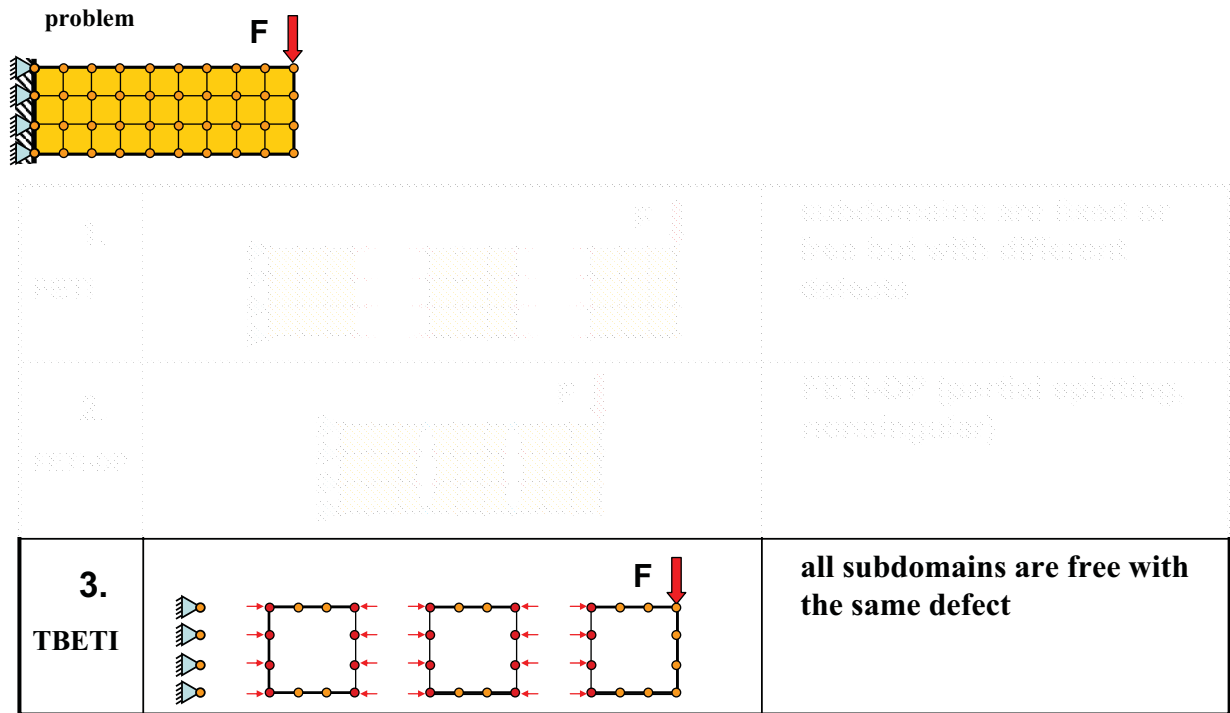
MatSol

Library with scalable solvers based on FETI and BETI domain decomposition methods

T. Kozubek, T. Brzobohatý, A. Markopoulos  
Z. Dostál, V. Vondrák, R. Kučera, M. Sadowská



<p>1. FETI</p>		<p>subdomains are fixed or free but with different defects</p>
<p>2. FETI-DP</p>		<p>FETI-DP (partial splitting, nonsingular)</p>
<p>3. TFETI</p>		<p>all subdomains are free with the same defect</p>



## Total FETI – primal formulation

$$\min \frac{1}{2} u^T K u - u^T f$$

$u$  displacement  
 $K$  stiffness matrix  
 $B$  constraint matrix  
 $c$  constraint vector

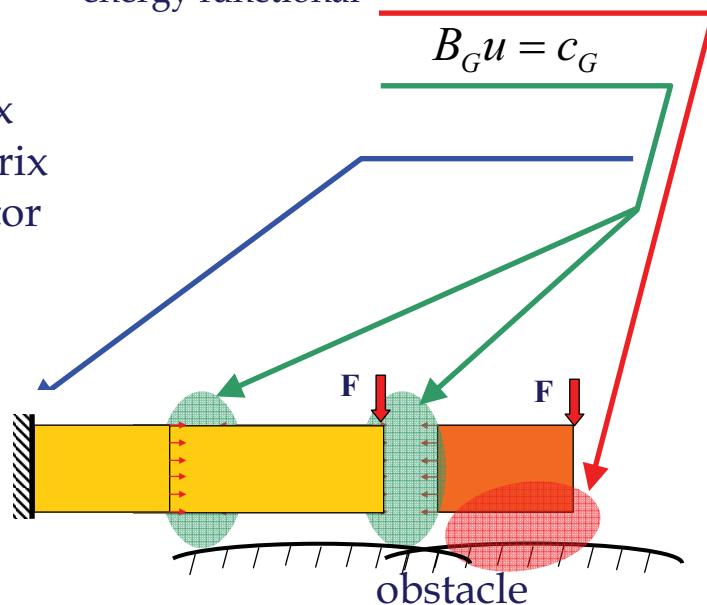
energy functional  $B_I u \leq c_I$

$$B_G u = c_G$$

### Total FETI

Dirichlet b.c. are enforced by LM,

$$B_B u = c_B$$





## Total FETI – dual formulation

$$\min \frac{1}{2} \lambda^T F \lambda - \lambda^T \hat{d} \quad \text{subject to } \lambda_I \geq 0, G\lambda = e \quad \text{a}$$

$$F = BK^+ B^T$$

$$G = R^T B^T$$

$$\hat{d} = BK^+ f - c$$

$$e = R^T f \quad \text{b}$$

$$B = \begin{bmatrix} B_I \\ B_G \\ B_B \end{bmatrix} = \begin{bmatrix} B_I \\ B_E \end{bmatrix}, c = \begin{bmatrix} c_I \\ c_G \\ c_B \end{bmatrix} = \begin{bmatrix} c_I \\ c_E \end{bmatrix}, \lambda = \begin{bmatrix} \lambda_I \\ \lambda_E \end{bmatrix} \quad \text{c}$$

$R$  basis of the kernel of  $K$ , rigid body motions

$\alpha$  amplitudes d

Relation between primal  
and dual variables:

$$u = K^+ (f - B^T \lambda) + R\alpha \quad \text{e}$$

## Homogenization of equality constraints

$$\min \frac{1}{2} \lambda^T F \lambda - \lambda^T \hat{d} \quad \text{subject to } \lambda_I \geq 0, G\lambda = e$$

$$G\hat{\lambda} = e, \hat{\lambda} = G^T (GG^T)^{-1} e$$

$$G\lambda = e, \lambda = \mu + \hat{\lambda} \Leftrightarrow G\mu = 0,$$

$$\lambda_I \geq 0 \Leftrightarrow \mu_I \geq -\hat{\lambda}_I$$

$$\min \frac{1}{2} \lambda^T F \lambda - \lambda^T d \quad \text{subject to } \lambda_I \geq -\hat{\lambda}_I, G\lambda = 0$$

$$\text{with } d = \hat{d} - F\hat{\lambda}.$$

## Applying natural coarse grid preconditioner

*Natural coarse grid projectors :*

$$Q = G^T (GG^T)^{-1} G$$

$$P = I - Q$$

$$\text{Im } Q = \text{Im } G^T$$

$$\text{Im } P = \text{Ker } G$$

$$\min \frac{1}{2} \lambda^T PFP \lambda - \lambda^T P d \quad \text{subject to } \lambda_l \geq -\hat{\lambda}_l, G \lambda = o$$

## Optimal estimates

**Theorem :** The following bounds for  $FPF$  hold :

$$\lambda_{\min}(FPF | \text{Im } P) \geq C_1$$

$$\lambda_{\max}(FPF | \text{Im } P) = \|FPF\| \leq C_2 \frac{H}{h}$$

$$\kappa(FPF | \text{Im } P) \leq C_3 \frac{H}{h}$$

with constants  $C_1, C_2, C_3$  independent on both  $H$  and  $h$

**Proof in C. Farhat, J. Mandel and F. - X. Roux CMAME 1994**  
**BETI J. Bouchala, Z. Dostal, M. Sadowska, Computing 2009**

## Optimality and scalability

**Theorem:**

The solutions of the discretized model problem with

$$H/h \leq C$$

and a given relative precision may be obtained by SMALBE/MPRGP at

$O(1)$  **matrix / vector multiplications.**

**Z.Dostal, D. Horak, SINUM 2007 (scalar case)**

**Z. Dostal, T. Kozubek, V. Vondrak, A. Markopoulos, T. Brzobohaty, IJNME 2009**

**J. Bouchala, Z. Dostal, M. Sadowska, Computing 2008, 2009**

## Many of this and much much more ....

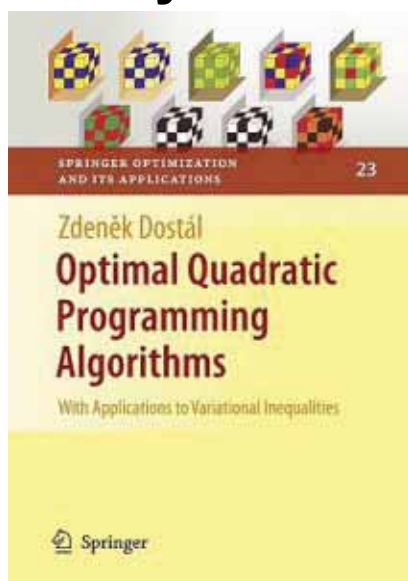


Table of Contents - Preface.

### Part I. Background

1. Linear Algebra.- 2. Optimization.

### Part II. Algorithms

3. CG for Unconstrained Minimization  
 4. Equality Constrained Minimization  
 5. Bound Constrained Minimization  
 6. Bound and Equality Constrained Minimization

### Part III. Applications to Variational Inequalities

7. Solution of a Coercive Variational Inequality by FETI-DP method  
 8. Solution to a Semicoercive Variational Inequality by TFETI Method.- References.- Index.

**Z. Dostál: Theoretically supported scalable algorithms for contact problems, next presentation, at 14.00.**

## Primal formulation with Tresca friction

$$\min \frac{1}{2} u^T K u - u^T f + \sum_{i=1}^{m_c} \Psi_i \|T_i u\| \quad \text{s.t. } B_I u \leq c_I, B_E u = c_E$$

$T_i u$  ... jump of the (master and slave) displacement at projected to the tangent vector in 2D and to the tangential plane in 3D

associated slip bound

$\Psi_i$  ...

## Removing non-differentiability

$$\sum_{i=1}^{m_c} \Psi_i \|T_i u\| = \sum_{i=1}^{m_c} \max_{\tau_i^T \leq \Psi_i} \tau_i^T T_i u$$

## Dual formulation with Tresca friction

$$\min \frac{1}{2} \lambda^T F \lambda - \lambda^T \hat{d} \quad \text{s.t. } \lambda_I \geq 0, \tau_i^T \leq \Psi_i \forall i, G \lambda = e \quad \text{a}$$

$$F = B K^+ B^T$$

$$G = R^T B^T$$

$$\hat{d} = B K^+ f - c$$

$$e = R^T f \quad \text{b}$$

$$\lambda = \begin{bmatrix} \lambda_I \\ \tau \\ \lambda_E \end{bmatrix}$$

$$B = \begin{bmatrix} B_I \\ T \\ B_E \end{bmatrix}$$

$$c = \begin{bmatrix} c_I \\ 0 \\ c_E \end{bmatrix} \quad \text{c}$$

$R$  basis of the kernel of  $K$ , rigid body motions  
 $\alpha$  amplitudes d

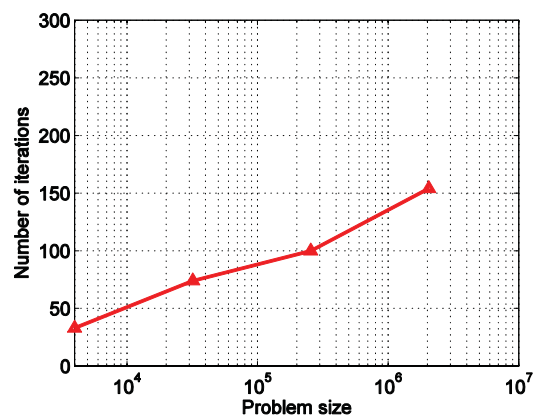
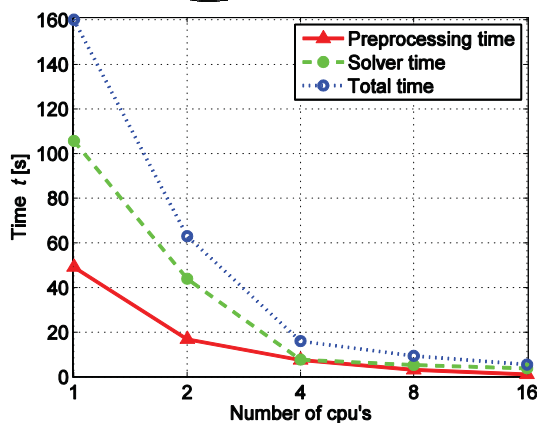
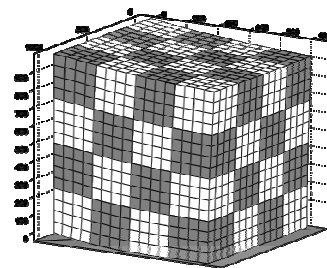
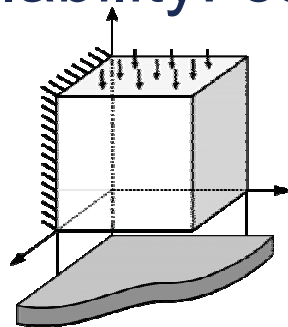
Relation between primal and dual variables:

$$u = K^+ (f - B^T \lambda) + R \alpha \quad \text{e}$$

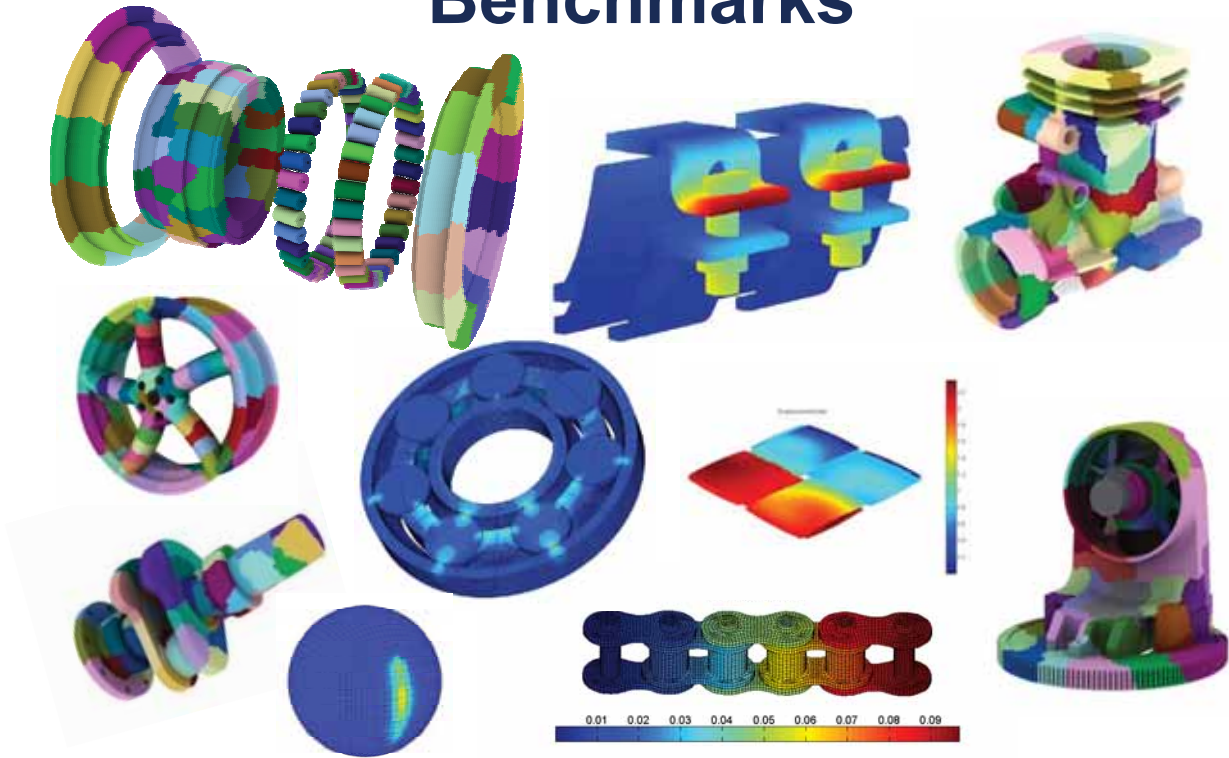
**Remark.** The Tresca friction is a simple friction law which violates some natural physical principles, but it can be used to define a mapping whose fixed point is a solution to the problem with the Coulomb friction.

- For more details: *Hlaváček I, Haslinger J, Nečas J, Lovíšek J. Solution of Variational Inequalities in Mechanics, Springer Verlag, Berlin, 1988.*

## Scalability: cube over the obstacle



# Benchmarks



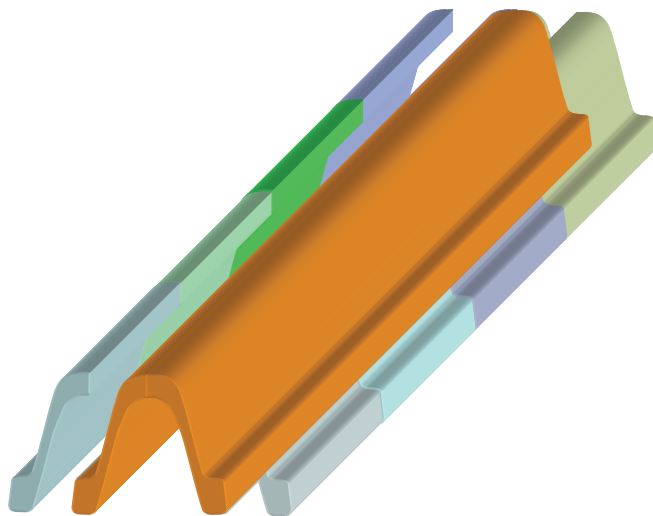
1-3 December, 2010

Comp. mech. II, 2010

17

## 1. ingredient: parallel implementation

Block diagonal structure of the stiffness matrix => suitable for parallel implementation



$$K = \begin{pmatrix} K^1 & O & \vdots & O \\ O & K^2 & \vdots & O \\ \dots & \dots & \ddots & \dots \\ O & O & \vdots & K^n \end{pmatrix}$$

Coercive and semicoercive problems may be solved!

1-3 December, 2010

Comp. mech. II, 2010

18

# Parallel programming

## Typical use cases

- Parallel for-Loops
  - Many iterations loop
  - Long iterations loop
- Offloading Work
- Large Data Sets

Cluster HP model BLc7000 (c-class).

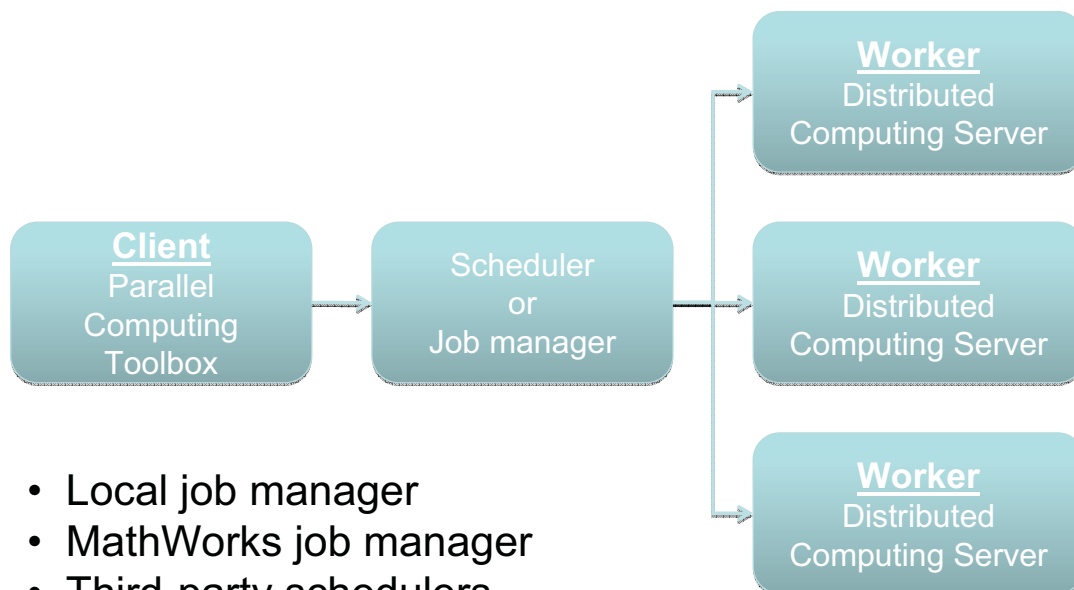
Configuration of the computational node  
2x dual core CPU AMD Opteron 2210 HE  
8GB ECC DDR2 667MHz RAM



IT4Innovations, Centrum excellence,  
Ostrava, Czech Republic, cluster with  
more than 30,000 processors.  
<http://www.it4i.eu>



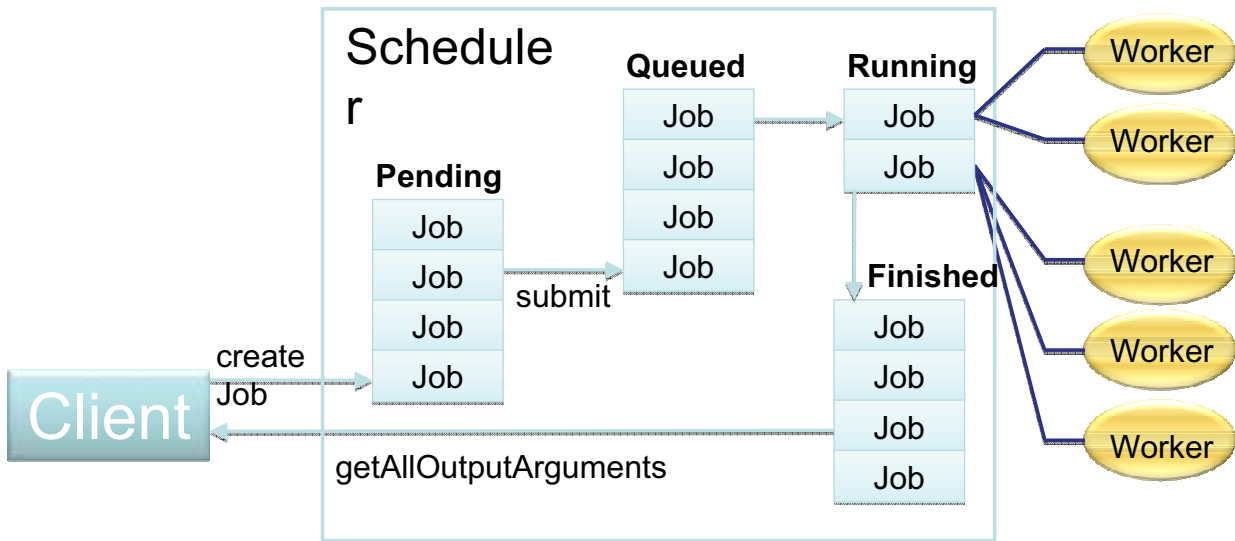
# Matlab Distributed Computing Server



- Local job manager
- MathWorks job manager
- Third-party schedulers  
(Windows CCS, PBS Pro, LSF)



# Life cycle of a job



# Distributed computations

1. Find scheduler or job manager
 

```
>>sched=findResource('scheduler', 'type','local');
```
2. Create a job
 

```
>>job=createJob(sched);
```
3. Create tasks and associate them with the job
 

```
>>createTask(job,@rand,1,{3,3});
            >>createTask(job,@eye,1,{4});
            >>createTask(job,@ones,1,{{4},{3}});
```
4. Send job to the front
 

```
>>submit(job);
```
5. Wait until job finishes
 

```
>>waitForState(job);
```
6. Gather results
 

```
>>results=getAllOutputArguments(job)
```
7. Destroy job
 

```
>>destroy(job);
```



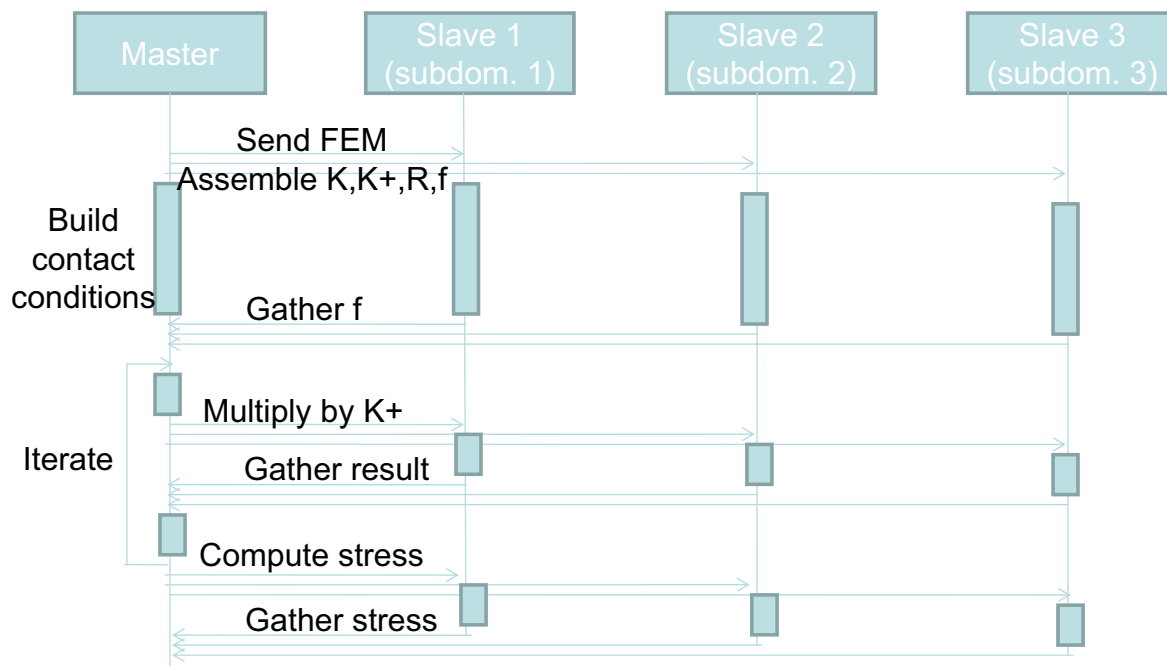
# Parallel computations

1. Find scheduler or job manager `>> sched=findResource('scheduler',...  
'type','local');`
2. Create a parallel job and sets the number of tasks `>> pjob=createParallelJob(sched);  
set(pjob,'MaximumNumberOfWorkers',4);  
set(pjob,'MinimumNumberOfWorkers',4);`
3. Create parallel tasks `>> createTask(pjob,@MyParTask,1,{});`
4. Send job to the front `>> submit(pjob);`
5. Wait until job finishes `>> waitForState(pjob);`
6. Gather results `>> results=getAllOutputArguments(pjob)`
7. Destroy job `>> destroy(pjob);`

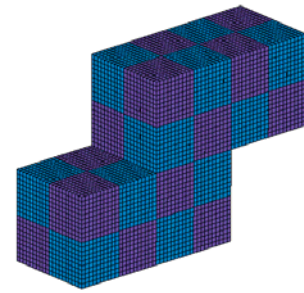
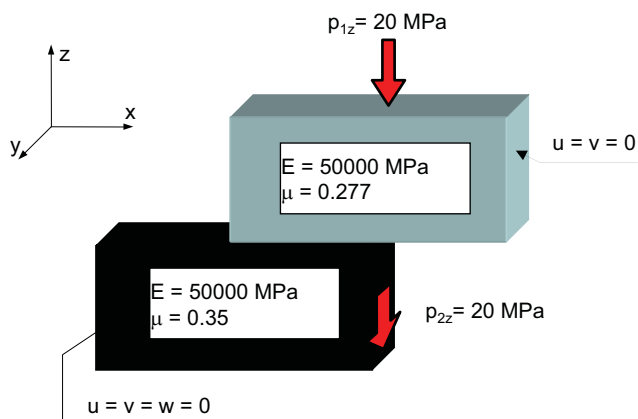
MPT functions: numlabs, labindex, labBarrier, labBroadcast, labProbe, labReceive, labSend, labSendReceive

# Parallel computation scenario

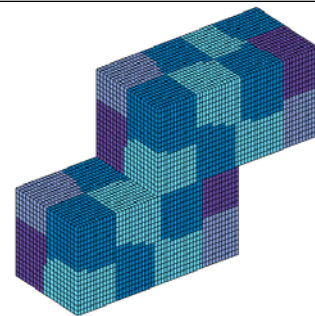
Send FEM models to workers and parallelize assembling of  $K$ ,  $K^+$ ,  $R$ ,  $f_v$ , stresses, searching contact pairs, multiplication procedures.



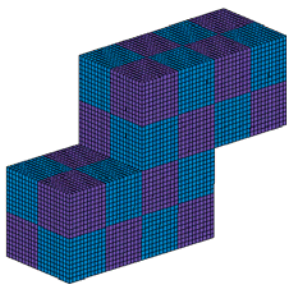
semi-coercive problem



uniform decomposition



METIS decomposition

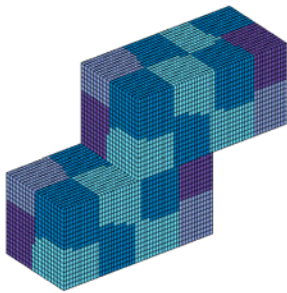


**Numerical scalability**

Tresca friction ( $f = 80$ )

uniform domain decomposition

Number of subdomains	4	64	1,024
Number of CPUs	4	24	24
Primal variables	15,972	255,552	4,088,832
Dual variables	1,694	50,634	942,954
Hessian multiplications	76	216	325
Total time (s)	13.81	141.8	4,330.01

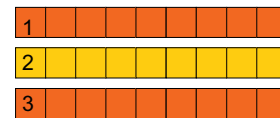
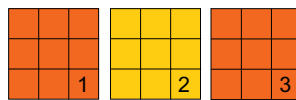


## Numerical scalability

Tresca friction ( $f = 80$ )

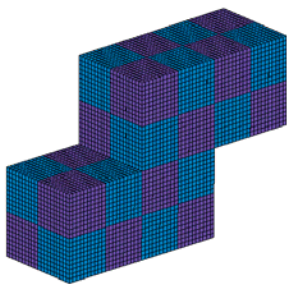
METIS domain decomposition

Number of subdomains	4	64	1024
Number of CPUs	4	24	24
Primal variables	15,972	259,902	4,125,570
Dual variables	1,694	54,984	1,024,898
Hessian multiplications	76	324	1,289
Total time (s)	13.16	206.21	16,865.10



$\kappa$  = condition number

$$\kappa_1 < \kappa_2$$

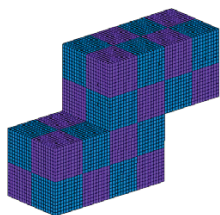


## Numerical scalability

Coulomb friction ( $f = 0.1$ )

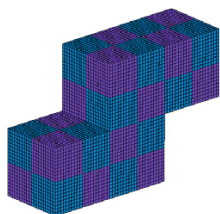
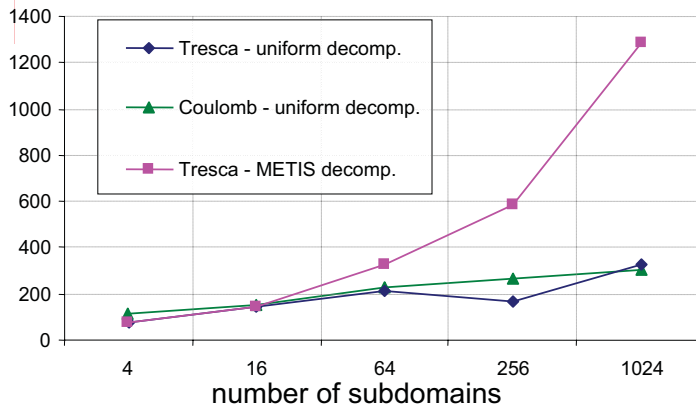
uniform domain decomposition

Number of subdomains	4	64	1,024
Number of CPUs	4	24	24
Primal variables	15,972	255,552	4,088,832
Dual variables	1,694	50,634	942,954
Hessian multiplications	115	226	301
Total time (s)	19.34	143.02	4,216.34



## Numerical scalability

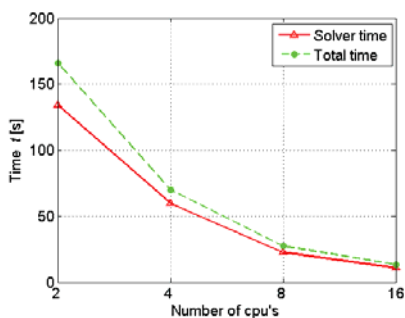
### matrix vector multiplication



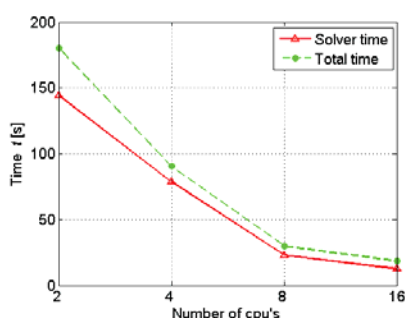
## Parallel scalability

fixed number of elements 11 664

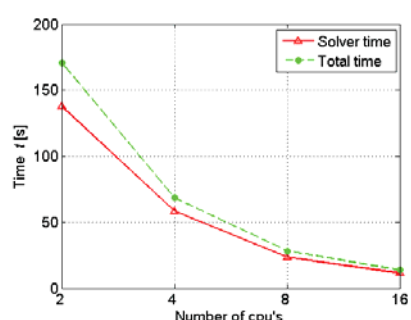
Tresca friction ( $f = 80$ )  
uniform domain  
decomposition



Tresca friction ( $f = 80$ )  
METIS domain  
decomposition



Coulomb friction ( $f = 0.1$ )  
uniform domain  
decomposition



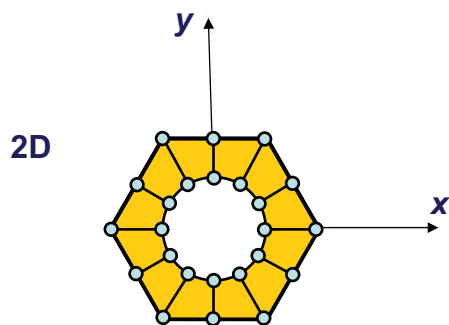
## 2. ingredient: stable pseudoinverse computation

### Rigid body motions in 2D elastic structure

- in x-direction
- in y-direction
- rotation

$$Ku = f, \quad f \in \text{Im } K$$

$$u = K^\dagger f + R\alpha, \quad R^T f = 0$$



screw female

$$KK^\dagger K = K$$

$$R^T = \begin{bmatrix} 1 & 0 & 1 & 0 & \cdots & 0 \\ 0 & 1 & 0 & 1 & \cdots & 1 \\ -y_1 & x_1 & -y_2 & x_2 & \cdots & x_n \end{bmatrix}$$

## Stable pseudoinverse computation

$$x = K^\dagger y \Leftrightarrow Kx = y$$

### 1. Singular Choleski factorization

$$L_{i,i} < \varepsilon, \quad \varepsilon = ?$$

universal  $\varepsilon$  doesn't exist

### 2. Choleski factorization combined with SVD

if a suspected 'zero' pivot appears  
use the **SVD decomposition** proposed by  
C. Farhat, M. Géradin.

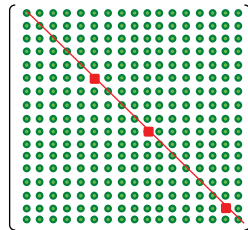
**Active choice of the nonsingular and SVD part using fixing nodes.**

**Proposed by** Z. Dostal, T. Kozubek, P. Kovar, A. Markopoulos, T. Brzobohatý, Cholesky-SVD decomposition with fixing nodes to stable computation of a generalized inverse of the stiffness matrix of a floating structure, IJNME 2010

# Stable pseudoinverse computation

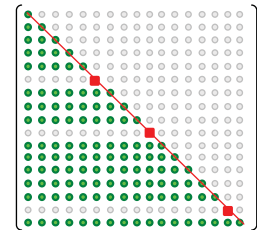
## 1. Singular Choleski factorization

$$K =$$



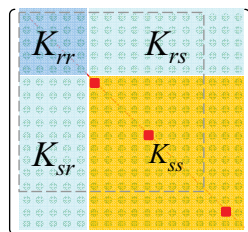
number of zero pivots = defect(K)

$$L =$$

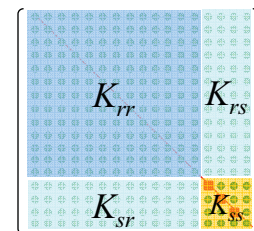


## 2. Choleski factorization combined with SVD

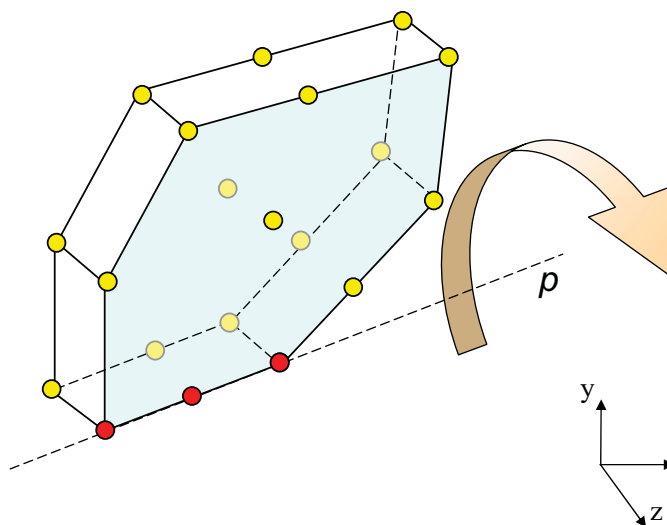
$$K =$$



Active choice of the SVD part

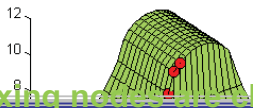


# Stable pseudoinverse computation

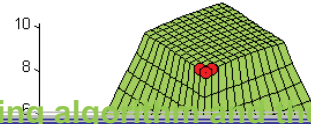


$$PKP^T = \begin{pmatrix} K_{rr} & K_{rs} \\ K_{sr} & K_{ss} \end{pmatrix}$$

$P$  ...reordering into singular and regular parts and sparse reordering



$$K_{rr} u = \vec{1}$$

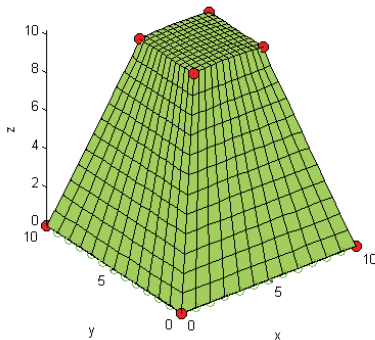


Fixing nodes are chosen using a graph partitioning algorithm and the Perron vector

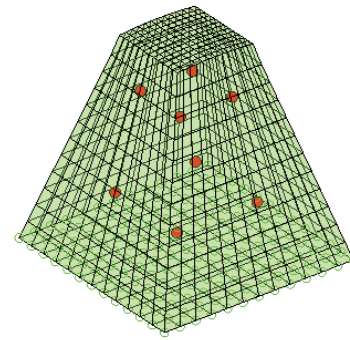
Z. Dostal, T. Kozubek, P. Kovar, A. Markopoulos, T. Brzobohatý, Cholesky-SVD decomposition with fixing nodes to stable computation of a generalized inverse of the stiffness matrix of a floating structure submitted to LINME 2010

Cond=1e8, n.iter=708

Cond=7.5e7, n.iter = 635



Cond=13359, n.iter = 306



Cond=2643, n.iter = 198

1-3 December, 2010

Comp. mech. II, 2010

35

## Algorithm for choosing $M$ uniformly distributed fixing nodes.

Given mesh and  $M > 0$ .

1. Split the mesh into  $M$  submeshes using the mesh partitioning algorithm.
2. Verify whether the resulting submeshes are connected. If not a graph postprocessing may be used to get connected submeshes.
3. Take a node lying near the center of each submesh.



## Graph preliminaries

**Adjacency matrix  $D$**  – entry  $d_{ij}$  is equal to 1 if the corresponding nodes  $i$  and  $j$  are adjacent in the mesh, and zero otherwise.

**Walk of length  $k$**  – a sequence of distinct nodes of the given mesh  $(v_1, v_2, \dots, v_k)$  such that all the edges are present in the mesh for all  $i = 1, 2, \dots, k-1$ . In other words

$$d_{v_i, v_{i+1}} = 1 \quad \forall i = 1, \dots, k-1.$$

**Lemma.** Let  $D$  be the adjacency matrix of a given mesh and let

$$B = D^k.$$

Then each entry  $b_{ij}$  of  $B$  gives the number of distinct  $(i,j)$ -walks of length  $k$  in the mesh.

**Corollary.** Let  $D$  be the adjacency matrix of a given mesh and  $e = [e_i]$ ,  $e_i = 1$ ,  $i=1, \dots, n$ .

Then the number  $w(i,k)$  of distinct walks of length  $k$  starting at node  $i$  is given by

$$w(i,k) = [D^k e]_i.$$



**Remark 1.** Since the mesh is approximately regular, we expect that more walks originate from the nodes that are near a center of the mesh rather than from vertices that are far from it.

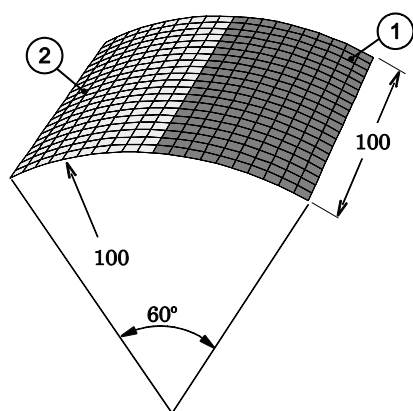
**Remark 2.** The node with index  $i$  which satisfies

$$w(i, k) \geq w(j, k) \quad \forall j$$

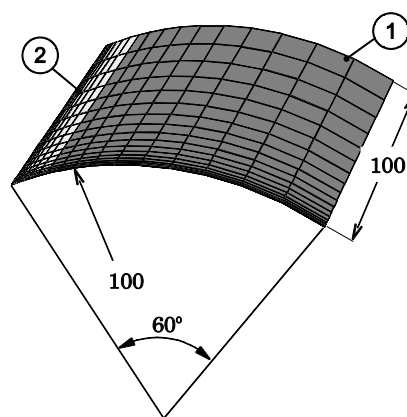
for sufficiently large  $k$  is in a sense near to the center of the subdomain associated with the submesh.

**Remark 3.** Notice that the vector  $p = \lim_{k \rightarrow \infty} \|D^k e\|^{-1} D^k e$  is a unique nonnegative eigenvector which corresponds to the largest eigenvalue of  $D$  (known as the Perron vector of  $D$ ).

## Variant A



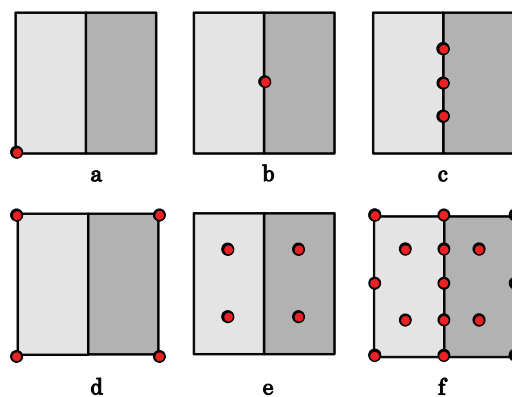
## Variant B



**material A:**  $E = 2.1e5$  MPa,  $\mu = 0.3$ ,  $t = 1$  mm

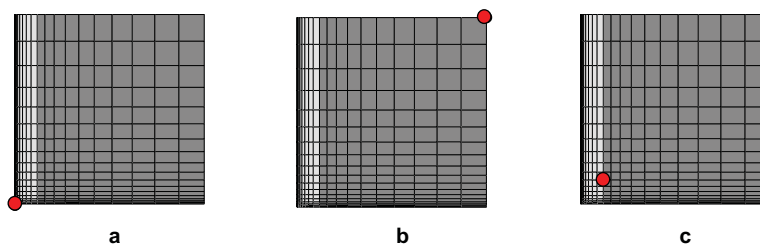
**material B:**  $E = 2.1e3$  MPa,  $m = 0.3$ ,  $t = 1$  mm

## Variant A



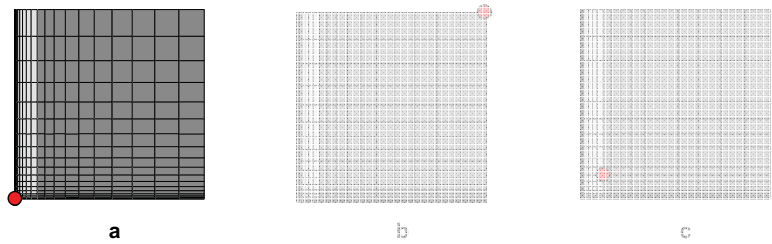
	a	b	c	d	e	f
cond(A)	2.27E+07	2.27E+07	2.27E+07	2.27E+07	2.27E+07	2.27E+07
cond(A <sub>JJ</sub> )	2.79E+11	3.97E+08	3.03E+07	7.52E+06	6.49E+06	9.72E+05
cond(A <sup>+</sup> )	2.79E+11	3.97E+08	3.03E+07	6.60E+07	2.29E+07	2.35E+07

## Variant B

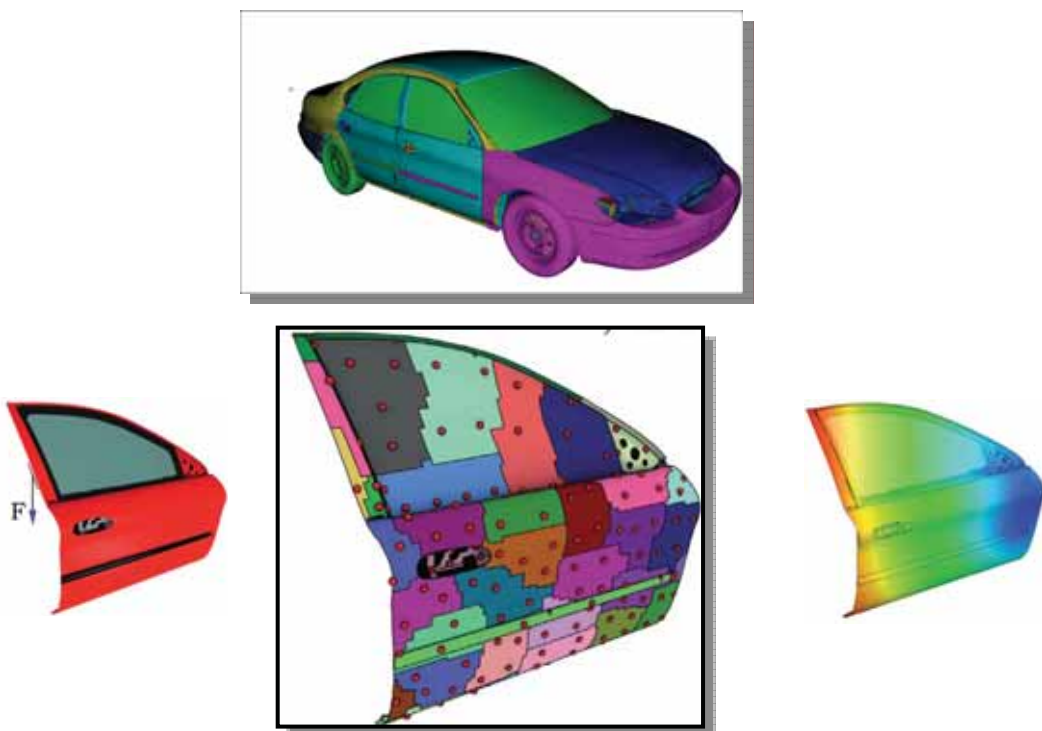


	a	b	c
cond(A)	3.44E+012	3.44E+12	3.44E+12
cond(A <sub>JJ</sub> )	1.79E+18	3.44E+12	3.44E+12
cond(A <sup>+</sup> )	2.62E+18	3.44E+12	3.44E+12

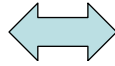
## Variant B



Matlabs function Chol applied on the matrix  $A_{jj}$  of the order 2640 finished with zero pivot at the line 2636. The results indicate that our method can be especially useful for large shells with irregular discretization.

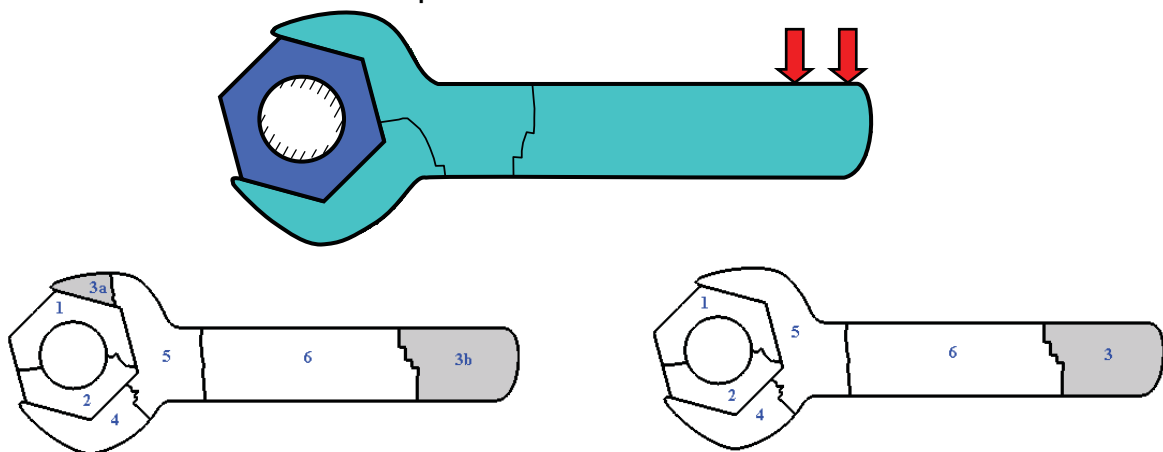


# Moore-Penrose pseudoinverse, $K$ is SPS

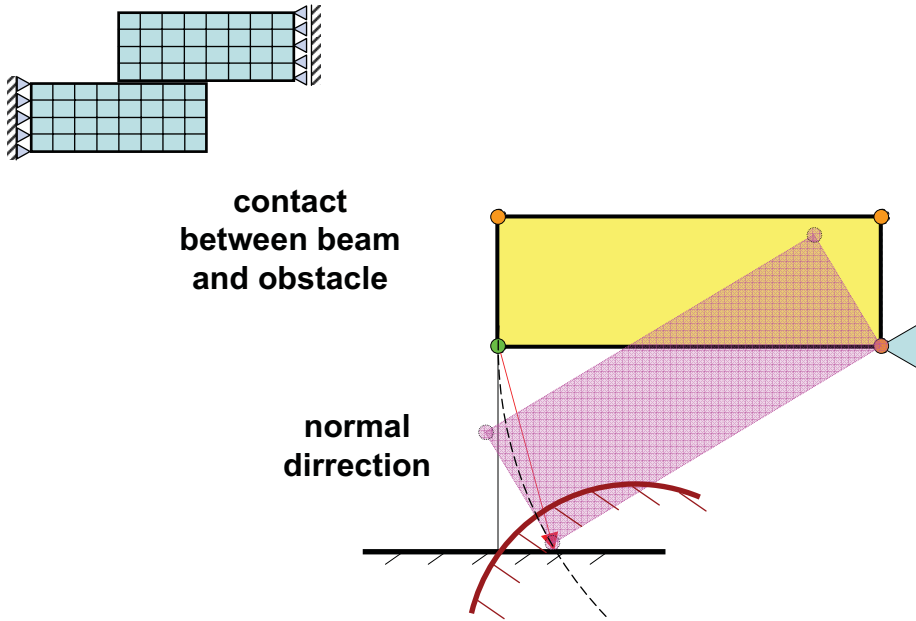


## 3. ingredient: domain decomposition correction

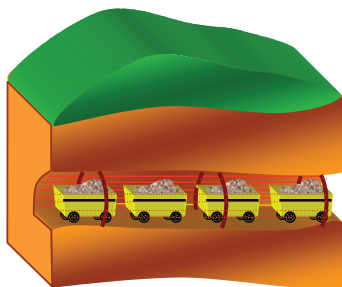
Spanner with a screw female



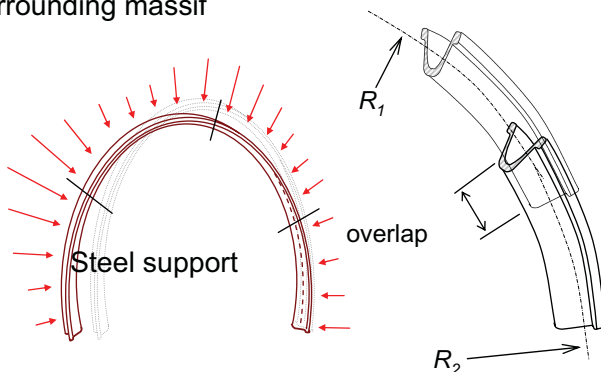
## 4. ingredient: contact direction correction



## Mining industry: clamp joint of the steel arc support



Pressure arising from the surrounding massif



Coulomb friction

$f = 0.1$

$E = 2.1e5 \text{ MPa,}$

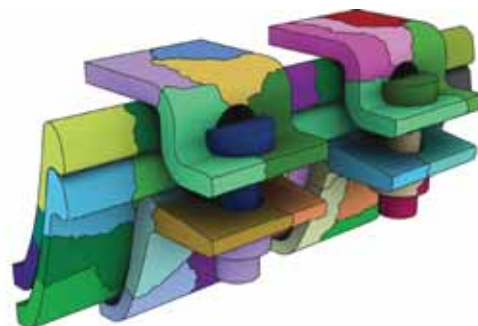
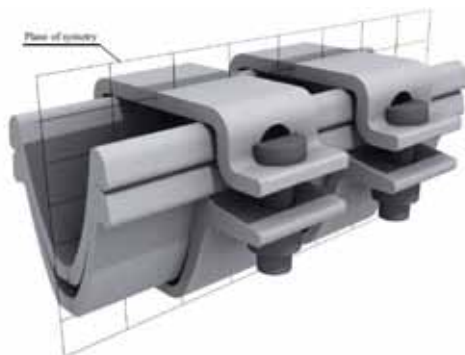
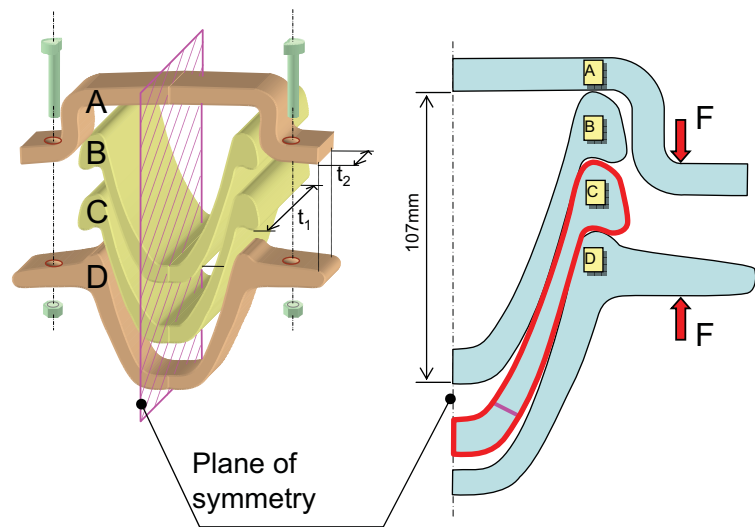
$\mu = 0.3$

$t_A = t_D = 10 \text{ mm}$

$t_B = t_C = 40 \text{ mm}$

primal variables 65562

dual variables 3112

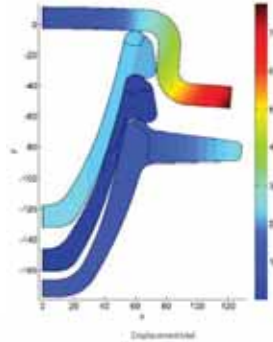


8 bodies  
 7 floating

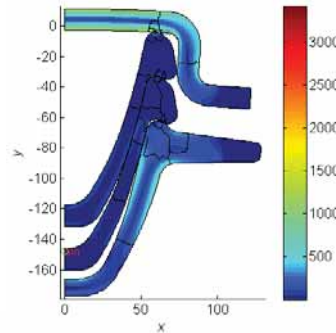
# Mining industry: clamp joint of the steel arc support

2D

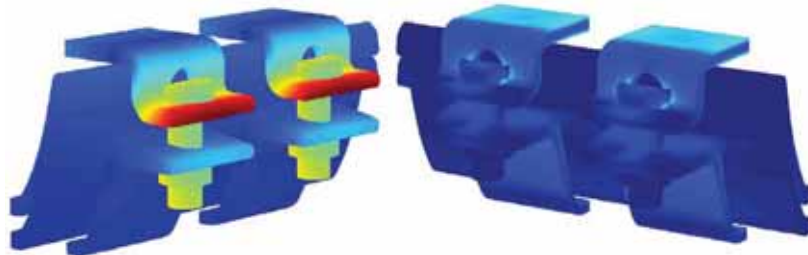
Displacements



HMH stress



3D

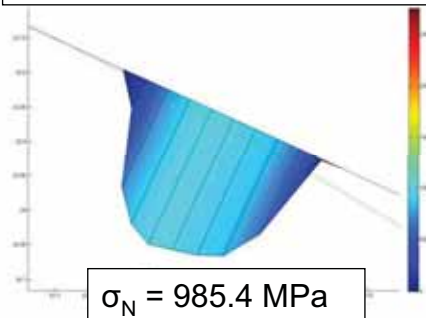


1-3 December, 2010

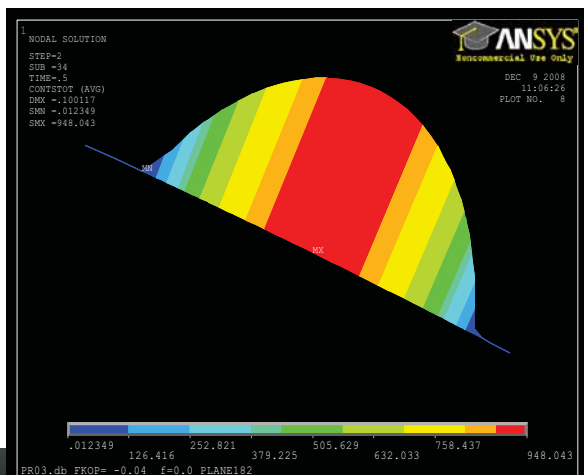
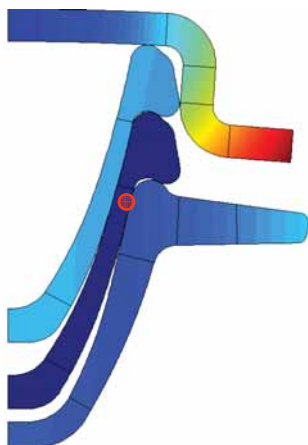
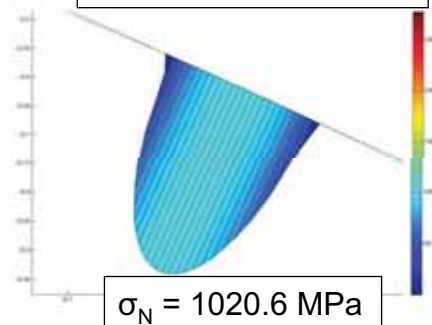
Comp. mech. II, 2010

51

without direction corrections



3 direction corrections



PARALLEL  
 ANSYS dynamic  
 solution: 27  
 hours

PARALLEL  
 ANSYS static  
 solution: 1  
 hour

MATSOL static with  
 direction  
 corrections: 15 mins

1-3 December, 2010

seq version 7 mins



## Comparing TBETI and TFETI

250 subdomains  $f = 0.1$

Solution time	2.41 hr.
Total time	2.55 hr.
matrix-vector multiplications	2 126
primal variables	1 592 853
dual variables	261 553
max(abs(u))	1.303 mm
max(totalU)	1.548 mm

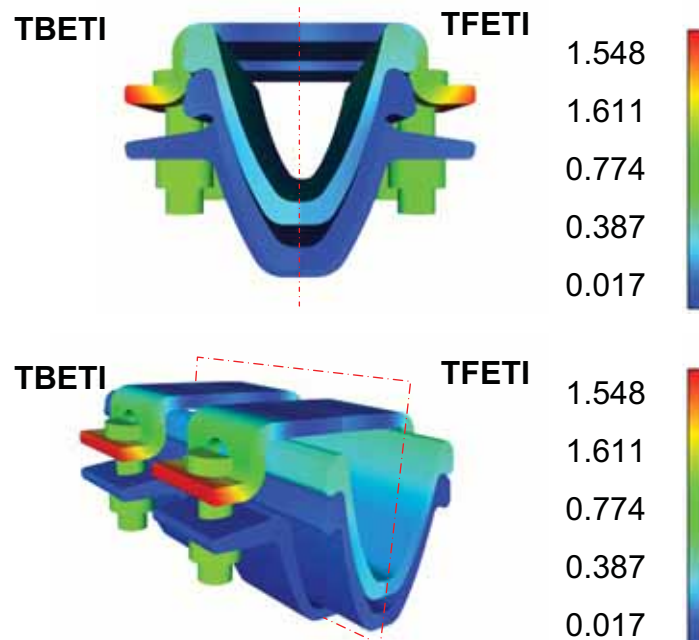
FETI

Solution time	2.54 hr.
Total time	3.33 hr.
matrix-vector multiplications	1 882
primal variables	713 751
dual variables	261 553
max(abs(u))	1.378 mm
max(totalU)	1.616 mm

BETI

## Comparing TBETI and TFETI

Total displacements  
 [mm]

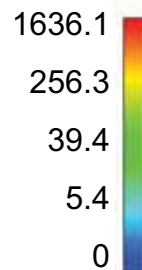
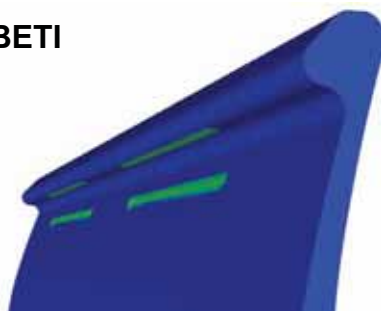




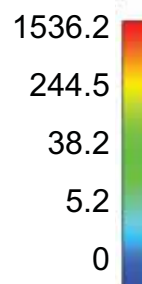
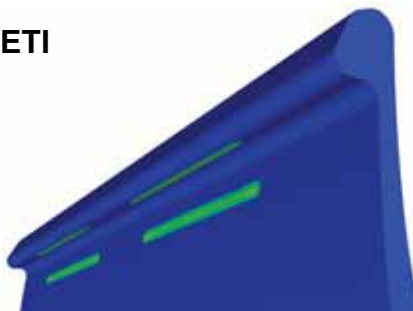
## Comparing TBETI and TFETI

Normal contact stress  
[MPa]

TBETI



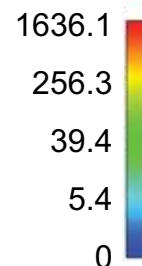
TFETI



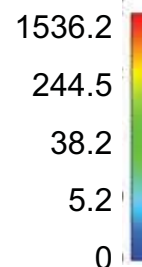
## Comparing TBETI and TFETI

Normal contact stress  
[MPa]

TBETI



TFETI

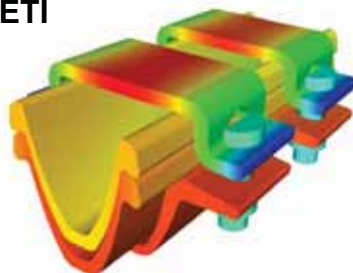


## Comparing TBETI and TFETI

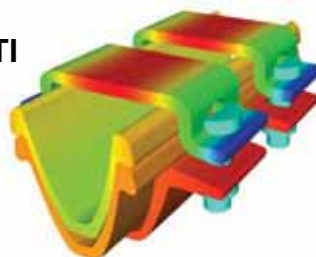
Displacement  $u_y$

[mm]

TBETI



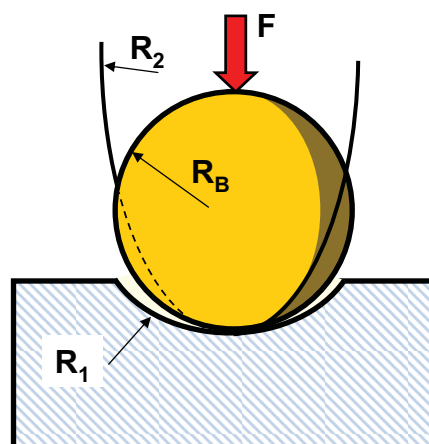
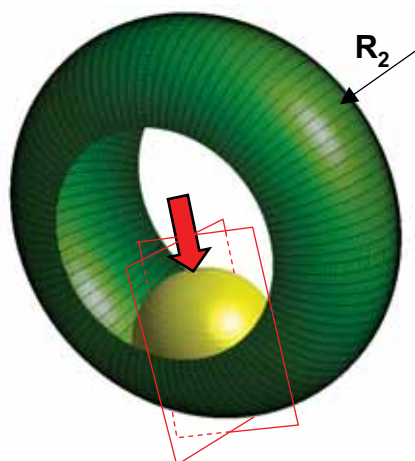
TFETI



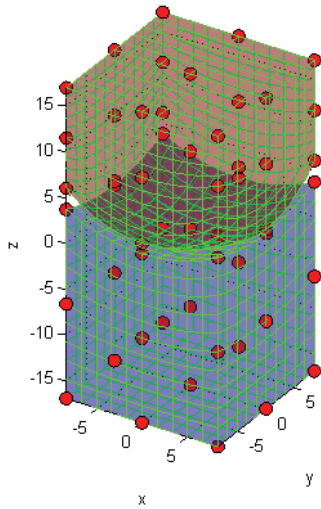
## Comparing TBETI and TFETI

$R_1 = 15 \text{ mm}$   
 $R_2 = 17.5 \text{ mm}$   
 $R_3 = 25 \text{ mm}$

$E_1 = E_2 = 2.1 \times 10^5 \text{ MPa}$   
 $\mu_1 = \mu_2 = 0.3$   
 $F = 5 \text{ kN}$



## Comparing TBETI and TFETI



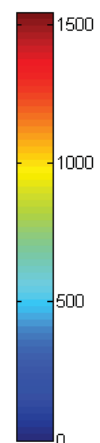
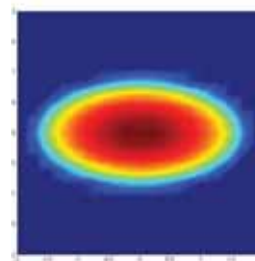
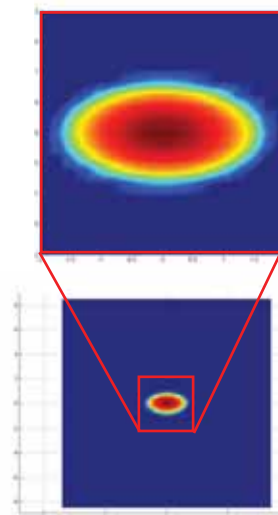
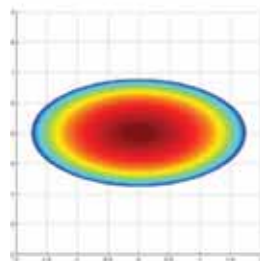
Method	TFETI	TBETI
Solution time	1.82 hr.	1.51 hr.
Total time	2.17 hr.	3.06 hr.
subdomains	1 024	1 024
matrix-vector multiplications	593	667
primal variables	4 088 832	1 849 344
dual variables	926 435	926 435

## Comparing TBETI and TFETI

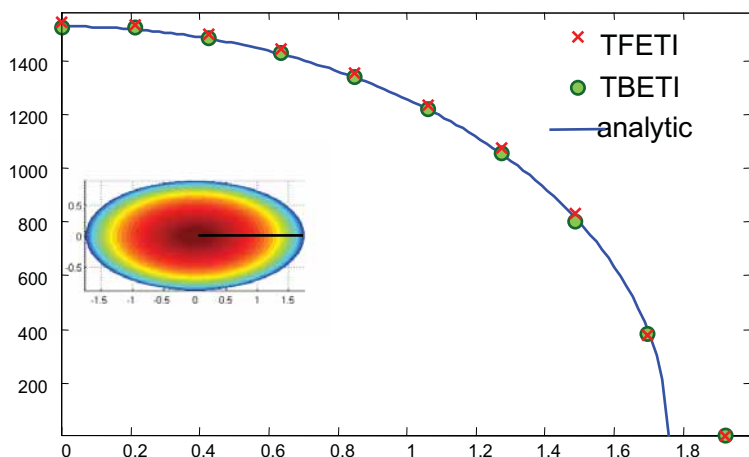
analytical solution

TFETI

TBETI



## Comparing TBETI and TFETI

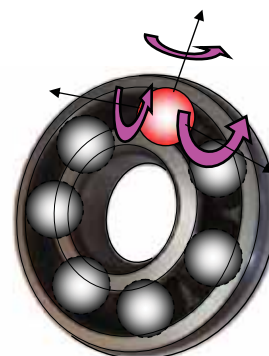
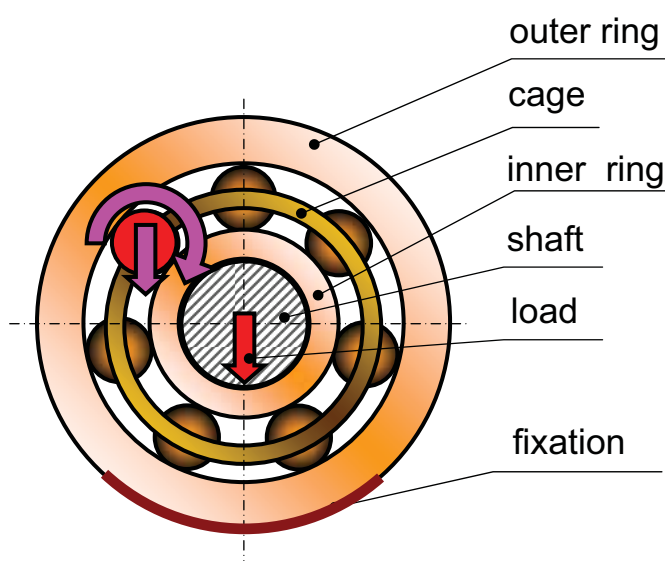


max contact stress

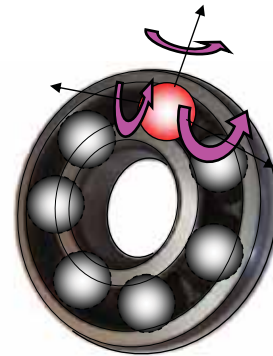
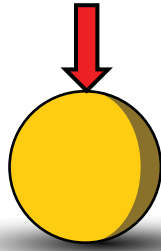
TFETI relative error = 1.1759 %

TBETI relative error = 0.6324 %

## 5. ingredient: fixing rigid body motions



## Fixing rigid body motions



$$\min \frac{1}{2} u^T K u - u^T f$$

$$B_I u \leq c_I$$

$$B_E u = o$$

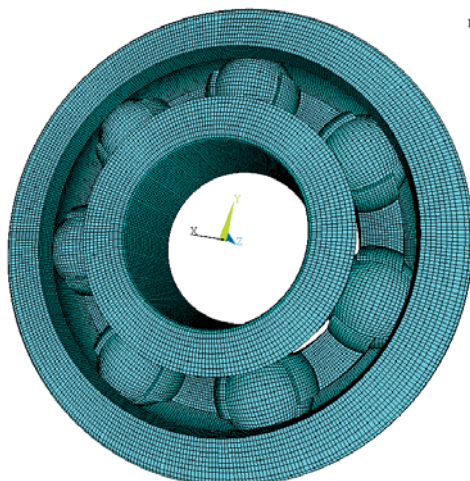
$$B_B u = c_B$$

additional  
condition

$$B_r u = o$$

$$R^T = \begin{bmatrix} 1 & 0 & 0 & 1 & 0 & 0 & \dots & 0 \\ 0 & 1 & 0 & 0 & 1 & 0 & \dots & 0 \\ 0 & 0 & 1 & 0 & 0 & 1 & \dots & 1 \\ -y_1 & x_1 & 0 & -y_2 & x_2 & 0 & \dots & 0 \\ -z_1 & 0 & x_1 & -z_2 & 0 & x_2 & \dots & x_n \\ 0 & -z_1 & y_1 & 0 & -z_2 & y_2 & \dots & y_n \end{bmatrix} \begin{matrix} x \\ y \\ z \\ xy \\ xz \\ yz \end{matrix}$$

ELEMENTS



ANNOI  
 NOV 10 2008  
 15:00:13

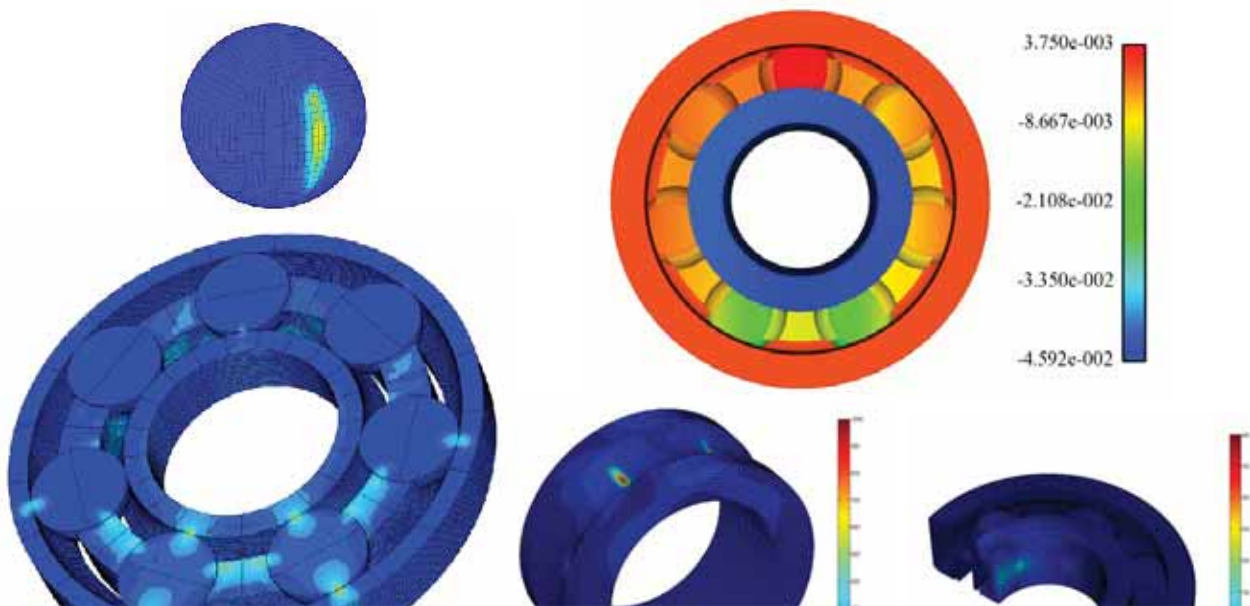


- 1 688 000 primal variables
- 408 000 dual variables
- 10 bodies, 9 floating
- 700 subdomains
- 2364 matrix-vector multiplications

	Parallel
Solution time	1.75 hr
Total time	1.83 hr

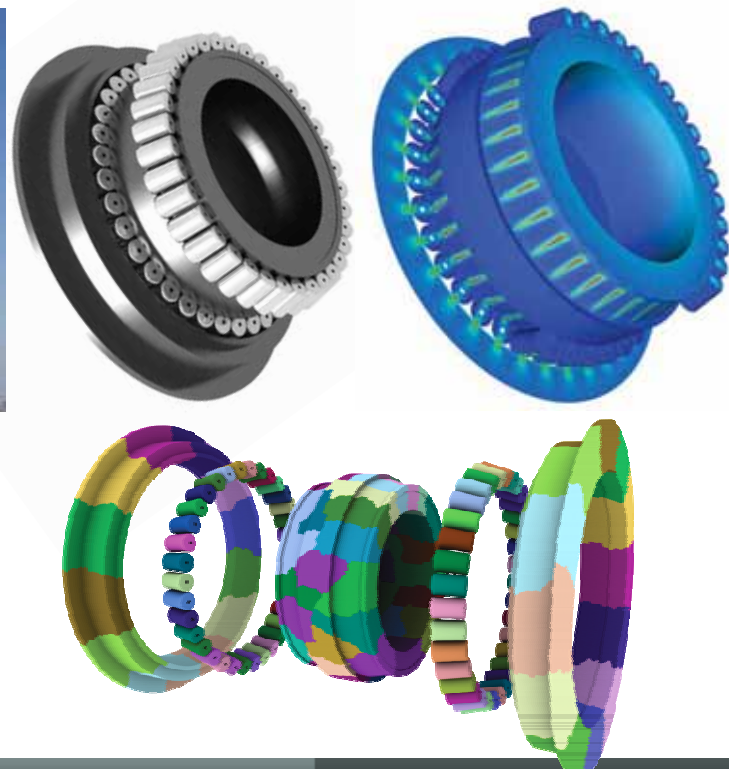


## Car industry: ball bearing



Scalable TFETI algorithm for the solution of multibody contact problems of elasticity (IJNME 2009), Z. Dostál, T. Kozubek, V. Vondrák, T. Brzobohatý, A. Markopoulos

## Roller bearing of wind generator



Statistics	
Bodies	73
Subdomains	700
Primal variables	2,73 M
Dual variables	459,8 k
Iterations	4270

## Visteon Headlight

12 bodies



1-3 December, 2010

Comp. mech. II, 2010

67

## Visteon Headlight

64 subdomains

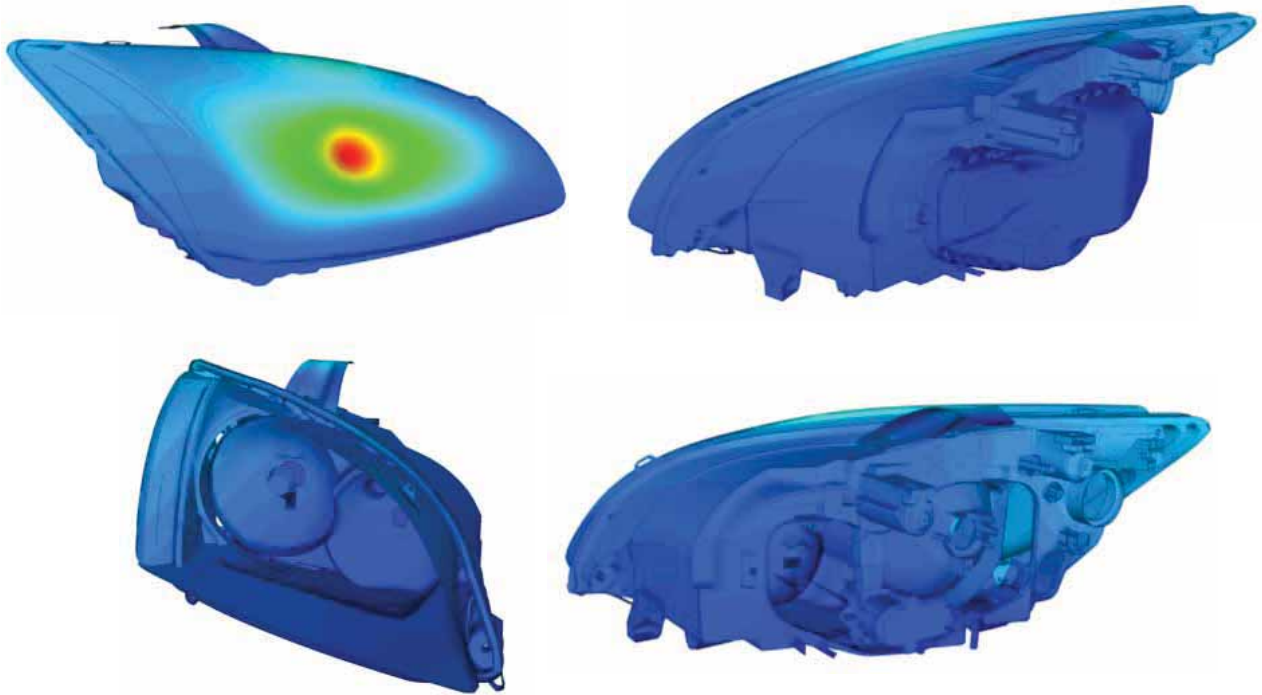


1-3 December, 2010

Comp. mech. II, 2010

68

## Visteon Headlight - Total Displacement



700 bodies  
3000 subdomains





# Extension to dynamics

Contact stabilized Newmark scheme combined with MPGRP algorithm

R. Krause, M. Walloth, *A Time Discretization Scheme Based on Rothe's Method for Dynamical Contact Problems with Friction - Computer Methods in Applied Mechanics and Engineering*, Vol. 199, pages 1-19 (December 2009). - Available as INS Preprint No. 0802.

begin [for  $\tau \in \langle 0, T \rangle$ ,  $0 = \tau_0 < \tau_1 \dots < \tau_n = T, \tau_i = i\Delta\tau$ ]

Step 1. { Solution of predictor displacement}

$$\min \left[ \frac{1}{2} (u_{\tau+\Delta\tau}^{pred})^T M (u_{\tau+\Delta\tau}^{pred}) - (Mu_{\tau} + \Delta\tau Mu_{\tau})^T u_{\tau+\Delta\tau}^{pred} \right]$$

subject to  $B_I u_{\tau+\Delta\tau}^{pred} \leq c_I$ , and  $B_E u_{\tau+\Delta\tau}^{pred} = c_E$

Step 2. { Solution of contact stabilized displacement}

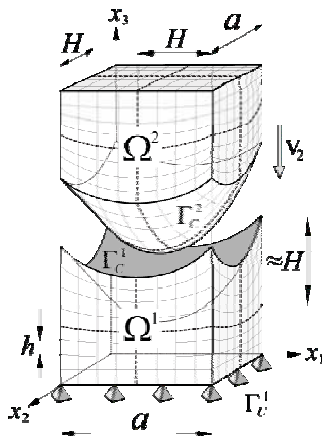
$$\min \left[ \frac{1}{2} (u_{\tau+\Delta\tau})^T K (u_{\tau+\Delta\tau}) - \left( \frac{2}{\Delta\tau^2} Mu_{\tau+\Delta\tau}^{pred} - \frac{1}{2} Au_{\tau} + \frac{1}{2} (f_{\tau+\Delta\tau} + f_{\tau}) \right)^T u_{\tau+\Delta\tau} \right]$$

subject to  $B_I u_{\tau+\Delta\tau} \leq c_I$  and  $B_E u_{\tau+\Delta\tau} = c_E$

Step 3. { Solution of velocity}

$$u_{\tau+\Delta\tau} = u_{\tau} + \frac{2}{\Delta\tau} (u_{\tau+\Delta\tau} - u_{\tau+\Delta\tau}^{pred})$$

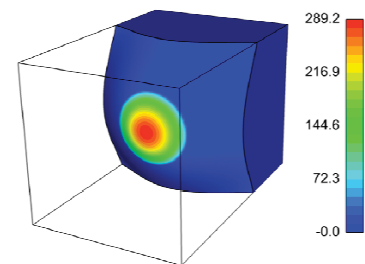
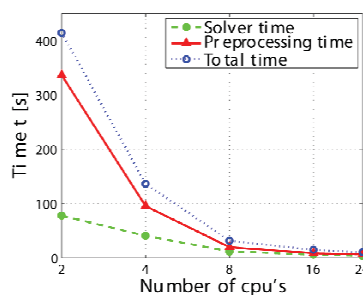
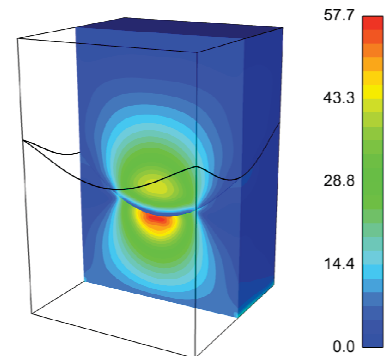
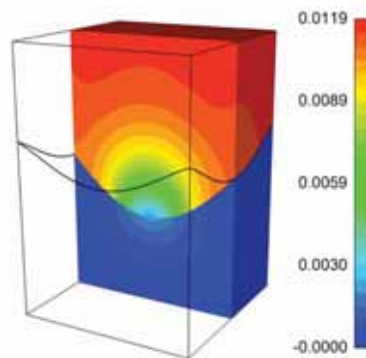
end



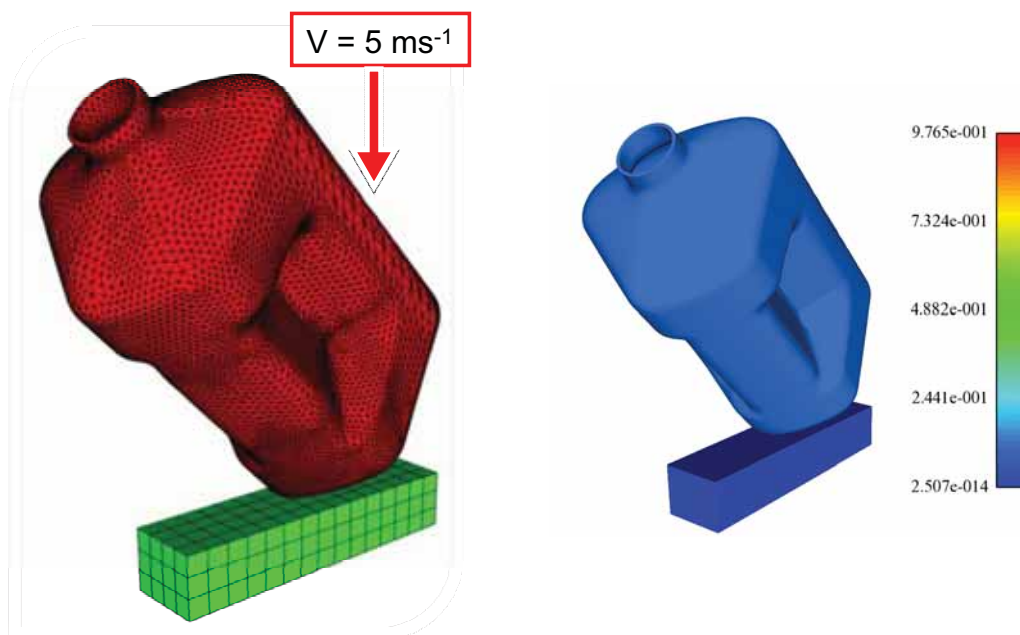
2 739 198 primal

596 771 dual

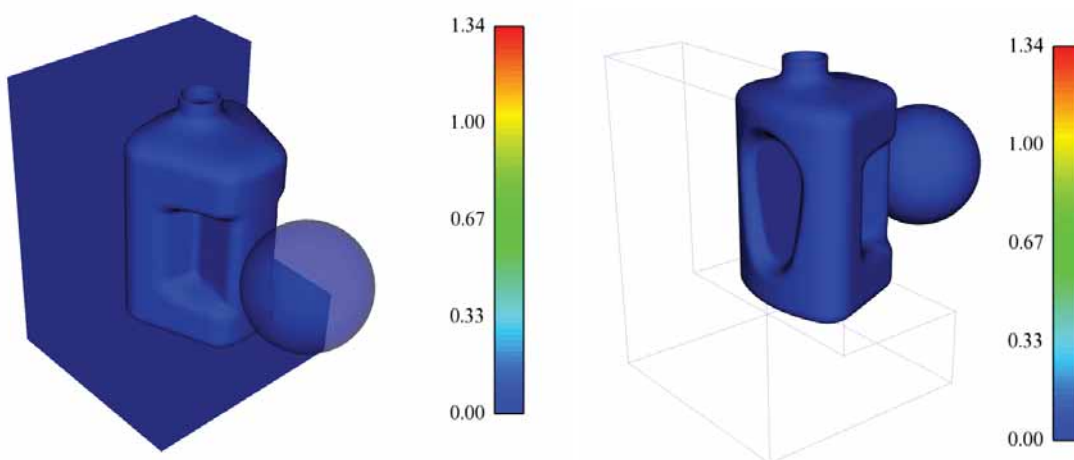
Solver time of one step 50s



## Extension to dynamics



## Extension to dynamics



1. Brzobohaty, T., Dostal, Z., Kovar, P., Kozubek, T., Markopoulos, A.: Cholesky–SVD decomposition with fixing nodes to stable evaluation of a generalized inverse of the stiffness matrix of a floating structure. Accepted for publishing in IJNME, 2010.
2. Dostal, Z., Kozubek, T., Vondrak, V., Brzobohaty, T., Markopoulos, A.: Scalable TFETI algorithm for the solution of multibody contact problems of elasticity. Int J Numer Meth Eng 82, No. 11, p. 1384-1405 (2010),
3. Dostal, Z., Kozubek, T., Horyl, P., Brzobohaty, T., Markopoulos, A.: Scalable TFETI algorithm for two dimensional multibody contact problems with friction. J Comput Appl Math. 2010, 235(2) (2010), 403-418.
4. Dostal, Z., Kozubek, T., Markopoulos, A., Brzobohaty, T., Vondrak, V., Horyl, P.: Theoretically supported scalable TFETI algorithm for the solution of multibody 3D contact problems with friction. Accepted for publishing in CMAME 2010.
5. Dostal, Z., Kozubek, T., Markopoulos, A., Brzobohaty, T., Vlach, O. Scalable TFETI with preconditioning by conjugate projector for transient contact problems of elasticity, in preparing 2010.

# Thank you for your attention

## Efficient parallel contact shape optimization

*V. Vondrák, T. Kozubek, A.  
Markopoulos, M. Sadowská and Z.  
Dostál*

*Dept. of Applied Math., VŠB-TU Ostrava  
Czech Republic*

## Outline

- *Contact shape optimization problem*
  - Parallel sensitivity analysis
  - 3D Hertz optimization problem
  - Numerical results
- *Total FETI & BETI domain decomposition*
  - Parallel solution of state problem
  - BETI & FETI methods
  - Sensitivity analysis
- *Conclusions and future work*

## Contact shape optimization

$$\min_{\alpha \in U_{ad}} \mathfrak{J}(\alpha, u(\alpha))$$

$\mathfrak{J}(\alpha, u(\alpha))$ ... objective function

$u(\alpha)$  solves contact problem

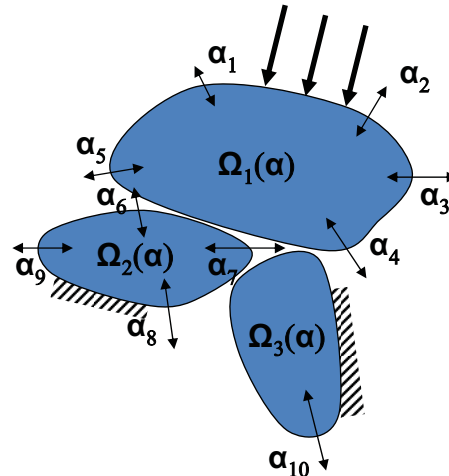
Variational inequality

$$a_\alpha(u, v - u) \geq b_\alpha(v - u), \quad \forall v \in C_\alpha$$

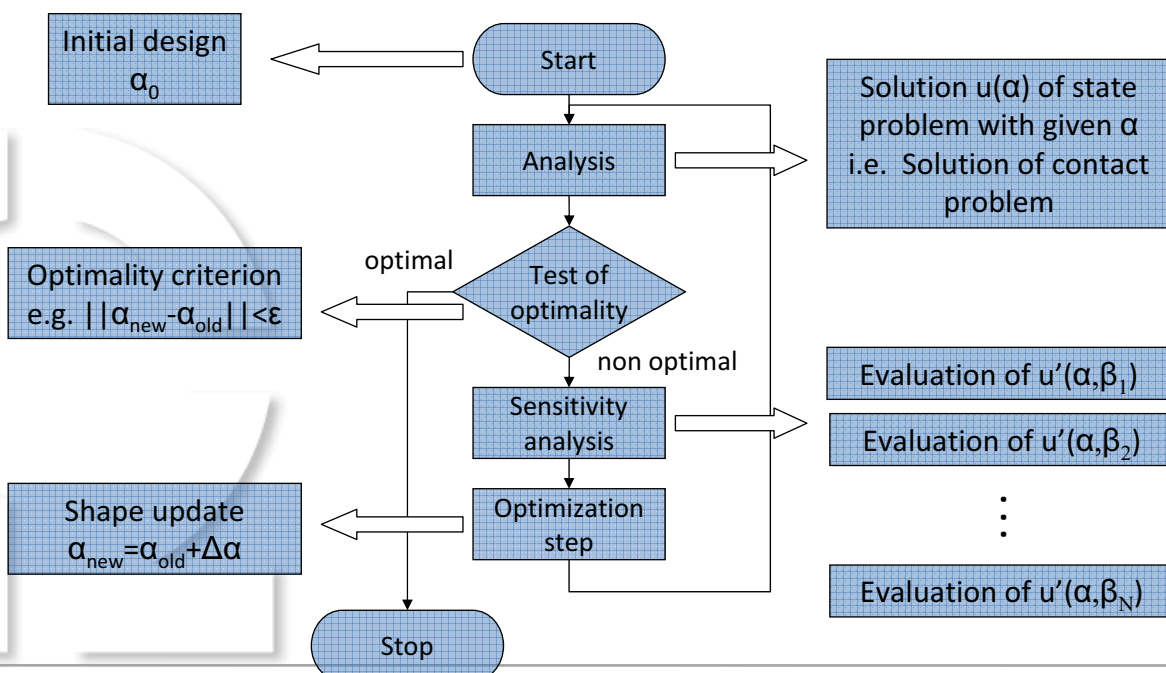
↓

$$\min \frac{1}{2} u^T K(\alpha) u - u^T f(\alpha),$$

s.t.  $B(\alpha)u \leq c(\alpha)$



## General shape optimization scheme



## Solution using MatSol

*function fem=problem(alpha)*

*Settings of*

*fem.geom ...Geometry def.*

*fem.mesh ...Mesh informations*

*fem.opt*

*fem.opt.dv ...Design variables*

*fem.opt.lb ... Lower bounds*

*fem.opt.ub ... Upper bounds*

*fem.opt.Aeq...Equality constr.*

*fem.opt.beq*

*fem.opt.Aiq ...Inequality constr.*

*fem.opt.biq*

*function*

*alphaopt=optimize(objective)*

*...*

*opt=feval(problem)*

*...*

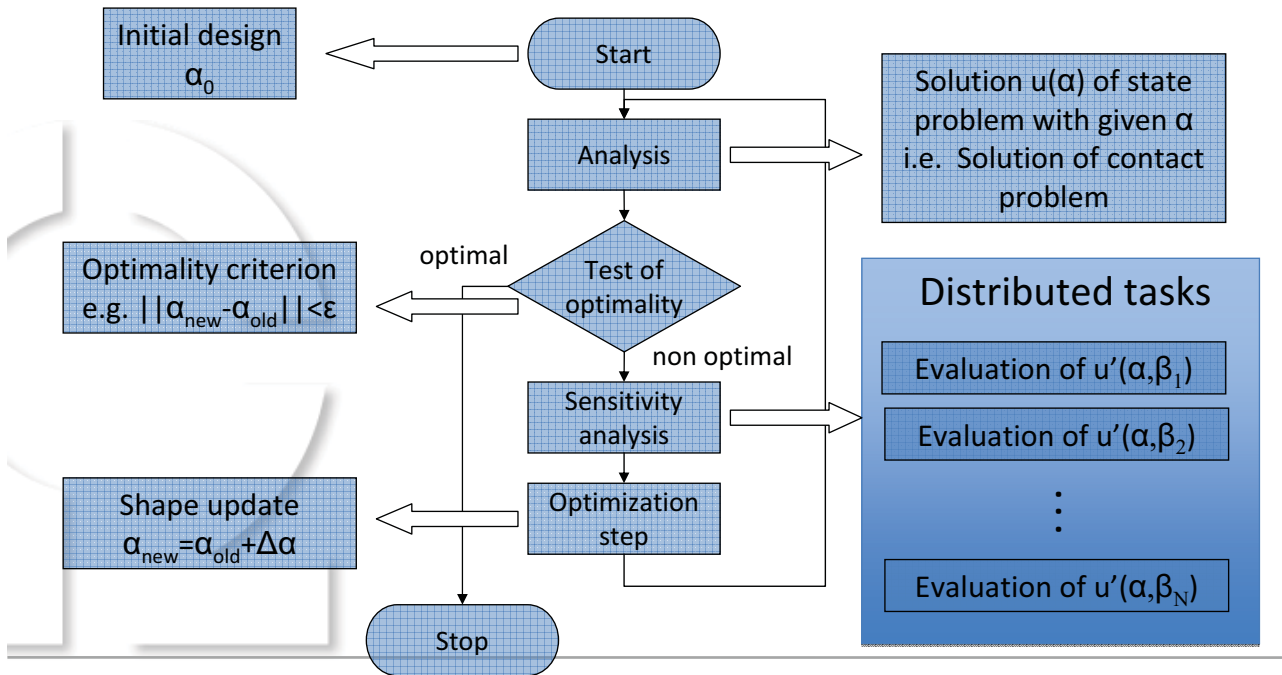
*alphaopt = fmincon(objective,  
opt.dv, opt.Aiq, opt.biq,  
opt.Aeq, opt.biq, opt.lb, opt.ub,  
optimoptions)*

*Function [f,g]=objective(alpha)*

*Solves state problem and  
sensitivity analysis*

## How to speed-up optimization process?

## General shape optimization scheme



## Finite difference sensitivity analysis

$$\frac{\partial u(\alpha)}{\partial \alpha_i} \approx \frac{u(\alpha + h e_i) - u(\alpha)}{h}$$

where

$u(\alpha + h e_i)$  solves

$$\min \frac{1}{2} u^T K(\alpha + h e_i) u - u^T f(\alpha + h e_i)$$

$$\text{subject to } B(\alpha + h e_i) u \leq c(\alpha + h e_i)$$

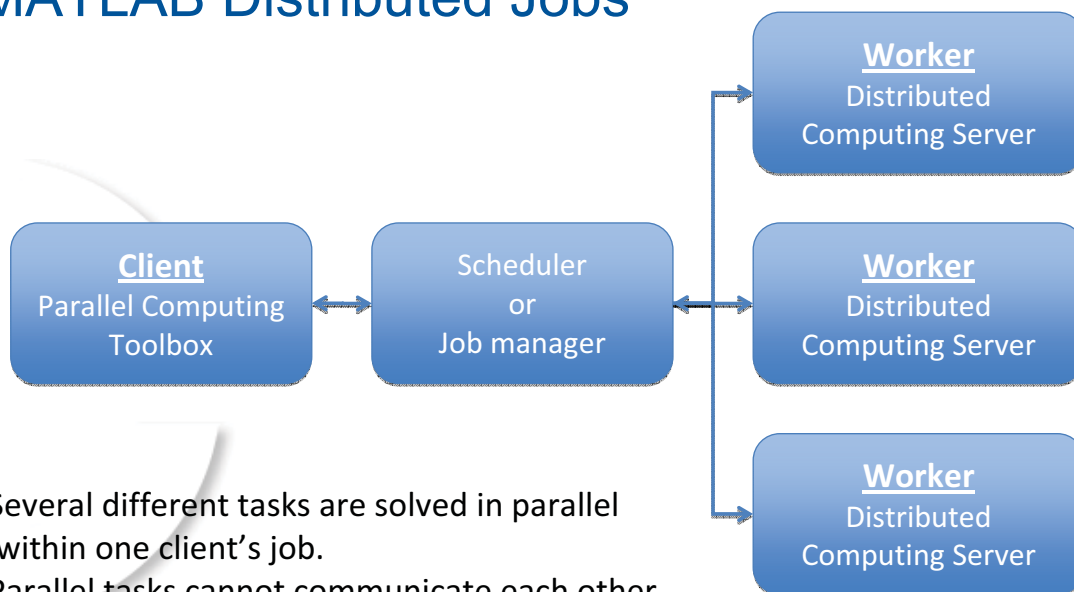
and  $e_i = (0, \dots, 0, \underset{i}{1}, 0, \dots, 0), i = 1, \dots, m$

- *Advantage*
  - Simple implementation
- *Disadvantages*
  - $m+1$  assemblies of stiffness matrix
  - $m+1$  solution of contact problem ( $m+1$  decompositions of  $K$ )
  - numerically unstable

## Parallel MATLAB and MatSol

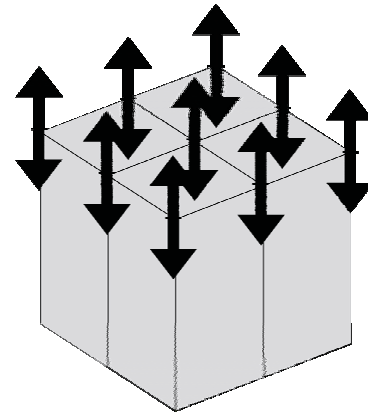
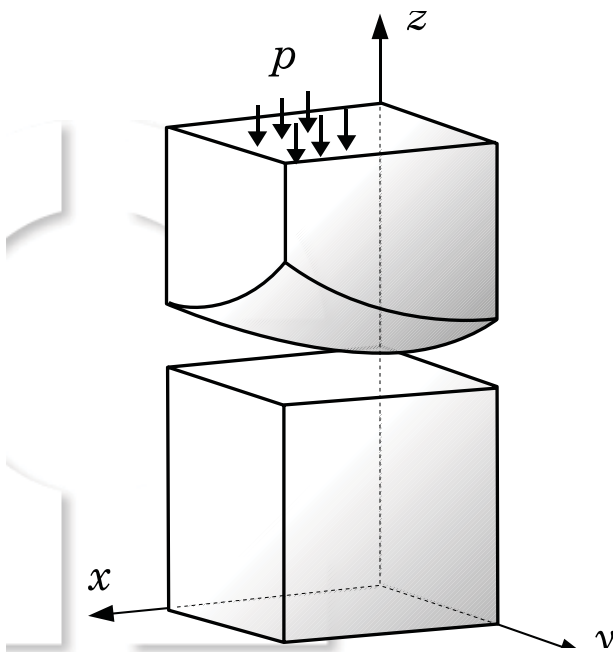
- *Parallel MATLAB – what does it mean?*
  - MATLAB® Distributed Computing Server™
  - Parallel Computing Toolbox™
  - Job managers or schedulers (local job manager, Mathworks job manager, Windows CCS, LSF, PBS Pro, ...)
  - <http://www.mathworks.com/products/distriben/>
- *MatSol uses Parallel Computing Toolbox*
  - Parallel implementation of algorithms
  - Parallel preprocessing and postprocessing
- *Star-P: alternative solution of Parallel MATLAB*
  - <http://www.interactivesupercomputing.com/>

## MATLAB Distributed Jobs



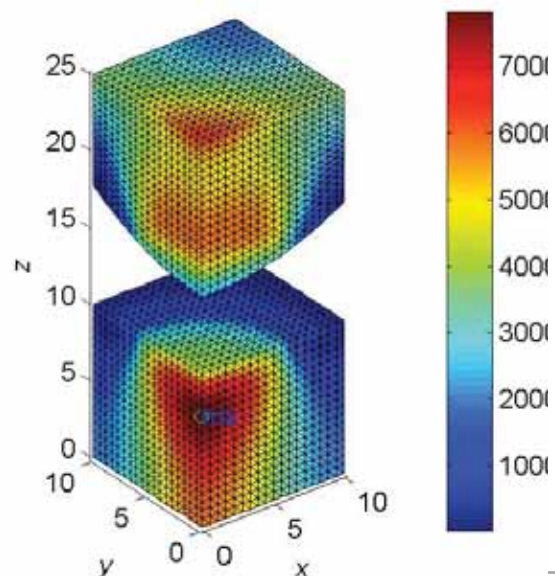
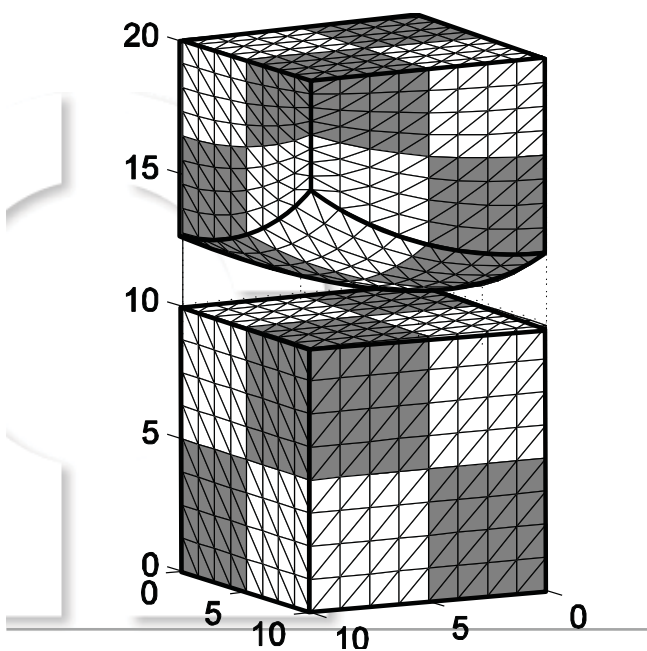


## 3D Hertz optimization problem



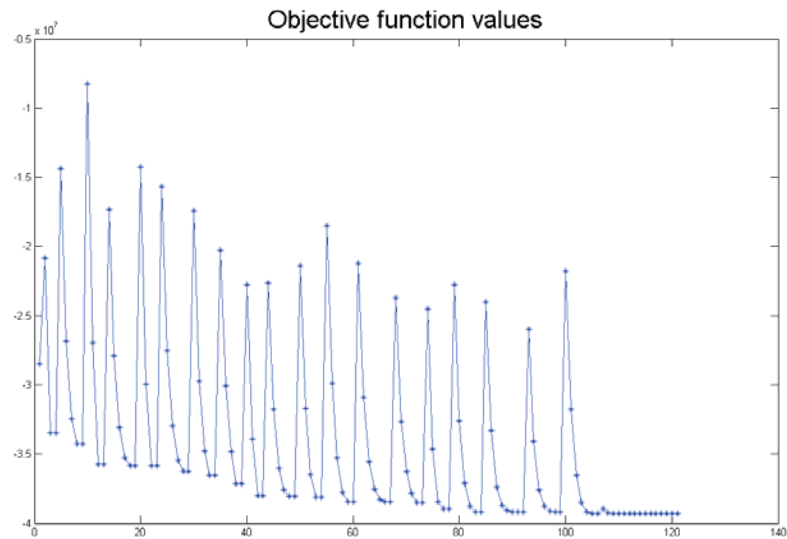
- $\min \frac{1}{2}u^TKu-u^Tf$
- 9 and 16 design variables with box constraints
- $\text{Vol}(\Omega)=\text{Vol}(\Omega_0)$

## 3D Hertz problem – initial design



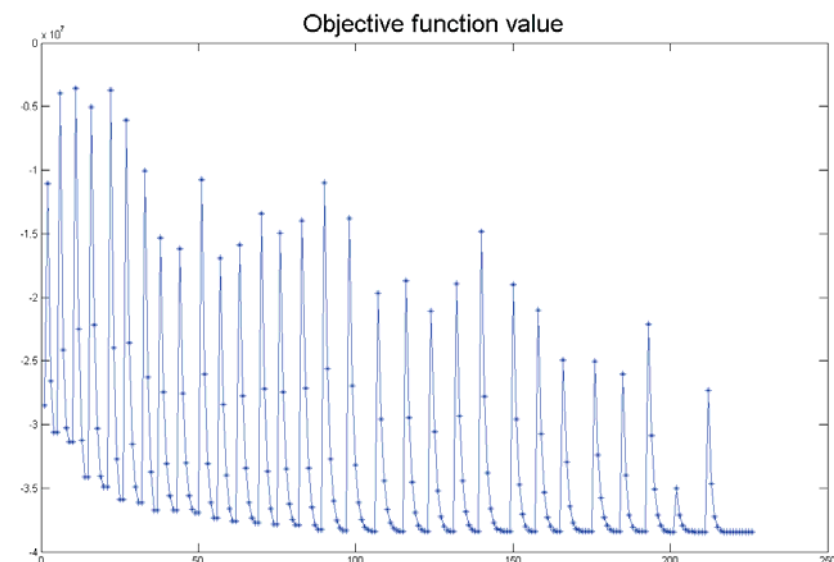
## 3D Hertz problem – optimized

Cubic spline function with 3x3 nodes = 9 design variables



## 3D Hertz problem – optimized

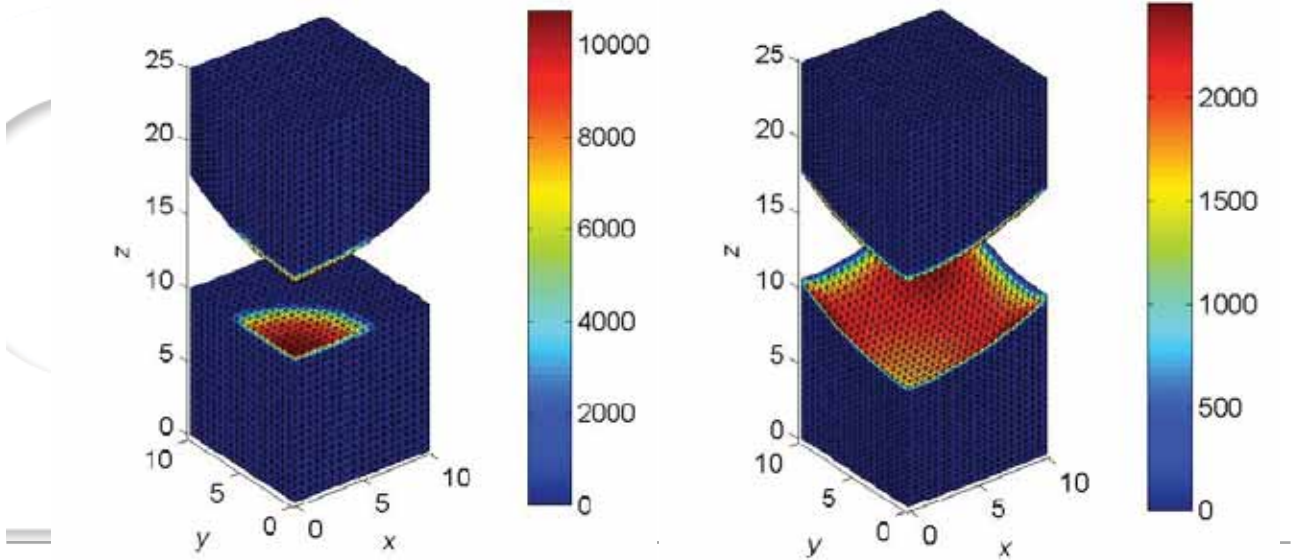
Cubic spline function with 4x4 nodes = 16 design variables



### 3D Hertz problem – contact pressure

Initial design

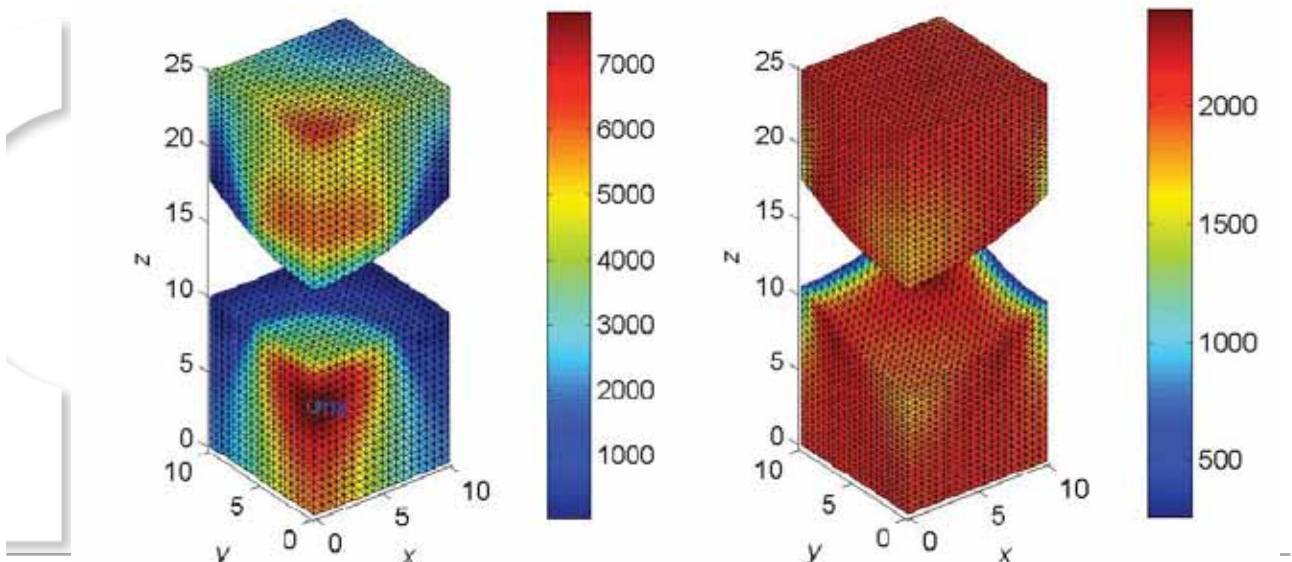
Optimized design



### 3D Hertz problem – von Mises stress

Initial design

Optimized design



## Parallel speed-up

Úloha	State problem		Sensitivity analysis	
		Sequential	Parallel	Speed-up
2D Hertz 5DV	0.4s	2s	5s	0.4x
2D Hertz 10DV	0.4s	4s	6s	0.67x
3D Hertz 9DV	15s	135s	30s	4.5x
3D Hertz 16DV	15s	240s	40s	6x

### Cluster COMSIO

HP Blade server, 18x AMD Opteron Dual Core 1.8GHz,  
 16x4GB +2x6GB, total 76GB  
 Infiniband interconnect  
 MATLAB Distributed Computing Server – 24 licences



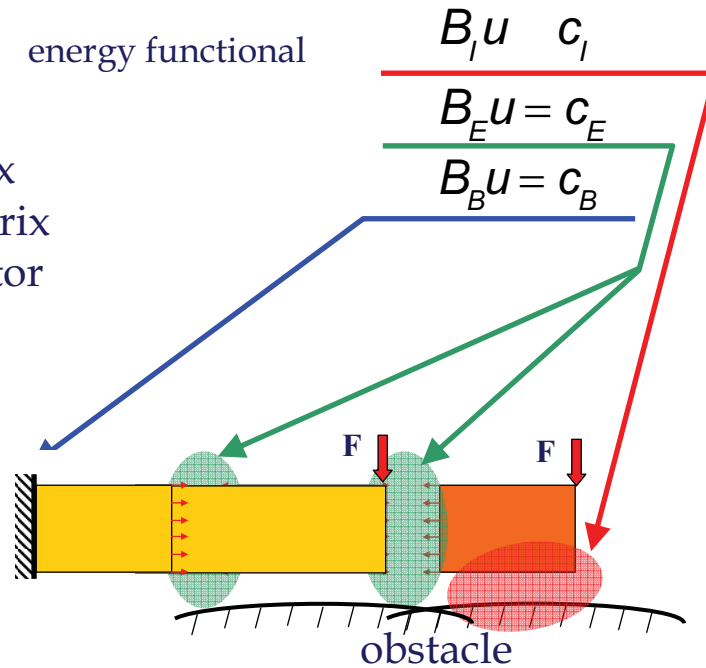
Number of parallel processes is limited by number of design variables!



# Total FETI – primal formulation

$$\min \frac{1}{2} u^T K u - u^T f \quad \text{energy functional}$$

$u$  displacement  
 $K$  stiffness matrix  
 $B$  constraint matrix  
 $c$  constraint vector



## Total FETI

Dirichlet b.c. are enforced by Lagrange multipliers

# Total FETI solution of state problem

$$\min \frac{1}{2} \lambda^T F(\alpha) \lambda - \lambda^T d(\alpha) \quad \text{subject to } \lambda_i \geq 0, E(\alpha) \lambda = g(\alpha)$$

$$\begin{aligned}
 F(\alpha) &= B(\alpha) K^+(\alpha) B(\alpha)^T \\
 d(\alpha) &= B(\alpha) K^+(\alpha) f(\alpha) - c(\alpha) \\
 E(\alpha) &= R(\alpha)^T B(\alpha)^T \\
 g(\alpha) &= R(\alpha)^T f(\alpha)
 \end{aligned}$$

$R(\alpha)$  is a-priori known!

$$\begin{aligned}
 K^+(\alpha) &= \text{diag} \left( K_1^+(\alpha), \dots, K_N^+(\alpha) \right) \\
 \lambda &= \begin{bmatrix} \lambda_B \\ \lambda_E \\ \lambda_I \end{bmatrix}, \quad B = \begin{bmatrix} B_B \\ B_E \\ B_I \end{bmatrix}, \quad c = \begin{bmatrix} 0 \\ 0 \\ c_I \end{bmatrix} \\
 \text{span} \{ R_{*,i}(\alpha) \} &= \text{null } K(\alpha)
 \end{aligned}$$

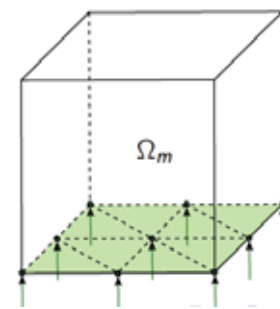
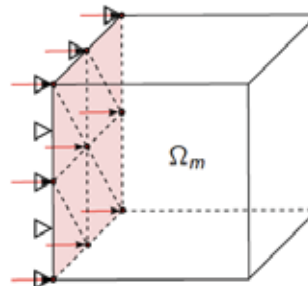
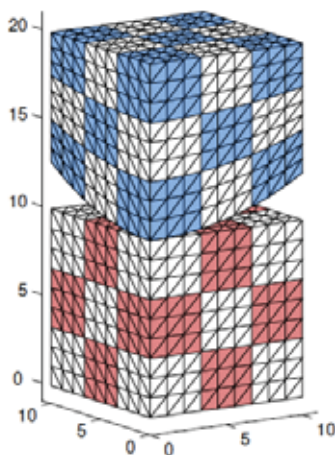
Reconstruction formula

$$\begin{aligned}
 u(\alpha) &= K^+(\alpha) \left( f(\alpha) - B(\alpha)^T \lambda(\alpha) \right) + R(\alpha) \xi \\
 &\text{with appropriate vector } \xi \in \mathbb{R}^{6N}
 \end{aligned}$$

Changing the shape of the bodies, they  
 have to be remeshed in each design  
 optimization step!



## Total BETI solution of state problem



$$\min J(u) \quad \text{subject to} \\
 B_I u = c_I, B_E u = 0, B_B u = 0$$

$$J(u) = \frac{1}{2} u^T S(\alpha) u - u^T r(\alpha) \\
 S(\alpha) = \text{diag}(S_1(\alpha), \dots, S_N(\alpha))$$

$$S_i(\alpha) = D_i + \left( \frac{1}{2} M_i + K_i \right)^T V_i^{-1} \left( \frac{1}{2} M_i + K_i \right) \\
 r_i(\alpha) = M_i^T V_i^{-1} N_i^0$$



# Total BETI solution of state problem

$$\min \frac{1}{2} \lambda^T F(\alpha) \lambda - \lambda^T d(\alpha) \text{ subject to } \lambda_i \geq 0, E(\alpha) \lambda = g(\alpha)$$

$$\begin{aligned} F(\alpha) &= B(\alpha) S^+(\alpha) B(\alpha)^T \\ d(\alpha) &= B(\alpha) S^+(\alpha) r(\alpha) - \alpha(\alpha) \\ E(\alpha) &= R(\alpha)^T B(\alpha)^T \\ g(\alpha) &= R(\alpha)^T r(\alpha) \end{aligned}$$

**$R(\alpha)$  is a-priori known!**

$$\begin{aligned} S^+(\alpha) &= \text{diag} \left( S_1^+(\alpha), \dots, S_N^+(\alpha) \right) \\ \lambda &= \begin{bmatrix} \lambda_B \\ \lambda_E \\ \lambda_I \end{bmatrix}, B = \begin{bmatrix} B_B \\ B_E \\ B_I \end{bmatrix}, c = \begin{bmatrix} c \\ c \\ c \end{bmatrix} \\ \text{span} \{ R_{\cdot i}(\alpha) \} &= \text{null } S(\alpha) \end{aligned}$$

Reconstruction formula  $u(\alpha) = S^+(\alpha) \left( r(\alpha) - B(\alpha)^T \lambda(\alpha) \right) + R(\alpha) \xi$   
with appropriate vector  $\xi \in \mathbb{R}^{6N}$

# Finite difference sensitivity analysis

$$\frac{\partial u(\alpha)}{\partial \alpha_i} \approx \frac{u(\alpha + h e_i) - u(\alpha)}{h}$$

where

$u(\alpha + h e_i)$  solves

$$\min \frac{1}{2} u^T K(\alpha + h e_i) u - u^T f(\alpha + h e_i)$$

$$\text{subject to } B(\alpha + h e_i) u \leq c(\alpha + h e_i)$$

$$\text{and } e_i = (0, \dots, 0, \underset{i}{1}, 0, \dots, 0), i = 1, \dots, m$$

- *Advantage*
  - Simple implementation
- *Disadvantages*
  - $m+1$  assemblies of stiffness matrix
  - $m+1$  solution of contact problem ( $m+1$  decompositions of  $K$ )
  - $m+1$  constructions of  $R$
  - numerically unstable
- *Does "semi-analytical" method exist?*

## Semi-analytical sensitivity analysis

$I_C = \{i : B_{i,*}(\alpha)u(\alpha) = c_i(\alpha)\}$  ... indices of nodal variables in contact

$I_S = \{i : i \in I_C \wedge \lambda_i(\alpha) > 0\}$  ... indices of nodal variables in strong contact

$I_W = \{i : i \in I_C \wedge \lambda_i(\alpha) = 0\}$  ... indices of nodal variables in weak contact

$$u'(\alpha, \beta) = \lim_{h \rightarrow 0} \frac{1}{h} (u(\alpha + h\beta) - u(\alpha))$$

solves

$$\min \frac{1}{2} z^T K(\alpha) z - z^T \bar{f}(\alpha, \beta)$$

$$\text{s.t. } B_W(\alpha) z \leq c_W(\alpha, \beta), B_S(\alpha) z = c_S(\alpha, \beta)$$

$$\bar{f}(\alpha, \beta) = f'(\alpha, \beta) - K'(\alpha, \beta)u(\alpha) + B'^T(\alpha, \beta)\lambda(\alpha)$$

$$B_S(\alpha) = [B_i(\alpha)]_{i \in I_S}, c_S(\alpha, \beta) = [f'_i(\alpha, \beta) - B'_{i,*}(\alpha, \beta)u(\alpha)]_{i \in I_S}$$

$$B_W(\alpha) = [B_i(\alpha)]_{i \in I_W}, c_W(\alpha, \beta) = [f'_i(\alpha, \beta) - B'_{i,*}(\alpha, \beta)u(\alpha)]_{i \in I_W}$$

Only one assembly and  
one decomposition of  
stiffness matrix for all  
 $\beta = e_i, i=1, \dots, m$

## BETI & FETI based sensitivity analysis

$$\min \frac{1}{2} \mu^T \bar{F}(\alpha) \mu - \mu^T \bar{d}(\alpha, \beta) \quad \text{s.t.} \quad \mu_w \geq 0, \bar{E}(\alpha) \mu = \bar{g}(\alpha, \beta)$$

where

$$\bar{F}(\alpha) = \bar{B}(\alpha) K^+(\alpha) \bar{B}^T(\alpha), \quad \bar{d}(\alpha, \beta) = \bar{B}(\alpha) K^+(\alpha) \bar{f}(\alpha, \beta) - \bar{c}(\alpha, \beta),$$

$$\bar{E}(\alpha) = R^T(\alpha) \bar{B}^T(\alpha), \quad \bar{g}(\alpha, \beta) = R^T(\alpha) \bar{f}(\alpha, \beta)$$

$$\bar{B}(\alpha) = \begin{bmatrix} B_W(\alpha) \\ B_S(\alpha) \end{bmatrix}, \quad \bar{c}(\alpha, \beta) = \begin{bmatrix} c_W(\alpha, \beta) \\ c_S(\alpha, \beta) \end{bmatrix}, \quad \mu = \begin{bmatrix} \mu_W \\ \mu_S \end{bmatrix}, \quad z(\alpha, \beta) = u'(\alpha, \beta)$$

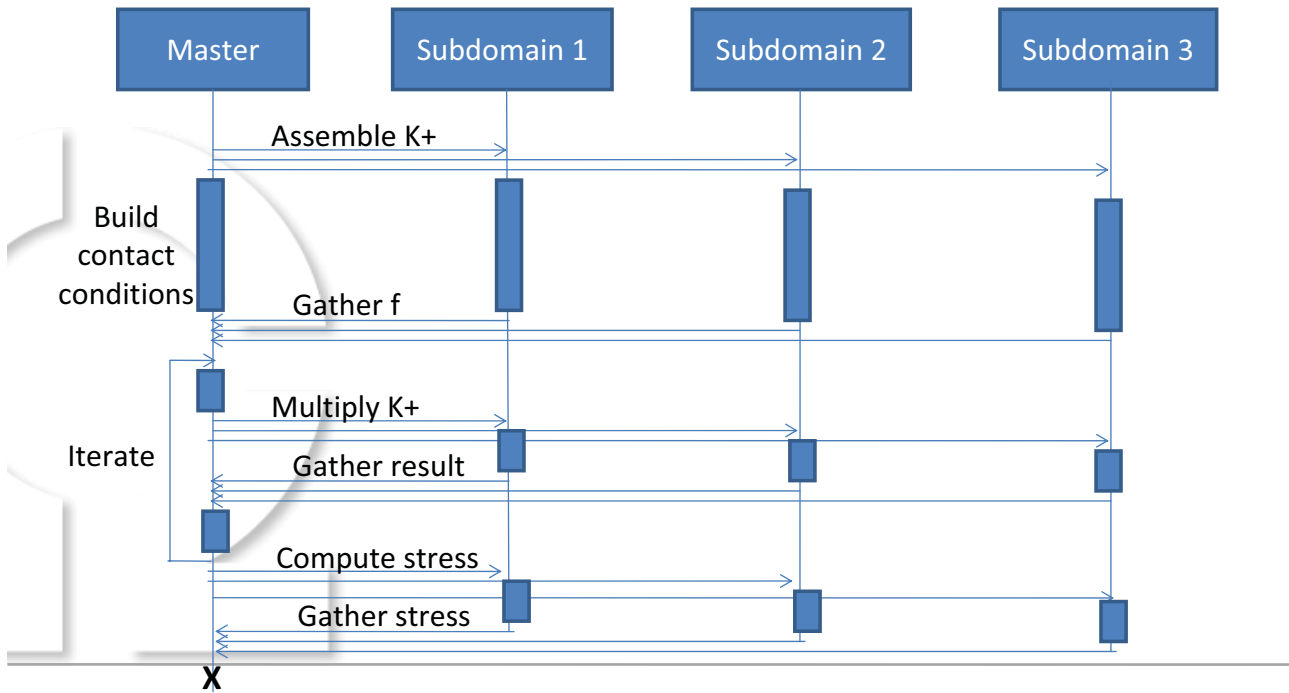
$$u'(\alpha, \beta) = K^+(\alpha) (\bar{f}(\alpha, \beta) - \bar{B}(\alpha)^T \mu(\alpha, \beta)) + R(\alpha) \zeta$$

with such appropriate  $\zeta$

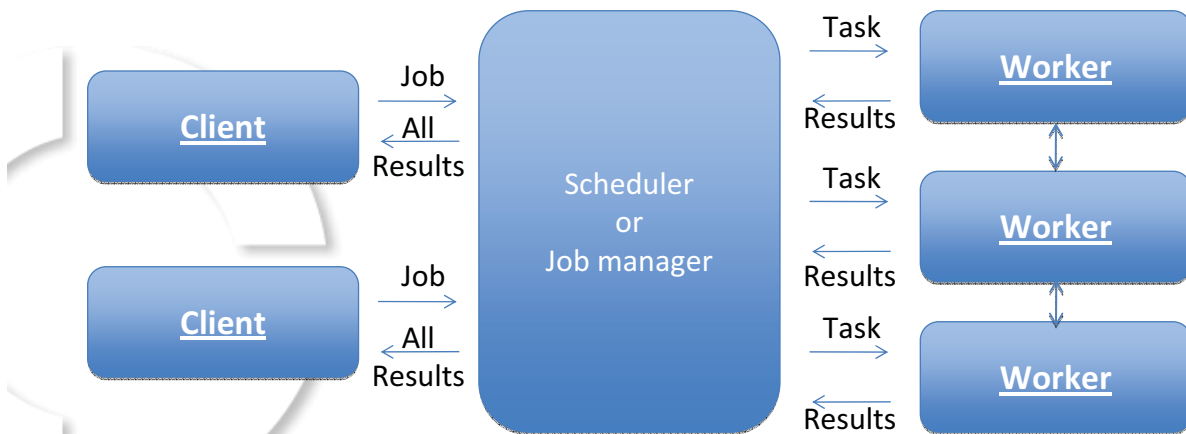
$K^+$  and  $R$  is known from state problem analysis,  $I_W$  is empty in reality!



## Scenario of parallel solution



## MATLAB Parallel Jobs



Only one task is solved in parallel within one client's job.  
 Parallel tasks can communicate each other.

## Total BETI vs. Total FETI-sequential code

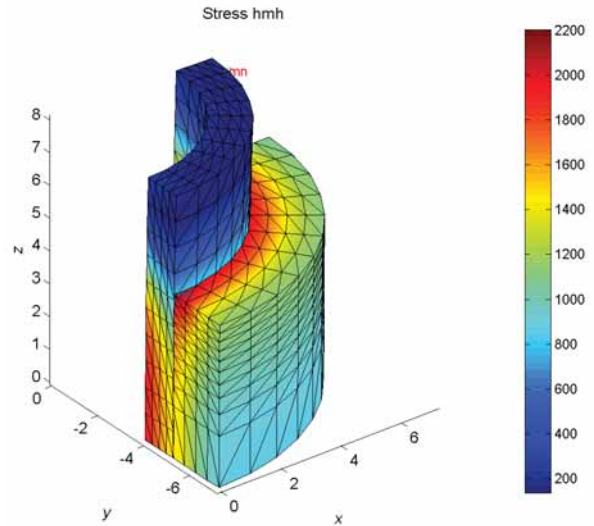
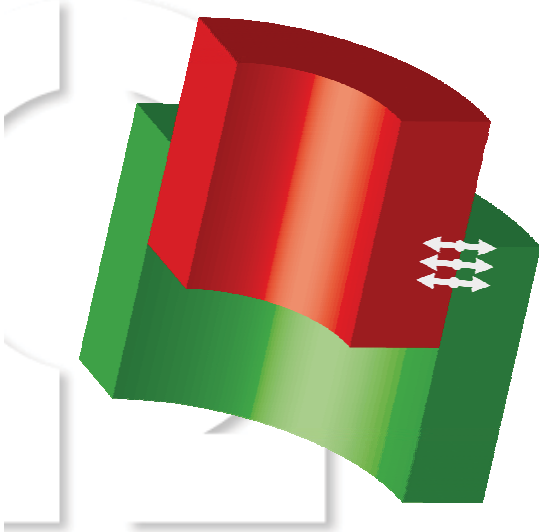
State problem				Sensitivity analysis		
Prim/Dual	Pre-Post	Sol	Total	Pre-Post	Sol	Total
10368/6480	48s 16s	10s 8s	58s 24s	768s 256s	160s 128s	928s 384s
48000/20256	470s 44s	30s 30s	500s 74s	7520s 704s	480s 480s	8000s 1184s
279936/70848	7680s 350s	500s 430s	8180s 780s	122880s 5600s	8000s 6880s	130880s 12480s
10368/6480	3x	1.25x	2.4x	3x	1.25x	2.4x
48000/20256	10.7x	1x	6.8x	10.7x	1x	6.8x
279936/70848	22x	1.2x	10.5x	22x	1.2x	10.5x

## Total BETI vs. Total FETI-parallel code

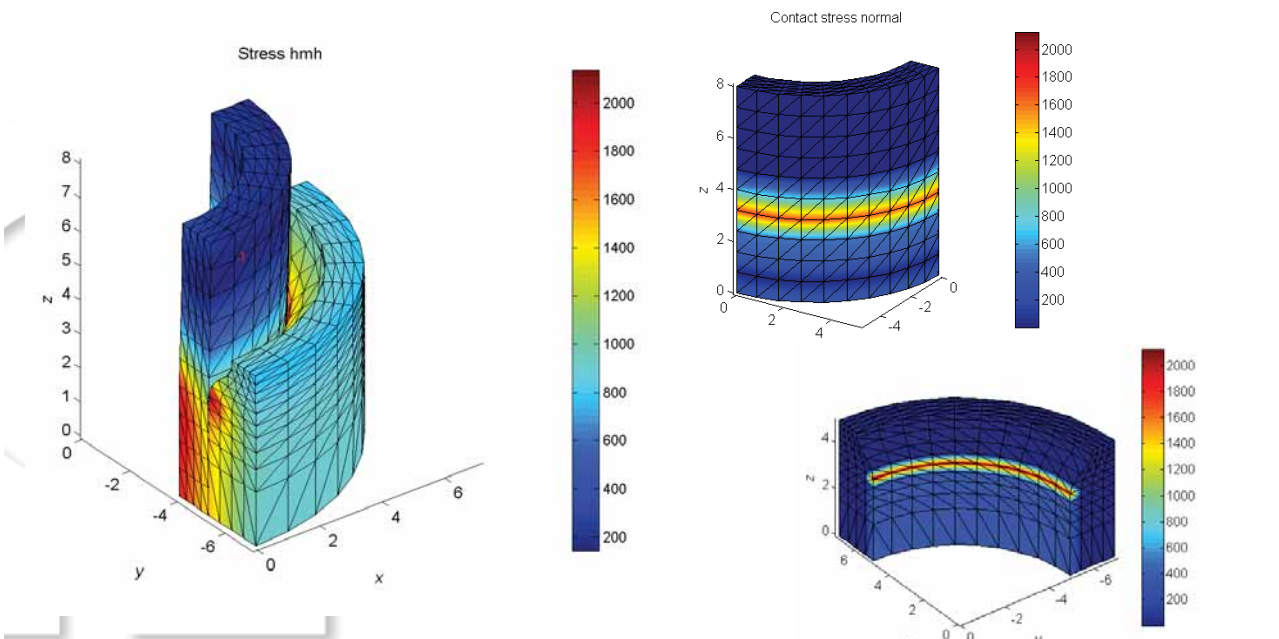
State problem				Sensitivity analysis		
Prim/Dual	Pre-Post	Sol	Total	Pre-Post	Sol	Total
10368/3108	34s 24s	2s 2s	36s 26s	243s 151s	13s 14s	256s 165s
48000/9021	152s 29s	6s 8s	158s 37s	1370s 258s	50s 66s	1420s 324s
279936/30036	3500s 143s	49s 150s	3549s 393s	31500s 1959s	441s 972s	31941s 2931s
10368/3108	1.4x	1x	1.4x	1.6x	0.9x	1.6x
48000/9021	5.2x	0.75x	4.3x	5.3x	0.75x	4.4x
279936/70848	24x	0.33x	9x	16x	0.45x	11x

## Two Cylinders

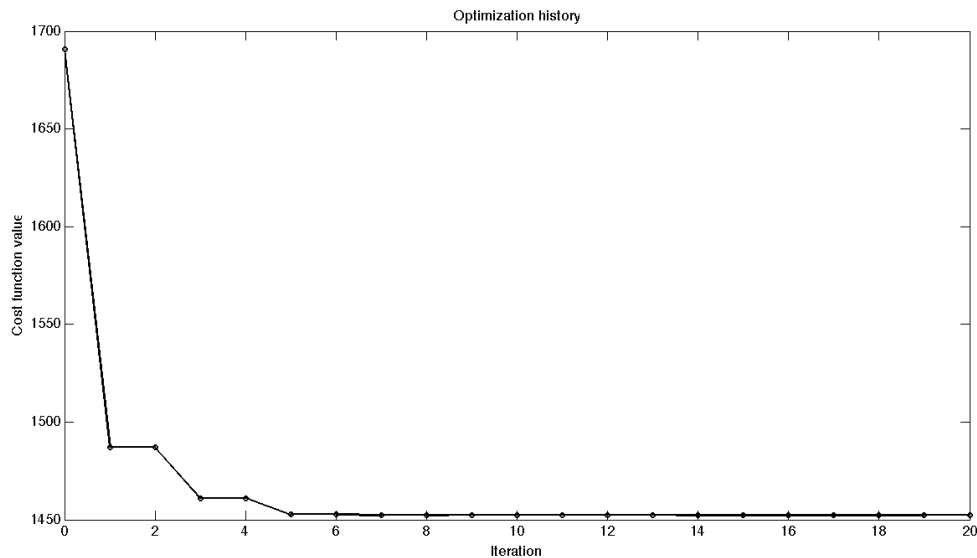
- $\min \frac{1}{2}u^TKu-u^Tf$
- 3 design variables box constrained



## Two Cylinders - optimization



## Two Cylinders - history



## Conclusions and future works

- *Efficient solution on parallel computers*
  - MATLAB distributed computing server
  - Scalable Total FETI algorithm
  - Efficient sensitivity analysis
- *BETI vs. FETI*
  - BETI do not need remeshing of interior of bodies
  - Matrices resulting from BETI are full
  - Assembling of BETI operator is very time consuming
- *Future works*
  - Fast sparse approximation for BETI
  - Massive parallel solution – both sensitivity and domain decomposition parallelism



*Thank you*

**[HTTP://WWW.AM.VSB.CZ/MATSO](http://www.am.vsb.cz/matso)**  
**L**

---

# Computational (geo) micromechanics

---

R. Blaheta, P. Byczanski,  
R. Kohut, V. Sokol et al.  
Computational Mechanics II, Ostrava

---

1

---

## Context



- Project GACR: Multiscale modelling and X-Ray tomography in geotechnics
- Experience
  - X-ray CT
  - Laboratory preparation and testing of geocomposites
  - FE modelling
- Aims – interconnection of the knowledge, better understanding of behaviour of geocomposites, development of homogenization techniques, FE software and solvers

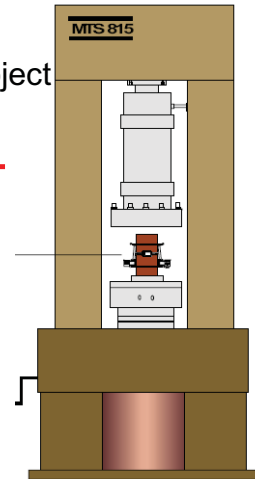
---

2

U Kumamoto  
CTU Prague  
new ICT project



Zwick 1494  
(600 kN)  
new ICT project

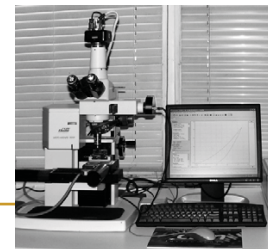


- load
- ultra-sound
- AE
- permeability
- ...

IGN - Hubert  
32-core SMP system  
128GB RAM  
new IT4 project



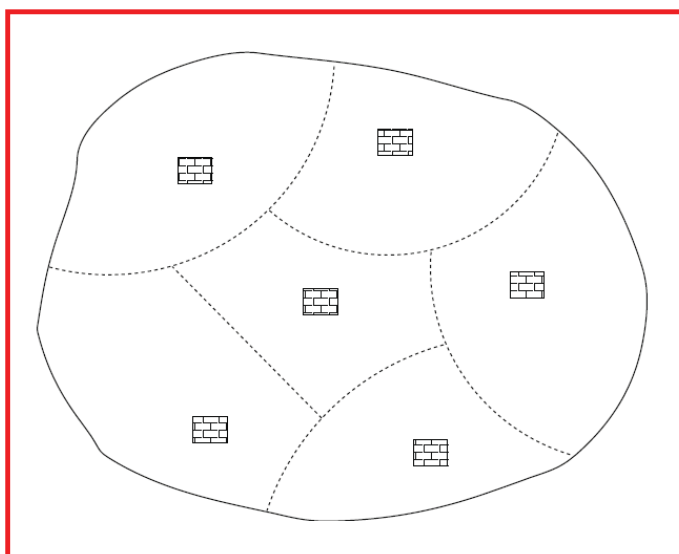
Micro Hardness Tester  
CSM Instruments



3

## Multiscale Heterogeneity

- Large difference in characteristic dimensions
- Impossible to cover by unique model
- Requirement for special approaches



MACROSCALE

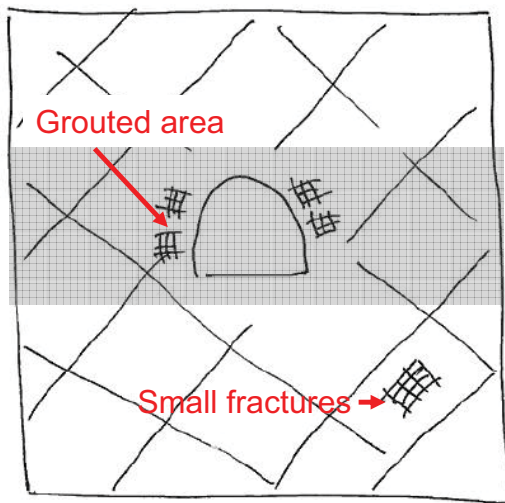


up-  
scaling

MICROSCALE

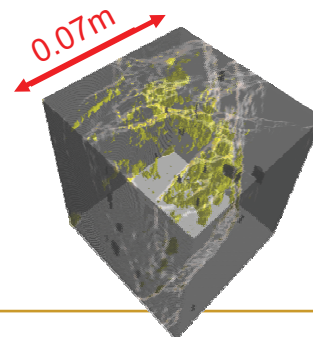
4

# Grouting and geocomposites

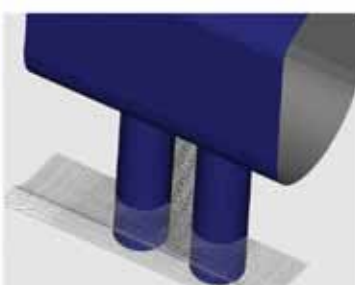
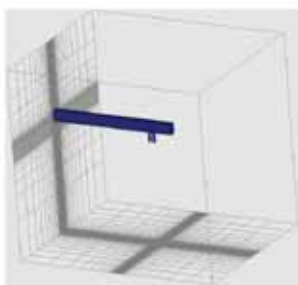


- Macroscale 50-100m
- Global model = rock blocks and main fractures
- Microscale 0.001m – small fractures, grouted fractures

Microscale properties influence the macroscale behaviour



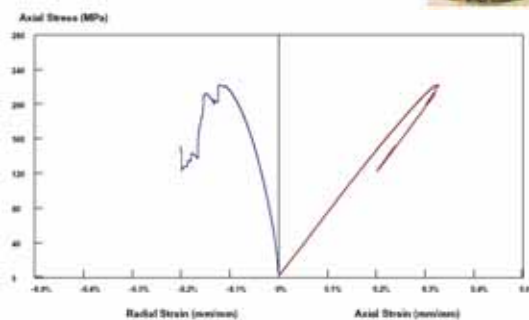
# Decovalex -APSE damage of granite rocks



Damage of granite is also included by macrostress due to continuum damage model

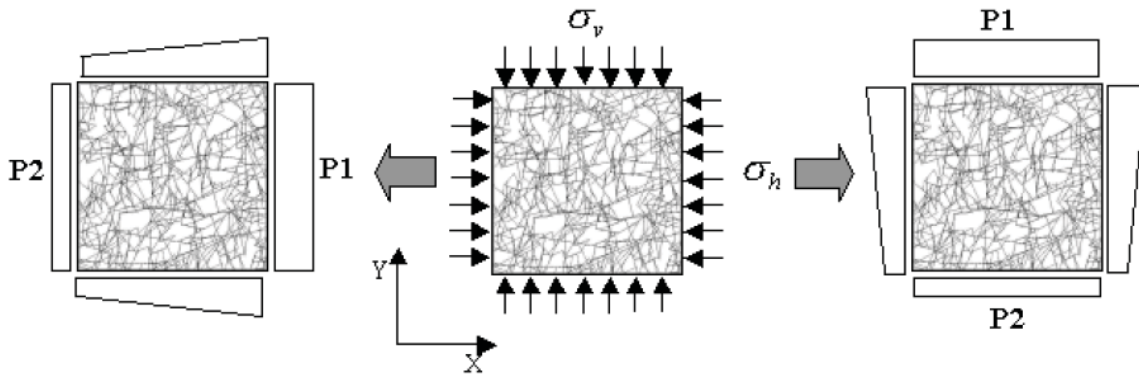


- Macro stress influences damage in microscale
- Damage influences flow in macroscale



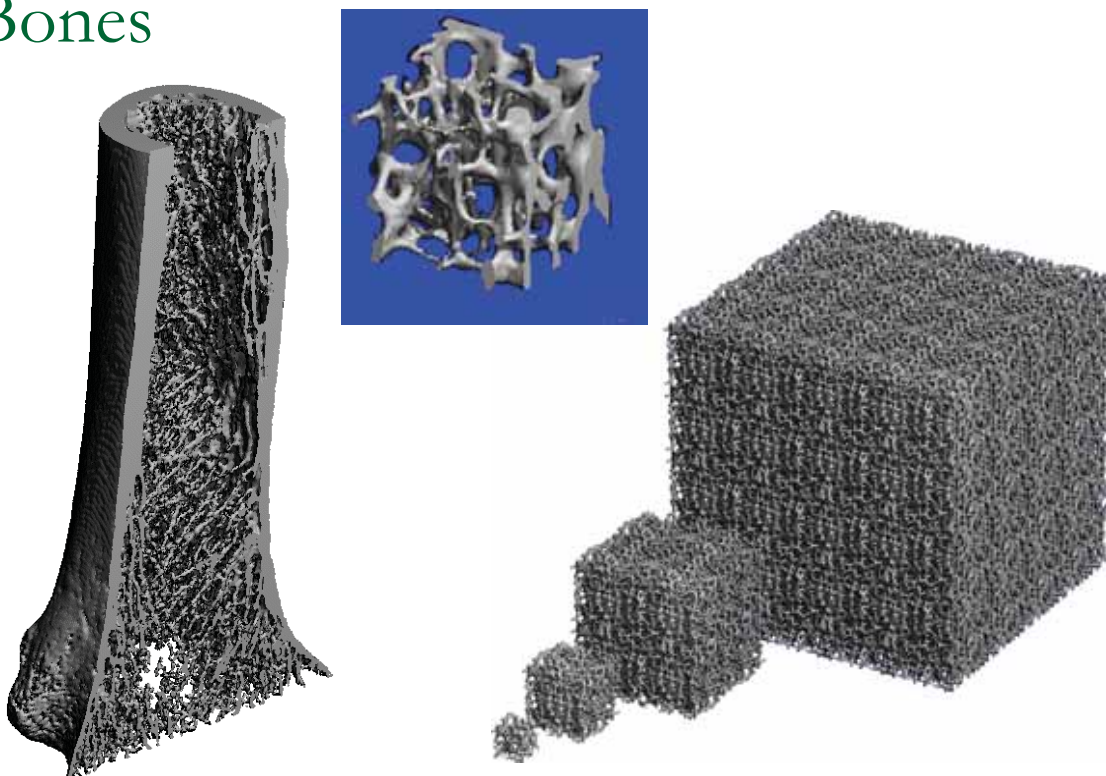


# Decovalex – flow in fractured rocks



7

# Bones

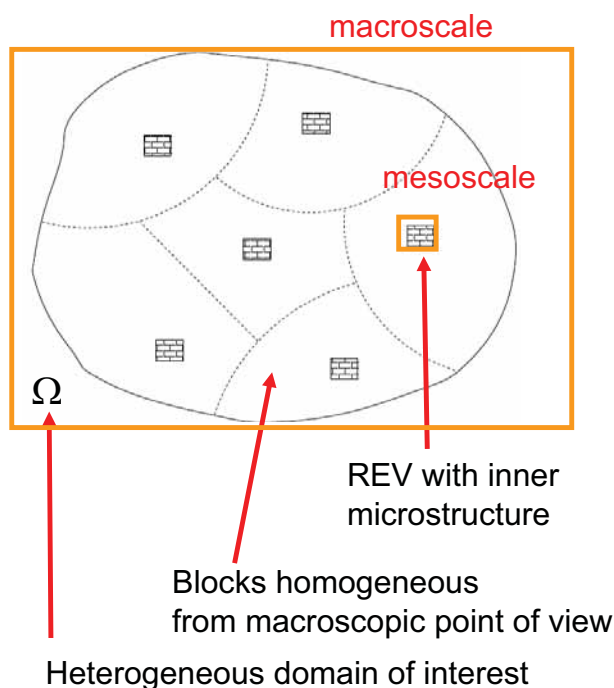


8

# Multiscale - scale separation

- Macro – meso - micro scale
- REV representative volume element
- Upscaling and homogenization
- Special case: periodic and layered structures

# Heterogeneity & multiscale



$$\varepsilon(x) = \bar{\varepsilon}(x) + \tilde{\varepsilon}(x)$$

$$\sigma(x) = \bar{\sigma}(x) + \tilde{\sigma}(x)$$

Microscale variables =  
macroscopic fields  
+ local microscale fluctuations

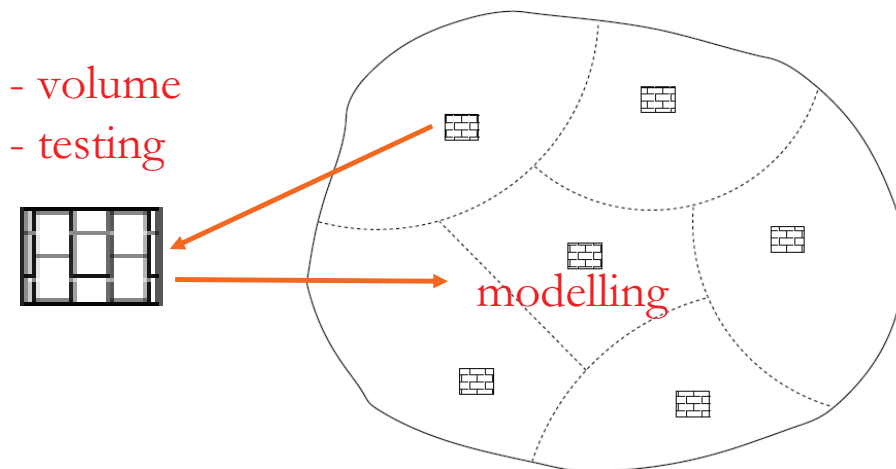
$$\bar{\varepsilon} = \frac{1}{V} \int_V \varepsilon(x) dV =$$

$$= \frac{1}{2V} \int_S (u \otimes n + n \otimes u) dS$$

$$\bar{\sigma} = \frac{1}{V} \int_V \sigma(x) dV =$$

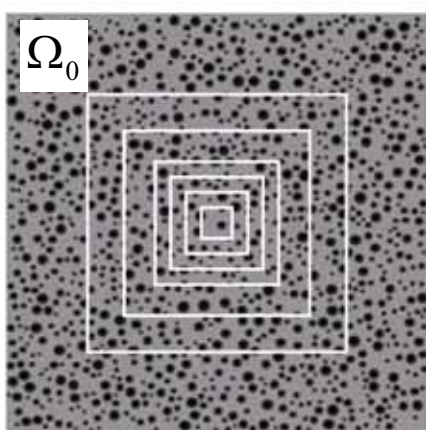
$$= \frac{1}{V} \int_S (t(x) \otimes x) dS$$

# Upscaling

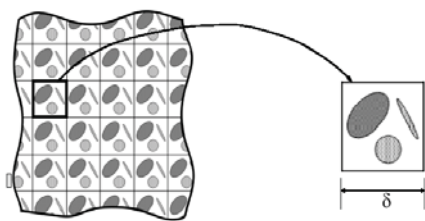


11

# RVE – representative volume element $V$



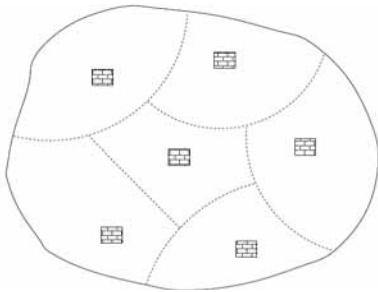
- Definition I: RVE is a **cell** that sufficiently accurately **represents the overall macroscale properties** of interest (increasing the size does not change calculated material parameters (Size effect))
- Definition II: **statistically homogeneous**



$\Omega_0$  a unit **periodic cell** for periodic microstructure

# Upscaling scheme

$\Omega$



scale separation

macroscale

$$L_h u_h = L_h(\bar{k}) u_h = f_h \text{ in } \Omega + BC$$

$$L_h u_h = -\text{div } \sigma, \sigma = \bar{k} \varepsilon, \varepsilon = \varepsilon(u_h)$$

mesoscale - microscale

$$\tilde{L}_h u_h = \tilde{L}_h(k) u_h = 0 \text{ in } V + BC$$

$$\tilde{L}_h \tilde{u}_h = -\text{div } \sigma, \sigma = k \varepsilon, \varepsilon = \varepsilon(\tilde{u}_h)$$

$$\bar{\sigma} = \langle \sigma \rangle = |V|^{-1} \int_V \sigma(x) dx$$

$$\bar{k}: \bar{\sigma} = \bar{k} \bar{\varepsilon} \text{ or } \overline{\sigma \cdot \varepsilon} = \bar{k} \bar{\varepsilon} \cdot \bar{\varepsilon}$$

# Homogenization $\tilde{L}_h u_h = \tilde{L}_h(k) u_h = 0 \text{ in } V + BC$

- $\varepsilon_0$ -KUBC  $u(x) = \varepsilon_0 \cdot x \text{ on } \partial\Omega$
- $\sigma_0$ -SUBC  $t = \sigma \cdot n = \sigma_0 \cdot n \text{ on } \partial\Omega$
- periodic  $u(x) = \varepsilon_0 \cdot x + v(x) \text{ on } \partial\Omega, v(x) \text{ periodic}$
- mixed  $(u(x) - \varepsilon_0 \cdot x)(\sigma(x) \cdot n(x) - \sigma_0 \cdot n(x)) = 0 \text{ on } \partial\Omega$

$$\langle \varepsilon \rangle = \varepsilon_0, \quad \langle \sigma \rangle = \sigma_0 \quad \begin{aligned} \langle \sigma \rangle &= C_\varepsilon^{app} \varepsilon_0 \Rightarrow C_\varepsilon^{app} \\ \langle \varepsilon \rangle &= S_\sigma^{app} \sigma_0 \Rightarrow C_\sigma^{app} = (S_\sigma^{app})^{-1} \end{aligned}$$

# Influence of BC and test volume size

- The homogenized coefficients are **unique** only for well separated scales and REV size of Test Volume

- Otherwise there is a dependence on **BC**

$$C_{\sigma}^{app} \leq C^{app} \leq C_{\varepsilon}^{app}$$

cf. Reuss lower – Voigt upper bounds

- And there is a size effect regarding **size of SD** – partition of sample and averaging of the test results for subsamples gives

$$\langle S_{\sigma,k}^{app} \rangle^{-1} \leq C_{\sigma}^{app} \leq C_{\varepsilon}^{app} \leq \langle C_{\varepsilon,k}^{app} \rangle$$

difference and SD size

- Equivalence of mechanical and energetic definition as well as size criterion – **Hill condition**

$$\langle \varepsilon : \sigma \rangle = \langle \varepsilon \rangle : \langle \sigma \rangle$$

## 1D homogenization

1D periodic microstructure problem

$$-[k(x)u'(x)]' = 0 \text{ in } \Omega$$

Reference cell (0,1)

$$k(x) = \begin{cases} k_1 & \text{in } (0, \frac{1}{2}) \\ k_2 & \text{in } (\frac{1}{2}, 1) \end{cases}$$

$$BC: \sigma \cdot n = \sigma_0 \cdot n \text{ on } \partial\Omega$$

$$\bar{\sigma} = \sigma_0 = \sigma$$

$$\bar{\varepsilon} = \frac{1}{2} \frac{\sigma_0}{k_1} + \frac{1}{2} \frac{\sigma_0}{k_2}$$

$$\frac{\bar{\varepsilon}}{\bar{\sigma}} = \frac{1}{\bar{k}} = \frac{1}{2} \left( \frac{1}{k_1} + \frac{1}{k_2} \right)$$

$$BC: u = \varepsilon_0 \cdot x + p \text{ on } \partial\Omega$$

$$\bar{\varepsilon} = \varepsilon_0, \text{ piecewise constant } \varepsilon_a, \varepsilon_b$$

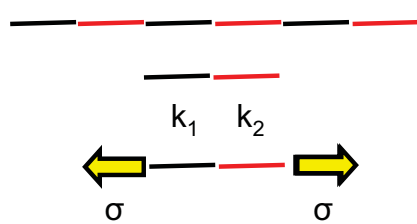
$$\bar{\varepsilon} = \frac{1}{2} \varepsilon_a + \frac{1}{2} \varepsilon_b$$

$$\bar{\sigma} = \sigma \text{ constant} = k_1 \varepsilon_a = k_2 \varepsilon_b$$

$$\Rightarrow \left(1 + \frac{k_1}{k_2}\right) \varepsilon_a = 2\bar{\varepsilon}$$

$$\Rightarrow \bar{\sigma} = 2k_1 \left(1 + \frac{k_1}{k_2}\right)^{-1} \bar{\varepsilon}$$

# Homogenization – 1D periodic medium



1D periodic medium  
 Basic cell, RVE  
 Material coefficients  
 Application of load, flux => constant flux

$$\bar{\varepsilon} = \frac{1}{|V|} \int_V \varepsilon dV = \frac{1}{2} \left( \frac{\sigma}{k_1} + \frac{\sigma}{k_2} \right) = \frac{\sigma}{\bar{k}}$$

$$\bar{k} = \frac{2k_1k_2}{k_1 + k_2}$$

Application of different BC:  
 here preserve constant flux  
 => give the same result  $\bar{k}$

## NOTES

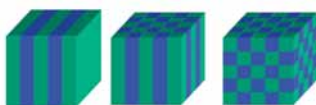
- The same result for any test volume being a multiple of basic cell (the same proportion of material components)
- **Big difference from arithmetic average**

# Asymptotic theory for periodic media

$$\frac{\partial}{\partial x} \left( A \left( \frac{x}{\varepsilon} \right) \frac{\partial u}{\partial x} \right) = 0$$

$$u_\varepsilon \rightarrow u^*$$

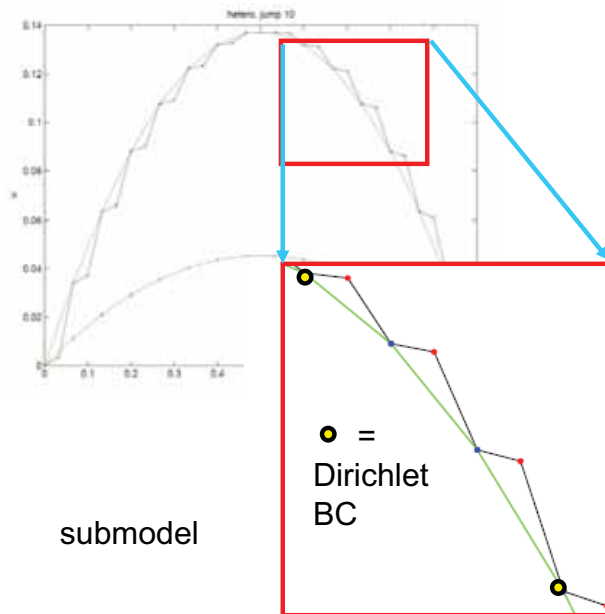
$$\frac{\partial}{\partial x} \left( A^* \frac{\partial u}{\partial x} \right) = 0$$



- PDE with rapidly oscillating periodic coefficients,  $\varepsilon=l/L$ ,  $A_\varepsilon=A(x/\varepsilon)$
- $u_\varepsilon \rightarrow u^*$  – boundedness in  $H^1$ , weak convergence
- $u^*$  is solution of a boundary value problem with constant coefficients  $A^*$
- $A^*$  is constant, known as effective property
- local correctors

## Local correctors

- Local – global approaches



## FEM analysis

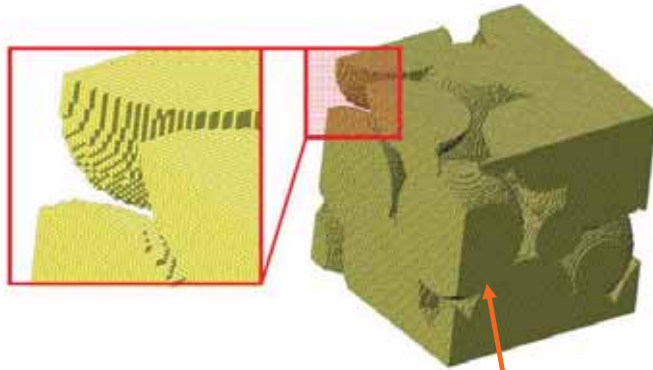
- Standard FEM on macroscale
- Standard FEM on mesoscale
  - BC, pure Neumann
  - Aligned and nonaligned (voxel) grids
- Accuracy and heterogeneity
- Heterogeneity and efficient solvers

# FEM – voxel/aligned grids

Discretization by standard  
finite elements



Voxel discretization



H. Andrä,  
Workshop on Microstructure Simulation and Virtual  
Material Design, Kaiserslautern, 2006

CT

## Solvers

- Large scale problems
- Jumps in coefficients



# Parallel solver – P. Arbenz, ETH

- PCG with smoothed aggregation (SA) multilevel preconditioning

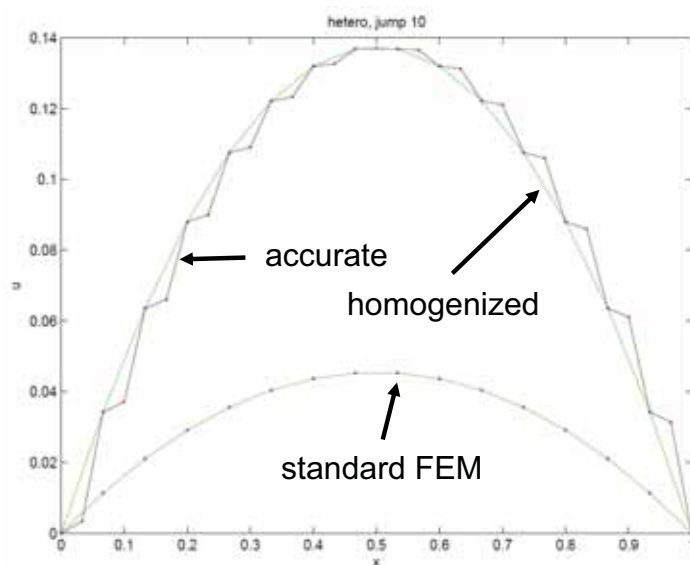
$$AB^{-1}\mathbf{y} = \mathbf{b}, \quad \mathbf{y} = B\mathbf{x}.$$

Solving with  $B$  means applying one multigrid  $V$ -cycle.

- P. Arbenz, G.H. van Lenthe, U. Mennel, R. Müller, and M. Sala: "A Scalable Multi-level Preconditioner for Matrix-Free  $\mu$ -Finite Element Analysis of Human Bone Structures". *Internat. J. Numer. Methods Engrg.* 73 (7): 927-947 (2008), doi:10.1002/nme.2101.

23

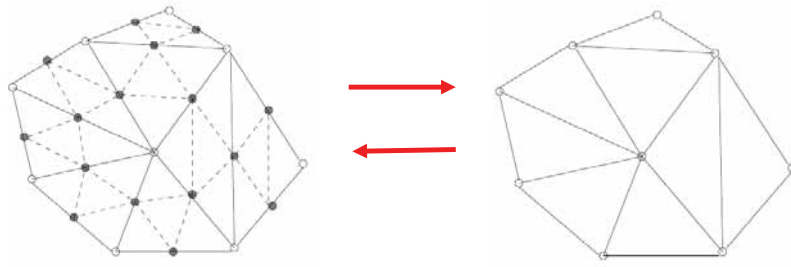
# FEM on macro and mesoscale



- Figure:  
 $-(ku')' = 1$  in  $(0, 1)$   
 $k \in \{1; 10\}$ ,  
periodic  $\varepsilon = 1/30$   
hom. Dirichlet BC

- **accurate** = P1 solution,  $h = 1/30$
- **standard FEM** = P1 solution,  $h = 1/15$
- **homogenized** = P1 solution,  $h = 1/15$ , homogen. coeff. (constant)

## Efficient multilevel solvers



- Multigrid, AMG, AMLI, DD methods
- Fine and (auxiliary) coarse grids/problems
- Intergrid transfers
- Coarse grid elements homo/heterogeneous
- Analogy with multiscale

25

## Multigrid – auxiliary macroscale

- Two Grid method Two scales
- initial  $u_h, r_h = b - Au_h$
- while  $\|r_h\| > \varepsilon$ 
  - Smoothing  $u_h \leftarrow u_h + \omega D^{-1}(b - Au_h)$
  - Coarse grid correction  $u_h \leftarrow u_h + R^T A_H^{-1} R (b - Au_h)$
  - Smoothing  $u_h \leftarrow u_h + \omega D^{-1}(b - Au_h)$
- end

**Multigrid** = system with  $A_H$  is solved iteratively by TG using still coarser level(s)

---

## Efficient multigrid

$-(ku')'=1$  in  $(0, 1)$ ,  $k \in \{1;10\}$ , periodic  $\varepsilon=1/30$   
hom. Dirichlet BC

$A_H =$  coarse grid, homogenized coeff.

$$R = \begin{pmatrix} x & & & & \\ & 1/2 & 1 & 1/2 & \\ & & & & \\ & & & 1/2 & 1 & 1/2 \\ & & & & & \ddots \\ & & & & & & \ddots \end{pmatrix} + \begin{pmatrix} 0 & & & & \\ & c & 0 & -c & \\ & & & & \\ & & & c & 0 & -c \\ & & & & & \ddots \end{pmatrix}$$

$$c = H(x_{i+1/2}) = \int_{x_i}^{x_{i+1/2}} \left( \frac{\bar{k}}{k(x)} - 1 \right) dx \quad A_H = RA_hR^T$$

---

27

---

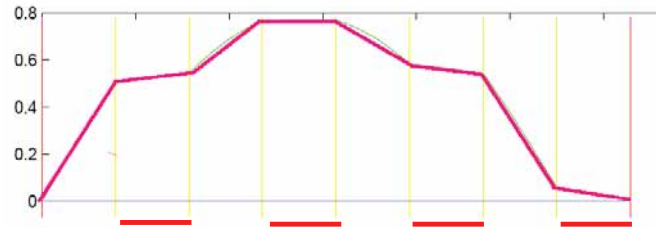
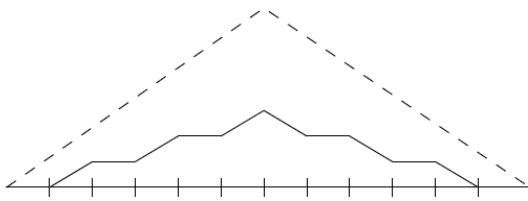
## Aggregations

$$R = \begin{pmatrix} x & & & & \\ & 1 & 1 & & \\ & & & & \\ & & & 1 & 1 \\ & & & & & \ddots \end{pmatrix}$$

---

28

# Aggregations – jumping coefficients



- we shall investigate aggregations within the two-level Schwarz framework
- show that if elements in aggregations are at least as stiff like elements in the surrounding THEN the two-level Schwarz is robust w.r.t. coefficient jumps

29

## Stiff aggregations

$$-\text{div}(\mathbf{k} \text{ grad}(u)) = f$$

$V_h = \text{span} \{ \phi_1, \dots, \phi_n \}$ , FE space and nodal basis functions

$V_0 = \text{span} \{ \psi_1, \dots, \psi_N \}$ , aggregations  $N < n$

$$\psi_i = \sum_j \varphi_{ij} \phi_j, \varphi_{ij} \in \{0, 1\}, \sum_j \varphi_{ij} \leq m_a \quad \forall_j \exists! i : \varphi_{ij} = 1$$

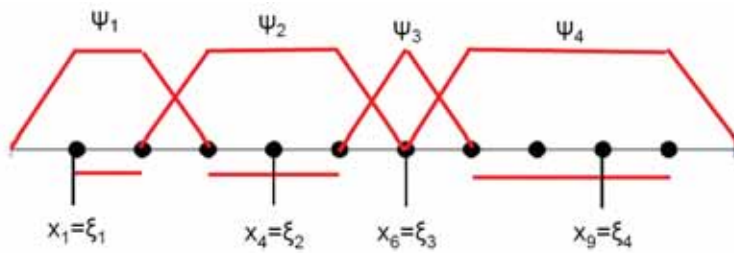
$$\mathcal{T}_h = \mathcal{T}_h^a \cup \mathcal{T}_h^b \quad \begin{aligned} T \in \mathcal{T}_h^a &\Leftrightarrow \text{ex. } i : T \subset \text{interior}(\text{supp}\{\psi_i\}) \\ T \in \mathcal{T}_h^b &\Leftrightarrow T \in \mathcal{T}_h \setminus \mathcal{T}_h^a. \end{aligned}$$

$$T \in \mathcal{T}_h^b \Rightarrow S_T = \{ S \in \mathcal{T}_h^a, \exists i : T, S \subset \overline{\text{supp}\{\psi_i\}} \}$$

$$\text{STIFF AGGREGATIONS } \forall T \in \mathcal{T}_h^b \quad \forall S \in S_T \quad k_T \leq k_S$$

30

# Stiff aggregations



$$(i) Qv = v_0, v_0 = \sum_1^N \alpha_i \psi_i, \alpha_i = v(\xi_i)$$

$$(ii) \dots, \alpha_i = |\text{supp}\{\psi_i\}|^{-1} \int_{\text{supp}\{\psi_i\}} v(x) dx$$

- Stability constant  $K_0$  does not depend on  $h$ ,  $k_{\max} / k_{\min}$
- Constant  $K_1$  depends on the domain decomposition ( $K_1=3$  for layered decomposition)
- Efficient and robust two-level method

31

# Multilevel methods – model 1D problem

$k_1$ $k_2$	$k_1/k_2 =$	1/1e0	1/1e1	1/1e2	1/1e3	1/1e4
standard TG method		7	46	451	-	-
TGH=TG+homogenized coarse problem		7	27	-	-	-
TGHC=TGH+corrected transfer		7	7	7	7	7
AG=TG+aggregation transfer		23	10	8	8	8

Numbers of iterations - solving the system from FE discretization of a 1D model problem with periodic microstructure, period size 1/15, discretization  $h=1/30$  (microstructure is fully resolved on fine grid), coarse system from discretization with  $H=1/15$  and the variants exploiting homogenization ideas.

# Schwarz – exact solvers

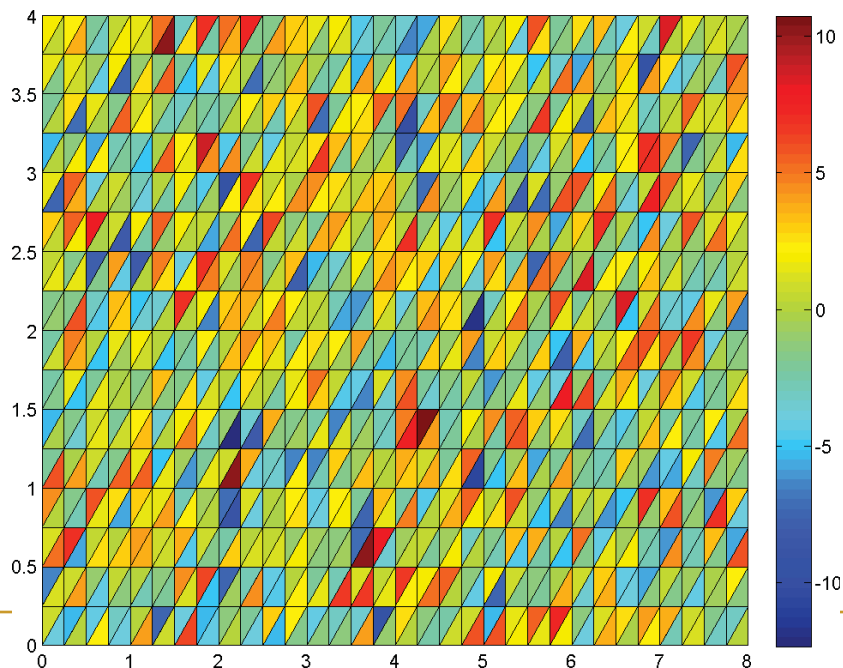
Stability estimate :  $v = \sum_k v_k, \quad v_k = \Pi_h(\Theta_k v).$

$$\begin{aligned} \sum \|v_k\|_A^2 &= \sum_{\Omega_k} \int k \|\nabla(\Pi_h(\Theta_k v))\|^2 dx \\ &\leq c \sum_T \int k \|\theta_k\|_\infty^2 \|\nabla v\|^2 dx + c \sum_T \int k \|\nabla \theta_k\|_\infty^2 \|v\|^2 dx \\ &\leq K_0 \int_\Omega k \|\nabla v\|^2 dx \end{aligned}$$

- Heterogeneity outside overlap
- Inside overlap
- Two-level methods

33

# Heterogeneity

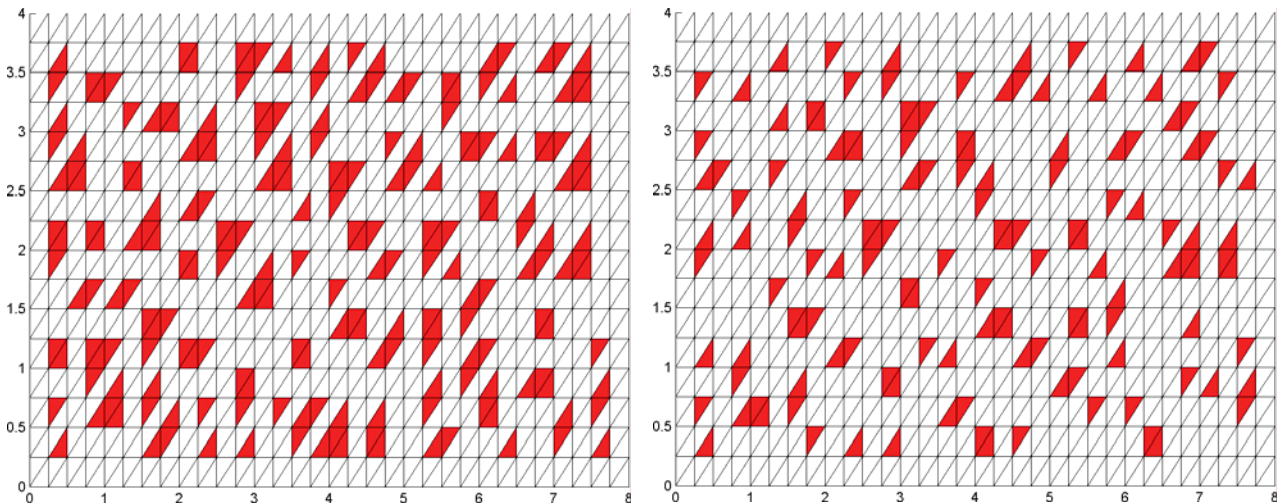


34

# Aggregations

■ thresholding to  $p=0.3$

■ thresholding to  $p=0.7$



35

# Numerical results

■ number of iterations (32385 DOFs)

$\frac{k_{max}}{k_{min}}$	CG	$p = 0.1$	$p = 0.3$	$p = 0.5$	$p = 0.7$	$p = 0.9$
$10^0$	365	14	14	14	14	14
$10^2$	695	11	11	10	9	7
$10^4$	1538	11	10	9	8	6
$10^6$	4046	11	10	9	8	6
$10^8$	10273	13	11	9	8	6
$10^{10}$	25735	14	12	10	8	6

(b)  $H/h = 8, H = 1/16$

■ size coarse spaces

$h$	$\frac{k_{max}}{k_{min}} = 1$	$\frac{k_{max}}{k_{min}} > 1$				
		$p = 0.1$	$p = 0.3$	$p = 0.5$	$p = 0.7$	$p = 0.9$
1/32	719	855	927	1059	1231	1666
1/64	2463	2988	3377	3871	4613	6301
1/128	9023	11361	12716	14795	18098	24757

36

## Homogenized parameters of geocomposite

BC	3aBC		1aBC	
loading	E(MPa)	$\nu$	E(MPa)	$\nu$
<i>direction x</i>	2367.82	0.2861	2318.21	0.3060
<i>direction y</i>	1947.20	0.3054	2018.21	0.2676
<i>direction z</i>	2369.74	0.2860	2319.60	0.3043

Reuss bound :  $E_R = 1837.71$  MPa,  $\nu_R = 0.2565$

Voight bound:  $E_V = 2387.57$  MPa,  $\nu_V = 0.3141$

Reuss and Voight bounds for E and  $\nu$  are determined from  
Reuss and Voight bounds for the effective material tensor  $C_{\text{eff}}$

Geocomposite seems to be softer in direction y

37

## Sensitivity of macro response to changes in local material properties (+10 %)

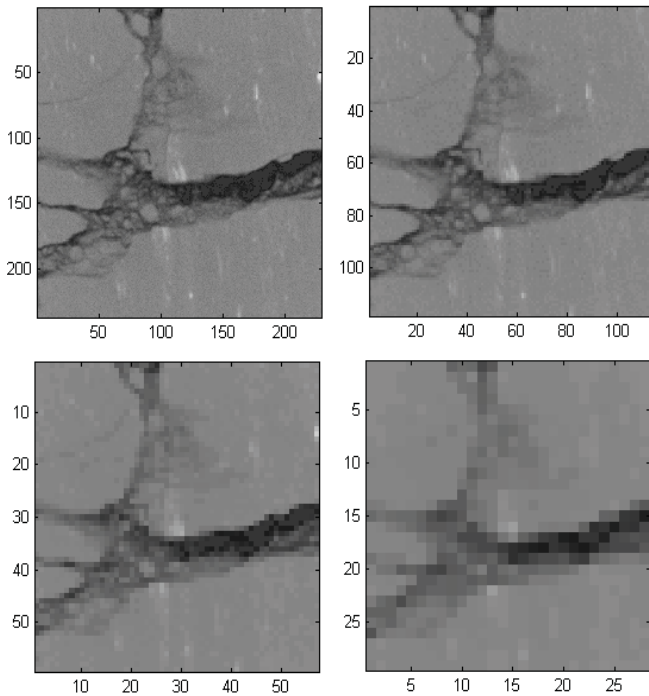
	3aBC(z)		1aBC(z)	
	$\Delta E_{\text{hom}}$ [%]	$\Delta \nu_{\text{hom}}$ [%]	$\Delta E_{\text{hom}}$ [%]	$\Delta \nu_{\text{hom}}$ [%]
$E_1^+$	+0.01	+0.07	+0.04	+0.00
$\nu_1^+$	-0.00	+0.00	-0.00	+0.00
$E_2^+$	+0.14	+0.28	+0.22	+0.00
$\nu_2^+$	-0.01	+0.07	-0.01	+0.23
$E_3^+$	+0.99	+0.17	+1.04	+0.03
$\nu_3^+$	+0.01	+0.80	-0.03	+0.82
$E_4^+$	<b>+8.81</b>	-0.59	<b>+8.60</b>	+0.10
$\nu_4^+$	+0.77	<b>+9.06</b>	+0.08	<b>+9.00</b>
<i><math>E, \nu</math> initial</i>	2369.74	0.2860	2319.60	0.3043

Sensitivity to changes in coal parameters

38



## Sensitivity to selected voxel grid



- grid 1:  $230 \times 238 \times 37 = 2\,025\,380$  nodes (6 076 140 degrees of freedom),
- grid 2:  $115 \times 119 \times 37 = 506\,345$  nodes (1 519 035 degrees of freedom),
- grid 3:  $58 \times 60 \times 37 = 128\,760$  nodes ( 386 280 degrees of freedom),
- grid 4;  $29 \times 30 \times 37 = 32\,190$  nodes ( 96 570 degrees of freedom).

39

## Sensitivity of macro response to voxel grid density

Material	$E_i$ [MPa]	$\nu_i$ [--]	grid 1	grid2	grid 3	grid 4
0 void	0.01	0.001	0.735	0.705	0.600	0.387
1 PUR 1	200	0.100	1.386	1.108	0.855	0.667
2 PUR 2	500	0.175	5.543	5.466	4.870	3.640
3 PUR 3	2100	0.250	9.670	10.226	11.545	13.379
4 coal	2600	0.320	82.667	82.495	82.131	81.927

The elasticity parameters of the individual materials and the volume fractions of materials

40

## Sensitivity of macro response to voxel grid density

type of BC	E [MPa]	Change in [%] of the homogenized $E$		
	grid 1	grid 2	grid 4	grid 4
3aBC(x)	2368	1	2	3
3aBC(y)	1947	2	5	12
3aBC(z)	2370	0	1	2
1aBC(x)	2318	1	2	4
1aBC(y)	2018 ?	1	4	10
1aBC(z)	2319 ?	0	1	3
averaged values	2223	1	2	6
Voight bound	2383	0	1	2

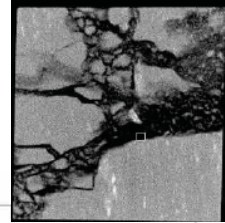
The sensitivity of the homogenized elasticity modulus to the grid density

41

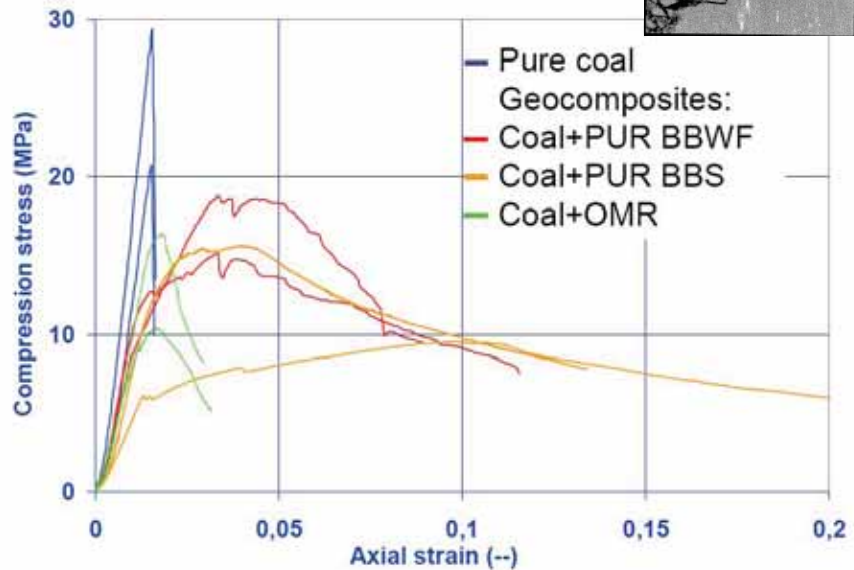
- I. The computation of elastic behaviour of geocomposites is
  - Possible
  - Stable
  - Verified with laboratory experiments
- II. Strength and nonlinear behaviour
- III. Some challenges

42

# Nonlinear geocomposite

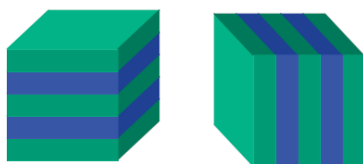
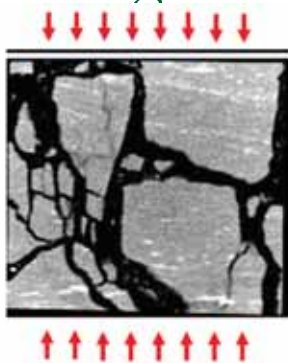


Coal – PE  
composite



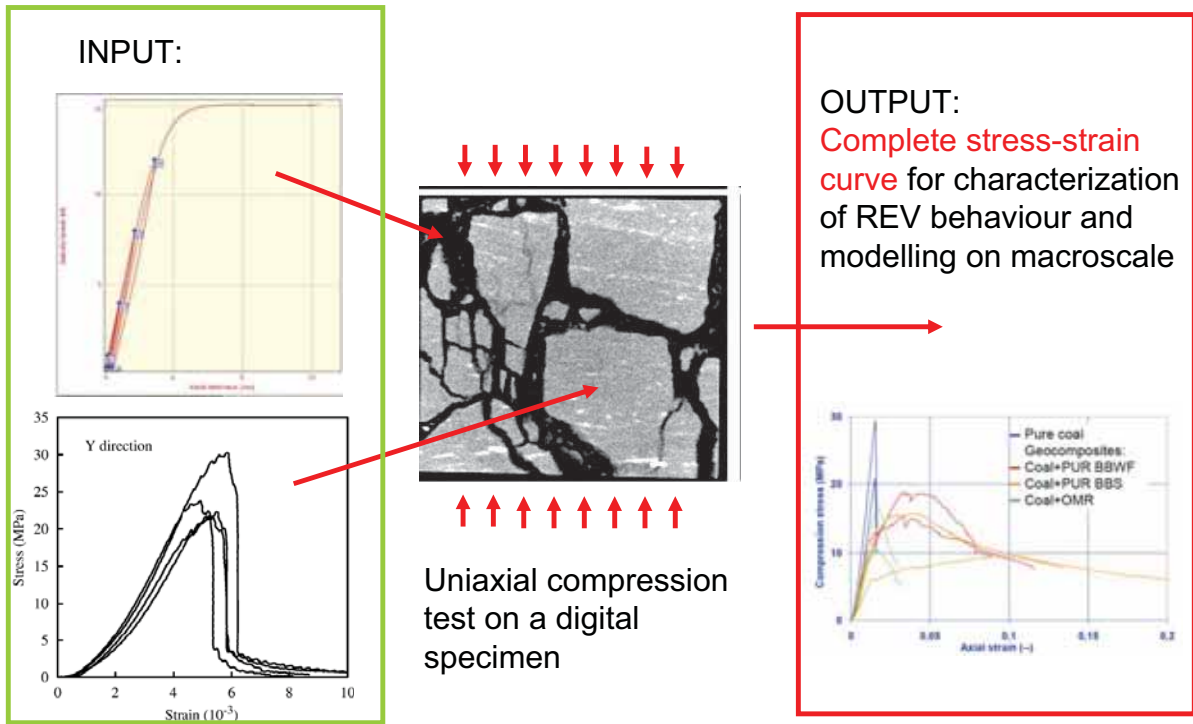
quasi-brittle/plastic behaviour

## Inelastic behaviour in uniaxial/triaxial loading



- Finding the ultimate load
  - Anisotropic strength
  - Depends heavily on local stress singularities
    - Nonlocal approach
  - Need for knowledge of local material properties
  - continuum/discrete models
  - Inverse analysis
- Finding the full strain-stress curve

# Homogenization of inelastic features

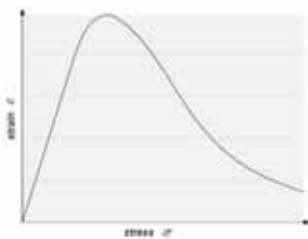
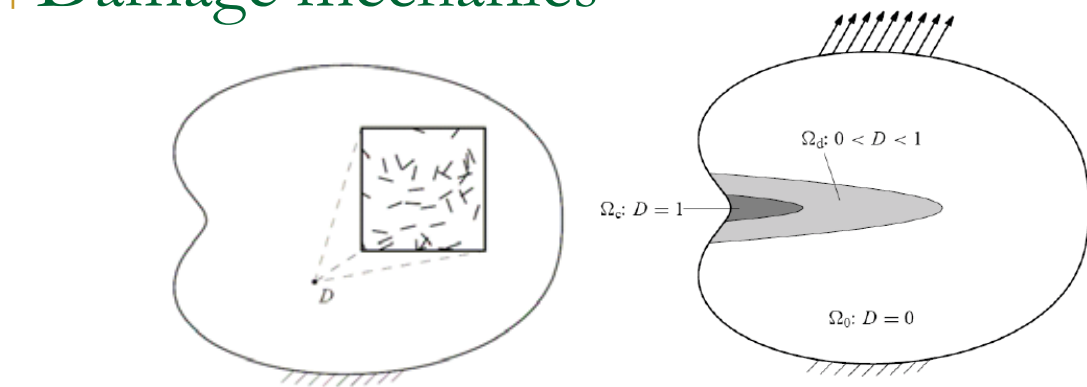


1/30/2011

Micromechanics of Geomaterials, Ostrava,  
September 2010

45

# Damage mechanics



(a)  $\varepsilon, \kappa, \sigma$

(b)  $f(\varepsilon, \kappa) = \bar{\varepsilon} - \kappa \leq 0$

(c)  $\dot{\kappa} \geq 0, \dot{\kappa} f(\varepsilon, \kappa) = 0$

(d)  $\omega = g(\kappa), g' \geq 0$

(e)  $\sigma = (1 - \omega)E\varepsilon$

$\kappa$  is internal damage parameter,  $f$  damage function, (b) admissibility condition, (c) complementarity cond., (d) damage law, (e) secant type Hooke law

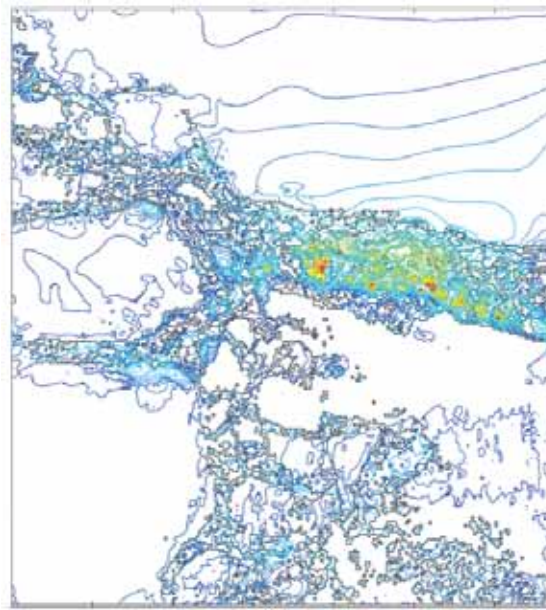
1/30/2011

Micromechanics of Geomaterials, Ostrava,  
September 2010

46

# Local failure

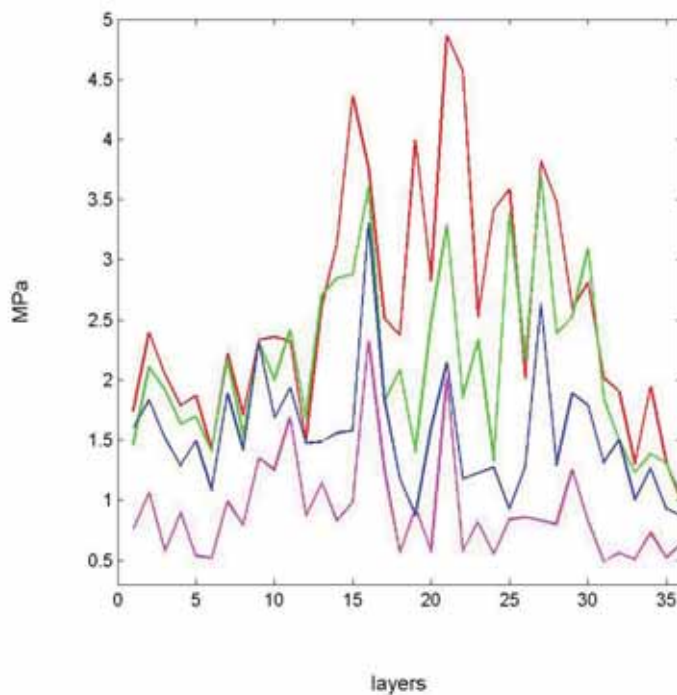
Stress analysis in in coal geocomposite sample under compressive loading



30/01/2011

47

## Max tension in layers – loading 10 MPa



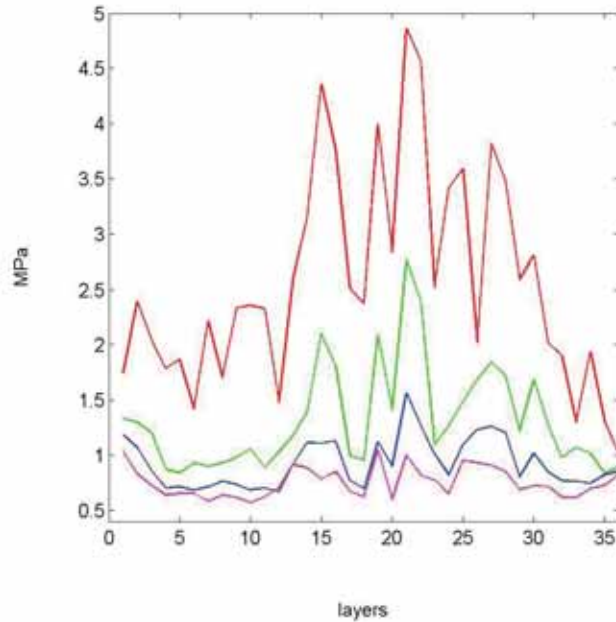
— mesh j1  
— mesh j4  
— mesh j2  
— mesh j8

**j1: 230x238x37**  
**j2: 115x119x37**  
**j4: 58x 60x37**  
**j8: 29x 30x37**  
**nodes**

48

# Nonlocal stress

pressure 10 MPa, 1aBC  
s3 - max. principal tension (>0) in layers (mesh j1, aver.1,2,3)  
coal



— mesh j1  
— mesh j1-aver.2  
— mesh j1-aver.1  
— mesh j1-aver.3

aver1 – 1 layer neighborhood  
(27 hexahedra)  
aver2 – 2 layer neighborhood  
(125 hexahedra)  
aver3 – 3 layer neighborhood  
(343 hexahedra)

49

$$\Lambda_M(\sigma(y), y) = \sqrt{[(\sigma_1(y) - \sigma_2(y))^2 + (\sigma_2(y) - \sigma_3(y))^2 + (\sigma_3(y) - \sigma_1(y))^2] / (2\sigma_c^2(y))}$$

$$\underline{\Lambda}(\sigma, y) = \Lambda(\tilde{\sigma}(y), y)$$

$$\tilde{\sigma}_{ij}(y) = \int_{\Omega} \varphi(x, y) \sigma_{ij}(x) dx$$

$$\varphi(x, y) = \begin{cases} \frac{3}{4\pi d^3} & |x - y| < d \\ 0 & |x - y| \geq d \end{cases}$$

50

---

local strength condition for  
micro-stresses

$$\sup_{y \in \Omega} \Lambda(\sigma(y), y) < 1.$$

(point) non-local strength  
condition

$$\Lambda^\odot(\sigma; y) := \Lambda(\sigma^\odot(y), y)$$

$$\Lambda^\odot(\sigma; y) < 1$$

non-local strength condition for the  
whole body

$$\sup_{y \in \Omega} \Lambda(\sigma^\odot, y) < 1$$

---

51

---

## S.E. Mikhailov

- local strength condition for micro-stresses

$$\sup_{y \in \Omega} \Lambda(\sigma(y), y) < 1.$$

- (point) non-local strength condition

$$\Lambda^\odot(\sigma; y) < 1$$

$$\Lambda^\odot(\sigma; y) := \underline{\Lambda}(\sigma, y) = \Lambda(\tilde{\sigma}(y), y), \quad \tilde{\sigma}_{ij}(y) = \int_{\Omega} \varphi_{ijkl}(x, y) \sigma_{kl}(x) dx$$

- non-local strength condition for the whole body

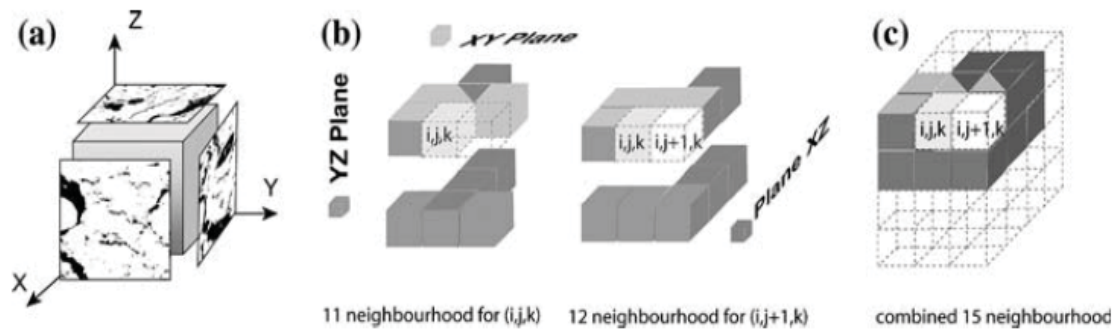
$$\sup_{y \in \Omega} \Lambda(\sigma^\odot, y) < 1$$

---

52



# Stochastic: Paper 3D Stochastic Modelling of Heterogeneous Porous Media 2006



- Determination of probabilities of neighbourhoodness of given components
- Frontal type stochastic generation
- Monte Carlo, Markov chain
- Checking global properties – mercury porosimetry
- Data for Liberec-type granite

Thank you for your attention !





# Identification of material parameters / Calibration of models

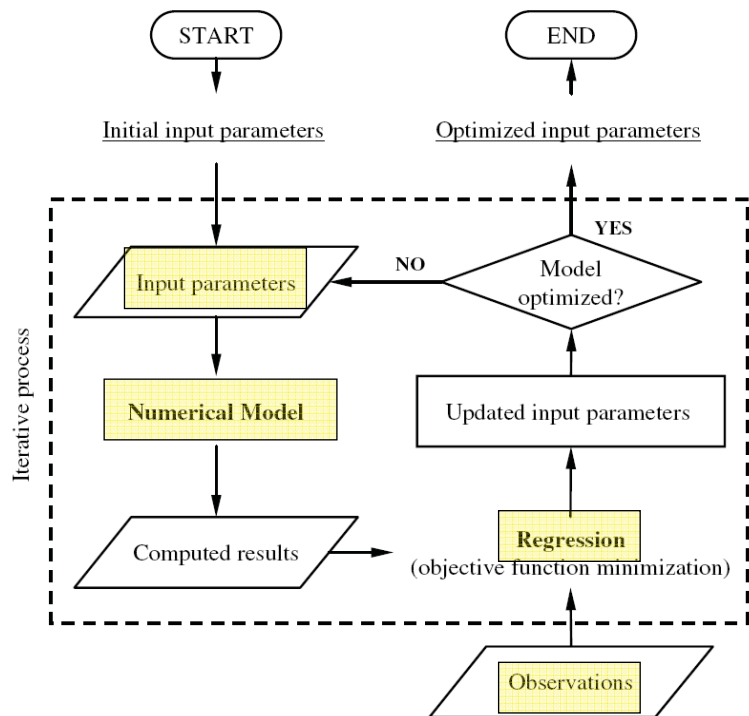
R. Blaheta, R. Hrtus, R. Kohut,  
O. Jakl, J. Starý et al.  
Computational Mechanics II, Ostrava

## Outline

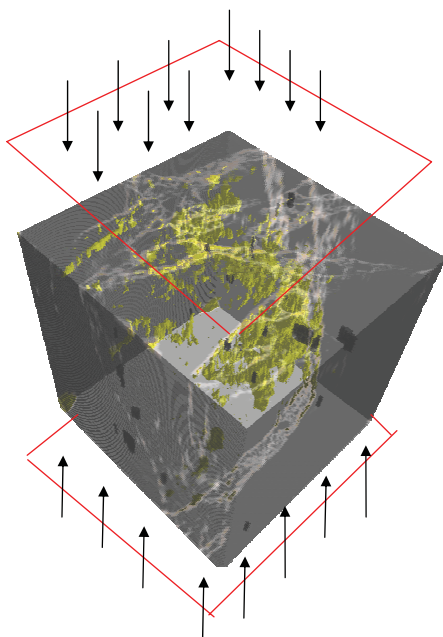
- Inverse problems
  - Identification of material parameters or calibration of the model - tasks requiring optimization of the difference between computed and measured data
  - Inverse problem with apriori given (heterogeneous) distribution of material but unknown material properties
  - Solution scheme and parallelization
- Geo-application
- Discrete model - Least-squares formulation
- NM, GA and gradient methods
- Numerical experiments with NM and GA
- Conclusions

# Parameter identification

- use for **identification** of problem parameters
- use for **calibration** of the model
- **numerical model** = FEM solution of time depend./indep. heat conduction
- **regression** = least square minimization



# Identification of parameters

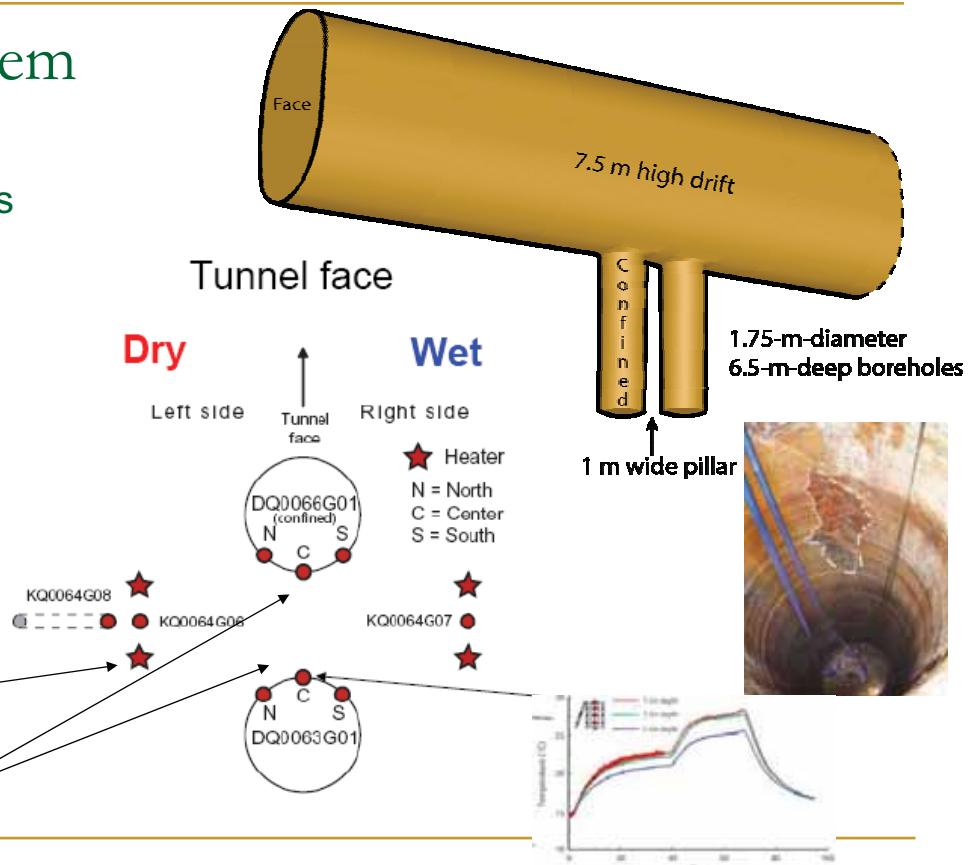


- Geocomposites
- CT scan of sample
- Materials – CT values
- Identification of local material properties
- Identification with use of several loading cases

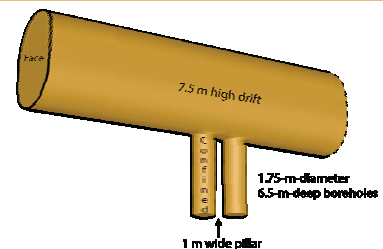
# APSE problem

- I. Initial stress
- II. Elastic stress due to construction phases
- III. Heating phase
- IV. Damage, spalling, EDZ evolution
- ...

Heaters  
Sensors in diff. depths



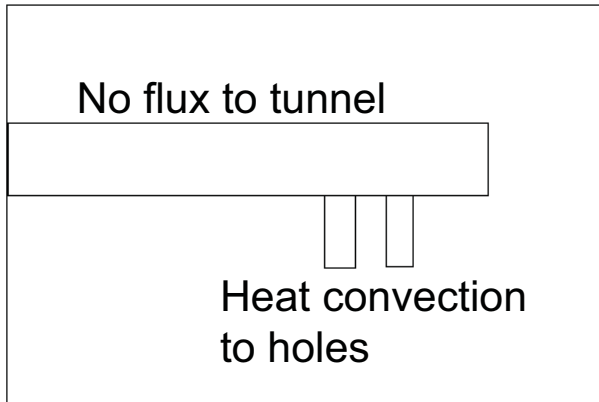
# Calibration



- Due to an underground water flow in a vicinity of the pillar it is difficult to use simple heat conduction model with heat capacity and conductivity from lab tests
- Therefore, we consider heat capacity and conductivity and heat convection parameters as unknown and try to fit the measured temperatures
- Change of heat conductivity a capacity induce change in heat flow in the model.
- Correctness of the calibrated model. The change of parameters provides model, which meets the observation data and seems to provides reasonable results (to justify physical correctness is generally difficult)

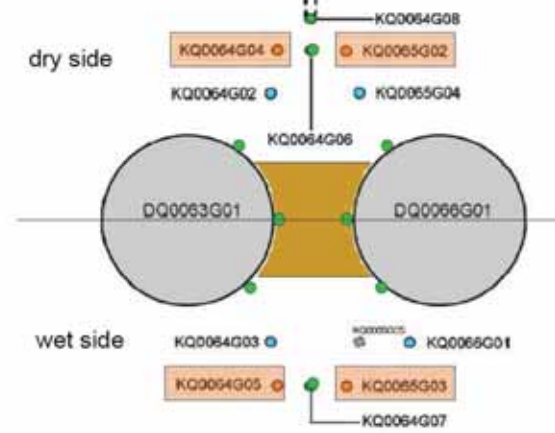
# The calibrated model

Boundary conditions:



Temperature 14.5 °C at the whole outer boundary

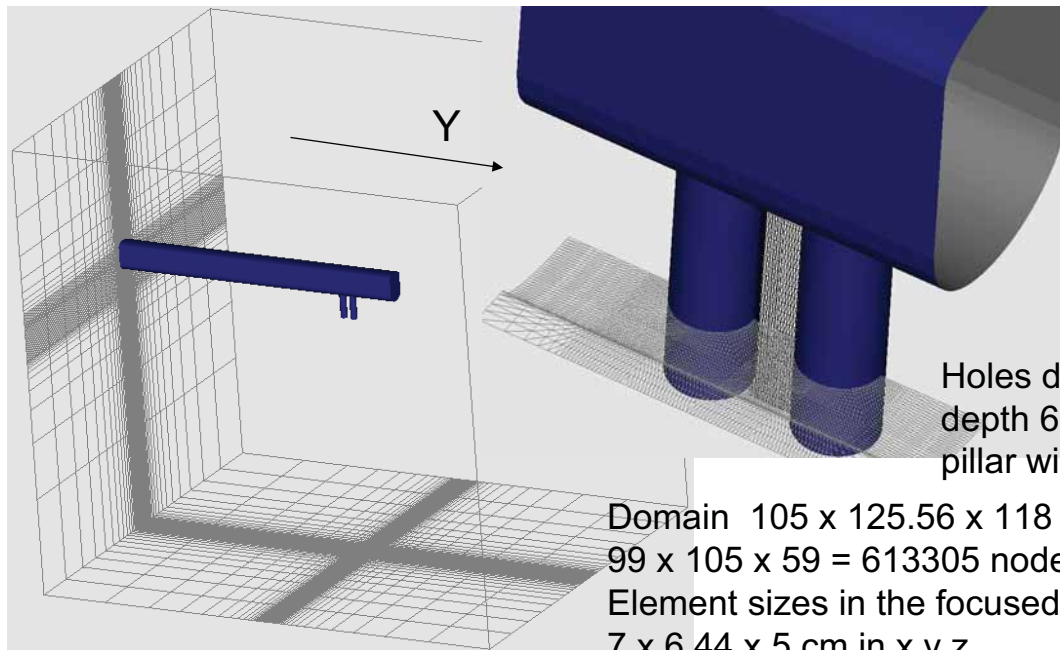
Linear heaters  
(nonstationary)



Linear heaters

Parameters:  $k_1, k_2, k_3$   
 $c_1, c_2, c_3$   
 $h_1, h_2, h_3$

# Discretization/computation with GEM sw



Holes diam. 1.75m,  
depth 6.5m  
pillar width 1.03 m

Domain 105 x 125.56 x 118 m  
99 x 105 x 59 = 613305 nodes  
Element sizes in the focused area  
7 x 6.44 x 5 cm in x,y,z.

Time stepping: 580 time steps

# Calibration via parameter identification

$$FEM : (k_1, k_2, c_1, c_2, \dots) \rightarrow u_{FEM}$$

$$F(k_1, k_2, c_1, c_2, \dots) = \sum_{ij} [u_{FEM}(x_i, t_j) - u_{ij}]^2$$

$$(k_1, k_2, c_1, c_2, \dots) = \arg \min F(k_1, k_2, c_1, c_2, \dots)$$

We use the **discrete heat conduction model**. Calibration of discretized model. Mesh dependence of optimal parameters? Objective function includes the model evaluation. Another point of view: model create a constraint for the aim function.

**Properties? Weighting, regularization in the objective function.**

## Parameters

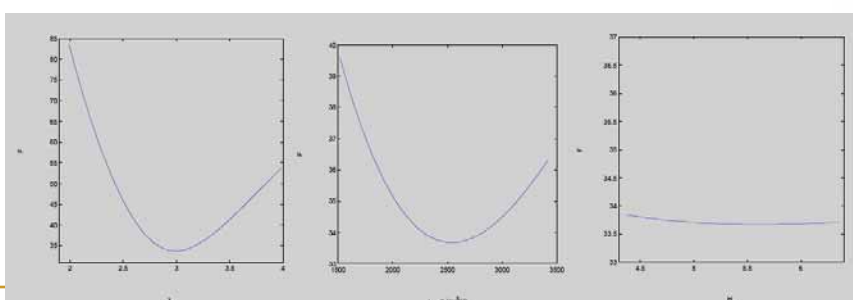
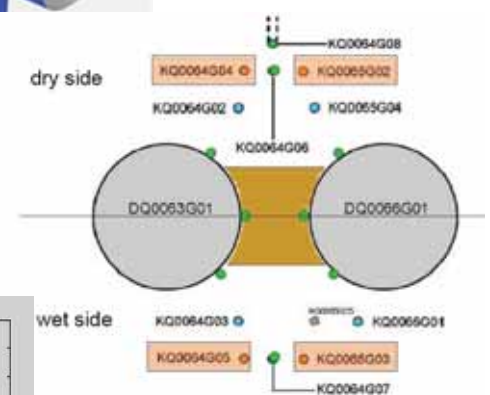
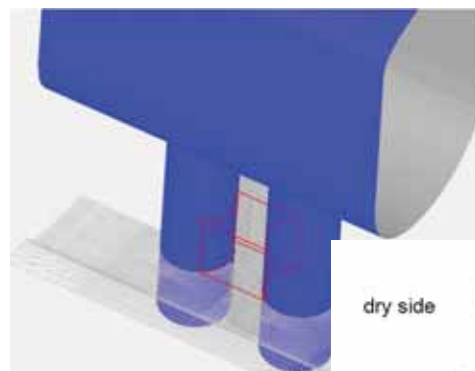
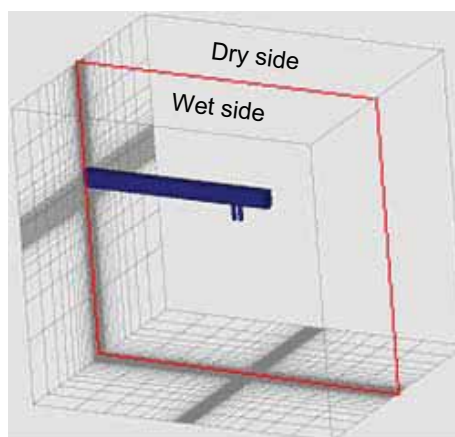
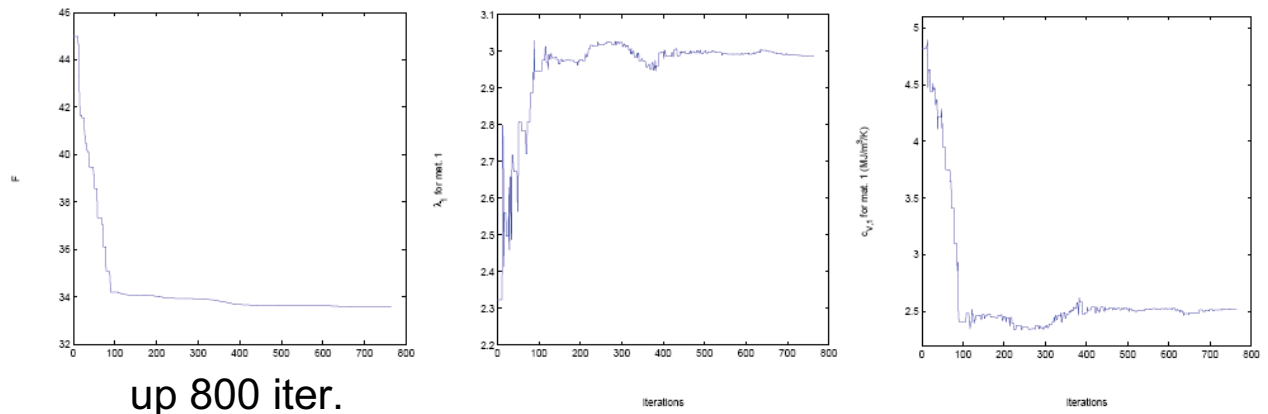


Figure 3: The dependence of the cost functional  $F$  on  $\lambda_1$  (left),  $c_1$  (center) and  $H_1$  (right).

# Convergence of MN for 9 parameters



up 800 iter.

Figure 2: The convergence of - the cost functional  $F$  (left), parameter  $\lambda_1$  (center) and  $c_1$  (right).

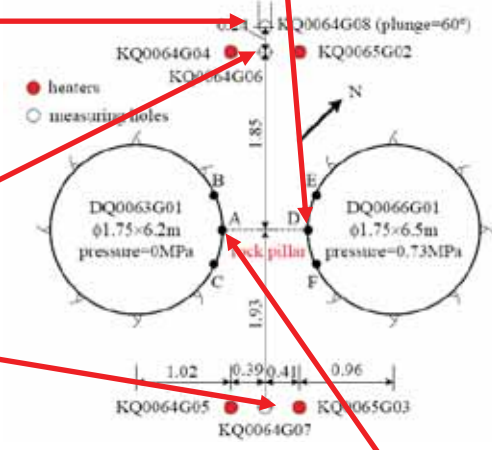
- Stop criterion  $\Delta F, \Delta p < 0.001$

## Accuracy

KQ0064G08	
2.75	5.5
0.23	0.12

DQ0066G01		
1.5	3.5	5.5
0.24	0.33	0.91

KQ0064G06		
1.5	3.5	5.5
2.96	6.67	4.52

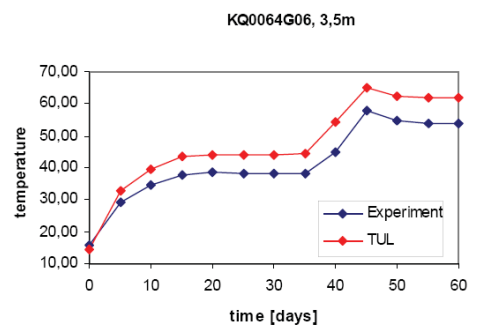
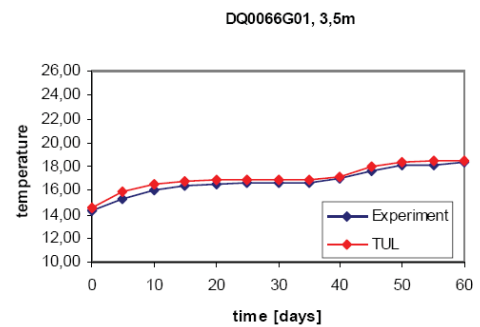


KQ0064G07		
1.5	3.5	5.5
2.59	3.02	1.78

Time averages

$$\varepsilon_T = \left( \frac{1}{12} \sum_{j=1}^{12} [u_{FEM}(x_i, t_j) - u_{ij}]^2 \right)^{1/2}$$

DQ0063G01		
1.5	3.5	5.5
0.68	0.63	0.62

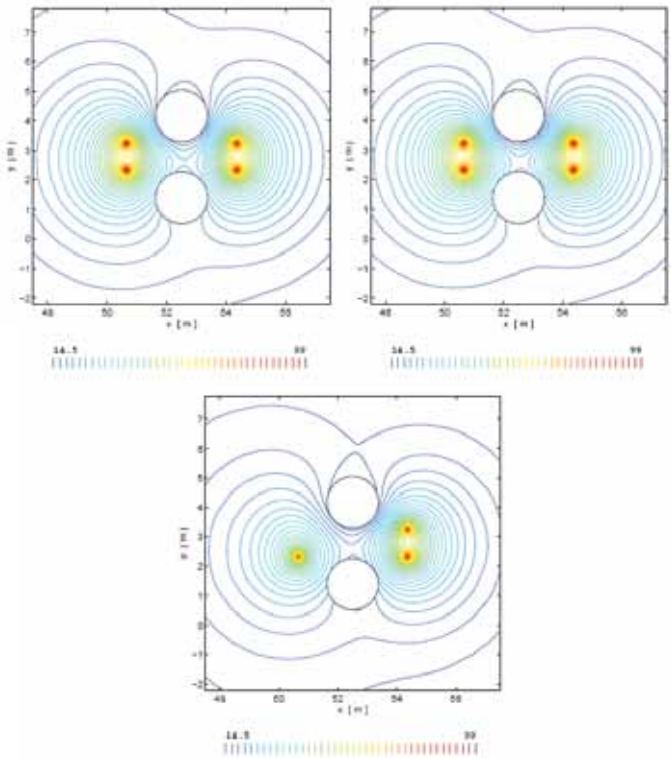
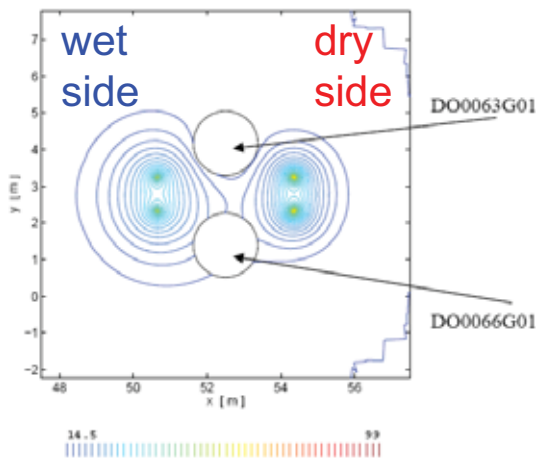




# Temperature fields

**Right:** After 60 days of heating, depths 1.5, 3.5 and 5.5m

**Below:** After 5 days, depth 3.5m



## Decrease of computational work: continuation in discretization parameter $\Delta t$

9 parameters,

$FEM(\Delta t = 0.0005,$

580 steps)

stop if  $\Delta F \leq 10^{-3}$

realistic initial guess

540 iterations of MN

790 calls of FEM

F = 33.6283

time = 56h52m04s

FEM	560	time	steps
# p	# it	time [s]	
2	1372	418	
4	1398	262	
8	1476	181	

A

$FEM(\Delta t = 0.01, 28 \text{ steps})$

stop if  $\Delta F \leq 10^{-1}$

realistic initial guess

167 iterations of MN

249 calls of FEM

F = 36.0679

time = 8h40m58s

B

$FEM(\Delta t = 0.001, 280 \text{ steps})$

stop if  $\Delta F \leq 10^{-2}$

guess from A

161 iterations of MN

220 calls of FEM

F = 33.6357

time = 14h19m08s

C

$FEM(\Delta t = 0.0005, 560 \text{ steps})$

stop if  $\Delta F \leq 10^{-3}$

guess from B

36 iterations of MN

62 calls of FEM

F = 33.6323

time = 4h27m47s

Convergence  
from both realistic  
and non realistic  
initial guess

Twice shorter time,

Twice less NM iterations

# Gradient methods - nonlinear least squares

$$F(k_1, k_2, c_1, c_2, \dots) = F(p) = R(p)^T R(p)$$

$$R: R^N \rightarrow R^M, N \text{ parameters}, M \text{ measurements}, (N < M)$$

$p > 0$ , unconstrained after an exponential transformation

- $R$  is differentiable,  $R(p) \approx M_c(p) = R(p_c) + J(p_c)(p - p_c)$   
 Gauss – Newton method, Levenberg – Marquardt  
 $p^c \rightarrow p^+ = \arg \min M_c(p)^T M_c(p)$  (linear LS)  
 $p^+ = p^c - [J(p^c)^T J(p^c) + \mu_c I]^{-1} J(p^c)^T R(p^c)$ , GN  $\Rightarrow \mu_c = 0$
- Convergence dependent on nonlinearity of  $R$  and residuum  $R(p^*)$

# Nelder-Mead (simplex) method

$$K^{(k,1)}, \dots, K^{(k,p+1)}$$

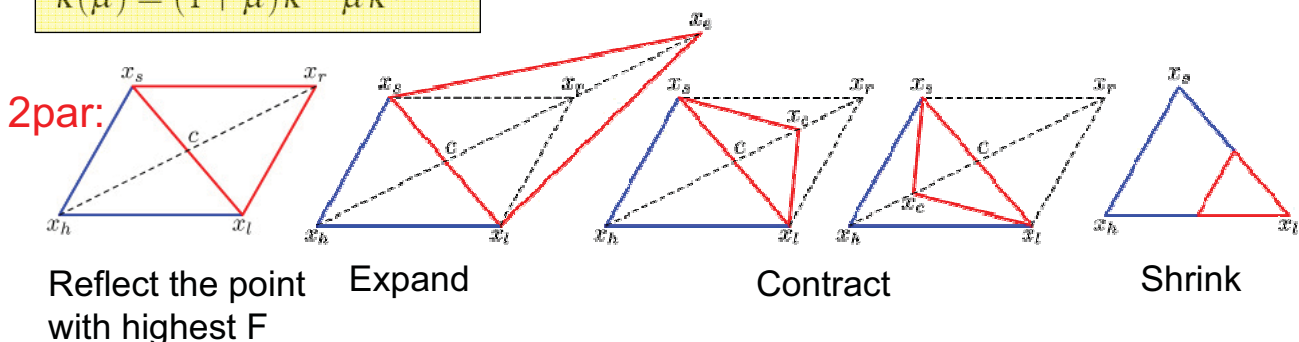
$$F(K^{(k,1)}) \leq F(K^{(k,2)}) \leq \dots \leq F(K^{(k,p+1)})$$

$$K(\mu) = (1 + \mu)\bar{K} - \mu K^{(k,p+1)}$$

Initial simplex  
 around initial  
 guess  $x_0$ ,  
 generally in  $R^N$

$\Rightarrow$

New simplex  
 Adaptation to local  
 landscape, decreasing  
 values at vertices



**Stop** – small decrease of functional & small size of simplex  
 Easier when the aim is decrease of  $F$  not exactly finding  $\min F$   
 - typically only 1-2 function evaluations at each step, while many other direct search methods use #param. or even more function evaluations.



# Genetic algorithms

## GA with $N = N_{GA}$ individuals

- (1) generate  $N$  random vectors  $\kappa^{(i)} \in \mathcal{H}$ ,  $i = 1, \dots, N$
- (2) for given generation, evaluate (in parallel)  
 $F_i = F(\kappa^{(i)})$ , if  $F_i$  is not known yet,
- (3) select  $\tau N$  parameter vectors  $\kappa^{(i)}$  with smallest values  $F_i$ ; so called parents. Then create  $(1 - \tau)N$  new vectors (childrens) by crossing randomly selected parents,
- (4) create a new generation by taking the selected parents and created childrens with mutating some of them,
- (5) evaluate stopping test and GOTO (2) if results are still not satisfactory.

$$K = \prod \langle a_i, b_i \rangle$$

For vectors  $x, y$

### Crossing

$$z_i = x_i + \alpha_i(y_i - x_i),$$

$\alpha_i$  randomly selected

### Mutation

$$z_i = x_i \pm \Delta_i 2^{-k\alpha},$$

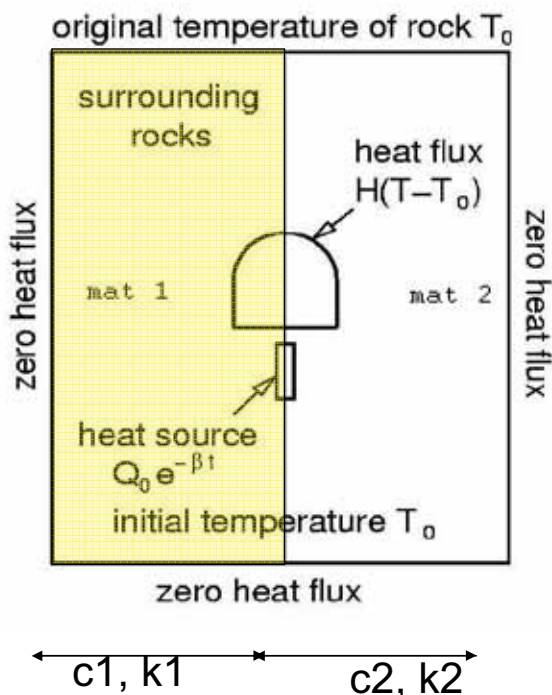
$\alpha$  randomly selected,  
mutat. range  $\Delta_i$

## NM vs. GA, problem with 8 parameters

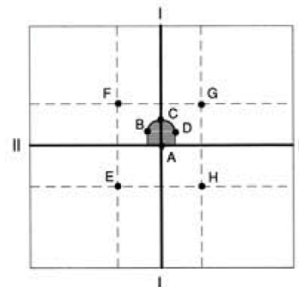
- $N$  – size of generation = 20
- $\frac{1}{2}$  of parents are selected,  $\frac{1}{2}$  new off is generated
- Coincidence  $F(GA) = 34.381 < F(NM)$
- In 24 generations – lucky guess
- Method is sensitive to parameter bounds
- Heat conductivity  $\lambda$  [W/(m·K)], volume heat capacity  $c$  [MJ/(m<sup>3</sup>·K)], heat conduction coefficient  $H$  [W/(m<sup>2</sup>·K)].

	$\lambda_1$	$c_1$	$\lambda_2$	$c_2$	$\lambda_3$	$c_3$	$H_1$	$H_2$
NelderMead	2.984	2.640	4.605	1.504	5.478	1.830	5.524	8.284
GA.	3.008	2.559	4.460	1.811	8.635	2.890	5.662	7.346

# A model problem and testing



- Identification of 4 material parameters



- Measured=computed temperatures in 8 points and 8 times ( 0.2, 0.5, 1.0, 4.0, 20.0, 30.0, 50.0,100.0) years

## Comparison of methods 20 member populations

algorithm	nمبر of solutions	$\lambda_1$	$c_1$	$\lambda_2$	$c_2$	F
NM	150	2.9996	2.4046	5.9994	4.8041	0.0025
DR	740=200 +27*20	3.0653	2.4672	5.9338	4.7471	0.0404
EIR	1220=200 +51*20	3.0158	2.4209	5.9809	4.7868	0.0119
ELR	890=200 +34*20	3.0828	2.4628	5.9308	4.7629	0.0506
exact	-	3.0000	2.4030	6.0000	4.8060	0

**Stopping rule:**

NM : the difference  $F(\text{par}_{\text{worst}}) - F(\text{par}_{\text{best}})$  in the simplex  $< 0.001$

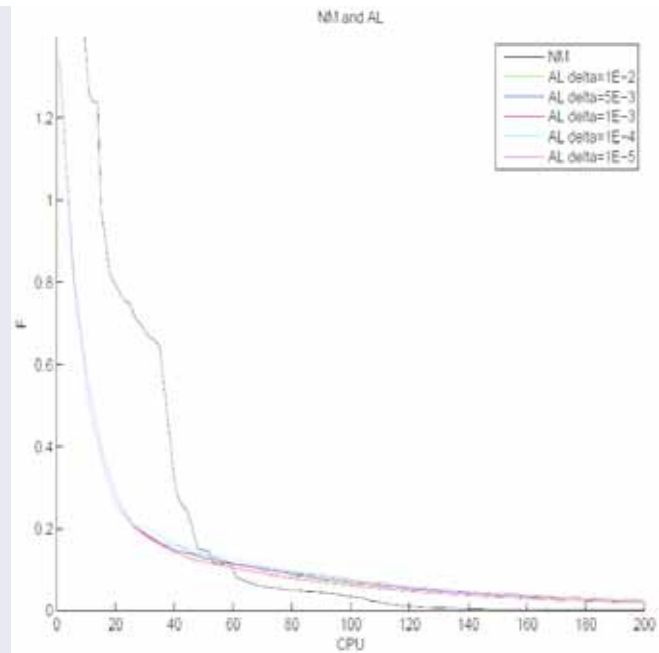
DR,EIR,ELR: the difference  $F(\text{par}_{\text{worst}}) - F(\text{par}_{\text{best}})$  in the family  $< 0.001$

# Steepest descent with apriori line search

```

Input:  $p^0, \epsilon, \Delta$ 
Output:  $p^r$ 
for ( $k = 0, 1, 2, \dots$ ) do
   $g^k \leftarrow \text{app\_grad}(F, x^k, \Delta)$ ;
   $d_i^k \leftarrow \frac{g_i^k}{\|g^k\|}$ ;
   $t^k \leftarrow \text{LINESEARCH}$ ;
   $p^{k+1} \leftarrow p^k + t^k d^k$ ;
  if  $|F(p^{k+1}) - F(p^k)| < \epsilon$  then
    BREAK;
  end
end
 $r \leftarrow k$ ;
return  $p^r$ ;

```



$$\min_{x \in \mathbb{R}^n} F(x).$$

We solve above equation iteratively- each iteration has a form

$$x^{k+1} = x^k + t_k d^k, \quad d^k = -G^k \nabla F(x^k),$$

stepsize  $t^k = \rho^{j_k}$ , such that  $j_k$  is the smallest nonnegative integer  $j$  satisfying the following inequality for constants  $\sigma \in (0, 1)$  and  $\rho \in (0, 1)$

$$F(x^k + \rho^j d^k) - F(x^k) \leq \sigma \rho^j \nabla F(x^k)^T d^k$$

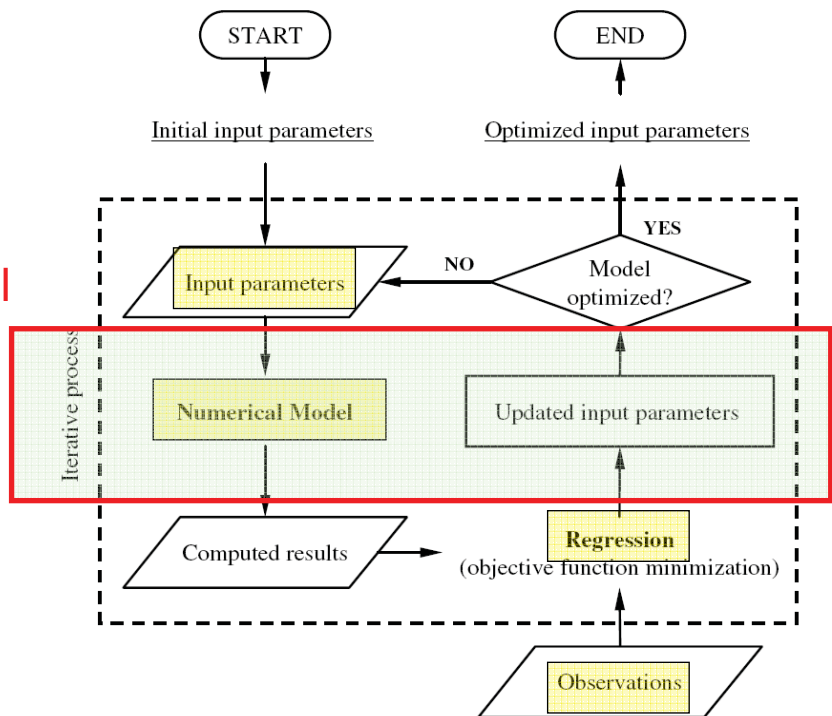
and using assumption that there exist constants  $\lambda_* > 0$  and  $\lambda^* > 0$  such that

$$\lambda_* \|d\|^2 \leq d^T G^k d \leq \lambda^* \|d\|^2,$$

then if  $(G^k = I) \inf_{x \in \mathbb{R}^n} \{F(x)\} = \lim_{k \rightarrow \infty} F(x^k)$

# Parallel processing

- Application of parallel computing
  - within numerical model = FEM solution of
  - within an optimization method for regression

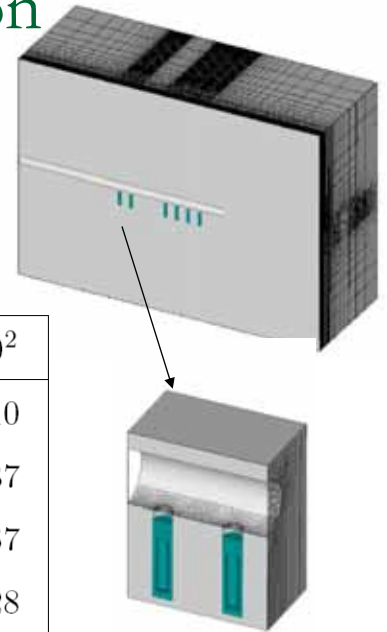


# Optimization method and parallelization

- Gradient methods
  - //: computation of gradient
  - //: starting from different initial values to avoid local minima
- Nelder-Mead (simplex) direct method
  - //: starting from different initial values to avoid local minima
- Genetic algorithms
  - //: easy, parallel evaluation of new generation
- Combinations

# Parallelization in model evaluation

- FEM + backward Euler
- one – level Schwarz method for systems  $M + \Delta t A$ , ILU on subdomains



>2.5 mil. DOF

#P \ $\Delta t$	$10^{-4}$	$10^{-3}$	$10^{-2}$	$10^{-1}$	$10^0$	$10^1$	$10^2$
1	12	12	17	27	39	61	110
4	14	14	17	25	40	68	137
8	16	18	22	25	40	84	167
16	16	18	22	25	41	99	228
24	16	18	22	26	42	97	262

Table: #iterations (Time step size x #subdomains)

# APSE problem

*FEM 560 time steps*

*# p # it time [s]*

2 1372 418

4 1398 262

8 1476 181

Efficiency

x

x

BG Blue Gene

---

## Continuous (not discretized) formulation

discrete measurements  $\Rightarrow$  function  $z = z(x, t)$

min LS functionals

$$1) J(k) = \frac{1}{2} \int_{T-\sigma}^T dt \int_{\Omega} k |u(k, x, t) - z(x, t)|^2 dx + \alpha \int_{\Omega} |\nabla k|^2 dx$$

subjected to :  $u(k, x, t)$  is solution of the given parabolic problem with heat conduction coefficient  $k$

$$2) J(k, v) = \frac{1}{2} \int_{T-\sigma}^T \left\| \frac{\partial}{\partial t} (v(t) - z(t)) - \nabla \cdot (k \nabla (v(t) - z(t))) \right\|_{L^2}^2 dx + \beta |k|_{H^2}^2$$

subjected to :  $e(k, v) = 0$ , where  $e$  is the solution of "error equation"

$$\frac{\partial}{\partial t} e + \Delta e = \frac{\partial}{\partial t} v + \nabla \cdot (k \nabla v) - f \text{ in } \Omega \times (0, T)$$

$$e(x, 0) = v(x, 0) - u_0(x) + BC$$

---

---

## Summary

- We discuss identification/calibration of model with application in geoenvironmental engineering
  - Discuss numerical realization of identification using discrete parabolic model
  - NM robust, reasonably efficient
  - GA less robust, efficient on parallel platforms, incomplete convergence
  - Combination, multiple run
  - Continuation approach recommended
  - Choice of parameters – stable and unstable minima
  - Other applications
-

---

# Conclusions

- We saw an application problem(s) for identification/calibration
  - Discuss numerical realization of identification using discrete parabolic model
    - Choice of optimization method
    - Experience with Nelder – Mead algorithm
    - Discussion of other optimization algorithms
    - Choice of parameters – stable and unstable minima
    - Computational expense, parallel computing, continuation approach
  - Use of continuous (not discretized) model
- 

---

# Conclusions

- Adaptation of the thermal model to real situation

- Calibration parameters
- Accuracy

- Inverse analysis

- Nelder – Mead algorithm
- Gauss-Newton
- Genetics algorithms

NM robust, reasonably efficient  
GA less robust, efficient on parallel platforms, incomplete convergence  
Combination, multiple run  
Continuation approach recommended  
Choice of parameters  
– stable and unstable minima

- Modifications of the price functional

- Weights  $\sum w_{ij} |u_{FEM} - u_{ij}|$
  - Relative differences  $\sum w_{ij} |u_{FEM} - u_{ij}| / |u_{ij}|$
  - Stresses  $\sum w_{ij} |u_{FEM} - u_{ij}| / |u_{ij}| - w|\sigma_{ij}|$
-

---

Thank you for your attention  
and comments



# Semismoothness and other properties of elastoplastic operator

*Stanislav Sysala*

Department of Applied Mathematics and Computer Science  
Institute of Geonics AS CR, Ostrava

email: sysala@ugn.cas.cz

## Motivation

### Nonsmooth Newton method

System of non-linear equations:

$$F : \mathbb{R}^n \rightarrow \mathbb{R}^n : F(\mathbf{u}) = \mathbf{f}$$

- $F$  is generally non-differentiable and implicit function
- $F$  is locally Lipschitz function

Nonsmooth Newton iterates:

$$\mathbf{u}_{j+1} := \mathbf{u}_j + \mathbf{V}_j^{-1}(\mathbf{f} - F(\mathbf{u}_j)), \quad \mathbf{V}_j \in \partial F(\mathbf{u}_j)$$

## Local convergence assumptions (Kummer 1988; Qi, J. Sun 1991)

- $F$  is locally Lipschitz function,
- $F$  is semismooth at  $\mathbf{u}$ ,
- all  $\mathbf{V} \in \partial F(\mathbf{u})$  are non-singular.

Other useful property:

- $F$  has a potential (generalized derivatives are symmetric)
  - $F$  is strictly monotone (generalized derivatives are positively definite)
- Semismoothness, Lipschitz continuity, monotonicity and potentiality will be investigated for the elastoplastic operator.
- Non-singularity of the generalized Jacobians depends generally on the load increment.

## Contents

1. Semismooth functions.
2. Generalized projected mapping onto a convex set.
3. Elastoplastic constitutive problem.
4. One-time-step elastoplastic problem.
5. Classical isotropic yield functions.
6. Example of elastoplastic operator.
7. Conclusion.

# 1 Semismooth functions

## Clarke's generalized derivative

$X, Y$  - finite dimensional spaces,  $F : X \rightarrow Y$  - locally Lipschitz function

$\mathcal{D}_F$  - set of points in  $X$  where  $F$  is Fréchet differentiable

$DF(x)$ ,  $x \in \mathcal{D}_F$ , - Fréchet derivative of  $F$  at  $x$

Generalized derivative (Clarke 1983):

$$\partial F(x) := \text{conv} \left\{ \lim_{x_i \rightarrow x, x_i \in \mathcal{D}_F} DF(x_i) \right\}$$

Example:  $F(x) := \max\{0, x\}$ ,  $\lim_{x \rightarrow 0^+} DF(x) = 1$ ,  $\lim_{x \rightarrow 0^-} DF(x) = 0$ ,

$$\partial F(0) = \text{conv}\{0, 1\} = [0, 1]$$

## Definition of semismooth function (Qi, J. Sun 1993)

$F : X \rightarrow Y$  - locally Lipschitz continuous function is

semismooth at  $x \in X$  if

- (i)  $F$  is directionally differentiable at  $x$ ,
- (ii) for any  $\Delta x \in X$ ,  $\Delta x \rightarrow 0$ , and  $F^o \in \partial F(x + \Delta x)$ ,

$$F(x + \Delta x) - F(x) - F^o \Delta x = o(\|\Delta x\|).$$

strongly semismooth at  $x \in X$  if

- (ii)\* for any  $\Delta x \in X$ ,  $\Delta x \rightarrow 0$ , and  $F^o \in \partial F(x + \Delta x)$ ,

$$F(x + \Delta x) - F(x) - F^o \Delta x = O(\|\Delta x\|^2).$$

## Examples and properties of semismooth functions

- $C^1(\mathcal{O})$ -functions are semismooth on  $\mathcal{O} \subset X$ .
- $C^{1,1}(\mathcal{O})$ -functions are strongly semismooth on  $\mathcal{O} \subset X$ .
- Max-function is strongly semismooth.
- Scalar product, sum, compositions of (strongly) semismooth functions are (strongly) semismooth.
- If  $F$  is Lipschitz continuous on  $X$  and (strongly) semismooth a.e. on  $X$  then  $F$  is (strongly) semismooth on  $X$ .
- Let  $F : X \rightarrow X$  be Lipschitz continuous and strictly monotone on  $X$ . Then  $F$  is (strongly) semismooth on  $X$  if and only if  $F^{-1}$  is (strongly) semismooth on  $X$  (Gowda 2004, Meng, D. Sun, Zhao 2005).

## Implicit function theorem for semismooth functions

Let  $\mathcal{I} : Y \times X \rightarrow X$  be a locally Lipschitz function in a neighborhood of  $(\bar{y}, \bar{x})$ , which solve  $\mathcal{I}(\bar{y}, \bar{x}) = 0$ . Let

$$[\partial_y \mathcal{I}(y, x), \partial_x \mathcal{I}(y, x)] := \partial \mathcal{I}(y, x).$$

If  $\partial_x \mathcal{I}(\bar{y}, \bar{x})$  is of maximal rank, i.e.

$$\mathcal{I}_x^o \Delta x = 0, \mathcal{I}_x^o \in \partial_x \mathcal{I}(\bar{y}, \bar{x}) \implies \Delta x = 0,$$

then there exist an open neighborhood  $\mathcal{O}_{\bar{y}}$  of  $\bar{y}$  and a function  $F : \mathcal{O}_{\bar{y}} \rightarrow X$  such that  $F$  is locally Lipschitz continuous in  $\mathcal{O}_{\bar{y}}$ ,  $F(\bar{y}) = \bar{x}$  and for every  $y$  in  $\mathcal{O}_{\bar{y}}$

$$\mathcal{I}(y, F(y)) = 0.$$

Moreover, if  $\mathcal{I}$  is (strongly) semismooth at  $(\bar{y}, \bar{x})$ , then  $F$  is (strongly) semismooth at  $\bar{y}$ . (Clarke 1983, D. Sun 2001)

## 2 Generalized projective mapping onto a convex set

### Assumptions

$W$  is finite dimensional space,  $G : W \rightarrow W$  fulfils:

(G1)  $G$  is Lipschitz continuous on  $W$ , i.e.  $\exists L > 0$  :

$$\|G(\Theta_1) - G(\Theta_2)\| \leq L\|\Theta_1 - \Theta_2\| \quad \forall \Theta_1, \Theta_2 \in W,$$

(G2)  $G$  is strictly monotone on  $W$ , i.e.  $\exists \alpha > 0$

$$(G(\Theta_1) - G(\Theta_2), \Theta_1 - \Theta_2) \geq \alpha\|\Theta_1 - \Theta_2\|^2 \quad \forall \Theta_1, \Theta_2 \in W,$$

(G3)  $G$  is (strongly) semismooth on  $W$

(G4)  $G$  is potential on  $W$ , i.e.  $\exists \Psi_G : W \rightarrow \mathbb{R}$ :

$$D\Psi_G(\Theta) = G(\Theta) \quad \forall \Theta \in W.$$

## 2 GENERALIZED PROJECTIVE MAPPING ONTO A CONVEX SET

### Definition and basic properties of the projection

$K$  - closed, convex and non-empty set in  $W$

$\Pi_K : W \rightarrow K$ ,  $\Sigma := \Pi_K(P)$ :

$$(P - G(\Sigma), \Theta - \Sigma) \leq 0 \quad \forall \Theta \in K$$

Let (G1), (G2) hold. Then

- $\Pi_K$  is a single-valued mapping onto  $K$ ,
- $\Pi_K(G(\Pi_K(P))) = \Pi_K(P)$ ,
- $\Pi_K(P) = G^{-1}(P)$  if and only if  $G^{-1}(P) \in K$ ,
- $(\Pi_K(P_1) - \Pi_K(P_2), P_1 - P_2) \geq \alpha\|\Pi_K(P_1) - \Pi_K(P_2)\|^2 \quad \forall P_1, P_2 \in W$ ,
- $\|\Pi_K(P_1) - \Pi_K(P_2)\| \leq \frac{1}{\alpha}\|P_1 - P_2\| \quad \forall P_1, P_2 \in W$ .

**Potential function  $\Pi_K$** 

Let (G1), (G2), (G4) hold and  $\Psi_G$  is a potential to  $G$ . Let

$$\Psi_{\Pi}(P) := (P, \Pi_K(P)) - \Psi_G(\Pi_K(P)), \quad P \in W.$$

Then

$$D\Psi_{\Pi}(P) = \Pi_K(P) \quad \forall P \in W.$$

Proof idea: using of a proximal mapping (Moreaux 1965):

$f$  - convex, proper, lower semicontinuous function on  $W$ :

$$\text{prox}_f(P) = \arg \min_{\Theta \in W} \left\{ \frac{1}{2} \|P - \Theta\|^2 + f(\Theta) \right\}$$

The mapping  $P \mapsto \Pi_K(\alpha P)$  is a proximal mapping with

$$f(\Theta) := \frac{1}{\alpha} \Psi_G(\Theta) - \frac{1}{2} \|\Theta\|^2 + I_K(\Theta)$$

**Specification of the set  $K$** 

$K := \{\Theta \in W : \Phi(\Theta) \leq 0\}$ ,  $\Phi : W \rightarrow \mathbb{R}$  fulfils

( $\Phi$ 1)  $\Phi$  is convex on  $W$ ,

( $\Phi$ 2)  $\Phi(0) < 0$ ,

( $\Phi$ 3)  $\Phi$  is a.e. differentiable on  $W$ .

( $\Phi$ 4)  $\Phi$  is a.e. differentiable on  $\partial K$ .

( $\Phi$ 5) If  $\Theta \in \mathcal{D}_{\Phi}$ , then  $\exists \mathcal{O}_{\Theta}$  such that  $\Phi \in C^1(\mathcal{O}_{\Theta})$  and  $D\Phi$  is (strongly) semismooth on  $\mathcal{O}_{\Theta}$ .

( $\Phi$ 6) If  $\Theta \in \partial K$  and  $\Theta \in \mathcal{D}_{\Phi}$ , then  $D\Phi(\Theta) \neq 0$ .

## Semismoothness of $\Pi_K$

**Theorem 1** *Let  $G$  fulfil (G1)-(G3) and  $\Phi$  fulfil ( $\Phi$ 1)-( $\Phi$ 6). Then  $\Pi_K$  is (strong) semismooth on  $W$ .*

Idea of the proof:

1.  $W$  - space partition:

$$\begin{aligned} M_1 &:= \{P \in W : \Sigma = \Pi_K(P) = G^{-1}(P) \in \text{int}(K)\}, \\ M_2 &:= \{P \in W : \Sigma = \Pi_K(P) \in \partial K, P \in \text{int}(N_{K,\Pi}(\Sigma))\}, \\ N_{K,\Pi}(\Sigma) &:= \{P \in W : \Pi_K(P) = \Sigma\}, \\ M_3 &:= \{P \in W : \Sigma = \Pi_K(P) \in \partial K, \Sigma \in \mathcal{D}_\Phi\}. \end{aligned}$$

It is only sufficient to prove the semismoothness on  $M_1$ ,  $M_2$  a  $M_3$  since the measure of  $W \setminus (M_1 \cup M_2 \cup M_3)$  in  $W$  vanishes.

## Idea of the proof - continuation

2. Semismoothness on  $M_1 = \{P \in W : \Sigma = \Pi_K(P) = G^{-1}(P) \in \text{int}(K)\}$ :  
 $\Sigma = \Pi_K(P) = G^{-1}(P)$ ,  $G^{-1}$  is (strongly) semismooth,  $M_1$  is open.
3. Semismoothness on  $M_2 = \{P : \Sigma = \Pi_K(P) \in \partial K, P \in \text{int}(N_{K,\Pi}(\Sigma))\}$ :  
 $\Pi_K$  is constant in a neighborhood of  $P \in M_2$ .
4. Semismoothness on  $M_3 = \{P \in W : \Sigma = \Pi_K(P) \in \partial K, \Sigma \in \mathcal{D}_\Phi\}$ :  
 Let  $\bar{P} \in M_3$  and  $\bar{\Sigma} := \Pi_K(\bar{P})$ . KKT conditions:

$$G(\bar{\Sigma}) - \bar{P} + \bar{\gamma} D\Phi(\bar{\Sigma}) = 0,$$

$$\Phi(\bar{\Sigma}) \leq 0, \bar{\gamma} \geq 0, \bar{\gamma} \Phi(\bar{\Sigma}) = 0, i = 1, \dots, m.$$

The second conditions can be equivalently rewritten:

$$\Phi(\bar{\Sigma}) + \max\{0, -\Phi(\bar{\Sigma}) - \bar{\gamma}\} = 0.$$

### Idea of the proof - continuation

Let  $\mathcal{I} : W \times W \times \mathbb{R} \rightarrow W \times \mathbb{R}$ ,

$$\mathcal{I}(P; \Sigma, \gamma) = \begin{pmatrix} G(\Sigma) - P + \gamma D\Phi(\Sigma) \\ \Phi(\Sigma) + \max\{0, -\Phi(\Sigma) - \gamma\} \end{pmatrix}.$$

Then

$$\mathcal{I}(\bar{P}; \bar{\Sigma}, \bar{\gamma}) = 0.$$

$\mathcal{I}$  is (strongly) semismooth in a neighborhood of  $(\bar{P}; \bar{\Sigma}, \bar{\gamma})$  and thus it is sufficient to prove

$$\mathcal{I}^\circ \begin{pmatrix} \delta\Sigma \\ \delta\gamma \end{pmatrix} = 0, \quad \mathcal{I}^\circ \in \partial_{(\Sigma, \gamma)} \mathcal{I}(\bar{P}; \bar{\Sigma}, \bar{\gamma}) \implies \begin{pmatrix} \delta\Sigma \\ \delta\gamma \end{pmatrix} = 0.$$

A similar implication is proved in (Meng, D. Sun, Zhao 2005).

### Derivative of $\Pi_K$ in a vector representation

Let  $G$  be differentiable,  $\Phi$  be twice differentiable,  $W = \mathbb{R}^n$  and

$$M_1 := \{\mathbf{P} \in \mathbb{R}^n : \Sigma = \Pi_K(\mathbf{P}) \in \text{int}(K)\},$$

$$M_2 := \{\mathbf{P} \in \mathbb{R}^n : \Sigma = \Pi_K(\mathbf{P}) \in \partial K, \mathbf{P} \in \text{int}(N_{K, \Pi}(\Sigma))\},$$

$$M_4 := \{\mathbf{P} \in \mathbb{R}^n : \Sigma = \Pi_K(\mathbf{P}) \in \partial K, \Sigma \neq G^{-1}(\mathbf{P}), \Sigma \in D_\Phi\}.$$

Then

$$D\Pi_K(\mathbf{P}) = \mathbf{C}(\Sigma, \gamma) = \begin{cases} (DG(\Sigma))^{-1}, & \mathbf{P} \in M_1, \\ \mathbf{0}, & \mathbf{P} \in M_2, \\ \mathbf{A}^{-1} + \mathbf{A}^{-1} \mathbf{B} (\mathbf{B}^T \mathbf{A}^{-1} \mathbf{B})^{-1} \mathbf{B}^T \mathbf{A}^{-1}, & \mathbf{P} \in M_4, \end{cases}$$

with

$$\mathbf{A} = DG(\Sigma) + \gamma D^2\Phi(\Sigma), \quad \mathbf{B} = D\Phi(\Sigma), \quad \Sigma = \Pi_K(\mathbf{P}).$$



### 3 Elasto-plastic constitutive problem

#### Notation and assumptions

1. Additive decomposition of the strain tensor:  $\boldsymbol{\varepsilon} = \boldsymbol{\varepsilon}^e + \boldsymbol{\varepsilon}^p$ .
2. Linear elastic law:  $\boldsymbol{\sigma} = \mathbf{D}^e \boldsymbol{\varepsilon}^e$ ,  $D_{ijkl}^e = D_{ijlk}^e = D_{klij}^e$ .
3. Simple combination of kinematic and non-linear isotropic hardening:

$$\boldsymbol{\beta} = a \mathbf{X}, \quad \kappa = H(\bar{\boldsymbol{\varepsilon}}^p), \quad a > 0, \quad H : \mathbb{R}^+ \rightarrow \mathbb{R}^+$$

$\mathbf{X}, \bar{\boldsymbol{\varepsilon}}^p$  - kinematic (tensor) and isotropic (scalar) hardening variables,  
 $\boldsymbol{\beta}, \kappa$  - corresponding hardening thermodynamical forces,  
 $H$  fulfils (G1)-(G4) and  $H(0) = 0$  and can be extended on  $\mathbb{R}$ .

4. Generalized stress and strain:  $\Sigma := (\boldsymbol{\sigma}, \boldsymbol{\beta}, \kappa)$  and  $G(\Sigma) = (\boldsymbol{\varepsilon}^e, \mathbf{X}, \bar{\boldsymbol{\varepsilon}}^p)$ ,  
 $G : W \rightarrow W$ ,  $W := S \times S \times \mathbb{R}$ ,  $G(\Theta) := ((\mathbf{D}^e)^{-1} \Theta_{\boldsymbol{\sigma}}, a^{-1} \Theta_{\boldsymbol{\beta}}, H^{-1}(\Theta_{\kappa}))$

#### Notation and assumptions - continuation

5. Yield function:  $\Phi : W \rightarrow \mathbb{R}$ ,  $\Phi(\boldsymbol{\sigma}, \boldsymbol{\beta}, \kappa) := \varphi(\boldsymbol{\sigma} - \boldsymbol{\beta}) - (\sigma_{y_0} + \kappa)$ ,  
 $\sigma_{y_0} > 0$  ... initial yield stress or shear yield stress or cohesion or...  
 $\varphi : S \rightarrow \mathbb{R}$ ,  $S = \mathbb{R}_{sym}^{3 \times 3}$ ,  $\Phi$  fulfils  $(\Phi_1)$ - $(\Phi_6)$ .

6. Principle of maximum plastic dissipation:

$$\text{find } \Sigma := (\boldsymbol{\sigma}, \boldsymbol{\beta}, \kappa) \in K : \quad \Upsilon^p(\dot{P}; \Sigma) \geq \Upsilon^p(\dot{P}; \Theta) \quad \forall \Theta \in K$$

$K := \{\Theta \in W : \Phi(\Theta) \leq 0\}$  ... set of admissible generalized stresses

$\Upsilon^p(\dot{P}; \Theta) := \langle \dot{\boldsymbol{\varepsilon}}^p, \Theta_{\boldsymbol{\sigma}} \rangle + \langle -\dot{\mathbf{X}}, \Theta_{\boldsymbol{\beta}} \rangle + (-\dot{\bar{\boldsymbol{\varepsilon}}}^p) \Theta_{\kappa}$  ... dissipation functional,

$\dot{P} := (\dot{\boldsymbol{\varepsilon}}^p, -\dot{\mathbf{X}}, -\dot{\bar{\boldsymbol{\varepsilon}}}^p) = (\dot{\boldsymbol{\varepsilon}} - \dot{\boldsymbol{\varepsilon}}^e, -\dot{\mathbf{X}}, -\dot{\bar{\boldsymbol{\varepsilon}}}^p)$  ... plastic strain rate

Equivalent formulation:

$$\text{find } \Sigma \in K : \quad (\dot{P}, \Theta - \Sigma) \leq 0 \quad \forall \Theta \in K \quad \text{or} \quad \dot{P} \in N_K(\Sigma).$$

### Elasto-plastic constitutive initial value problem

Given:

- the history of the strain tensor  $\boldsymbol{\varepsilon} = \boldsymbol{\varepsilon}(t)$ ,  $t \in [0, t_{\max}]$ ,
- the initial values

$$\boldsymbol{\varepsilon}(0) = 0, \quad \boldsymbol{\varepsilon}^e(0) = 0, \quad \bar{\boldsymbol{\varepsilon}}^p(0) = 0, \quad \mathbf{X}(0) = 0.$$

Find:

- the generalized stress  $\Sigma(t) = (\boldsymbol{\sigma}(t), \boldsymbol{\beta}(t), \kappa(t)) \in K$ :

$$(\dot{P}, \Theta - \Sigma) \leq 0 \quad \forall \Theta \in K, \quad \dot{P} = (\dot{\boldsymbol{\varepsilon}} - \dot{\boldsymbol{\varepsilon}}^e, -\dot{\mathbf{X}}, -\dot{\bar{\boldsymbol{\varepsilon}}}^p),$$

- the generalized strain

$$(\boldsymbol{\varepsilon}^e(t), \mathbf{X}(t), \bar{\boldsymbol{\varepsilon}}^p(t)) = G(\Sigma(t)).$$

### Time discretization of constitutive elasto-plastic problem

Time discretization:  $0 = t_0 < t_1 < \dots < t_k < \dots < t_N = t_{\max}$ .

Implicit Euler method:

$$\dot{P}_k \equiv \dot{P}(t_k) \approx \frac{P(t_k) - P(t_{k-1})}{\Delta t_k} = \frac{P_k^t - G(\Sigma_k)}{\Delta t_k},$$

with

$$\Sigma_k \equiv \Sigma(t_k) = (\boldsymbol{\sigma}_k, \boldsymbol{\beta}_k, \kappa_k).$$

and a trial generalized strain

$$P_k^t = (\boldsymbol{\varepsilon}_{k-1}^e + \Delta \boldsymbol{\varepsilon}_k, \mathbf{X}_{k-1}, \bar{\boldsymbol{\varepsilon}}_{k-1}^p), \quad \Delta \boldsymbol{\varepsilon}_k = \boldsymbol{\varepsilon}_k - \boldsymbol{\varepsilon}_{k-1},$$

## One-time-step elasto-plastic constitutive problem

Given:

- $P_{k-1} = (\boldsymbol{\varepsilon}_{k-1}^e, \mathbf{X}_{k-1}, \bar{\varepsilon}_{k-1}^p)$  such that  $\Sigma_{k-1} = G^{-1}(P_{k-1}) \in K$
- $\Delta \boldsymbol{\varepsilon}_k = \boldsymbol{\varepsilon}_k - \boldsymbol{\varepsilon}_{k-1}$

Find:  $\Sigma_k = (\boldsymbol{\sigma}_k, \boldsymbol{\beta}_k, \kappa_k) \in K$ :

$$(P_k^t - G(\Sigma_k), \Theta - \Sigma_k) \leq 0 \quad \forall \Theta \in K, \quad P_k^t = (\boldsymbol{\varepsilon}_{k-1}^e + \Delta \boldsymbol{\varepsilon}_k, \mathbf{X}_{k-1}, \bar{\varepsilon}_{k-1}^p),$$

or

$$\Sigma_k = \Pi_K(P_k^t),$$

Compute:

$$P_k = (\boldsymbol{\varepsilon}_k^e, \mathbf{X}_k, \bar{\varepsilon}_k^p) = G(\Sigma_k).$$

## Correctness of the extended function $H$

$H : \mathbb{R}^+ \rightarrow \mathbb{R}^+$  fulfils (G1)-(G4) and  $H(0) = 0, \kappa = H(\bar{\varepsilon}^p)$

- possible extension to the whole  $\mathbb{R}$  such that (G1)-(G4) hold
- it is necessary to verify that  $\kappa_k \geq 0$ , where  $\Sigma_k = \Pi_K(P_k^t)$
- it holds

$$0 = \kappa_0 \leq \kappa_1 \leq \dots \leq \kappa_k \leq \dots \leq \kappa_N$$

- this is in accordance with mechanical assumptions

## 4 One-time-step elastoplastic problem

$\Omega \subset \mathbb{R}^3$  - investigated domain with partially fixed boundary

$V \subset [H^1(\Omega)]^3$  - space of kinematically admissible displacement

$f \in V^*$  - the load (a combination of surface and volume loads)

Find:  $\mathbf{u}_k \in V$ ,  $\boldsymbol{\sigma}_k, \boldsymbol{\beta}_k, \kappa_k, \boldsymbol{\varepsilon}_k^e, \mathbf{X}_k, \bar{\boldsymbol{\varepsilon}}_k^p$ :

$$\int_{\Omega} \langle \boldsymbol{\sigma}_k, \boldsymbol{\varepsilon}(\mathbf{v}) \rangle d\mathbf{x} = f_k(\mathbf{v}) \quad \forall \mathbf{v} \in V,$$

$$(\boldsymbol{\sigma}_k, \boldsymbol{\beta}_k, \kappa_k) = \Pi_K(\boldsymbol{\varepsilon}_{k-1}^e + \boldsymbol{\varepsilon}(\Delta \mathbf{u}_k), \mathbf{X}_{k-1}, \bar{\boldsymbol{\varepsilon}}_{k-1}^p) \quad \text{a.e. in } \Omega,$$

$$(\boldsymbol{\varepsilon}_k^e, \mathbf{X}_k, \bar{\boldsymbol{\varepsilon}}_k^p) = G(\boldsymbol{\sigma}_k, \boldsymbol{\beta}_k, \kappa_k) \quad \text{a.e. in } \Omega,$$

where  $\Delta \mathbf{u}_k = \mathbf{u}_k - \mathbf{u}_{k-1}$ .

## Reformulation of the one-time-step problem

Let

$$(\Pi_{K,\sigma}(P), \Pi_{K,\beta}(P), \Pi_{K,\kappa}(P)) := \Pi_K(P), \quad P \in W,$$

$$T_k : S \rightarrow S, \quad T_k(\boldsymbol{\eta}) := \Pi_{K,\sigma}(\boldsymbol{\varepsilon}_{k-1}^e + \boldsymbol{\eta}, \mathbf{X}_{k-1}, \bar{\boldsymbol{\varepsilon}}_{k-1}^p) - \boldsymbol{\sigma}_{k-1}$$

Then

$$\Delta \boldsymbol{\sigma}_k := \boldsymbol{\sigma}_k - \boldsymbol{\sigma}_{k-1} = T_k(\Delta \boldsymbol{\varepsilon}_k).$$

Find:  $\mathbf{u}_k \in V$ ,  $\boldsymbol{\sigma}_k, \boldsymbol{\beta}_k, \kappa_k, \boldsymbol{\varepsilon}_k^e, \mathbf{X}_k, \bar{\boldsymbol{\varepsilon}}_k^p$ :

$$\int_{\Omega} \langle T_k(\boldsymbol{\varepsilon}(\Delta \mathbf{u}_k)), \boldsymbol{\varepsilon}(\mathbf{v}) \rangle d\mathbf{x} = \Delta f_k(\mathbf{v}) \quad \forall \mathbf{v} \in V,$$

$$(\boldsymbol{\sigma}_k, \boldsymbol{\beta}_k, \kappa_k) = \Pi_K(\boldsymbol{\varepsilon}_{k-1}^e + \boldsymbol{\varepsilon}(\Delta \mathbf{u}_k), \mathbf{X}_{k-1}, \bar{\boldsymbol{\varepsilon}}_{k-1}^p) \quad \text{a.e. in } \Omega,$$

$$(\boldsymbol{\varepsilon}_k^e, \mathbf{X}_k, \bar{\boldsymbol{\varepsilon}}_k^p) = G(\boldsymbol{\sigma}_k, \boldsymbol{\beta}_k, \kappa_k) \quad \text{a.e. in } \Omega,$$

### Properties of $T_k(\boldsymbol{\eta}) = \Pi_{K,\sigma}(\boldsymbol{\varepsilon}_{\mathbf{k}-1}^e + \boldsymbol{\eta}, \boldsymbol{\beta}_{\mathbf{k}-1}, \kappa_{\mathbf{k}-1}) - \boldsymbol{\sigma}_{\mathbf{k}-1}$

Let

- the constitutive mapping  $G$  fulfils (G1)-(G4),
- the yield function  $\Phi$  fulfils  $(\Phi1) - (\Phi6)$ ,

Then

- $\Psi_{T_k}(\boldsymbol{\eta}) = \langle \boldsymbol{\eta}, T_k(\boldsymbol{\eta}) + \boldsymbol{\sigma}_{\mathbf{k}-1} \rangle - \frac{1}{2} \langle (\mathbf{D}^e)^{-1} T_k(\boldsymbol{\eta}), T_k(\boldsymbol{\eta}) \rangle$ ,  $D\Psi_{T_k} = T_k$ ,
- $T_k$  is Lipschitz continuous and monotone on  $S$ ,
- $T_k$  is (strongly) semismooth on  $S$ ,
- the generalized derivative of  $T_k$  are symmetric and positively semidefinite.

### Derivative of the elastoplastic operator $T_k$

Let

$$\begin{aligned} P_\eta &:= (\boldsymbol{\varepsilon}_{\mathbf{k}-1}^e + \boldsymbol{\eta}, \mathbf{X}_{\mathbf{k}-1}, \bar{\boldsymbol{\varepsilon}}_{\mathbf{k}-1}^p) \in \mathcal{D}_{\Pi_K}, \\ \Pi_K(P_\eta) &:= (\Pi_{K,\sigma}(P_\eta), \Pi_{K,\beta}(P_\eta), \Pi_{K,\kappa}(P_\eta)), \\ T_k(\boldsymbol{\eta}) &:= \Pi_{K,\sigma}(P_\eta) - \boldsymbol{\sigma}_{\mathbf{k}-1}. \end{aligned}$$

Then

$$DT_k(\boldsymbol{\eta}) = \frac{\partial \Pi_{K,\sigma}(P_\eta)}{\partial \boldsymbol{\sigma}}.$$

If  $G^{-1}(P_\eta) = (\boldsymbol{\sigma}_{\mathbf{k}-1} + \mathbf{D}^e \boldsymbol{\eta}, \boldsymbol{\beta}_{\mathbf{k}-1}, \kappa_{\mathbf{k}-1}) \in \text{int}(K)$  (elastic region), then

$$T_k(\boldsymbol{\eta}) = \mathbf{D}^e \boldsymbol{\eta}, \quad DT_k(\boldsymbol{\eta}) = \mathbf{D}^e.$$

## FEM discretization of elastoplastic problem

$\tau_h$  - triangulation of  $\Omega$  with linear simplex elements

$V_h$  - approximation of  $V_h$  (piecewise linear functions)

Non-linear operator:  $F_{k,h} : V_h \rightarrow V_h$

$$(F_{k,h}(\mathbf{v}_h), \mathbf{w}_h)_h := \sum_{\mathcal{K} \in \tau_h} |\mathcal{K}| \langle T_k(\boldsymbol{\varepsilon}(\mathbf{v}_h)|_{\mathcal{K}}), \boldsymbol{\varepsilon}(\mathbf{w}_h)|_{\mathcal{K}} \rangle d\mathbf{x} \quad \forall \mathbf{v}_h, \mathbf{w}_h \in V_h.$$

Vector representation:  $\mathbf{v}_h \in V_h \mapsto \mathbf{v} \in \mathbb{R}^n$ ,  $\mathbf{f}_h \in V_h \mapsto \mathbf{f} \in \mathbb{R}^n$ ,

$$\mathcal{F}_k : \mathbb{R}^n \rightarrow \mathbb{R}^n, \quad \mathcal{F}_k(\mathbf{v}) = F_{k,h}(\mathbf{v}_h) \quad \forall \mathbf{v}_h \in V_h.$$

One-time step elastoplastic problem:

$$\text{find } \Delta \mathbf{u}_k \in \mathbb{R}^n : \quad \mathcal{F}_k(\Delta \mathbf{u}_k) = \Delta \mathbf{f}_k.$$

$\mathcal{F}_k$  - similar properties as  $T_k$ , semismoothness depends on  $h$ .

## 5 CLASSICAL ISOTROPIC YIELD FUNCTIONS

### 5 Classical isotropic yield functions

#### Scalar isotropic functions

Definition:  $S := \mathbb{R}_{sym}^{3 \times 3}$ ,

$$\varphi : S \rightarrow \mathbb{R}, \quad \varphi(\boldsymbol{\sigma}) = \varphi(\mathbf{Q}\boldsymbol{\sigma}\mathbf{Q}^T) \quad \forall \mathbf{Q} \in Orth$$

Eigenvalues representation:  $\boldsymbol{\sigma} = \sum_{i=1}^3 \sigma_i \mathbf{e}_i \otimes \mathbf{e}_i$

$$\varphi(\boldsymbol{\sigma}) = \hat{\varphi}(\sigma_1, \sigma_2, \sigma_3) = \hat{\varphi}(\sigma_2, \sigma_1, \sigma_3) = \hat{\varphi}(\sigma_1, \sigma_3, \sigma_2) \quad \forall \boldsymbol{\sigma} \in S,$$

First derivative (Ogden 1984):

$$\frac{\partial \varphi}{\partial \boldsymbol{\sigma}} = \sum_{i=1}^3 \frac{\partial \hat{\varphi}}{\partial \sigma_i} \mathbf{e}_i \otimes \mathbf{e}_i$$

### Second derivative of isotropic function (Carlson, Hoger 1986)

Let  $\boldsymbol{\sigma} \in S$ ,  $\sigma_1 \neq \sigma_2 \neq \sigma_3 \neq \sigma_1$ . Then the eigenprojections of  $\boldsymbol{\sigma}$  fulfil

$$\mathbf{E}_i = \prod_{j=1, j \neq i}^3 \frac{1}{(\sigma_i - \sigma_j)} (\boldsymbol{\sigma} - \sigma_j \mathbf{I}) = e_i \otimes e_i, \quad i = 1, 2, 3.$$

$$D^2\varphi(\boldsymbol{\sigma}) = \sum_{i,j=1}^3 \frac{\partial^2 \hat{\varphi}}{\partial \sigma_i \partial \sigma_j} \mathbf{E}_i \otimes \mathbf{E}_j + \sum_{a=1}^3 \frac{\partial \hat{\varphi} / \partial \sigma_a}{(\sigma_a - \sigma_b)(\sigma_a - \sigma_c)} \left\{ \frac{\partial \boldsymbol{\sigma}^2}{\partial \boldsymbol{\sigma}} - (\sigma_b + \sigma_c) \mathbf{I}_\sigma - [(\sigma_a - \sigma_b) + (\sigma_a - \sigma_c)] \mathbf{E}_a \otimes \mathbf{E}_a - (\sigma_b - \sigma_c) (\mathbf{E}_b \otimes \mathbf{E}_b - \mathbf{E}_c \otimes \mathbf{E}_c) \right\},$$

where  $a \neq b \neq c \neq a$  and

$$(\partial \boldsymbol{\sigma}^2 / \partial \boldsymbol{\sigma}) \mathbf{T} = \boldsymbol{\sigma} \mathbf{T} + \mathbf{T} \boldsymbol{\sigma}, \quad \mathbf{I}_\sigma \mathbf{T} = \mathbf{T}, \quad (\mathbf{E}_i \otimes \mathbf{E}_j) \mathbf{T} = \langle \mathbf{E}_j, \mathbf{T} \rangle \mathbf{E}_i \quad \forall \mathbf{T} \in S$$

### The second derivative of scalar-valued isotropic functions (Carlson, Hoger 1986)

- Isotropic function  $\varphi$  is twice continuously differentiable in a neighborhood of  $\boldsymbol{\sigma} \in S$ ,  $\sigma_1 \neq \sigma_2 \neq \sigma_3 \neq \sigma_1$  if  $\hat{\varphi}$  is twice continuously differentiable in a neighborhood of  $(\sigma_1, \sigma_2, \sigma_3)$ .

- The same implication holds for semismoothness of  $D\varphi$  a neighborhood of  $\boldsymbol{\sigma} \in S$ ,  $\sigma_1 \neq \sigma_2 \neq \sigma_3 \neq \sigma_1$

### Assumptions on isotropic function

$$\Phi : W \rightarrow \mathbb{R}, \quad \Phi(\boldsymbol{\sigma}, \boldsymbol{\beta}, \kappa) := \varphi(\boldsymbol{\sigma} - \boldsymbol{\beta}) - (\sigma_{y0} + \kappa)$$

$\varphi : S \rightarrow \mathbb{R}$ ,  $\varphi$  is isotropic,  $\varphi(\mathbf{0}) = 0$  and

( $\varphi$ 1)  $\varphi$  is convex on  $S$ ,

( $\varphi$ 2)  $\varphi$  is a.e. differentiable on  $S$ .

( $\varphi$ 3)  $\varphi$  is a.e. differentiable on the set

$$K_c := \{\boldsymbol{\sigma} \in S : \varphi(\boldsymbol{\sigma}) = c\}, \quad c > 0.$$

( $\varphi$ 4) If  $\boldsymbol{\sigma} \in \mathcal{D}_\varphi$ , then  $\exists \mathcal{O}_{\boldsymbol{\sigma}}, \varphi \in C^2(\mathcal{O}_{\boldsymbol{\sigma}})$ .

( $\varphi$ 5) If  $\boldsymbol{\sigma} \in K_c$  and  $\boldsymbol{\sigma} \in \mathcal{D}_\varphi$ , then  $D\varphi(\boldsymbol{\sigma}) \neq \mathbf{0}$ .

### Von Mises yield function

$$\Phi(\boldsymbol{\sigma}, \boldsymbol{\beta}, \kappa) = \varphi(\boldsymbol{\sigma} - \boldsymbol{\beta}) - (\sigma_{y0} + \kappa), \quad \varphi(\boldsymbol{\sigma}) := \sqrt{\frac{3}{2}} \|\text{dev}(\boldsymbol{\sigma})\|_F,$$

$$p(\boldsymbol{\sigma}) := \frac{1}{3} \text{tr}(\boldsymbol{\sigma}) = \frac{1}{3}(\sigma_{11} + \sigma_{22} + \sigma_{33}), \quad \text{dev}(\boldsymbol{\sigma}) = \boldsymbol{\sigma} - p(\boldsymbol{\sigma})\mathbf{I}.$$

- $\varphi$  is isotropic and convex on  $S$ ,  $\varphi(\mathbf{0}) = 0$
- $\varphi$  is not differentiable only for  $\boldsymbol{\sigma} = p(\boldsymbol{\sigma})\mathbf{I}$ , otherwise is  $C^\infty$  smooth
- $\varphi$  is differentiable on  $K_c = \{\boldsymbol{\sigma} : \varphi(\boldsymbol{\sigma}) = c\}$ ,  $c > 0$

$$D\varphi(\boldsymbol{\sigma}) = \sqrt{\frac{3}{2}} \hat{\mathbf{n}}(\boldsymbol{\sigma}), \quad D^2\varphi(\boldsymbol{\sigma}) = \frac{\mathbf{I}_{\text{dev}} - \hat{\mathbf{n}}(\boldsymbol{\sigma}) \otimes \hat{\mathbf{n}}(\boldsymbol{\sigma})}{\|\text{dev}(\boldsymbol{\sigma})\|_F},$$

$$\hat{\mathbf{n}}(\boldsymbol{\sigma}) = \frac{\text{dev}(\boldsymbol{\sigma})}{\|\text{dev}(\boldsymbol{\sigma})\|_F}, \quad \mathbf{I}_{\text{dev}}\boldsymbol{\sigma} = \text{dev}(\boldsymbol{\sigma}).$$



## Drucker-Prager yield function

$$\Phi(\boldsymbol{\sigma}, \boldsymbol{\beta}, \kappa) = \varphi(\boldsymbol{\sigma} - \boldsymbol{\beta}) - \xi(c_0 + \kappa), \quad \varphi(\boldsymbol{\sigma}) := \sqrt{\frac{1}{2}} \|\text{dev}(\boldsymbol{\sigma})\|_F + \eta p(\boldsymbol{\sigma}),$$

$$p(\boldsymbol{\sigma}) := \frac{1}{3} \text{tr}(\boldsymbol{\sigma}) = \frac{1}{3}(\sigma_{11} + \sigma_{22} + \sigma_{33}), \quad \text{dev}(\boldsymbol{\sigma}) = \boldsymbol{\sigma} - p(\boldsymbol{\sigma})\mathbf{I},$$

$c_0 > 0$  - initial cohesion,  $\eta, \xi > 0$  - given parameters

- $\varphi$  is isotropic and convex on  $S$ ,  $\varphi(\mathbf{0}) = 0$
- $\varphi$  is not differentiable only for  $\boldsymbol{\sigma} = p(\boldsymbol{\sigma})\mathbf{I}$ , otherwise is  $C^\infty$  smooth
- $\varphi$  is not differentiable on  $K_c = \{\boldsymbol{\sigma} : \varphi(\boldsymbol{\sigma}) = c\}$  only at  $\boldsymbol{\sigma} = (\xi c / \eta)\mathbf{I}$

$$D\varphi(\boldsymbol{\sigma}) = \sqrt{\frac{3}{2}} \hat{\mathbf{n}}(\boldsymbol{\sigma}) + \frac{\eta}{3} \mathbf{I}, \quad D^2\varphi(\boldsymbol{\sigma}) = \frac{\mathbf{I}_{\text{dev}} - \hat{\mathbf{n}}(\boldsymbol{\sigma}) \otimes \hat{\mathbf{n}}(\boldsymbol{\sigma})}{\|\text{dev}(\boldsymbol{\sigma})\|_F},$$

## Tresca yield function

$$\Phi(\boldsymbol{\sigma}, \boldsymbol{\beta}, \kappa) = \varphi(\boldsymbol{\sigma} - \boldsymbol{\beta}) - (\sigma_{y_0} + \kappa), \quad \varphi(\boldsymbol{\sigma}) = \hat{\varphi}(\sigma_1, \sigma_2, \sigma_3) := \sigma_{\max} - \sigma_{\min},$$

- convexity of  $\varphi$  follows from

$$\sigma_{\max} = \sup_{\|\boldsymbol{\nu}\|=1} (\boldsymbol{\sigma}\boldsymbol{\nu}, \boldsymbol{\nu}), \quad \sigma_{\min} = \inf_{\|\boldsymbol{\nu}\|=1} (\boldsymbol{\sigma}\boldsymbol{\nu}, \boldsymbol{\nu})$$

- $\hat{\varphi}$  is  $C^\infty$  smooth at  $(s_1, s_2, s_3) \in \mathbb{R}^3$ ,  $s_i \neq s_j$ ,  $i \neq j$
- hence  $\varphi$  is  $C^\infty$  smooth at  $\boldsymbol{\sigma} \in \mathbb{S}$ ,  $\sigma_i \neq \sigma_j$ ,  $i \neq j$
- $\hat{\varphi}$  is a.e. differentiable on  $\hat{K}_c = \{(s_1, s_2, s_3) : \hat{\varphi}(s_1, s_2, s_3) = c\}$ ,  $c > 0$
- hence  $\varphi$  is a.e. differentiable on  $K_c = \{\boldsymbol{\sigma} : \varphi(\boldsymbol{\sigma}) = c\}$ ,  $c > 0$

## Derivative of Tresca yield function

Let  $s_1 > s_2 > s_3$ . Then  $\hat{\varphi}(s_1, s_2, s_3) = s_1 - s_3$  and

$$D_1\hat{\varphi} = 1, \quad D_2\hat{\varphi} = 0, \quad D_3\hat{\varphi} = -1, \quad D^2\hat{\varphi} = 0.$$

Then

$$D\phi(\boldsymbol{\sigma}) = \mathbf{e}_1 \otimes \mathbf{e}_1 - \mathbf{e}_3 \otimes \mathbf{e}_3 = \mathbf{E}_1 - \mathbf{E}_3, \quad \sigma_1 > \sigma_2 > \sigma_3,$$

$$\begin{aligned} D^2\varphi(\boldsymbol{\sigma}) = & \frac{1}{(\sigma_1 - \sigma_2)(\sigma_1 - \sigma_3)} \left\{ \frac{\partial \sigma^2}{\partial \boldsymbol{\sigma}} - (\sigma_2 + \sigma_3)\mathbf{I}_\sigma - \right. \\ & \left. - [(\sigma_1 - \sigma_2) + (\sigma_1 - \sigma_3)]\mathbf{E}_1 \otimes \mathbf{E}_1 - (\sigma_2 - \sigma_3)(\mathbf{E}_2 \otimes \mathbf{E}_2 - \mathbf{E}_3 \otimes \mathbf{E}_3) \right\} \\ & - \frac{1}{(\sigma_3 - \sigma_1)(\sigma_3 - \sigma_2)} \left\{ \frac{\partial \sigma^2}{\partial \boldsymbol{\sigma}} - (\sigma_1 + \sigma_2)\mathbf{I}_\sigma - \right. \\ & \left. - [(\sigma_3 - \sigma_1) + (\sigma_3 - \sigma_2)]\mathbf{E}_3 \otimes \mathbf{E}_3 - (\sigma_1 - \sigma_2)(\mathbf{E}_1 \otimes \mathbf{E}_1 - \mathbf{E}_2 \otimes \mathbf{E}_2) \right\} \end{aligned}$$

## Mohr-Coulomb yield function

$$\Phi(\boldsymbol{\sigma}, \boldsymbol{\beta}, \kappa) = \varphi(\boldsymbol{\sigma} - \boldsymbol{\beta}) - 2(c_0 + \kappa) \cos \psi,$$

$$\begin{aligned} \varphi(\boldsymbol{\sigma}) = \hat{\varphi}(\sigma_1, \sigma_2, \sigma_3) & := (\sigma_{\max} - \sigma_{\min}) + (\sigma_{\max} + \sigma_{\min}) \sin \psi \\ & = (1 + \sin \psi)\sigma_{\max} - (1 - \sin \psi)\sigma_{\min} \end{aligned}$$

$c_0 > 0$  - initial cohesion

$\psi \in [0, \pi/2)$  - frictional angle

- similar properties and derivatives as Tresca yield function

## 6 Example of elastoplastic operator

### Von Mises yield criterion with nonlinear isotropic hardening

$$\Phi(\boldsymbol{\sigma}, \kappa) = \sqrt{\frac{3}{2}} \|\text{dev}(\boldsymbol{\sigma})\|_F - (\sigma_{y0} + \kappa), \quad \mathbf{D}^e \boldsymbol{\varepsilon}^e = \lambda \text{tr}(\boldsymbol{\varepsilon}^e) \mathbf{I} + 2\mu \boldsymbol{\varepsilon}^e, \quad \kappa = H(\bar{\varepsilon}^p)$$

$$T_k(\boldsymbol{\eta}) = \mathbf{D}^e \boldsymbol{\eta} - 2\mu \sqrt{\frac{3}{2}} \gamma^+ \hat{\mathbf{n}}(\boldsymbol{\sigma}(\boldsymbol{\eta})),$$

$$\sqrt{\frac{3}{2}} \|\text{dev}(\boldsymbol{\sigma}(\boldsymbol{\eta}))\|_F - 3\mu\gamma - (\sigma_{y0} + H(\bar{\varepsilon}_{k-1}^p + \gamma)) = 0 \quad \text{if } \Phi(\boldsymbol{\sigma}(\boldsymbol{\eta}), \kappa_{k-1}) > 0,$$

$$\hat{\mathbf{n}}(\boldsymbol{\sigma}) = \frac{\text{dev}(\boldsymbol{\sigma})}{\|\text{dev}(\boldsymbol{\sigma})\|_F}, \quad \boldsymbol{\sigma}(\boldsymbol{\eta}) = \boldsymbol{\sigma}_{k-1} + \mathbf{D}^e \boldsymbol{\eta}$$

### Potential and derivative of the von Mises operator

$$\begin{aligned} \Psi_{T_k}(\boldsymbol{\eta}) &= \langle \boldsymbol{\eta}, T_k(\boldsymbol{\eta}) + \boldsymbol{\sigma}_{k-1} \rangle - \frac{1}{2} \langle (\mathbf{D}^e)^{-1} T_k(\boldsymbol{\eta}), T_k(\boldsymbol{\eta}) \rangle = \\ &= \frac{1}{2} \langle (\mathbf{D}^e)^{-1} \boldsymbol{\sigma}(\boldsymbol{\eta}), \boldsymbol{\sigma}(\boldsymbol{\eta}) \rangle - 3\mu^2 (\gamma^+)^2. \end{aligned}$$

$$DT_k(\boldsymbol{\eta}) = \begin{cases} \mathbf{D}^e, & \Phi(\boldsymbol{\sigma}(\boldsymbol{\eta}), \kappa_{k-1}) < 0, \\ \mathbf{D}^e - 2\mu(\bar{\beta} \mathbf{I}_{\text{dev}} + \bar{\gamma} \hat{\mathbf{n}} \otimes \hat{\mathbf{n}}), & \Phi(\boldsymbol{\sigma}(\boldsymbol{\eta}), \kappa_{k-1}) > 0, \end{cases}$$

$$\bar{\beta}(\boldsymbol{\eta}) = \sqrt{\frac{3}{2}} \gamma \|\text{dev}(\boldsymbol{\sigma}(\boldsymbol{\eta}))\|_F^{-1}, \quad \bar{\gamma}(\boldsymbol{\eta}) = \frac{3\mu}{3\mu + H'(\bar{\varepsilon}_{k-1}^p + \gamma)} - \bar{\beta}(\boldsymbol{\eta})$$

Properties of  $T_k$  and  $DT_k$  ensuring quadratic convergence of the Newton method was investigated in (Blaheta, 1997).

## 7 Conclusion

- Elastoplastic problem was formulated by the generalized projective mapping.
- Such a formulation is suitable for investigation of the operator properties like semismoothness, differentiability or potentiality.
- It is possible to consider some generalization like non-linear elastic law, perfect plasticity, other hardening law or non-associative plasticity.
- Positive definiteness of the tangential operator for plasticity with hardening has not been investigated within this framework yet.

Thank you for your attention.